MOLECULAR CHARACTERIZATION OF PULMONARY LIPID PHOSPHATE PHOSPHOHYDROLASE: IMPLICATIONS IN LUNG AND TYPE II CELLS

by

MEERA NANJUNDAN

Graduate Program in Biochemistry

Submitted in partial fulfilment
of the requirements for the degree of
Doctor of Philosophy

Faculty of Graduate Studies
The University of Western Ontario
London, Ontario
February, 2001

ABSTRACT

Lipid phosphate phosphohydrolase (LPP) catalyzes the hydrolysis of phosphatidic acid (PA) to diacylglycerol. We demonstrate that LPP is N-ethylmaleimide-insensitive, Mg^{+2}-independent whose function in lung is unknown. Initial studies characterized LPP activity in rat lung microsomes where it was inhibited by sphingoid bases including sphingosine. LPP activity was enriched in lung plasma membranes (PM) and in isolated surfactant secreting type II cells where it could potentially be involved in signaling. LPP hydrolyzed PA and lyso-PA (LPA) with high specific activities while the activity against sphingosine-1-phosphate (S-1-P) was very low. The substrate specificity of pulmonary LPP appeared different to that of rat liver LPP which suggested the potential presence of a novel LPP isoform in lung. Cloning of LPPs by reverse-transcriptase polymerase chain reaction (RT-PCR) generated LPP1, up to three LPP1 variants (LPP1a and two novel truncated isoforms, LPP1b and LPP1c), and LPP3 cDNAs. Further investigation of the LPP1b isoform revealed that its mRNA was present across a variety of tissues and exists in equal abundance to the LPP1/1a isoform in lung. The developmental patterns for LPP, PLD, PKC isoforms, and Edg receptors indicate potential roles in the control of lung vasculogenesis, alveolar development, and surfactant phospholipid secretion. LPP activity was enriched in caveolin-enriched domains (CEDs) isolated from rat lung tissue, isolated rat type II cells, and in mouse type II-like cell lines (MLE12 and MLE15). LPP3 protein localized predominantly to rat lung CEDs while LPP1/1a protein is present in purified caveolae from MLE15 cells. Since total plasma membranes had a higher

abundance of LPP1/1a protein with low LPP activity and phorbol ester treatment caused an increase in LPP specific activity in MLE CEDs, the activated form of LPP1/1a may be recruited into caveolae-rafts. The concerted actions of LPP, PLD, and PKC may be implicated in the transdifferentiation of type II cells to a type I cell during lung development and injury. Thus, LPP localization to caveolae-rafts is consistent with a role in caveolae/raft signaling and caveolar dynamics. LPP is proposed to act sequentially to PLD and control LPA/S-1-P effects mediated through Edg to regulate cellular proliferation, differentiation, migration, and apoptosis.

KEYWORDS

phosphatidate phosphohydrolase, lipid phosphate phosphohydrolase, phosphatidic acid, diacylglycerol, lysophosphatidic acid, sphingosine-1-phosphate, ceramide-1-phosphate, phospholipid signaling, phospholipase D, diacylglycerol kinase, protein kinase C, sphingolipid signaling, plasma membranes, caveolae/rafts, novel isoforms, rat lung, MLE12, MLE15, type II cells, type I cells, surfactant secretion, lung development, epithelial cell growth

CO-AUTHORSHIP

The following thesis contains material from previously published and submitted manuscripts co-authored by Meera Nanjundan and Fred Possmayer. The experimental work presented in this thesis was performed by Meera Nanjundan with the exception of the isolation of alveolar epithelial cells from fetal tissue (19 days gestation and 21 days gestation) which was performed by Irene Tseu in the laboratory of Dr. Martin Post (Hospital for Sick Children, Toronto, Canada). The original manuscript, a version which appears in Chapter 2 of this thesis, was written by Meera Nanjundan and Fred Possmayer. The copyright release of the original manuscript that appears in Chapter 2 is in the Appendices section.

ACKNOWLEDGEMENTS

I would like to express my sincere appreciation to my supervisor, Dr. Fred Possmayer, for his support, guidance, and understanding during my graduate studies.

I would also like to thank my advisory committee, Dr. Eric Ball, Dr. David Litchfield, Dr. Paul Walton, and Dr. Ruud Veldhuizen, for their advice and assistance. I would like to thank Dr. David Brindley, Dr. Andrew Morris, Dr. Sylvain Bourgoin, and Dr. Martin Post for providing antibodies and cells for work presented in this thesis as well as for invaluable discussions.

I extend my appreciation to Anne Brickenden for her wonderful technical assistance and encouragement.

I would also like to thank past and present members of the Possmayer laboratory. I thank Kevin Inchley, Steven Hearn, Dr. Shou-Hwa Yu, Dr. Lin Zhao, Dr. Karina Rodriguez-Capote, and Jonathan Faulkner for their support and assistance. I am also grateful to the work-study students who have assisted in the laboratory.

Finally, I express my sincere gratitude to my mother, father, and my sister for their unending support and constant encouragement.

TABLE OF CONTENTS

LIST OF FIGURES

ABBREVIATIONS

ATP	adenosine triphosphate
AEC	alveolar epithelial cell
bp	base pair(s)
^0C	degrees celsius
cAMP	cyclic adenosine monophosphate
cDNA	complementary deoxyribonucleic acid
CDP	cytidine diphosphate
CED	caveolin-enriched domain
CPT	cholinephosphotransferase
CMV	cytomegalovirus
CYT	choline:phosphate cytidyltransferase
C-1-P	ceramide-1-phosphate
C-terminal	carboxy-terminal
cDNA	complementary deoxyribonucleic acid
dNTP	deoxyribonucleotide triphosphate
DAG	diacylglycerol
DGPP	diacylglycerol pyrophosphate
DMEM	Dulbecco's eagle medium
DNAse-1	deoxyribonuclease 1
DTT	dithiothreitol
Edg	endothelial differentiation gene

EDTA	ethylenediaminetetraacetic acid
EGTA	ethylene glycol-bis (β-aminoethyl ether)-tetraacetic acid
GFP	green fluorescent protein
HEK	human embryonic kidney
HEPES	(N-[2-Hydroxyethyl]piperazine-N'-[2-ethanesulfonic acid])
IPTG	isopropylthio-β-D-galactoside
kDa	kilodalton
LPA	lysophosphatidic acid
LPP	lipid phosphate phosphohydrolase
M	molar
MAO	monoamine oxidase
MAP	mitogen activated protein
MEM	minimal essential media
min	minute(s)
MLE	mouse lung epithelial
mRNA	messenger ribonucleic acid
NEM	N-ethylmaleimide
nmol	nanomole
N-terminal	amino terminal
PA	phosphatidic acid
PAGE	polyacrylamide gel electrophoresis
PAP	phosphatidate phosphohydrolase
PBS	phosphate buffered saline

PC	phosphatidylcholine
PCR	polymerase chain reaction
PIP_2	phosphatidylinositol bisphosphate
PKA	protein kinase A
PKC	protein kinase C
PLD	phospholipase D
PMA	phorbol 12-myristate 13-acetate
P_{2u}	purinergic receptor subtype 2u
RNAse	ribonuclease
RT	reverse transcriptase
SDS	sodium dodecyl sulphate
SSC	sodium citrate saline
SM	sphingomyelin
SV40 T	simian virus large T antigen
TBST	tris-buffered saline with Tween 20
TLC	thin layer chromatography
tris	tris (hydroxymethyl) aminomethane
S-1-P	sphingosine-1-phosphate
UTP	uridine triphosphate

Chapter 1

Introduction

1.1 Characterization of Pulmonary Phosphatidate Phosphohydrolase Activities

Phosphatidate phosphohydrolase (PAP) catalyzes the hydrolysis of phosphatidic acid (PA) to diacylglycerol (DAG) and was first described in plants by Kates in 1955 (1). Early studies on PAP in liver, brain, kidney, intestine, and erythrocytes demonstrated that most of the enzymatic activity was associated with the particulate fractions although further investigations indicated that the cytosolic fraction contained a factor, which stimulated the production of DAG from PA (2). Casola and Possmayer (3) initially measured PAP activity using labelled PA that was endogenously generated on lung microsomes from glycerol-3-P^{32}-phosphate (PA_{mb}). A large proportion of this PA activity was found in the cytosolic fractions with a small proportion in the microsomal fraction. Triton X-100 stimulated the membrane-bound PA (PA_{mb}) PAP activity in the cytosol and microsomes but inhibited the activity against aqueously dispersed PA ((PA_{aq}) PAP) (4). Furthermore, PA_{mb} PAP activity could be distinguished from the PA_{aq} PAP activity on the basis of pH, ions, and magnesium (3). However, these results did not exclude the possibility that these differences in the activity could arise from alterations in the physical state of the substrate rather than the presence of independent enzymatic activities.

Based on the susceptibility of PA_{mb} PAP activity to trypsin and heat in contrast to PA_{aq} PAP activity which was unaffected, lung could contain two potentially distinguishable activities (5). Furthermore, separation of these two activities by purification of rat lung cytosols by gel filtration indicated that greater

than 55% of the PA_{mb} PAP activity eluted at a molecular weight of 390 kDa with a minor peak at 110 kDa and greater than 75% of the PA_{aq} PAP eluted at 130 kDa and 25% at 110 kDa (5). During these studies, it was observed that the 390 kDa peak could hydrolyze PA_{aq} substrate in the presence of magnesium. This was the first indication of a PAP activity which showed absolute magnesium dependency. Hence, a major difference between the activities observed with the two substrates may have been related to the presence of magnesium in the membrane-bound substrate since the radioactive PA_{mb} was prepared in the presence of magnesium while sodium PA was used to prepare the PA_{aq}. Further differences between PA_{aq} and PA_{mb} PAP activities were observed during rat lung development (6). The specific activity of PA_{mb} PAP increased 1.5-fold between 18 and 21 days gestation (22 days term). In contrast, PA_{aq} PAP activity did not change in the fetus but increased significantly after birth. These results provided strong evidence that separate enzymes were responsible for the degradation of membrane-bound and aqueous dispersions of PA.

1.2 Pulmonary PAP1

Further characterization of the magnesium-dependent isozyme, PAP1, was performed by Walton and Possmayer who assayed the activity using mixed lipid vesicles of equimolar egg PA and dipalmitoylphosphatidylcholine (DPPC) (7). The addition of magnesium produced a two-fold increase in activity with the microsomal fraction and a 9.5-fold increase with the cytosolic fraction (7). Sturton *et al* (8) have observed with rat liver microsomes that P^{32} can be released from radioactive PA by

a combination of phospholipase, PLA_1 and PLA_2, activities followed by the degradation of glycerol-3-P^{32}-phosphate to yield glycerol and P^{32}-inorganic phosphate. In order to ensure that a similar activity was not interfering with phosphohydrolase activities in lung, similar studies were performed in lung microsomes and cytosol using P^{32}-PA and C^{14}-PA (9). The magnesium-dependent release of radioactive DAG accounted for 94% of the radioactivity from P^{32}-PA while the C^{14} label in monoacylglycerol, glycerol, and glycerol-3-phosphate accounted for less than 7%. Furthermore, extraction with molybdate indicated that 90% of the radioactivity released from P^{32}-PA was due to inorganic phosphate. Thus, phospholipase activities in lung fractions do not appear to lead to an overestimation of inorganic phosphate release in the measurement of PAP activity (9).

1.2.1 Phosphatidylcholine (PC) Biosynthesis

The formation of PA is an important step in the biosynthesis of PC (Figure 1.1) (10). PC can be formed through the initial acylation of either sn-glycerol-3-phosphate or its more oxidized glycolytic precursor, dihydroxyacetone phosphate. This is followed by a reductive step yielding 1-acyl-sn-glycerol-3-phosphate or lysophosphatidic acid (LPA) which is rapidly acylated to PA in lung. PA is then hydrolyzed to diacylglycerol (DAG) and P_i by PAP. The combination of DAG with CDP choline is catalyzed by cholinephosphotransferase to generate PC and CMP. PA is at an important branchpoint in the biosynthetic pathway and can also be utilized for the formation of acidic phospholipids including phosphatidylinositol (PI) and phosphatidylglycerol (PG).

Figure 1.1. Glycerolipid biosynthesis. Acylation of glycerol-3-phosphate (G-3-P) or dihydroxyacetone phosphate (DHAP) occurs by G-3-P acyltransferase (**1a**) and 1-acylglycerol-3-phosphate acyltransferase (**1b**) or DHAP acyltransferase (**1c**) to generate phosphatidic acid (PA). PA is then dephosphorylated by phosphatidic acid phosphohydrolase (**2**) to produce diacylglycerol (DAG). Cholinephosphotransferase (CPT, **3**) will generate phosphatidylcholine (PC) from DAG and CDP-choline (generated by the sequential action of choline kinase (CK, **4**) and the rate-limiting enzyme choline:phosphate cytidylyltransferase (CT, **5**)). PC can also be synthesized through the methylation of phosphatidylethanolamine (PE) by ethanolamine phosphotransferase (EPT, **6**) and PE methyltransferase (PEMT, **7**). PE can be used for the synthesis of PS by PS synthase (PSS, **8**). PA can also be used for the synthesis of PI in this pathway through CDP-DAG synthase (**9**) and PI synthase (**10**).

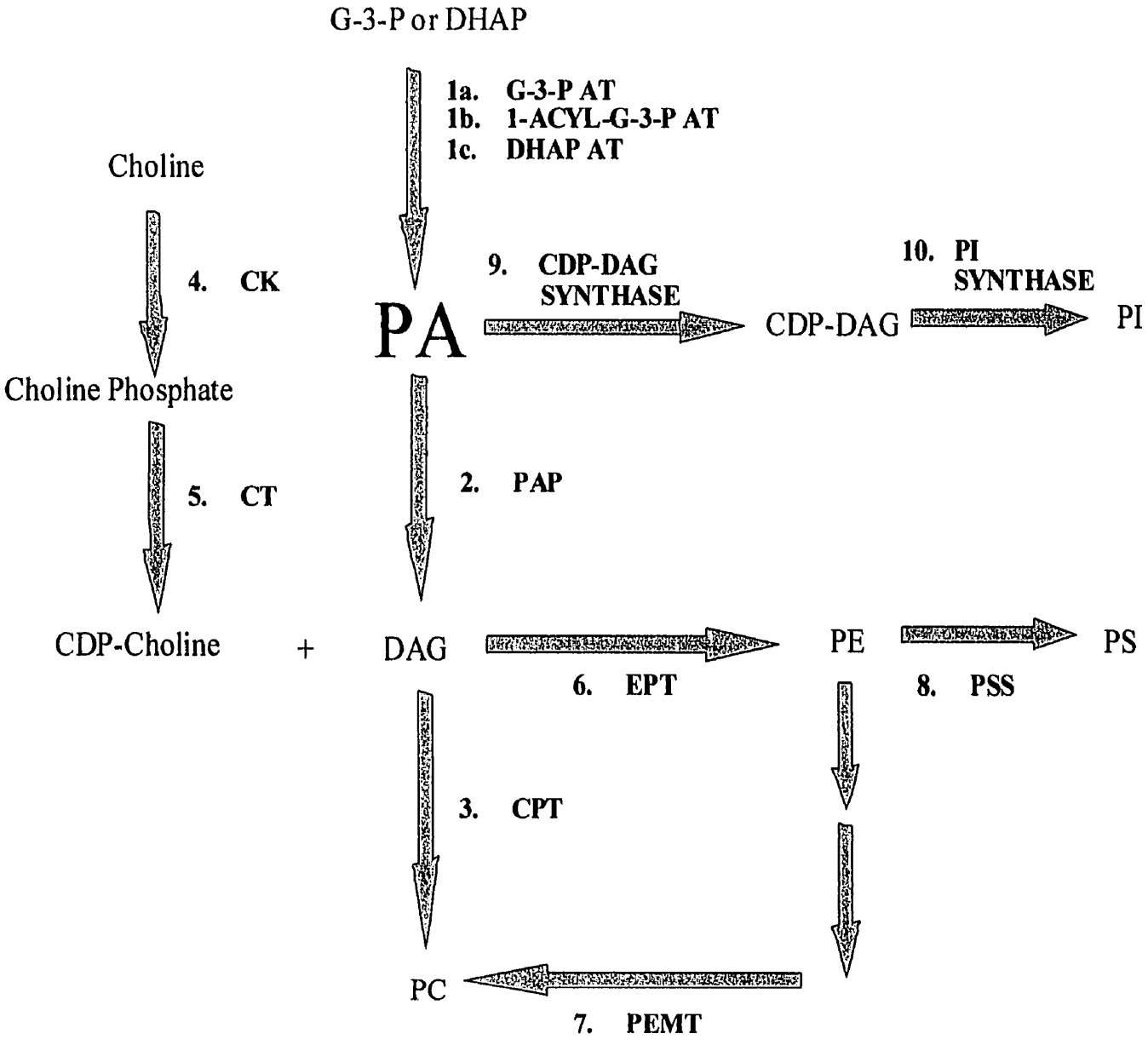
G-3-P or DHAP
1a. G-3-P AT
1b. 1-ACYL-G-3-P AT
1c. DHAP AT
Choline
4. CK
Choline Phosphate
5. CT
CDP-Choline
+
PA
9. CDP-DAG SYNTHASE
CDP-DAG
10. PI SYNTHASE
PI
2. PAP
DAG
6. EPT
PE
8. PSS
PS
3. CPT
PC
7. PEMT

Walton and Possmayer (11) identified the PAP activity responsible for the production of DAG for the formation of triacylglycerol (TAG), phosphatidylethanolamine (PE), and phosphatidylcholine (PC) through salt washing studies. Rat lung microsomes were washed with increasing concentrations of NaCl which led to a progressive increase in the proportion of radioactivity in PA from 63% to over 90% with a decrease in the labeling of DAG and TAG from 37% to less than 10%. The salt washing did not affect PAP2 but reduced PAP1 activity. The ability of the salt washed microsomes to metabolize PA was resolved by the addition of the washings, cytosol, or partially purified PAP1. Thus, PAP1 was shown to be essential for glycerolipid biosynthesis leading to neutral glycerolipids and PC. The effects of a novel inhibitor of PAP1, bromoenol lactone, showed that this PAP isoform participates in triacylglycerol (TAG) synthesis in mouse macrophages (12).

PAP1 is a magnesium-dependent cytosolic enzyme which can translocate to the endoplasmic reticulum where it was shown to have a role in phospholipid biosynthesis. The translocation of soluble PAP1 to the microsomal fractions has been observed in a number of systems. Evidence in lung for translocation has been obtained with A549 cells, a transformed alveolar type II-like cell line. Exposure of A549 cells to free fatty acids produced a rapid decrease in the proportion of PAP1 activity which was released from digitonin-permeabilized cells while there was no effect on PAP2 activity (13).

1.2.2 Signaling

In addition to phospholipid biosynthesis, PAP1 may also be involved in cell signaling. Upon cell stimulation, the type I enzyme may translocate to plasma membranes to generate DAG sequentially to phospholipase D (PLD) activation. Truett *et al* (14) suggest that the regulation of the conversion of PA to DAG by PAP1 may be integral to the control of certain human polymorphonuclear leukocyte (PMN) responses. Their studies indicate that after chemoattractant stimulation, magnesium-dependent PAP activity decreased in the soluble fraction and increased in the particulate fraction suggesting that the enzyme may participate in signal transduction in the PMN. Jiang *et al* (15) examined the effect of epidermal growth factor (EGF) on PAP1 activity in human epidermoid A431 cells. In unstimulated cells, they found that PAP1 activity co-immunoprecipitates with the EGF receptor. With EGF treatment, PAP1 was found to associate with protein kinase C (PKC-ε). It is possible that PKC-ε may serve to allosterically modify PAP1 or localize PAP to appropriate membrane locations where PA substrate is localized. Furthermore, Johnson *et al* determined the involvement of PAP1 as a key regulatory element leading to arachidonic acid mobilization (16) and the induction of cyclooxygenase-2 (COX2) (17) in human WISH cells, which are crucial events for the eicosanoid response.

1.3 Pulmonary PAP2

PAP2 is a magnesium-independent membrane-bound enzyme whose function in lung to date is unclear. Casola and Possmayer (6) observed that

membrane-bound PAP2 activity in rat lung tissue did not change appreciably in the fetus but increased significantly after birth. In rabbit lung, Casola and Possmayer (18) observed a doubling in microsomal PAP2 between 25 days gestation (dg) and term (30 dg) which correlated with choline incorporation into PC. Treatment with glucocorticoids, in fetal rabbit lung, led to an increase in PAP2 activity as well as enhanced incorporation of choline into PC (19). The specific activity of PAP2 also increased with the appearance of lamellar bodies (intracellular stored surfactant) in fetal rabbit lung (20). These changes in PAP2 activity appeared to parallel surfactant production. Pulmonary surfactant, composed of 90% phospholipid (mostly dipalmitoyl phosphatidylcholine (DPPC)) and 10% protein, is essential for normal lung function. Its main function is to maintain low surface tensions at the air-liquid interface and to prevent alveolar collapse upon expiration (21).

The presence of PAP2 activity in human amniotic fluid and the observation that this activity paralleled the increase in lecithin (PC) to sphingomyelin (SM) or the PC/SM ratio (L/S ratio) (22) stimulated a detailed study of this enzyme in lamellar bodies and in isolated surfactant. The specific activity of PAP2 in lamellar bodies was approximately double that in the microsomal fraction (23). Casola *et al* (24) confirmed the presence of PAP2 in rat lamellar bodies but noted that the presence of the activity was very low. Crecelius and Longmore (25) have investigated the subcellular localization of a magnesium-independent PAP activity in adult type II cells. The highest activities were found in the cytosolic fraction with smaller amounts in the lamellar bodies, microsomal, and mitochondrial fractions.

1.4 Characterization and Purification of NEM-Insensitive PAP2

Brindley and colleagues have developed an assay to measure the activity of magnesium-independent phosphatidate phosphohydrolase (26). In order to exclude possible interference from PAP1, N-ethylmaleimide (NEM) was utilized to distinguish between these two enzymatic activities. PAP1, a magnesium-dependent activity, was NEM-sensitive while PAP2, a magnesium-independent activity, was NEM-insensitive. A number of investigators have demonstrated that NEM-insensitive PAP activity is predominantly localized in the membrane fraction (27, 28, 29, 30, 31).

Kanoh *et al* (32) were the first group to purify PAP2, as an 83kDa protein, from porcine thymus membranes. Its properties indicated that it was magnesium-independent, NEM-insensitive, specific for PA, and activated by Triton X-100. An apparent molecular weight of 218kDa was obtained by gel filtration chromatography suggestive of an oligomeric structure. Brindley and colleagues (33) were also successful in purifying PAP2 from rat liver plasma membranes as two ionically separate forms: anionic PAP (53kDa, pI<4) and a cationic PAP (51kDa, pI=9). These investigators determined that cationic PAP was a desialated form of anionic PAP by neuraminidase treatment. Fleming and Yeaman (34) have also purified NEM-insensitive PAP from rat liver as two separate activities. One activity, PAP2A, was purified as an 83kDa protein and the other, PAP2B, as a combination of three polypeptides, 83kDa, 54kDa, and 34kDa. Native PAP2A and PAP2B eluted from gel filtration with apparent molecular masses of 265 kDa and 290/300 kDa, respectively,

suggesting at least two different isozymes may be present in rat liver. Both activities were magnesium-independent, NEM-insensitive, and inhibited by LPA.

A number of investigators have characterized and purified ecto-phosphatidic acid phosphohydrolase activities from various cells including neutrophilic leukocytes (35, 36), PAM 212 keratinocytes (37), and CD34+/CD38+ hematopoietic progenitor cells (38). These ecto-PAP activities are localized to the extracellular side of the plasma membranes and rapidly hydrolyze exogenous PA and LPA. Disruption of intact neutrophils did not further increase PAP2 activity indicating that the activity hydrolyzes primarily exogenous substrate. In *in gel* activity assays, PAP activity consistently localized with a 42-52kDa band (35).

1.5 Cloning of Mammalian NEM-Insensitive PAP2 Isoforms

A number of PAP2 isoforms have been recently cloned and have been renamed lipid phosphate phosphohydrolases (LPP) (Figure 1.2) due to their broad substrate specificity, which is later discussed in Section 1.10. Kai *et al* (39) were the first to identify and clone the cDNA of LPP. They previously described the purification of an 83kDa protein from porcine thymus but the cDNA failed to express LPP activity upon transfection in mammalian cells. They detected other minor proteins in their purified preparation and they later determined that a minor broad band of 35kDa accounted for the activity. N-terminal and internal sequences were obtained and the N-terminal sequence was found to be highly conserved to the internal sequence encoded by a mouse partial cDNA named Hic53, a H_2O_2-inducible gene (40). Mouse kidney PAP (mPAP) was cloned generating a cDNA that

Figure 1.2. Naming of phosphatidate phosphohydrolases.

Present Name	Previous Name
LPP1	PAP2, mPAP, PAP2a-α2
LPP1a	PAP2a-α1
LPP2	PAP2c
LPP3	PAP2b, Dri42

was highly similar to Hic53. These cDNAs could have been derived by alternative splicing or by artifactual sequencing of Hic53 resulting in a discrepant reading frame. Kai *et al* (39) noted that the amino acid sequence of the mouse PAP2 is 34% and 48% identical to Drosophila *wunen* (41) and to rat Dri42 (42), respectively. Zhang *et al* (43) proposed that *wunen* may be responsible for guiding the germ cells early in embryonic development from the lumen of the developing gut towards the overlying mesoderm. Barila *et al* (44) searched for novel genes that were up-regulated during development and differentiation of the epithelial cells of the intestinal mucosa which led to the isolation of the Dri42 cDNA clone encoding a 35.5kDa protein.

Kai *et al* (45) have further cloned two isozymes of the magnesium-independent PAP from human HepG2 cells. Human LPP1 and LPP3 consist of 284 (32.158kDa) and 311 amino acids (35.119kDa) with 47% sequence identity. Human LPP1 and mPAP share 83% identity and human LPP3 shares 94% identity with rat Dri42 protein. There is 39% and 34% sequence identity between *wunen* and human LPP1 and LPP3, respectively. Both activities were insensitive to NEM and independent of magnesium.

Hooks *et al* (46) reported the cloning of a novel PAP2 isoform, LPP2, which was identified by searching the database of expressed sequence tags (dbESTs). At the same time, Roberts *et al* (47) have cloned the three human LPP isoforms. LPP1, LPP2, and LPP3 comprise 289, 288, and 311 amino acids corresponding to 32.788, 32.577, and 35.120kDa. LPP2 is 54% identical to LPP1 and 42% identical to LPP3.

Leung *et al* (48) were the first to identify LPP1a, an apparent alternative spliced variant of the human LPP1 isoform with sequences diverging at a putative exon (32.154kDa with pI = 7.89) from a human lung cDNA library. Between the two alternatively spliced exons, there is an overall 40% amino acid match. Tate *et al* (49) have also cloned LPP1a from guinea pig airway smooth muscle cells. Guinea pig LPP1a and human LPP1a have 90% identity in their predicted amino acid sequences.

1.6 Yeast Lipid Phosphate Phosphohydrolases

Two types of PAP have been identified in Saccharomyces Cerevisiae: a magnesium-dependent and NEM-sensitive form as well as a magnesium-independent and NEM-insensitive form (50). Two membrane-associated forms (104 and 45kDa) of PAP1 have been purified and characterized in yeast which are regulated by phosphorylation by protein kinase A (PKA), phospholipids (CDP-DAG, cardiolipin, and phosphatidylinositol), sphingoid bases (sphingosine), and nucleotides (ATP and CTP) (51). PAP2 was first identified as a 34kDa diacylglycerol pyrophosphate (DGPP) phosphatase encoded by the DPP1 gene (52). The deletion of DPP1 in yeast resulted in the loss of all the detectable DGPP phosphatase activity with only 50% loss in magnesium-independent PAP activity (52). Recently, Carman and colleagues (53) showed that DPP1 was regulated by zinc. It has previously been proposed that DGPP may function in lipid signaling pathways (54). Studies with plants, where DGPP was first identified, have shown that this phospholipid accumulates upon G protein activation. DGPP has not been identified

in mammalian cells (54). However, Balboa *et al* (55) have shown that exogenous DGPP activates mouse macrophages for enhanced secretion of arachidonic acid metabolites which is a crucial event in the immunoinflammatory response of leukocytes. Carman and colleagues (56) recently reported the isolation and characterization of the LPP1 gene in yeast and show that the order of substrate preference was PA>LPA>DGPP. LPP1 null cells did not exhibit any growth defects (56). They suggest that LPP1 may play a role in the regulation of phospholipid metabolism and the cellular levels of PI and PA (56).

Katagiri and Shinozaki (57) have cloned two yeast PAP2 isoforms, ScPAP1 and ScPAP2, whose molecular weights are 33.5 and 31.2kDa, respectively. Hydropathy plot analyses of these two PAP2 yeast sequences indicate six transmembrane domains. These investigators isolated a ScPAP1 null mutant, which showed abnormal cell aggregation, abnormal cell shapes, and failed in cytokinesis while their nuclear division proceeded normally. Interestingly, these investigators found that Rho1 null mutant cells have a similar phenotype (58). Rho1 encodes a small GTP-binding protein of the Rho family which is involved in bud formation and is thought to function in signaling during cytokinesis (58). Faulkner *et al* (59) identified that LPP1 and DPP1 could account for most of the hydrolytic activities toward essential isoprenoid intermediates such as dolichyl pyrophosphate, dolichyl phosphate, farnesyl pyrophosphate, and geranylgeranyl pyrophosphate through the use of a double disruption mutant.

1.7 Expression of LPP

Western blotting using polyclonal antibodies generated against purified rat liver PAP2 (51-53kDa) (33) detected an 86kDa protein in brain as well as 17 and 36kDa proteins in thymus and spleen which may be tissue specific PAP isoforms. The antibody failed to immunoreact with lung and adipose tissue extracts (33). These tissues may express different isoforms of PAP for which these antibodies have low affinity. The existence of tissue specific isoforms is supported by observations that LPA failed to inhibit PAP purified from pig thymus and anti-thymus PAP (83kDa) failed to immunoprecipitate PAP activity from rat liver (32). An anti-LPP3 antibody developed by Morris and colleagues was used to screen its protein expression in various tissues from adult mouse which demonstrated its highest levels in brain, kidney, and lung (60) which correlates with the high PAP2 activities in rat brain, kidney, and lung (33). With regards to mRNA expression patterns, human LPP1 had distinct distribution patterns with little expression in placenta, thymus, and peripheral blood leukocytes but high expression in the prostate (45). Meanwhile, LPP3 mRNA was ubiquitously expressed (45). The LPP2 isoform revealed a more restrictive mRNA expression pattern being limited to brain, pancreas, and placenta (46). Leung *et al* (48) showed that human LPP1 mRNA was expressed in all tissues tested with the highest expression in heart, lung, uterus, and bladder. The size and sequence similarity between LPP1 and LPP1a isoforms did not allow these workers to distinguish the relative abundance of the two isoforms by northern analysis (48). Hence, RT-PCR was performed using primers specific to each individual exon showing that LPP1 mRNA was the predominant isoform in

kidney, lung, placenta, and liver while LPP1a mRNA was predominant in heart and pancreas (48).

1.8 Transmembrane Topology, N-linked Glycosylation, and Localization of LPP

Hydropathy plot analyses show that the LPPs are highly hydrophobic proteins containing six hydrophobic clusters of 17-23 amino acids (61). Both Kanoh's (62) and Brindley's group (63) obtained evidence that the N and C-termini of LPP1 are cytoplasmically oriented. The transmembrane disposition of Dri42, the rat LPP3 homolog, was investigated using *in vitro* insertion of Dri42-chloramphenicol acyltransferase (CAT) fusion proteins into microsomal membranes which indicated that both the N and C termini were cytoplasmically exposed (42) (Figure 1.3).

Purified PAP2 from rat liver plasma membranes (51-53kDa) migrated as a 28kDa band when treated with N-glycanase indicating that it contains N-linked polysaccharides (30). These sugars may be required for proper folding during synthesis, cellular localization, stability, or for biological function. Brindley and colleagues (64) later showed by site-directed mutagenesis that the glycosylation is not essential for enzymatic activity. mPAP, a 35kDa protein, migrated as a 29kDa band when treated with N-glycanase and was found to be resistant to endoglucosidase H indicating that the N-linked sugars are complex type suggestive of a post-Golgi localization (38). The mPAP sequence encodes two potential N-glycosylation sites at Asn 142 and Asn 276. The Dri 42 protein has one consensus sequence for N-linked glycosylation (Asn 171) (42). All of the cloned LPPs (LPP1,

Figure 1.3. Transmembrane topology of lipid phosphate phosphohydrolases. The N and C-termini of the various cloned LPP isoforms are cytoplasmically oriented. The active site, comprised of three domains, is proposed to face extracellularly or luminally. Regions I to VI represent transmembrane domains and the * represents an N-linked glycosylation site.

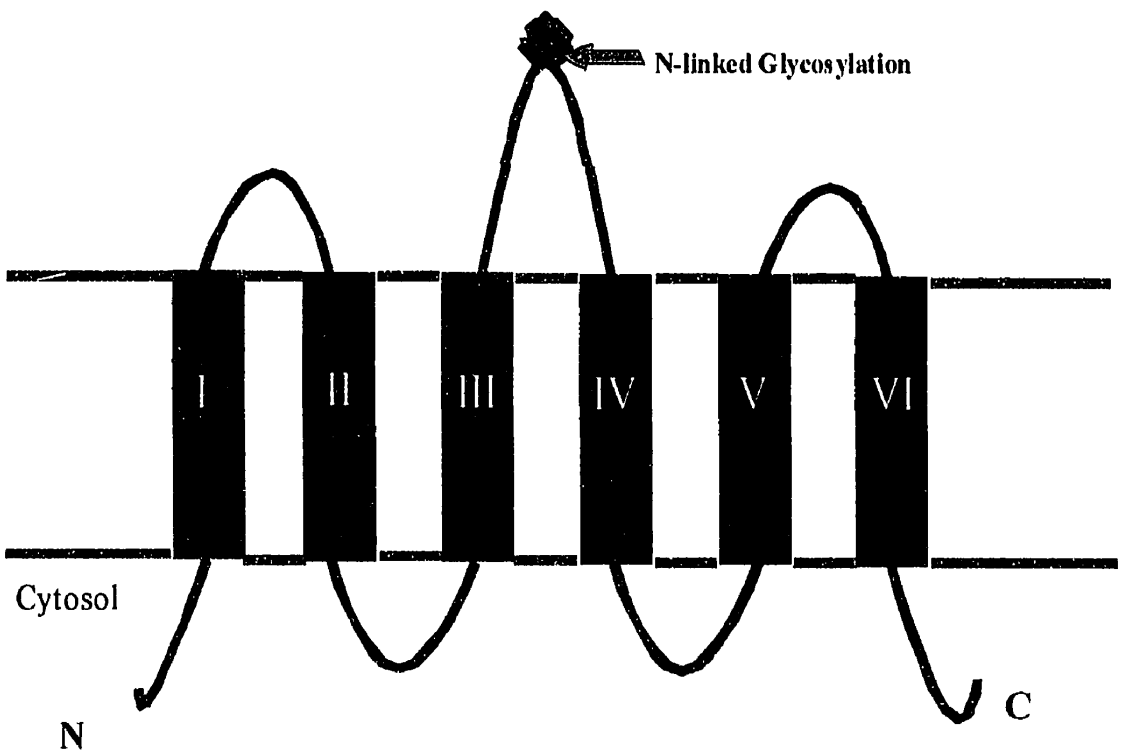
N-linked Glycosylation
I
II
III
IV
V
VI
Cytosol
N
C

LPP2, and LPP3) contain at least one single consensus site for N-linked glycosylation (39, 45, 46, 47).

The intracellular localization of Dri42, using polyclonal antibodies generated against Dri42-glutathione-S-transferase (GST) fusion proteins, was investigated by immunofluorescence studies in FRIC B (fetal rat intestinal cells), sections of the small intestine, and MDCK (Madin Darby canine kidney) cells overexpressing Dri 42-CAT fusion protein indicated localization to the endoplasmic reticulum (42). By immunofluorescence, endogenous LPP3 localized to the cell border and the perinuclear region in Swiss 3T3 (mouse fibroblasts) cells, at the cell periphery in LPP3 transiently transfected HEK 293 (human embryonic kidney) cells, and to the ER in COS7 (monkey kidney) cells (60). Therefore, the localization of LPP3 appears to be cell specific. Ishikawa *et al* (65) also define the localization of LPP3 as a green fluorescent protein (GFP) fusion protein in HEK 293 cells to the cell surface with some intracellular staining. Kanoh and colleagues (45) demonstrate plasma membrane localization of human LPP1 and LPP3 as GFP fusion proteins in HEK 293 cells. Jasinska *et al* (63) have localized mLPP1-GFP in rat 2 fibroblasts predominantly to the plasma membrane with some intracellular staining. Roberts and Morris (66) also show that a significant portion of LPP1 is localized to the surface of LPP1 stably transfected HEK 293 cells. Post-translational processing of PAP isoforms was investigated by pulse-chase studies, which further support the plasma membrane localization indicated by these subcellular localization studies (42, 45, 47, 60).

1.9 Active Site of LPP

Stukey and Carman (67) identified a novel, conserved phosphatase sequence motif, KXXXXXX**R**P- (X_{12-54})-XSG**H**- (X_{31-54})-S**R**XXXXX**H**XXXD, that is shared among several lipid phosphatases, including the mammalian glucose-6-phosphatases, chloroperoxidases, and bacterial nonspecific acid phosphatases. Essential features of their model includes: nucleophilic attack of the substrate's phosphoryl group by the histidine of domain 3 and production of a phosphoenzyme catalytic intermediate; involvement of conserved arginine residues of domains 1 and 3 in hydrogen binding to equatorial phosphoryl oxygens; and the histidine of domain 2 participating in the protonation of the substrate leaving group (67).

Zhang *et al* (64) provide evidence for structurally important domains of LPP1. They propose a theoretical structure for LPP1 in which the three conserved domains of the active site are located on the outer surface of the plasma membrane (Figure 1.4) (64). The investigators used site-directed mutagenesis to determine the three conserved domains of LPP1 which are required for catalytic activity (64). The mutations K120R, R127K, P128I, S169T, H171L, R217K, and H223L from the three domains decreased LPP activities by more than 95% compared to the wild-type mLPP1 construct (64). The G170A mutation showed 38% of the wild-type activity. Arg-127 donates hydrogen bonds to phosphate oxygen and may position the phosphate that binds to histidine (His-171) essential in acid-base group catalysis. His-223 is also essential for LPP1 enzyme activity. Lys-120, Ser-169, and Arg-217 may hydrogen-bond to the phosphate oxygen. Gly-170 may also be involved in forming hydrogen bonds with the oxygen atom (64). Pro-128 may create a kink in

Figure 1.4. Active site of LPP. The amino acids in the dark blue circles represent essential residues involved in the catalytic mechanism which resulted in a severe reduction in LPP activity when mutagenized. Amino acids in yellow circles represent residues, when mutated, which did not affect significantly the activity. Asn142 represents the glycosylation site which did not affect the enzymatic activity when mutated.

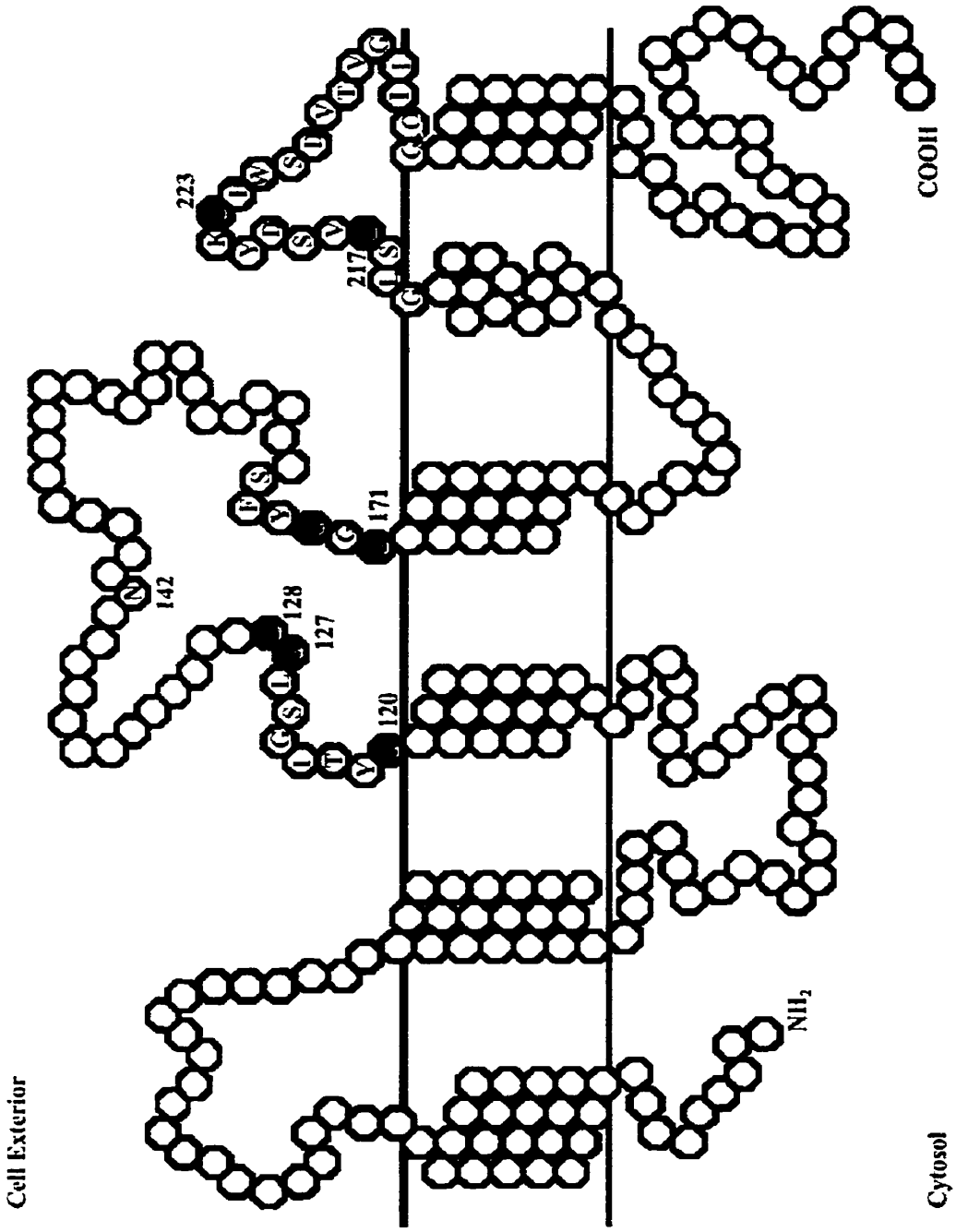
Cell Exterior
Cytosol
NH2
COOH
223
217
171
142
128
127
120

the LPP1 polypeptide chain and may be involved in the control of protein conformation rather than being an active-site residue (64). Brindley and coworkers also mutated the putative glycosylation site, Asn-142 (N142Q), and this decreased the molecular mass by about 4 kDa which is expected for the non-glycosylated protein while not affecting the enzymatic activity which is compatible with previous work in which the glycan of LPP was enzymatically removed (64).

1.10 Substrate Specificity of LPP

Waggoner *et al* (68) investigated the substrate specificity of purified phosphatidate phosphohydrolase from rat liver and found that it was capable of catalyzing the hydrolysis of ceramide-1-phosphate (C-1-P), LPA, and sphingosine-1-phosphate (S-1-P). They proposed that LPP could regulate signaling by these bioactive lipids and putative second messengers. The same preparation was also capable of dephosphorylating DAG pyrophosphate (DGPP) (69). Rat liver LPP is not a general phospholipase C as it did not hydrolyze glycerol-3-phosphate, phosphatidylcholine (PC), phosphatidylethanolamine (PE), phosphatidylserine (PS), phosphatidylinositol (PI), nor diphosphatidylglycerol (DPG) and these lipids also did not inhibit phosphatidic acid phosphohydrolase activity (68).

These various substrates were also tested for human LPP1 and LPP3 expressed in HEK 293 cells (45). LPP1 demonstrated high activity towards LPA while there was no increase in S-1-P (45). In contrast, LPP3 had increased activities to LPA, C-1-P, and S-1-P (45). The properties of LPP3 are more similar to those of the rat liver enzyme, which degrades all of these substrates at similar rates (45).

Hooks *et al* (46) developed kinetic profiles of the three human LPPs including LPP2 using P^{32}-labelled PA, LPA, and N-oleoyl ethanolamine PA (NOEPA), an LPA mimetic, in HEK 293 cells. For both LPP1 and LPP3, the maximum activity of the enzymes was approximately 30% higher with PA as the substrate than with LPA. In LPP2 transfected cells, the maximum activity was higher with LPA (46). The Km for PA was similar for all LPPs and LPA would appear to be a more selective substrate (46). All these LPP isoforms have a higher affinity for NOEPA than LPA (46).

Morris' group (47) infected Sf9 insect cells with baculovirus giving rise to 114, 460, and 540-fold increases in membrane–associated LPP1, LPP2, and LPP3 activities, respectively. These investigators also examined the cell surface activity of these LPP isoforms using intact Sf9 cells. Only overexpressed LPP1 Sf9 insect cells exhibited significantly elevated level of ecto-phosphohydrolase activity. Kinetic analysis of the LPP activity against substrates presented in nonionic detergent micelles showed that all three PAP enzymes were highly active against PA (47). The following is the order of substrate selectivity: LPP1, LPA > PA > S-1-P > C-1-P; LPP2, PA > C-1-P > LPA > S-1-P; LPP3, LPA ~ PA > C-1-P > S-1-P (44).

Jasinska *et al* (63) showed that overexpressed LPP1 degrades both glycerolipid and sphingolipid phosphate esters in rat 2 fibroblasts. LPP1 was also shown to increase the rate of dephosphorylation of exogenous LPA, PA and C-1-P (63). Ishikawa *et al* (65) investigated the degradation of LPA, dioctanoyl PA, and dioleoyl PA in intact HEK 293 cells overexpressing LPP3 as well as in *in vitro* assays. In intact cells, LPP3 markedly increased the dephosphorylation of

exogenously added LPA and dioctanoyl PA (65). However, the dephosphorylation of dioleoyl PA was extremely low in intact cells and increased to a negligible extent by transfection with LPP3 despite its high activity in *in vitro* assays (65).

Roberts and Morris (66) examined the substrate specificity of LPP1 in a HEK 293 stable cell line and through reconstitution experiments using purified enzymes. Overexpression of LPP1 in HEK 293 cells resulted in increases in PAP activity against exogenously provided substrates (66). They further showed that LPP1 is highly active against substrates in a lipid bilayer. In reconstitution experiments, the activity of LPP1 against LPA was approximately 12-fold greater than PA in a lipid bilayer (66). LPP1 activity was largely insensitive to dilution of the liposome preparation with assay buffer suggesting that LPP1 is preferentially active against substrates localized to the same membrane bilayer (66).

1.11 Regulation of LPP

The regulation of LPP is crucial in order to control cellular PA and DAG levels to regulate the cellular responses to extracellular stimuli. A comparison of the amino acid sequences of the LPP family suggests that there are a variety of protein kinase phosphorylation consensus sites (49, 61). There exist cytoplasmic protein kinase C (PKC) phosphorylation consensus sites (S/T-X-K/R; K/R-X-X-S/T; K/R-X-S/T) as well as cytoplasmic p42/p44 MAP kinase phosphorylation consensus sites (P-X-S/T-P; X-X-S/T-P).

Evidence that LPP can be phosphorylated arose very early from studies conducted by Brindley and colleagues (33) who performed band shift experiments

indicating that LPP is a phosphoprotein. Phosphorylation-dependent regulation of LPP has been implicated in previous work and could explain, in part, the difference in specific activity or stability of the two ionic forms of purified LPP (33). Furthermore, phosphorylation may also explain the lack of correlation between the specific activity of LPP and the intensity of the immunoreactive 51-53kDa proteins in the various tissues examined (33). However, Fleming and Yeamen (34) tested five different protein kinases for their ability to phosphorylate and regulate LPP (cAMP and AMP protein kinase, calmodulin (CaM) kinase, protein kinase C (PKC), and mitogen activated protein (MAP) kinase) *in vitro* but found no evidence that these could modulate LPP activity. Furthermore, incubation of their purified LPP with kinase and γP^{32}-ATP indicated that neither the 83kDa nor any other minor proteins were phosphorylated (34).

Interestingly, Brindley and colleagues (70) noted that the LPP activity was elevated in rat 2 cells harvested in the presence of vanadate and zinc which may indicate a role for tyrosine phosphorylation in regulating LPP activities. These agents inhibit protein tyrosine phosphatases which can be activated when cells are harvested. However, they could not demonstrate immunoprecipitation of LPP activities with anti-phosphotyrosine antibodies (70). Alternatively, LPP activities may not be a direct target for tyrosine phosphorylation but may be regulated by other proteins in the membranes which are themselves phosphorylated.

Ulrix *et al* (71) identified LPP1 as an androgen-regulated gene in the human prostatic adenocarcinoma cell line, LNCaP. These investigators have used a differential display technique to identify novel androgen-regulated genes that are

important for androgen action in the prostate (71). Androgens were found to induce a 4-fold increase in the levels of LPP1 mRNA in LNCaP cells, which was accompanied by an increase in magnesium-independent, NEM-insensitive PAP activity (71). The exact mechanism by which androgens affect LPP1 gene expression remains to be investigated and further studies will be required to determine whether androgen regulation of the LPP1 gene involves a direct interaction of the androgen receptor with a responsive element in the gene (71). Kanoh and colleagues (45) showed that epidermal growth factor (EGF) caused a sustained increase (3-fold) in LPP3 mRNA but not LPP1 in HeLa cells suggesting that the expression of LPP1 and LPP3 are regulated by distinct mechanisms.

1.12 Other Lipid Phosphate Phosphohydrolase Activities

It is highly probable that there exist yet other lipid phosphate phosphohydrolases that have not been cloned. Mandala *et al* (72) have recently cloned and characterized a lipid phosphohydrolase which degrades S-1-P from mouse brain (430 amino acids). The cDNA had little overall homology to the LPP phosphatases except at the conserved amino acids predicted to be in the active site. A hydropathy plot using the Kyte-Doolittle algorithm indicates 8-10 hydrophobic regions that are potential membrane spanning helices (72). They investigated S-1-P phosphohydrolase mRNA expression in adult mouse tissues by Northern blotting and found that it was highest in mouse liver and kidney with low levels in lung and undetectable in skeletal muscle (72). Interestingly, the expression of S-1-P phosphohydrolase in various mouse tissues does not correlate with the relative

phosphohydrolase activities measured in rat tissue extracts, as it was previously found that brain had about 3.5 times greater activity than liver or kidney (72).

Boudker and Futerman (73) characterized C-1-P phosphatase activity in rat liver plasma membranes. They found that the highest specific activity was observed in rat liver plasma membrane. The activity is not inhibited by NEM and is specific for C-1-P (73). A similar phosphatase activity that hydrolyzes C-1-P has also been detected in rat brain by Shinghal *et al* (74), where it is enriched in synaptic membranes. Subcellular fractionation studies suggest that C-1-P phosphatase is found in the synaptic terminal and is associated with both synaptic vesicles and plasma membranes. The activity was inhibited by magnesium and was insensitive to NEM (74).

Imai *et al* (75) showed that the gonadotropin releasing hormone (GnRH) agonist, buserelin, increased LPA phosphatase activity in plasma membranes of GnRH receptor-positive ovarian cells in the presence of the nonhydrolyzable GTP analog, GTP-γS. The enzyme activity was magnesium-independent and NEM-insensitive. Investigation of the substrate specificity demonstrated that S-1-P and C-1-P did not affect LPA hydrolysis (75).

Baker and Chang (76) presented evidence for the existence of a neuronal nuclear NEM-insensitive LPA phosphohydrolase. S-1-P inhibited the nuclear NEM-insensitive LPA phosphohydrolase activity while no inhibition was observed with PA (76). A nuclear PAP activity has been implicated in the production of diacylglycerol from phosphatidic acid produced by the action of a nuclear phospholipase D. Since the neuronal nuclear LPA phosphohydrolase activity was not inhibited by PA, it

appears to be distinct from the NEM-insensitive enzymes that hydrolyze this acidic phospholipid (76).

Frank and Waechter (77) purified and characterized a polyisoprenyl phosphate phosphatase from pig brain. The purified enzyme was a neutral phosphatase with maximal activity at pH 7 and had a molecular weight of 33 kDa (77). The activity was NEM-sensitive and magnesium-independent. A dolichol phosphatase could have important roles in the catabolism and biosynthesis of the glycosyl carrier lipid (77). The pig brain phosphatase catalyzes the enzymatic dephosphorylation of dolichol phosphate and PA with very similar catalytic efficiencies (77).

Hiroyama and Takenawa (78) characterized an LPA-specific phosphatase from bovine brain. This activity was present in the cytosolic fraction with a molecular weight of 44 kDa. The enzyme had no activity in the absence of detergent (78). The activity showed no activity towards C-1-P or S-1-P but showed a slight activity towards PA and p-nitro-phenyl-phosphate at pH 7.5. The activity was magnesium-independent and NEM-sensitive. These investigators have further reported the cloning of a cDNA for the LPA phosphatase (79).

Xie and Low (37) have shown that the ecto-lysoPAP activity in PAM 212 keratinocytes can be released by trypsin treatment. The solubilized enzyme appears to behave identically to the cell surface-associated enzyme based on substrate preference and inhibitor sensitivity studies. This enzyme prefers LPA and likely represents a distinct isoform to the cloned lipid phosphate phosphohydrolases.

1.13 Glycerolipid Signaling

1.13.1 DAG and PA as Second Messengers

There is considerable evidence supporting the involvement of phosphatidylinositol-specific phospholipase C (PI-PLC) in agonist stimulated breakdown of phosphatidylinositol bisphosphate (PIP_2) to inositol trisphosphate (IP_3) and DAG. These agonists also stimulate the breakdown of PC by PLD (80). It was postulated that PAP may be involved in cellular signal transduction following agonist stimulated breakdown of PC at the plasma membrane by phospholipase D (PLD) from experiments using PAP inhibitors such as propranolol and sphingosine (81). Thus, PAP may be involved in destroying PA, a second messenger, and creating another signal, DAG, required for PKC activation. This lipid signaling pathway generates biphasic DAG responses (80, 82). The early DAG phase normally lasts less than 1 minute and is generated primarily by PI-PLC breakdown of PIP_2. The more sustained DAG peak can be produced by LPP acting on PA generated by PLD. DAG activates protein kinase C (PKC) transiently and generation of prolonged DAG from PC could sustain PKC activation.

Evidence for agonist stimulated PC hydrolysis arises from: increased turnover of radiolabel in PC in cells prelabelled with [^{3}H]choline when stimulated with agonists; an increase in [^{3}H]choline/choline phosphate released into the media upon stimulation; and acyl chain analysis which indicated that both PC and PIP_2 can be the sources of agonist-stimulated DAG generation (80, 82). Pessin and Raben (83) as well as Wakelam and colleagues (84) analyzed derivatives of cellular DAGs that they separated by gas chromatography or high performance liquid

chromatography, respectively. Their studies demonstrated that PIP_2 hydrolysis is important for transient DAG generation (15 seconds) while PC hydrolysis contributes to the majority of the DAG in Swiss 3T3 cells after 5 minutes to 1 hour (83, 84).

There are three potential pathways of PC breakdown giving rise to DAG: PC-PLC, PLD/LPP, and sphingomyelin (SM) synthase. Convincing evidence is lacking for PC-PLC (85, 86) and only a few studies have investigated the possibility that DAG is generated as a consequence of stimulated SM synthesis (see section 1.14.1) (87, 88). However, there is extensive evidence for PLD in cells (80, 89). An experimentally invaluable characteristic of PLD is that it catalyzes a transphosphatidylation reaction in which a phosphatidyl-PLD intermediate utilizes water as a nucleophilic acceptor to generate PA (82, 90). Thus, short chain primary aliphatic alcohols (1-butanol) can substitute for water and generate phosphatidylalcohol (Pbut).

The initial phase of DAG generation is composed of polyunsaturated DAG species while the second phase contains predominantly more saturated species (82, 90). For example, bombesin stimulated a time-dependent increase in Swiss 3T3 cells in total DAG mass with changes in species profile (25 seconds- polyunsaturated and 5 to 30 minutes- saturated). In contrast, LPA stimulated a small increase in DAG in PAE (porcine aortic endothelial) cells only after 5 minutes (saturated and monounsaturated species) (91). In the presence of 0.3% butanol in 3T3 cells, Pbut formation accumulated and prevented the formation of DAG as a consequence of PLD activation; the DAG mass at 30 minutes was abolished but not

at shorter time periods. Therefore, the early rise can be attributed to the activation of PI-PLC and not PLD. Agonist stimulated PLD activity has been repeatedly proposed as providing the source of sustained DAG generation in cells leading to the sustained activation of PKC (80). However, it is becoming increasingly apparent that the PA product of PLD itself functions as an intracellular messenger (92). It was demonstrated that PA, generated by activation of PLD, can stimulate rho-mediated actin stress fiber formation in PAE cells (93). A variety of other signaling functions have been proposed for PLD-generated PA including the activation of a PA-regulated protein kinase (94), PKC-ζ (95), activation of Raf (96, 97), cAMP-specific phosphodiesterase (PDE_4D_3) (98), and tyrosine phosphorylation of MAP kinases (99).

There are only a few studies examining the importance of DAG acyl chain in the activation of PKC although all 1,2-DAGs appear to be able to activate PKCs *in vitro* (100, 101). Polyunsaturated DAGs such as 1-stearoyl-2-arachidonyl glycerol activate PKC more effectively than saturated DAG (102, 103). A combination of bombesin and TGF-β causes a sustained accumulation of poly-DAGs and sustained activation of various PKC isoforms (104) and in thrombin-stimulated platelets, activation of PKC correlates with transient production of PIP_2 derived poly-DAGs rather than with sustained DAG production (105). However, Ha and Exton (106) observed that PKCα was rapidly translocated by α-thrombin at 15 seconds but disappeared within 1 minute while PKCε was rapidly translocated and its membrane association was sustained for 60 minutes.

Wakelam and colleagues (107) have demonstrated that DAG kinase ζ selectively removes polyunsaturated DAG, inducing altered protein kinase C distribution in vivo. Furthermore, Shirai *et al* (108) observed activation of PKC and DAG kinase isoforms temporally and spatially to one another in response to various agonists. DAG kinase terminates the polyunsaturated DAG signal by forming polyunsaturated PA. This is the preferred substrate for an isoform of CDP-DAG synthase which is responsible for the formation of CDP-DAG. This liponucleotide is then utilized by PI synthase for PI synthesis followed by sequential phosphorylation to regenerate PIP_2 (107).

1.13.2 Phosholipase D (PLD)

The PLD family of enzymes consists of three distinct isoforms. PLD1 has been cloned from HeLa cells and requires PIP_2 for activity and is activated by ADP-ribosylation factor (ARF), the Rho family of GTPases, cdc42, and PKCα (109, 110). PLD2 has high basal activity and has been cloned from various human tissues (111). There exists an oleate-stimulated PLD activity which is insensitive to small GTPases which has yet to be cloned (112, 113). Provost and colleagues (114) used *in vitro* studies to examine the tissue distribution of ARF/RhoA activated PLD activity and found high levels of activity in lung, kidney, and spleen while muscle lacked this activity. The oleate-dependent enzyme was high in lung, epididymal fat, and heart but moderate in brain, skeletal muscle, spleen, kidney and low in intestinal mucosa, liver, and testis (115).

PLD is localized in a variety of subcellular compartments. Its plasma membrane localization is consistent with signaling and may be coupled to cell surface receptors (116). A nuclear PLD activity was identified in MDCK cells (117) and a nuclear residing RhoA has been implicated in the activation of this PLD resulting in the elevation of nuclear PA and DAG levels (118). The nuclear ARF/RhoA activated PLD is proposed to be involved in nuclear envelope signal transduction independent of the plasma membrane as well as in nuclear membrane dynamics during mitosis (119). PLD exists in the Golgi apparatus and Ktistakis *et al* (120) presented evidence in favor of a role for PLD in ARF-dependent Golgi transport by showing that the formation of COP1-coated vesicles was inhibited by ethanol and the requirement for ARF in coatomer binding can be bypassed by adding exogenous PLD. Siddhanta *et al* (121) further demonstrated that secretory vesicle budding from the trans-golgi network in rat anterior pituitary GH3 cells is mediated by phosphatidic acid generated by PLD. Another proposed function for PLD in mammalian cells is in mediating agonist-induced reorganization of the cytoskeleton (119). PLD1 was shown to associate with the octylglucoside-insoluble cytoskeletal fraction upon activation by GTPγS in permeabilized U937 cells (122).

Recently, a number of cytosolic, calcium-dependent, PI-specific PLD activities were identified in rat brain which are involved in the conversion of PI (3, 4, 5)P_3, produced by phosphatidylinositol-3-kinase (PI3K), to I(3, 4, 5)P_3 and PA (123). These inositol phosphates are key components in the activation of cell growth. Since PA is generated, these PI-PLDs may provide a putative link between PI3K and signaling pathways mediated by PA. Tsujioka and colleagues (124) have

identified a glycosylphosphatidylinositol (GPI)-PLD that is involved in releasing GPI-anchored proteins from membranes generating DAG for PKCα activation (124). GPI-anchors may also be involved in signal transduction since treatment of cells with hormones and cytokines induces their cleavage generating second messengers such as inositol phosphoglycans and PA.

Sciorra *et al* (60) present evidence for a functional role for LPP3 in the metabolism of PA derived from PLD activation. They report that the PLD/LPP pathway is operational in detergent resistant membrane microdomains, a type of specialized membrane compartment implicated in vesicular trafficking and signal transduction (60). PLD activity and LPP3 localize to and act sequentially to generate DAG in these specialized domains. They propose that the functional association between PLD and LPP3 is accomplished by colocalization of these enzymes to the same membrane compartments (60).

1.13.3 Diacylglycerol Kinase (DAG Kinase)

Nine mammalian isotypes of DAG kinases have been identified which differ in primary structure, substrate specificity, and tissue distribution (125, 126). DAG kinase phosphorylates DAG and is a potential terminator of DAG signaling and thus, downregulates membrane localization of PKC as shown by Shirai *et al* (108). DGKs contain a conserved catalytic domain and a number of other conserved motifs that are crucial in lipid-protein and protein-protein interactions (125, 126). Some isoforms are regulated by small GTPases of the Rho family. It was shown recently by Houssa

et al (127) that DAG kinase θ binds to and is negatively regulated by active Rho A. Rho family of GTPases (Rho A, Rac, and Cdc42) regulate cytoskeletal reorganization and gene transcription through protein kinases and lipid signaling enzymes (PLD, PI5K, and PI3K). These investigators report that when DAG kinase θ binds to active Rho A, it loses its catalytic activity. This observation suggests a role for DAG kinases in actin cytoskeletal rearrangement. Other DAG kinase isoforms are found in the nucleus in association with other regulatory enzymes of the PI cycle and may have an effect on cell cycle progression (128). Most DAG kinase isoforms show high expression in distinct regions of the brain (125, 126).

1.13.4 Protein Kinase C (PKC)

At least twelve different isozymes have been identified (129) and are classified into three groups (conventional, novel, and atypical) based on their structure and cofactor regulation. The conventional isoforms include α, βI, βII, and γ which are regulated by calcium. The novel PKC isoforms include δ, ε, θ, η, μ, and ν which do not appear to require calcium binding. The atypical PKCs include ζ and λ which do not respond to phorbol esters. Binding of DAG or other lipid activators produces conformational changes resulting in the movement of the pseudosubstrate domain from the active site causing the kinase to become active (130). PKC also binds acidic lipids such as PS which is responsible for calcium-dependence for the conventional type PKCs (130). These kinase isoforms phosphorylate serine and threonine residues on their substrates including myristoylated, alanine-rich C kinase

substrate (MARCKS) (131). PKCs play important roles in proliferation, differentiation, vesicle trafficking, and gene expression.

1.13.5 LPP and Edg Receptors

PAP2 localized on the plasma membranes has generally been thought to dephosphorylate PA generated by PLD. To participate in the metabolism of cellular PA, PAP2 at the plasma membrane should have its catalytic site oriented towards the inner leaflet of the bilayer or exposed on the cytoplasmic leaflet. However, the catalytic site of the cloned PAP2 isoforms have been predicted to be located at the putative extracellular loops and may be able to degrade extracellular substrates or those in the outer leaflet. This prediction suggests that the enzyme attenuates receptor-directed extracellular signals such as LPA and S-1-P.

LPA and S-1-P are phospholipid growth factors which are found in activated platelets, injured cells, and at μM concentrations in serum (132, 133). The biological responses to these phospholipid growth factors include stimulation of cellular proliferation, inhibition of apoptosis, aggregation of platelets, contraction of smooth muscle cells, neurite retraction, regulation of cell-cell aggregation and adhesion, and chemotaxis (132, 133). These responses are transduced by the endothelial differentiation gene (Edg) receptors coupled to various G proteins including G_q (PLC), G_i (cAMP), and $G_{12/13}$ (GTPase Rho). There are two classes of Edg receptors: LPA subtypes, Edg 2, 4, and 7; and S-1-P subtypes, Edg 1, 3, 5, 6, and 8 (134).

Brindley and colleagues reported that overexpression of LPP1 increased the hydrolysis of LPA in rat 2 fibroblasts (135). They further showed that LPP1 overexpression could decrease the activation of ERK1/ERK2 and DNA synthesis induced by LPA. They proposed that LPP1 may control the net interaction of LPA with these cells in order to regulate the activation of the Edg2 receptor (136). Antisense oligonucleotides designed against LPP1 decreased the dephosphorylation of exogenous LPA, increased the net association of LPA, increased the activation of ERK1/ERK2, and DNA synthesis. Possible mechanisms of action for LPA include LPA binding to Edg2 after association with the outer leaflet of plasma membrane and LPA dissociation from Edg2 into the membrane followed by its dephosphorylation by LPP1 or LPP1 regulation of the net amount of LPA available for activating Edg2 receptors.

1.14 Sphingolipid Signaling

1.14.1 *De novo* Biosynthesis of Sphingomyelin

Sphingolipid metabolism involves a number of biosynthetic and catabolic reactions in which ceramide has a crucial role (Figure 1.5) (137, 138). The *de novo* biosynthesis of sphingomyelin is initiated with the condensation of palmitoyl-CoA with serine which is catalyzed by the rate-limiting enzyme, serine palmitoyltransferase. Reducing and acylating steps are catalyzed by NADPH-dependent reductase followed by the actions of ceramide synthase and a dehydrogenase to generate ceramide. Ceramide can then be converted into sphingomyelin through the transfer of the choline phosphate group from

Figure 1.5. Sphingolipid metabolism. The synthesis of sphingomyelin is initiated with the condensation of palmitoyl-CoA with serine catalyzed by the rate limiting enzyme, serine palmitoyltransferase (Ser palmitoyltransferase, **1**). Ceramide, produced by the sequential action of NADPH-dependent reductase (**2**) and ceramide synthase (cer synthase, **3**), can be converted to sphingomyelin by sphingomyelin synthase (SM synthase, **4**). Ceramide can be phosphorylated by ceramide kinase (cer kinase, **8**) to generate C-1-P which can, itself, be dephosphorylated by C-1-P phosphohydrolase (CPP, **9**) to regenerate ceramide. Ceramidase (**5**) can also utilize ceramide to generate sphingosine which is phosphorylated by sphingosine kinase (SPH kinase, **6**) producing S-1-P. Dephosphorylation of S-1-P is catalyzed by S-1-P phosphohydrolase (SPP, **7**). Hydrolysis of sphingomyelin by sphingomyelinase (SMASE, **10**) will generate ceramide. Abbreviations: C-1-P, ceramide-1-phosphate, and S-1-P, sphingosine-1-phosphate.

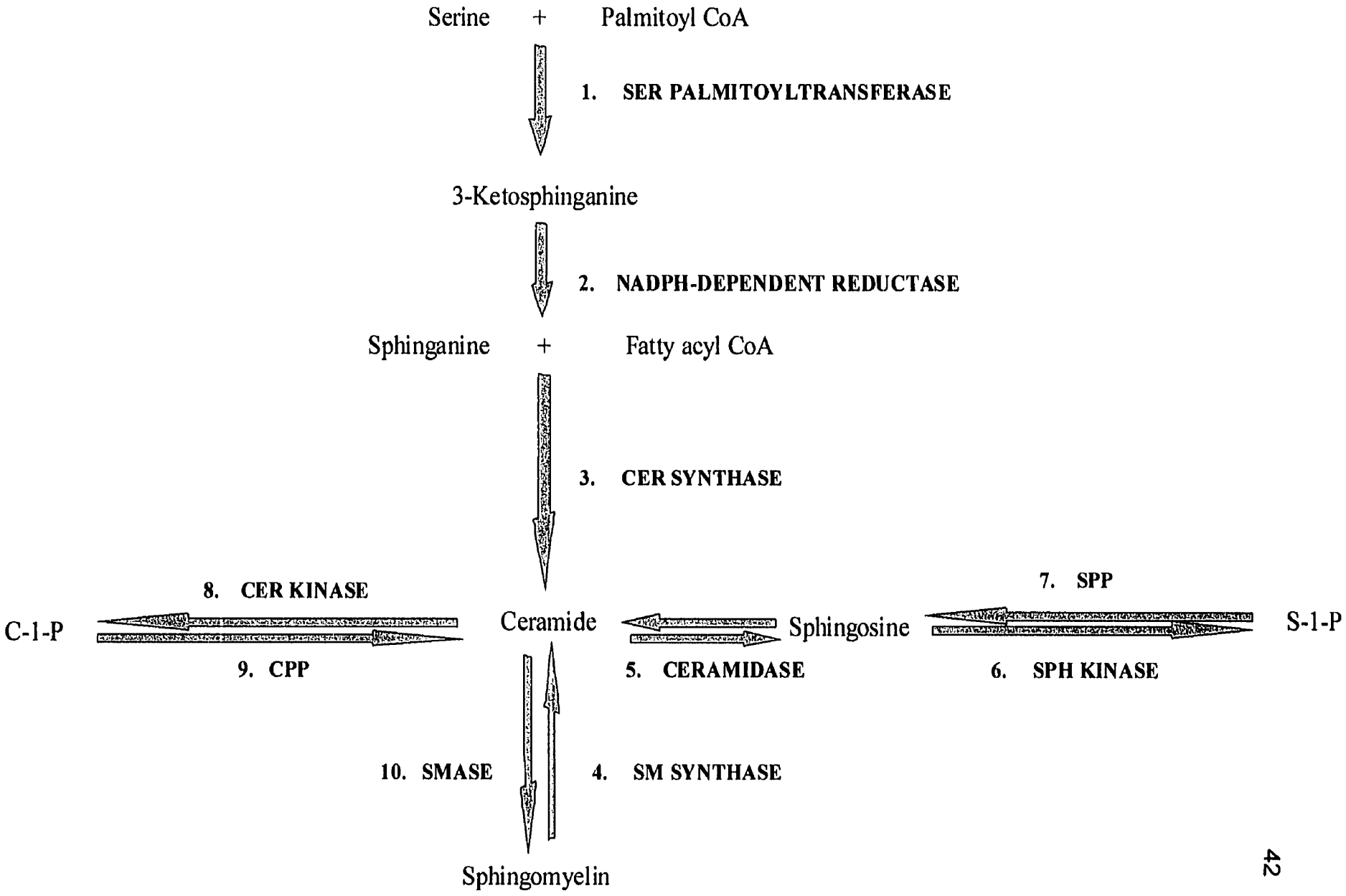
Serine + Palmitoyl CoA
1. SER PALMITOYLTRANSFERASE
3-Ketosphinganine
2. NADPH-DEPENDENT REDUCTASE
Sphinganine + Fatty acyl CoA
3. CER SYNTHASE
8. CER KINASE
C-1-P
9. CPP
Ceramide
Sphingosine
5. CERAMIDASE
7. SPP
S-1-P
6. SPH KINASE
10. SMASE
4. SM SYNTHASE
Sphingomyelin

phosphatidylcholine through the action of PC:ceramide phosphocholine transferase (SM synthase). Theoretically, this enzyme can regulate the levels of ceramide as well as DAG. Ceramide can also be utilized for generating cerebrosides and gangliosides through the sequential addition of carbohydrate units and sialic acid residues. Phosphorylation of ceramide at its 1-position by ceramide kinase will yield C-1-P.

1.14.2 Sphingolipids and their Role as Second Messengers

In contrast to the function of DAG in glycerolipid signaling, ceramide is a key regulator of antiproliferative and pro-apoptotic signaling pathways (137, 138). Ceramide exerts its effects through the activation of a ceramide-activated protein phosphatase (CAPP) leading to inhibition of cell growth and apoptosis (139, 140, 141). Ceramide accumulates in response to several different inducers such as TNFα, Ilβ1, IFN-γ, Fas, irradiation, and stresses such as serum deprivation and heat shock (142). The general response to these stresses is a growth-suppressed condition, cell cycle arrest or apoptosis. Serum deprivation induces an elevation of intracellular ceramide with a progressive arrest of the cell cycle in the G_0-G_1 phase (143). In contrast to ceramide, sphingosine was observed to stimulate the proliferation of Swiss 3T3 cells leading to PA accumulation generated by PLD (144) or a PKC-independent pathway (145).

Sphingomyelin can be hydrolyzed to ceramide (146) by sphingomyelinases which have been recently cloned by several groups (147, 148, 149). Ceramidases

can hydrolyze the generated ceramide into sphingosine and thus, modulate the levels of these two lipids. Various ceramidases (acid, neutral, and alkaline) have been cloned (150, 151) and overexpression of acid ceramidase was found to be capable of protecting cells from TNF-induced apoptosis (151). The generated sphingosine can then be phosphorylated by sphingosine kinase to produce the bioactive lipid, S-1-P. This enzyme has been cloned and characterized by Spiegel's group (152, 153). As previously described, S-1-P has diverse biological functions both intracellularly as well as extracellularly through Edg receptors (154). Intracellularly generated S-1-P may be converted back to sphingosine by the recently cloned S-1-P phosphohydrolase (72) which when overexpressed was found to increase ceramide levels leading to decreased cell survival. LPP isoforms, which have broad substrate specificity capable of hydrolyzing extracellularly presented substrates, may be involved in the regulation of S-1-P-mediated effects through Edg receptors. Ceramide, itself, can be phosphorylated by ceramide kinase generating C-1-P, which appears to have roles in neutrophil phagocytosis and vesicle fusion (155). C-1-P can be dephosphorylated by LPPs to generate ceramide. It is unknown whether LPP-generated ceramide contributes to the apoptotic response.

Recent studies showed that SV-40 transformation induced a significant increase in SM synthase activity in human lung fibroblasts (88). As a consequence of the elevated SM synthase activity in the transformed cells, there was a decrease in the intracellular ceramide and an increase in DAG (88). Cross-talk between sphingolipid signaling (ceramide) and glycerolipid signaling (DAG) adds further

complexity and the regulation of intracellular ceramide and DAG can be crucial in the control of cell viability and cell death.

1.15 Lung and the Alveolar Epithelium

1.15.1 Lung Development

Lung development is a highly complex process that involves morphogenesis, growth, and differentiation which is required for transition from an aqueous to an air-breathing environment (156). It is initiated in the embryo as a ventral outpouching of endodermal cells from the anterior foregut into the surrounding mesenchyme. There exist three phases of lung development: pseudoglandular, canalicular, and saccular. In rat, during the pseudoglandular phase (17 to 20 dg), branching occurs with the formation of bronchioles and alveolar ducts. The ductal epithelial cells remain undifferentiated. This is followed by the canalicular phase (21 dg) in which rapid growth diminishes with differentiation of epithelial cells lining the ducts, and the initiation of capillary growth. In the terminal sac phase (22 dg to after birth), capillaries continue to grow and epithelial cells undergo differentiation. Interactions between epithelial cells and the mesoderm are essential for the effects of growth and differentiation factors as well as hormones in various developmental processes including cellular differentiation, vasculogenesis, and the synthesis of surfactant lipids and proteins (156).

The structure of the alveolar epithelium consists of cuboidal type II cells in the alveolar corners and the squamous type I epithelium which covers the capillaries. The type I cells are long, squamous cells which comprise 96% of the

epithelial surface area which serves to minimize the distance between the alveolar air space and the capillaries in order to maximize gas exchange. Type II cells are cuboidal and cover only 4% of the surface area (157). There are a number of functions attributed to the type II cell including the synthesis and secretion of surfactant, involvement in pulmonary defense, and recovery from lung injury (157). Although type I cells are susceptible to lung injury, the type II cells appear to be more resistant being capable of proliferating and transdifferentiating into type I cells in order to restore the alveolar epithelium.

1.15.2 Type II Cell Surfactant Phospholipid Secretion

Surfactant phospholipid secretion by isolated type II cells can be stimulated by a variety of agonists acting by at least three signal transduction mechanisms: β_2 or A_2 receptor leading to the activation of adenylyl cyclase, P_{2u} receptor leading to the activation of calcium-calmodulin, and the activation of PKC (Figure 1.6) (158). The P_{2u} receptor, which is activated by the surfactant secretagogues, ATP and UTP, has been cloned by Rice *et al* (159). The receptor is a seven transmembrane G-protein coupled receptor containing two consensus sites for N-linked glycosylation at its N-terminus and phosphorylation sites in its cytoplasmic tail.

ATP has been reported to stimulate surfactant phospholipid secretion in isolated perfused lungs, lung slices, and primary cultures of type II cells from fetus, newborn, and adult rats (160). Cross-talk between different signaling pathways occurs in many systems and can have positive and negative effects on the final cellular response. 5'-(N-ethylcarboxyamido)adenosine (NECA) and ionomycin

Figure 1.6. Surfactant secretion: the P_{2u} purinergic signaling cascade. Transient elevations in DAG levels arising through phospholipase C (PLC) degradation of phosphatidylinositol bisphosphate (PIP_2) in alveolar type II cells can be extended through the stimulation of the phospholipase D (PLD)/LPP pathway. LPP is proposed to function in the regulation of surfactant phospholipid secretion. The signaling pathway would involve a plasma membrane localized LPP which would act sequentially to PLD in the purinergic P_{2u} receptor cascade where it would generate DAG from phosphatidylcholine (PC)-derived PA, thereby sustaining protein kinase C (PKC) activation and surfactant secretion

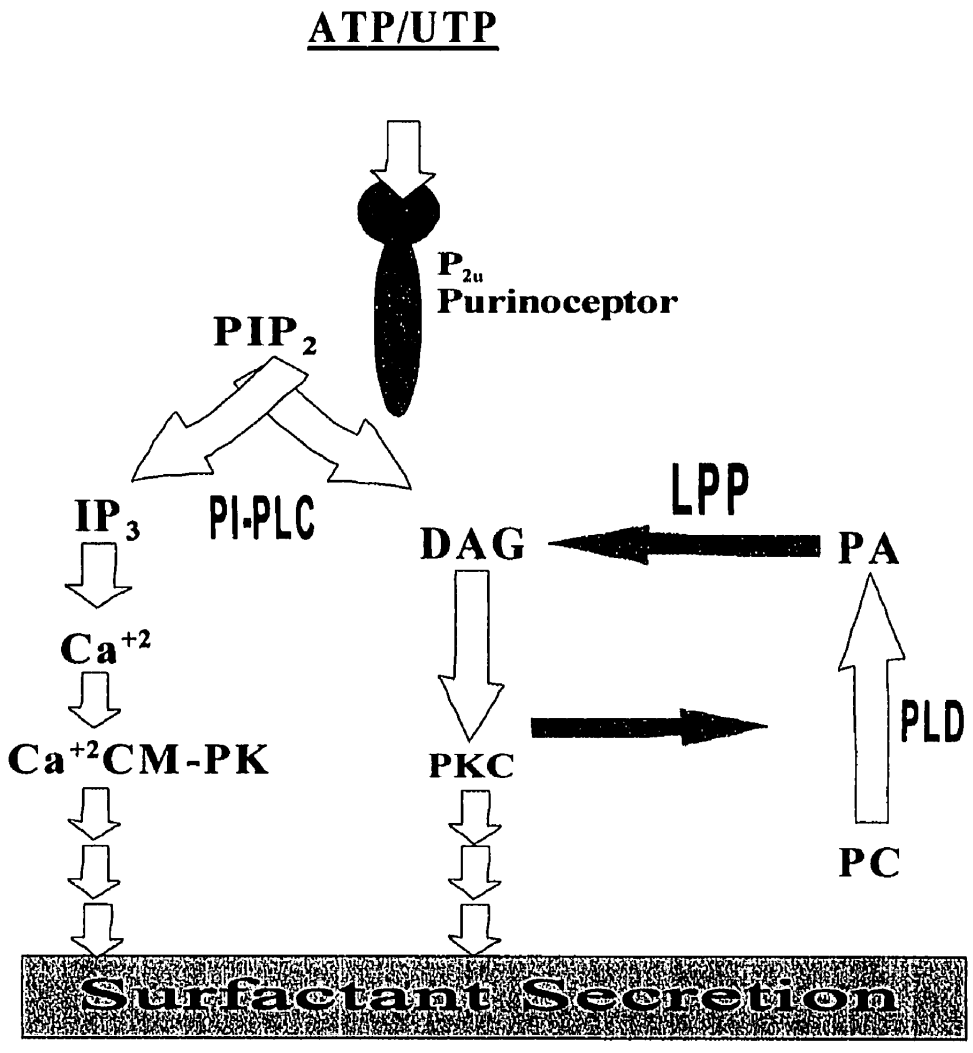
ATP/UTP
P2u
Purinoceptor
PIP2
IP3
PI-PLC
DAG
LPP
PA
Ca+2
Ca+2CM-PK
PKC
PLD
PC
Surfactant Secretion

increased PC secretion from a basal rate of 1.4% in 2 hours to 4% while ATP and TPA increased it to 5-7% (161). The combination of NECA, ATP, TPA, and ionomycin resulted in an increase to 13% (161). A large part of the effect of ATP on PC secretion may be mediated by activation of an adenosine A_2 receptor coupled to adenylate cyclase which was determined through the use of antagonists specific for each pathway (161).

Rooney and colleagues have investigated ATP-stimulation of surfactant secretion and inositol phospholipid metabolism in primary rat type II cells (162). The effect of ATP was examined in cells prelabeled with [^{3}H]-arachidonic acid or [^{3}H]-acetate. DAG formation was biphasic with an initial rapid transient increase (10 seconds) followed by a more prolonged peak between 5 and 10 minutes which returned to normal levels by 15 minutes (162). PA levels were also measured and were found to increase within 1 minute and remain constant for 30 minutes (162). These changes in DAG and PA were small but were consistently observed. Inositol phosphates (IP_3) were also measured and found to increase rapidly with a corresponding decrease in PIP_2 levels. Similar results were obtained with UTP, the P_{2u} receptor agonist (163). PC secretion could be detected as early as 15 minutes and was maintained up to 4 hours after ATP exposure. The second DAG peak could have been generated by at least two mechanisms: PC-PLC or PLD/LPP pathway. It was shown that the latter pathway was involved in the generation of the second DAG phase. These two pathways were distinguished through the use of an alcohol whereby PLD can catalyze a transphosphatidylation reaction leading to the formation of the corresponding phosphatidylalcohol (164). Gobran *et al* (165) have

further examined the PKC isoforms and other signaling proteins involved in surfactant secretion in developing rat type II cells. These investigators had previously reported that there is a developmental increase in the response of type II cells to surfactant secretagogues (166). They observed that there was a diminished response to ATP in newborn type II cells compared to adult and the response to UTP was not detected until 4 days after birth. Therefore, they concluded that there was a developmental delay in the expression of one or more components of the P_{2u} signaling mechanisms (166). These investigators have also found the following signaling proteins in type II newborn and adult type II cells: PKCα, PKCβI, PKCβII, PKCδ, PKCη, PKCζ, PKCθ, PKCμ, PLC-β3, and $G_q\alpha$ (167). They found differences between newborn (1-2 day (D) old) and adult in the following PKC isoforms and signaling proteins: PKCα, PKCβI, PKCβII, PKCζ, and PKCθ which were 43-54% the levels of adult in the neonate. The purinergic receptor, P_{2u}, was examined by RT-PCR and its mRNA expression was found to be the same in the newborn and adult type II cells. However, due to lack of antibodies against this receptor, changes in these protein levels could not be determined. Subsequently, Gobran and Rooney (167) examined the PKC isoforms that are activated in response to ATP and UTP. Western analysis indicated that the PKCμ isoform translocated to the membrane fraction in response to treatment with these secretagogues after 5 minutes.

1.15.3 Type II Cell Proliferation and Transdifferentiation

Cuboidal epithelial cells are the progenitor of other epithelial cells during lung development and for repair at the alveolar surface (168). Interactions between epithelial cells and fibroblasts appear to be crucial for epithelial cell function. During lung development, fibroblast factors secreted in response to steroids, induce surfactant synthesis in maturing type II cells (169). In lung fetal development, when epithelial growth slows and surfactant accumulation begins, there is increased disruption of the basal membrane leading to increased cell-cell contact between cuboidal cells and fibroblasts (168). Normally the proliferation rate of various pulmonary cells in lung is low. However, during lung injury such as exposure to 90% O_2 for 6 days and return to air, there is a burst of cell proliferation after 1 day and a return to normal mitotic indices after 3 days (168). The stimulating factor for type II cell division could include the loss of contact inhibition or it may involve a signal arising from different basal membrane composition (168). Epithelial and interstitial cell contacts have been described in developing fetal lung where their frequency increases sharply at a time when epithelial division slows down and surfactant synthesis begins (168).

Several growth factors have been shown to be capable of stimulating type II cell DNA synthesis and growth, including FGF, HGF, TGF-α, KGF, and EGF (170). Events operating late in G1 are essential in the control of transition of lung alveolar epithelial cells into and out of the proliferative state. Investigators have observed that transformed alveolar epithelial cells overexpress cyclin A compared to normal fetal and adult rat alveolar epithelial cells in primary culture (171). Thus, cyclin A may play a role in regulating the rapidly proliferative phenotype of

transformed alveolar epithelial cells (AEC). A suppression of cyclin D2 and cdc2 gene expression was observed during the development of normal rat AECs and induction or overexpression of the cdc2 gene in hyperoxic rat alveolar epithelial cells (172). There may exist an important functional role for cyclin D2 and cdc2 genes in determining the proliferative or nonproliferative phenotypes of normal AECs during lung development, injury, repair, and transformation. Wu *et al* (173) have concluded that cyclin D2 expression in 19 day gestation AECs (19dg canalicular phase) may play an important role in the regulation of type II cell proliferation.

1.15.4 Type II Cell Apoptosis

Apoptosis plays a central role in the cellular remodeling of the developing lung (174). Type II cell apoptosis was observed to increase with the transition from the canalicular (21 dg) to the terminal sac (22 dg) stage of development in the rabbit (175). It was also found that at this stage of development, there were increases in epithelial apoptosis as well as Fas ligand protein in type II cells (175). It was suggested that the Fas/Fas ligand system may be an important pathway in the control of postcanalicular alveolar differentiation (175).

Mallampalli and colleagues (176) showed that TNFα increases ceramide without inducing apoptosis in alveolar type II epithelial cells. Intratracheal administration of TNFα did not induce apoptosis in alveolar type II cells but TNFα was able to decrease sphingomyelin and increase ceramide levels in the lung with no alteration in the activity of serine palmitoyltransferase or sphingomyelin synthase

(176). TNFα could have induced cell death in other cells and it is possible that type II cells require other events for apoptosis.

Inflammatory diseases of the respiratory tract including Adult Respiratory Distress Syndrome (ARDS) are characterized by a large increase in inflammatory oxidants such as H_2O_2, which contribute to lung injury (175). The lung epithelium plays an important role in modulating the inflammatory response to lung injury where airway epithelial cells are targeted by H_2O_2 and other oxygen radicals (175). H_2O_2 was observed to activate a membrane sphingomyelinase leading to the generation of ceramide in HAE cells. Changes in cell morphology, apoptotic nuclear condensation, and segmentation were also observed (177). The regulation of sphingomyelinases and the mechanism by which H_2O_2 stimulates sphingomyelin hydrolysis is currently unknown. H_2O_2 stimulates the release of the mitochondrial protein cytochrome c and activates caspase 9, which leads to the activation of caspase 3, activation of c-fos and c-jun, and eventually apoptosis. Upstream membrane lipid signaling events may include H_2O_2 activation of PLD (178). H_2O_2 induced cell death was enhanced by pretreatment with 1-butanol suggesting that PLD activity might suppress the H_2O_2 induced cell death (178). H_2O_2 stimulated endogenous PLD activity and the overexpression of PLD2 led to a further increase in H_2O_2 induced PLD activity (178). Since LPP is proposed to act sequentially to PLD, it may be involved in the generation of DAG, from PLD-derived PA, for PKC activation in order to counter the effects of ceramide.

1.16 Summary

The overall goal of this thesis was to further expand our knowledge and understanding of LPP in lung and alveolar type II cells. We propose that LPP would have a role in the regulation of surfactant phospholipid secretion and in the control of cell growth. Chapter 2 of this thesis is entitled "Characterization of the Pulmonary N-Ethylmaleimide Insensitive Lipid Phosphate Phosphohydrolase". Previous studies performed in lung have demonstrated the existence of two different forms of PAPases, namely PAP1 and LPP (PAP2). The former pulmonary Mg^{+2}-dependent enzyme is N-ethylmaleimide (NEM)-sensitive, heat labile, and is involved in phospholipid biosynthesis. However, the function of the latter lung isozyme is unknown. LPP was selectively assayed using NEM in the absence of Mg^{+2}. Studies employing this assay and adult rat lung microsomal preparations demonstrated that LPP was inhibited by amphiphilic amines, sphingoid bases, products of the LPP reaction (monoacylglycerol (MAG) and diacylglycerol (DAG)), and substrate analogs such as LPA, C-1-P, and to a very small extent, S-1-P. Purified lung plasma membranes, prepared using discontinuous sucrose and Percoll gradients, showed that LPP activity was enriched 6.9±1.6-fold over the whole homogenate and was between the enrichment for plasma membrane markers, 5'-nucleotidase (14.7±0.3) and $Na^{+}K^{+}$-ATPase (4.0±0.2). Both PA and LPA were good substrates for LPP in this purified plasma membrane fraction. In contrast, S-1-P was a very poor substrate. LPP activity was slightly enriched in isolated type II cells and low in isolated rat lung fibroblasts. These studies show that lung contains LPP activity in plasma membranes and type II cells where it could play a role in signal

transduction, specifically in surfactant phospholipid secretion in the P_{2u} purinergic signaling cascade acting sequentially to PLD.

Chapter 3 entitled "Molecular Cloning and Expression of Pulmonary Lipid Phosphate Phosphohydrolases" identifies the LPP isoforms present in lung and type II cells. In Chapter 2, we observed that S-1-P was a relatively poor substrate in lung plasma membranes in contrast to purified rat liver LPP which suggested the potential presence of a novel LPP in lung. Thus, LPPs were cloned by reverse transcriptase-polymerase chain reaction (RT-PCR) from both adult rat lung and type II cell RNA. The RT-PCR generated LPP1 (849bp), up to three LPP1 variants, and LPP3 (936bp) cDNAs. The three LPP1 variants include LPP1a (852bp) and two novel isoforms, LPP1b (697bp) and LPP1c (1004bp). The pulmonary LPP1 and LPP3 isoforms are identical to the previously cloned rat liver and intestinal LPPs, respectively, and the LPP1a isoform has 80% sequence identity to the human homolog. The LPP2 isoform was not detected in lung by RT-PCR. Expression of LPP1, LPP1a, and LPP3 cDNAs in HEK 293 cells established that they encode functional lipid phosphate phosphohydrolases. In contrast, the novel isoforms, LPP1b and LPP1c, contain frameshifts which would result in premature termination producing putative catalytically inactive polypeptides of 30 and 76 amino acids, respectively. Further investigation of the LPP1b isoform revealed that it was present across a variety of tissues and exists in equal abundance to the LPP1/1a isoform in lung tissue. As expected, transient mammalian expression of LPP1b failed to alter PAP2 activity. Our initial investigations were directed to address the role of these cloned isoforms in surfactant phospholipid secretion in type II cells. However,

overexpression in type II cell lines (mouse lung epithelial cells (MLE)) was without success. These studies will await improved type II cell model systems and the analysis of type II cells from knock-out mice.

Chapter 4 is entitled "Developmental Patterns of Lipid Phosphate Phosphohydrolases in Rat Lung and Alveolar Type II Cells". These studies were initiated as a preliminary towards investigating the possible functions of the cloned LPP isoforms. The developmental patterns for LPP, PLD, Edg receptors, and various PKC isoforms suggest potential roles in epithelial growth, vasculogenesis, differentiation, and surfactant phospholipid secretion. Since type II cells comprises less than 10% of the lung cellular population, changes in LPP observed in the whole lung profile cannot be extrapolated to this cell type and thus, further investigations will await better type II model systems.

Chapter 5 entitled "Pulmonary Lipid Phosphate Phosphohydrolases in Plasma Membrane Signaling Platforms" was performed to investigate the localization of LPP in lipid-rich signaling platforms as it was recently reported that PLD isoforms and Edg receptors were localized to these lipid-rich signaling domains. Herein, LPP activity is reported to be enriched in lipid-rich signaling platforms isolated from rat lung tissue, isolated rat type II cells, and type II cell - mouse lung epithelial cell lines (MLE12 and MLE15). Lung and cell line caveolin-enriched domains (CEDs), prepared based on their detergent insolubility in Triton X-100, contain caveolin-1 and protein kinase C (PKC) isoforms. The LPP3 isoform was predominantly localized to rat lung CEDs. These lipid-rich domains, including those from isolated rat type II cells, were enriched both in

phosphatidylcholine/sphingomyelin (PC: SM) and cholesterol. The effect of saponin was also investigated, as it is known to sequester cholesterol thereby destabilizing the lipid-rich microdomain structure and rendering them sensitive to solubilization by nonionic detergents. Saponin-treatment of MLE15 cells shifted the LPP activity, cholesterol, PC: SM, and caveolin-1 from lipid microdomains to detergent soluble fractions. Elevated LPP activity and LPP1/1a protein are present in caveolae from MLE15 cells prepared using the cationic colloidal silica method. In contrast, total plasma membranes had a higher relative abundance of LPP1/1a protein with low LPP activity. Phorbol ester treatment caused a 3.8-fold increase in LPP specific activity in MLE12 CEDs. Thus, the activated form of LPP1/1a may be recruited into caveolae-rafts. Transdifferentiation of type II cells into a type I-like cell demonstrated enrichment in caveolin-1 levels and LPP activity. These results indicate that LPP is localized in caveolae and/or rafts in lung tissue, isolated type II cells, and type II cell lines consistent with a role for LPP in both caveolae/raft signaling and caveolar dynamics.

1.17 References

1. **Kates M.** 1955. Hydrolysis of lecithin by plant plastid enzymes. Can. J. Biochem. **35**: 575-589.

2. **Possmayer F.** 1988. Pulmonary phosphatidate phosphohydrolase and its relation to the surfactant system of the lung. In Phosphatidate Phosphohydrolase. Volume II. Brindley, D.N. (ed.) Boca Raton, CRC Press, pp.39-118.

3. **Casola PG and Possmayer F.** 1979. Pulmonary phosphatidic acid phosphatase. Properties of membrane-bound phosphatidate-dependent

phosphatidic acid phosphatase in rat lung. Biochim Biophys Acta. **574**:212-225.

4. **Casola PG and Possmayer F.** 1981. Pulmonary phosphatidic acid phosphohydrolase: further studies on the activities in rat lung responsible for the hydrolysis of membrane-bound and aqueously dispersed phosphatidate. Can J Biochem. **59**:500-510.

5. **Casola PG and Possmayer F.** 1981. Separation and characterization of the membrane-bound and aqueously dispersed phosphatidate phosphatidic acid phosphohydrolase activities in rat lung. Biophys Acta. **664**:298-315.

6. **Casola PG and Possmayer F.** 1981. Pulmonary phosphatidic acid phosphohydrolase. Developmental patterns in rat lung. Biochim Biophys Acta. **665**:177-185.

7. **Walton PA and Possmayer F.** 1985. Mg^{+2}-dependent phosphatidate phosphohydrolase of rat lung: development of an assay employing a defined chemical substrate which reflects the phosphohydrolase activity measured using membrane-bound substrate. Anal Biochem. **151**:479-486.

8. **Sturton RG and Brindley DN.** 1978. Problems encountered in measuring the activity of phosphatidate phosphohydrolase. Biochem J. **171**:263-266.

9. **Walton PA.** 1984. Characterization of pulmonary magnesium-dependent phosphatidate phosphohydrolase activity. Ph.D Thesis, University of Western Ontario, London, Ontario, Canada.

10. **Pelech SL and Vance DE.** 1984. Regulation of phosphatidylcholine biosynthesis. Biochim. Biophys. Acta. **779**: 217-251.

11. **Walton PA and Possmayer F.** 1984 The role of Mg2+-dependent phosphatidate phosphohydrolase in pulmonary glycerolipid biosynthesis. Biochim Biophys Acta. **796**:364-372.

12. **Balsinde J and Dennis EA.** 1996. Bromoenol lactone inhibits magnesium-dependent phosphatidate phosphohydrolase and blocks triacylglycerol biosynthesis in mouse P388D1 macrophages. J. Biol. Chem. **271**: 31937-31941.

13. **Walton PA and Possmayer F.** 1986. Translocation of Mg2+-dependent phosphatidate phosphohydrolase between cytosol and endoplasmic reticulum in a permanent cell line from human lung. Biochem Cell Biol. **64**:1135-1140.

14. **Truett AP, Bocckino SB, and Murray JJ.** 1992. Regulation of phosphatidic acid phosphohydrolase activity during stimulation of human polymorphonuclear leukocytes. FASEB J. **6**: 2720-2725.

15. **Jiang Y, Lu Z, Zang Q, and Foster DA.** 1996. Regulation of phosphatidic acid phosphohydrolase by epidermal growth factor. Reduced association with the EGF receptor followed by increased association with protein kinase C episilon. J. Biol. Chem. **271**: 29529-29532.

16. **Balboa MA, Balsinde J, and Dennis EA.** 1998. Involvement of phosphatidate phosphohydrolase in arachidonic acid mobilization in human amnionic WISH cells. J Biol Chem. **273**:7684-7690.

17. **Johnson CA, Balboa MA, Balsinde J, and Dennis EA.** 1999. Regulation of cyclooxygenase-2 expression by phosphatidate phosphohydrolase in human amnionic WISH cells. J. Biol. Chem. **274**: 27689-27693.

18. **Casola PG and Possmayer F.** 1981. Pulmonary phosphatidic acid phosphohydrolase. Developmental patterns in rabbit lung. Biochim. Biophys. Acta. **665**: 186-194.

19. **Brehier A, Benson BJ, Williams MC, Mason RJ, and Ballard PL.** 1977. Corticosteroid induction of phosphatidic acid phosphatase in fetal rabbit lung. **77**: 883-890.

20. **Douglas WHJ, Sommers-Smith SK, and Johnston JM.** 1983. Phosphatidate phosphohydrolase activity as a marker for surfactant synthesis in organotypic cultures of type II alveolar pneumocytes. J. Cell Sci. **60**: 199-207.

21. **Cockshutt AM and Possmayer F.** 1992. Metabolism of surfactant lipids and proteins in the developing lung. Ed: Robertson, van Golde LMG, and Batenburg JJ. Chapter 16, p339-397.

22. **Jimenez JM, Schultz FM, and Johnston JM.** 1975. Fetal lung maturation. III. Amniotic fluid phosphatidic acid phosphohydrolase (PAPase) and its relation to the lecithin/sphingomyelin ratio. Obstet Gynecol. **46**:588-590.

23. **Spitzer HL and Johnston JM.** 1978. Characterization of phosphatidate phosphohydrolase activity associated with isolated lamellar bodies. Biochim Biophys Acta. **531**:275-285.

24. **Casola PG, Macdonald PM, McMurray WC, and Possmayer F.** 1982. Concerning the coidentity of phosphatidic acid phosphohydrolase and

phosphatidylglycerophosphate phosphohydrolase in rat lung lamellar bodies. Exp Lung Res. **3**:1-16.

25. **Crecelius CA and Longmore WJ.** 1983. Phosphatidic acid phosphatase activity in subcellular fractions derived from adult rat type II pneumocytes in primary culture. Biochim Biophys Acta. **750**:447-456.

26. **Martin A, Gomez-Munoz A, Jamal Z, and Brindley DN.** 1991. Characterization and assay of phosphatidate phosphatase. Methods Enzymol. **197**: 553-563.

27. **Fleming IN and Yeaman SJ.** 1995. Subcellular distribution of N-ethylmaleimide-sensitive and -insensitive phosphatidic acid phosphohydrolase in rat brain. Biochim. Biophys. Acta. **1254**: 161-168.

28. **Hoer A and Oberdisse E.** 1994. Characterization of a phosphatidic acid phosphatase from rat brain cell membranes. Naunyn Schmiedebergs Arch Pharmacol. **350**: 653-661.

29. **Jamdar SC and Cao WF.** 1994. Properties of phosphatidate phosphohydrolase in rat adipose tissue. Biochem J. **301**: 793-799.

30. **Day CP and Yeaman SJ.** 1992. Physical evidence for the presence of two forms of phosphatidate phosphohydrolases in rat liver. Biochim. Biophys. Acta. **1127**: 87-94.

31. **Jamal Z, Martin A, Gomez-Munoz A, and Brindley DN.** 1991. Plasma membrane fractions from rat liver contain a phosphatidate phosphohydrolase distinct from that in the endoplasmic reticulum and cytosol. J. Biol. Chem. **266**: 2988-2996.

32. **Kanoh H, Imai S, Yamada K, Sakane F.** 1992. Purification and properties of phosphatidic acid phosphatase from porcine thymus membranes. J. Biol. Chem. **267**: 25309-25314.

33. **Waggoner DW, Martin A, Dewald J, Gomez-Munoz A, and Brindley DN.** 1995. Purification and characterization of a novel plasma membrane phosphatidate phosphohydrolase from rat liver. J. Biol. Chem. **270**: 19422-19429.

34. **Fleming IN and Yeaman SJ.** 1995. Purification and characterization of N-ethylmaleimide-insensitive phosphatidic acid phosphohydrolase (PAP2) from rat liver. Biochem J. **308**: 983-989.

35. **English D, Martin M, Harvey KA, Akard LP, Allen R, Widlanski TS, Garcia JGN, and Siddiqui RA.** 1997. Characterization and purification of neutrophil ecto-phosphatidic acid phosphohydrolase. Biochem J. **324**: 941-950.

36. **Perry DK, Stevens VL, Widlanski TS, and Lambeth JD.** 1993. A novel ecto-phosphatidic acid phosphohydrolase activity mediates activation of neutrophil superoxide generation by exogenous phosphatidic acid. J. Biol. Chem. **268**: 25302-25310.

37. **Xie M and Low MG.** 1994. Identification and characterization of an ecto-(lyso)phosphatidic acid phosphatase in PAM 212 keratinocytes. Arch. Biochem. Biophys. **312**: 254-259.

38. **Harvey KA, Siddiqui RA, Reeves M, Kovala T, Dugan M, Akard LP, and English D.** 1999. Characterization and partial purification of CD34+ progenitor cell ecto-phosphatidic acid phosphohydrolase. Biochem Mol. Biol. Int. **47**: 9-23.

39. **Kai M, Wada I, Imai S, Sakane F, and Kanoh H.** 1996. Identification and cDNA cloning of 35kDa phosphatidic acid phosphatase (type 2) bound to plasma membrane. Polymerase chain reaction amplification of mouse H_2O_2-inducible hic 53 clone yielded the cDNA encoding phosphatidic acid phosphatase. J. Biol. Chem. **271**: 18931-18938.

40. **Egawa K, Yoshiwara M, Shibanuma M, and Nose K.** 1995. Isolation of a novel ras-recision gene that is induced by hydrogen peroxide from a mouse osteoblastic cell line, MC3T3-E1. FEBS Lett. **372**: 74-77.

41. **Zhang N, Zhang J, Purcell KJ, Chang Y, and Howard K.** 1997. The Drosophila protein Wunen repels migrating germ cells. Nature. **385**: 64-67.

42. **Barila D, Plateroti M, Nobili F, Muda AO, Xie Y, Morimoto T, and Perozzi G.** 1996. The Dri 42 gene, whose expression is up-regulated during epithelial differentiation, encodes a novel endoplasmic reticulum resident transmembrane protein. J. Biol. Chem. **271**: 29928-29936.

43. **Zhang N, Zhang J, Cheng Y, and Howard K.** 1996. Identification and genetic analysis of wunen, a gene guiding Drosophila melanogaster germ cell migration. Genetics. **143**: 1231-1241.

44. **Barila D, Murgia C, Nobili F, Gaetani S, and Perozzi G.** 1994. Subtractive hybridization cloning of novel genes differentially expressed during intestinal development. Eur. J. Biochem. **223**: 701-709.

45. **Kai M, Wada I, Imai S, Sakane F, and Kanoh H.** 1997. Cloning and characterization of two human isozymes of Mg^{+2}-independent phosphatidic acid phosphatases. J. Biol. Chem. **270**: 24572-24578.

46. **Hooks SB, Ragan SP, and Lynch KR.** 1998. Identification of a novel human phosphatidic acid phosphatase.. FEBS Lett. **427**: 188-192.

47. **Roberts R, Sciorra VA, and Morris AJ.** 1998. Human type 2 phosphatidic acid phosphatases. Substrate specificity of the type 2a, 2b, and 2c enzymes and cell surface activity of the 2a isoform. J. Biol. Chem. **273**: 22059-22067.

48. **Leung DW, Tompkins CK, and White T.** 1998. Molecular cloning of two alternatively spliced forms of human phosphatidic acid phosphatase cDNAs that are differentially epxressed in normal and tumor cells. DNA and Cell Biol. **17**: 377-385.

49. **Tate R, Tolan D, and Pyne S.** 1999. Molecular cloning of magnesium-independent type 2 phosphatidic acid phosphatases from airway smooth muscle. Cell Signal. **11**: 515-522.

50. **Carman GM.** 1997. Phosphatidate phosphatases and diacylglycerol pyrophosphate phosphatases in Saccharomyces cerevisiae and Escherichia coli. Biochim. Biophys. Acta. **1348**: 45-55.

51. **Kocsis MG and Weselake RJ.** 1996. Phosphatidate phosphatases of mammals, yeast, and higher plants. Lipids. **31**:785-802.

52. **Toke DA, Bennett WL, Dillon, Wu WI, Chen X, Ostrander DB, Oshiro J, Cremesti A, Voelker DR, Fishli AS, and Carman GM.** 1998. Isolation and characterization of the Saccharomyces Cerevisiae DPP1 gene encoding diacylglycerol pyrophosphate phosphatase. J. Biol. Chem. **273**: 3278-3284.

53. **Han GS, Johnston CN, Chen X, Athenstaedt K, Daum G, and Carman GM.** 2001, Regulation of the Saccharomyces Cerevisiae DPP1-encoded diacylglycerol pyrophosphate phosphatase by zinc. J. Biol. Chem. In press.

54. **Munnik T, de Vrije T, Irvine RF, and Musgrave A.** 1996. Identification of diacylglycerol pyrophosphate as a novel metabolic product of phosphatidic acid during G-protein activation in plants. J. Biol. Chem. **271**: 15708-15715.

55. **Balboa MA, Balsinde J, Dillon DA, Carman GM, and Dennis EA.** 1999. Proinflammatory macrophage-activating properties of the novel phospholipid diacylglycerol pyrophosphate. J. Biol. Chem. **274**: 522-526.

56. **Toke DA, Bennett WL, Oshiro J, Wu WI, Voelker DR, and Carman GM.** 1998. Isolation and characterization of the Saccharomyces cerevisiae LPP1 gene encoding a Mg^{+2}-independent phosphatidate phosphatase. J. Biol. Chem. **273**: 14311-14338.

57. **Katagiri T and Shinozaki K.** 1998. Disruption of a gene encoding phosphatidic acid phosphatase causes abnormal phenotypes in cell growth and abnormal cytokinesis in Saccharomyces Cerevisiae. Biochem. Biophys. Res. Commun. **248**: 87-92.

58. **Yamochi W, Tanaka K, Nonaka H, Maeda A, Musha T, Takai Y.** 1994. Growth site localization of Rho1 small GTP-binding protein and its involvement in bud formation in Saccharomyces cerevisiae. J Cell Biol. **125:**1077-1093.

59. **Faulkner A, Chen X, Rush J, Horazdovsky B, Waechter CJ, Carman GM, and Sternweis PC.** 1999. The LPP1 and DPP1 gene products account for most of the isoprenoid phosphate phosphatase activities in Saccharomyces Cerevisiae. J. Biol. Chem. **274**: 14381-14837.

60. **Sciorra VA and Morris AJ.** 1999. Sequential actions of phospholipase D and phosphatidic acid phosphohydrolase 2b generate diglyceride in mammalian cells. Mol. Biol. Cell. **10**: 3863-3876.

61. **Brindley D and Waggoner D.** 1998. Mammalian lipid phosphate phosphohydrolases. J. Biol. Chem. **273**: 24281-24284.

62. **Kanoh H, Kai M, and Wada I.** 1999. Molecular characterization of the type 2 phosphatidic acid phosphatase. **98**: 119-126.

63. **Jasinska R, Zhang QX, Pilquil C, Singh I, Xu J, Dewald J, Dillon DA, Berthiaume LG, Carman GM, Waggoner DW, and Brindley DN.** 1999. Lipid phosphate phosphohydrolase-1 degrade exogenous glycerolipid and sphingolipid phosphate esters. Biochem J. **340**: 677-686.

64. **Zhang QX, Pilquil CS, Dewald J, Berthiaume LG, and Brindley DN.** 2000. Identification of structurally important domains of lipid phosphate phosphatase-1: implications for its sites of action. Biochem J. **345**: 181-184.

65. **Ishikawa T, Kai M, Wada I, and Kanoh H.** 2000. Cell surface activities of the human type 2b phosphatidic acid phosphatase. J. Biochem (Tokyo). **127**: 645-651.

66. **Roberts R and Morris AJ.** 2000. Role of phosphatidic acid phosphatase 2a in uptake of extracellular lipid phosphate mediators. Biochim. Biophys. Acta. **1487**: 33-49.

67. **Stukey J and Carman GM.** 1997. Identification of a novel phosphatase sequence motif. Protein Science. **6**: 469-472.

68. **Waggoner DW, Gomez-Munoz A, Dewald J, and Brindley DN.** 1996. Phosphatidate phosphohydrolase catalylzes the hydrolysis of ceramide-1-phosphate, lysophosphatidate, and sphingosine-1-phosphate. J. Biol. Chem. **271**: 16506-16509.

69. **Dillon DA, Chen X, Zeimetz GM, Wu WI, Waggoner DW, Dewald J, Brindley DN, and Carman GM.** 1997. Mammalian Mg^{+2}-independent phosphatidate phosphatase (PAP2) displays diacylglycerol pyrophosphate phosphatase activity. J. Biol. Chem. **272**: 10361-10366.

70. **Martin A, Gomez-Munoz A, Waggoner DW, Stone JC, and Brindley DN.** 1993. Decreased activities of phosphatidate phosphohydrolase and phospholipase D in ras and tyrosine kinase (fps) transformed fibroblasts. J. Biol. Chem. **268**: 23924-23932.

71. **Ulrix W, Swinnen JV, Heyns W, and Verhoeven G.** 1998. Identification of the phosphatidic acid phosphatase type 2a isozyme as an androgen-regulated gene in the human prostatic adenocarcinoma cell line LNCaP. J. Biol. Chem. **273**: 4660-4665.

72. **Mandala SM, Thornton R, Galve-Roperh I, Poulton S, Peterson C, Olivera A, Bergstrom J, Kurtz MB, and Spiegel S.** 2000. Molecular cloning and characterization of a lipid phosphohydrolase that degrades sphingosine-1-phosphate and induces cell death. Proc. Natl. Acad. Sci. USA. **97**: 7859-7864.

73. **Boudker O and Futerman AH.** 1993. Detection and characterization of ceramide-1-phosphate phosphatase activity in rat liver plasma membrane. J. Biol. Chem. **268**: 22150-22155.

74. **Shinghal R, Scheller RH, and Bajjalieh SM.** 1993. Ceramide 1-phosphate phosphatase activity in brain. J. Neurochem. 61:2279-2285.

75. **Imai A, Furui T, Tamaya T, and Mills GB.** 2000. A gonadotropin-releasing hormone-responsive phosphatase hydrolyses lysophosphatidic acid within the plasma membrane of ovarian cancer cells. J. Clin. Endocrinol. Metab. **85**: 3370-3375.

76. **Baker RR and Chang HY.** 2000. A metabolic path for the degradation of lysophosphatidic acid, an inhibitor of lysophosphatidylcholine lysophospholipase, in neuronal nuclei of cerebral cortex. Biochim. Biophys. Acta. **1483**: 58-68.

77. **Frank DW and Waechter CJ.** 1998. Purification and characterization of a polyisoprenyl phosphate phosphatase from pig brain. Possible dual specificity. J. Biol. Chem. **273**: 11791-11798.

78. **Hiroyama M and Takenawa T.** 1998. Purification and characterization of a lysophosphatidic acid-specific phosphatase. Biochem. J. **336**: 483-489.

79. **Hiroyama M and Takenawa T.** 1999. Isolation of a cDNA encoding lysophosphatidic acid phosphatase that is involved in the regulation of mitochondrial lipid biosynthesis. J. Biol. Chem. **274**: 29172-29180.

80. **Exton JH.** 1990. Signaling through phosphatidylcholine breakdown. J. Biol. Chem. **265**: 1-4.

81. **Brindley DN and Waggoner DW.** 1996. Phosphatidate phosphohydrolase and signal transduction. Chem. Phys. Lipids. **80**: 45-57.

82. **Wakelam MJO.** 1998. Diacylglycerol - when is it an intracellular messenger? Biochim. Biophys. Acta. **1436**: 117-126.

83. **Pessin MS and Raben DM.** 1989. Molecular species analysis of 1,2-diglycerides stimulated by alpha-thrombin in cultured fibroblasts. J. Biol. Chem. **264**: 8729-8738.

84. **Pettitt TR and Wakelam MJO.** 1993. Bombesin stimulates distinct time-dependent changes in the sn-1-2-diradylglycerol molecular species profile from Swiss 3T3 fibroblasts as analyzed by 3,5-dinitrobenzoyl derivatization and h.p.l.c. separation. Biochem J. **289**: 487-495.

85. **Schutze S, Potthoff K, Machleidt T, Berkovic D, and Wiegmann K.** 1992. TNF activates NF-kappa B by phosphatidylcholine-specific phospholipase C-induced "acidic" sphingomyelin breakdown. Cell. **71**: 765-776.

86. **Johansen T, Bjorkey G, Overvatn A, Diaz-Meco MT, Traavik T, and Moscat J.** 1994. NIH 3T3 cells stably transfected with the gene encoding phosphatidylcholine-hydrolyzing phospholipase C from Bacillus Cereus acquire a transformed phenotype. Mol. Cell Biol. **14**: 646-654.

87. **Hannun YA.** 1996. Functions of ceramide in coordinating cellular responses to stress. Science. **274**: 1855-1859.

88. **Luberto C and Hannun YA.** 1998. Sphingomyelin synthase, a potential regulator of intracellular levels of ceramide and diacylglycerol during SV40 transformation. Does sphingomyelin synthase account for the putative phosphatidylcholine-specific phospholipase C? J. Biol. Chem. **273**: 14550-14559.

89. **Cook SJ and Wakelam MJO.** 1991. Stimulated phosphatidylcholine hydrolysis as a signal transduction pathway in mitogenesis. Cell Signal. **3**: 273-282.

90. **Hodgkin MN, Pettitt TR, Martin A, Michell RH, Pemberton AJ, and Wakelam MJO.** 1998. Diacylglycerols and phosphatidates: which molecular species are intracellular messengers? TIBS. **23**: 200-204.

91. **Pettitt TR, Martin A, Horton T, Liossis C, Lord JM, and Wakelam MJO.** 1997. Diacylglycerol and phosphatidate generated by phospholipase C and D, respectively, have distinct fatty acid compositions and functions. J. Biol. Chem. **272**: 17354-17359.

92. **Waggoner DW, Xu J, Singh I, Jasinska R, Zhang QX, and Brindley DN.** 1999. Structural organization of mammalian lipid phosphate phosphatases: implications for signal transduction. Biochim. Biophys. Acta. **1439**: 299-316.

93. **Cross MJ, Roberts S, Ridley AJ, Hodgkin MN, Stewart A, Claesson-Welsh L, and Wakelam MJO.**1996. Stimulation of actin stress fibre formation mediated by activation of phospholipase D. Curr. Biol. **6**: 588-597.

94. **McPhail LC, Waite KA, Regier DS, Nixon JB, Qualliotine-Mann D, Zhang WX, Wallin R, and Sergeant S.** 1999. A novel protein kinase target for the lipid second messenger phosphatidic acid. Biochim. Biophys. Acta. **1439**: 277-290.

95. **Limatola C, Schaap D, Moolenaar WH, van Blitterswijk WJ.** 1994. Phosphatidic acid activation of protein kinase C-zeta overexpressed in COS cells: comparison with other protein kinase C isotypes and other acidic lipids. Biochem J. 304:1001-1008.

96. **Ghosh S, Strum JC, Sciorra VA, Daniel L, and Bell RM.** 1996. Raf-1 kinase possesses distinct binding domains for phosphatidylserine and phosphatidic acid. Phosphatidic acid regulates the translocation of Raf-1 in 12-O-tetradecanoylphorbol-13-acetate-stimulated Madin-Darby canine kidney cells. J. Biol. Chem. **271**: 8472-8480.

97. **Rizzo MA, Shome K, Vasudevan C, Stolz DB, Sung TC, Frohman MA, Watkins SC, and Romero G.** 1999. Phospholipase D and its product, phosphatidic acid, mediate agonist-dependent Raf-1 translocation to the plasma membrane and the activation of the mitogen-activated protein kinase pathway. J. Biol. Chem. **274**: 1131-1139.

98. **Grange M, Sette C, Cuomo M, Conti M, Lagarde M, Prigent AF, and Nemoz G.** 2000. The cAMP-specific phosphodiesterase PDE4D3 is regulated by phosphatidic acid binding. Consequences for cAMP signaling pathway, and characterization of a phosphatidic acid binding site. J. Biol. Chem. In press.

99. **Siddiqui RA and Yang YC.** 1995. Interleukin-11 induces phosphatidic acid formation and activates MAP kinase in mouse 3T3-L1 cells. Cell. Signal. **7**; 247-259.

100. **Mori T, Takai Y, Yu B, Takahashi J, Nishuzuka Y, and Fujikura T.** 1982. Specificity of the fatty acyl moieties of diacylglycerol for the activation of calcium-activated, phospholipid-dependent protein kinase. J. Biochem (Tokyo). **91**: 427-431.

101. **Go M, Sekigushi K, Nomura H, Kikkawa U, and Nishizuka Y.** 1987. Further studies on the specificity of diacylglycerol for protein kinase C activation.Biochem. Biophys. Res. Commun. **144**: 598-605.

102. **Marignani PA, Epand RM, Sebaldt RJ.** 1996. Acyl chain dependence of diacylglycerol activation of protein kinase C activity in vitro. Biochem. Biophys. Res. Commun. **225**: 469-473.

103. **Schachter JB, Lester DS, Alkon DL.**1996. Synergistic activation of protein kinase C by arachidonic acid and diacylglycerols in vitro: generation of a stable membrane-bound, cofactor-independent state of protein kinase C activity. Biochim. Biophys. Acta. **1291**: 167-176.

104. **Olivier AK, Hansra G, Pettitt TR, Wakelam MJO, and Parker PJ.** 1996. The co-mitogenic combination of transforming growth factor beta 1 and bombesin protects protein kinase C-delta from late-phase down-regulation, despite synergy in diacylglycerol accumulation. Biochem. J. **318**: 519-525.

105. **Baldassare JJ, Henderson PA, Burns D, Loomis C, and Fisher GJ.** 1992. Translocation of protein kinase C isozymes in thrombin-stimulated human platelets. Correlation with 1,2-diacylglycerol levels. J. Biol. Chem. **267**: 15585-15590.

106. **Ha K-S and Exton JH.** 1993. Differential translocation of protein kinase C isozymes by thrombin and platelet-derived growth factor. A possible function for phosphatidylcholine-derived diacylglycerol. J. Biol. Chem. **268**: 10534-10539.

107. **Pettitt TR and Wakelam MJO.** 1999. Diacylglycerol kinase ε, but not ζ, selectively removes polyunsaturated diacylglycerol, inducing altered protein kinase C distribution *in vivo*. J. Biol. Chem. **274**: 36181-36186.

108. **Shirai Y, Segawa S, Kuriyama M, Goto K, Sakai N, and Saito N.** 2000. Subtype-specific translocation of diacylglycerol kinase α and γ and its correlation with protein kinase C. J. Biol. Chem. **275**: 24760-24766.

109. **Hammond SM, Altshuller YM, Sung TC, Rudge SA, Rose K, Engebrecht J, Morris AJ, and Frohman MA.** 1995. Human ADP-ribosylation factor-activated phosphatidylcholine-specific phospholipase D defines a new and highly conserved gene family. J. Biol. Chem. **270**: 29640-29643.

110. **Houle MG and Bourgoin S.** 1999. Regulation of phospholipase D by phosphorylation-dependent mechanisms. Biochim. Biophys. Acta. **1439**: 135-150.

111. **Colley WC, Sung TC, Roll R, Jenco J, Hammond SM, Altshuller Y, Bar Sagi D, Morris AJ, and Frohman MA.** 1997. Phospholipase D2, a distinct phospholipase D isoform with novel regulatory properties that provokes cytoskeletal reorganization. Curr. Biol. **7**: 191-201.

112. **Massenburg D, Han JS, Liyanage M, Patton WA, Rhee SG, Moss J, and Vaughan M.** 1994. Activation of rat brain phospholipase D by ADP-ribosylation factors 1, 5, and 6: separation of ADP-ribosylation factor-dependent and oleate-dependent enzymes. Proc. Natl. Acad. Sci. USA. **91**: 11718-11722.

113. **Okamura S and Yamashita S.** 1994. Purification and characterization of phosphatidylcholine phospholipase D from pig lung. J. Biol. Chem. **269**: 31207-31213.

114. **Provost JJ, Fudge J, Israelit S, Siddiqi AR, Exton JH.** 1996. Tissue-specific distribution and subcellular distribution of phospholipase D in rat: evidence for distinct RhoA- and ADP-ribosylation factor (ARF)-regulated isoenzymes. Biochem. J. **319**: 285-291.

115. **Chalifour R and Kanfer JN.** 1982. Fatty acid activation and temperature perturbation of rat brain microsomal phospholipase D. J. Neurochem. **39**: 299-305.

116. **Liscovitch M, Czarny M, Fiucci G, and Tang X.** 2000. Phospholipase D: molecular and cell biology of a novel gene family. Biochem. J. **345**: 401-415.

117. **Balboa MA, Balsinde J, Dennis EA, and Insel PA.** 1995. A phospholipase D-mediated pathway for generating diacylglycerol in nuclei from Madin-Darby canine kidney cells. J. Biol. Chem. **270**: 11738-11740.

118. **Balboa MA and Insel PA.** 1995. Nuclear phospholipase D in Medin-Darby canine kidney cells. Guonisine 5'-O-(thiotriphosphate)-stimulated activation is mediated by RhoA and is downstream of protein kinase C. J. Biol. Chem. **270**: 29843-29847.

119. **Liscovitch M, Czarny M, Fiucci G, Lavie Y, and Tang X.** 1999. Localization and possible functions of phospholipase D isozymes. Biochim. Biophys. Acta. **1439**: 245-263.

120. **Ktistakis NT, Brown HA, Waters MG, Sternweis PC, and Roth MG.** 1996. Evidence that phospholipase D mediates ADP ribosylation factor-dependent formation of Golgi coated vesicles. J. Cell Biol. **134**: 295-306.

121. **Siddhanta A and Shields D.** 1998. Secretory vesicle budding from the trans-Golg i network is mediated by phosphatidic acid levels. J. Biol. Chem. **273**: 17995-17998.

122. **Iyer SS and Kusner DJ.** 1999. Association of phospholipase D activity with the detergent-insoluble cytoskeleton of U937 promonocytic leukocytes. J. Biol. Chem. **274**: 2350-2359.

123. **Ching T-T, Wang D-S, Hsu A-L, Lu P-J, and Chen C-S.** 1999. Identification of multiple phosphoinositide-specific phospholipase D as new regulatory enzymes for phosphatidylinositol 3,4,5-trisphosphate. J. Biol. Chem. **274**: 8611-8617.

124. **Tsuj ioka H, Takami N, Misumi Y, and Ikehara Y.** Intracellular cleavage of glycosylphosphatidylinositol by phospholipase D induces activation of protein kinase C α. Biochem. J. **342**: 449-455.

125. **Van Blitterswijk WJ and Houssa B.** 2000. Properties and functions of diacylglycerol kinases. Cell. Signal. **12**: 595-605.

126. **Topham MK and Prescott SM.** 1999.Mammalian diacylglycerol kinases, a family of lipid kinases with signaling functions. J. Biol. Chem. **274**: 11447-11450.

127. **Houssa B, de Widt J, Kranenburg O, Moolenaar WH, and van Blitterswijk WJ.** 1999. Diacylglycerol kinase theta binds to and is negatively regulated by active RhoA. J. Biol. Chem. **274**: 6820-6822.

128. **D'Santos CS, Clarke JH, and Divecha N.** 1997. Phospholipid signalling in the nucleus. Biochem. J. **327**: 569-576.

129. **Dempsey EC, Newton AC, Mochly-Rosen D, Fields AP, Reyland ME, Insel PA, and Messing RO.** 2000. Protein kinase C isozymes and the regulation of diverse cell responses. Am. J. Physiol. Lung Cell Mol. Physiol. **279**

130. **Bell RM and Burns DJ.** 1991. Lipid activation of protein kinase C. J. Biol. Chem. **266**: 4661-4664.

131. **Liu WS and Heckman CA.** 1998. The sevenfold way of PKC regulation. Cell Signal. **10**: 529-542.

132. **An S, Goetzl EJ, and Hsinyu L.** 1998. Signaling mechanisms and molecular characterization of G protein-coupled receptors for lysophosphatidic acid and sphingosine 1-phosphate. J. Cell. Biochem. (Supplements). **30/31**: 124-157.

133. **Goetzl EJ and An S.** 1998. Diversity of cellular responses and functions for the lysophospholipid growth factors lysophosphatidic acid and sphingosine 1-phosphate. FASEB J. **12**: 1589-1598.

134. **An S.** 2000. Identification and characterization of G-protein-coupled receptors for lysophophatidic acid and sphingosine-1-phosphate. Ann N.Y. Acad. Sci. **905**: 25-33.

135. **Xu J, Zhang QX, Pilquil C, Berthiaume LG, Waggoner DW, and Brindley DN.** 2000. Related lipid phosphate phosphatase-1 in the regulation of lysophosphatidate signaling. Ann N.Y. Acad. Sci. **905**: 81-90.

136. **Xu J, Love LM, Sing I, Zhang QX, Dewald J, Wang DA, Fisher DJ, Tigyi G, Berthiaume LG, Waggoner DW, and Brindley DN.** 2000. Lipid phosphate phosphatase-1 and Ca^{+2} control lysophosphatidate signaling through EDG-2 receptors. J. Biol. Chem. **275**: 27520-27530.

137. **Hannun YA.** 1994. The sphingomyelin cycle and the second messenger function of ceramide. J. Biol. Chem. **269**: 3125-3128.

138. **Luberto C and Hannun YA.** 1999. Sphingolipid metabolism in the regulation of bioactive molecules. Lipids. **34**: S5-S11.

139. **Galadari S, Kishikawa K, Kamibayashi C, Mamby MC, and Hannun YA.** 1998. Purification and characterization of ceramide-activated protein phosphatases. **37**: 11232-11238.

140. **Bialojan C and Takai A.** 1988. Inhibitory effect of a marine-sponge toxin, okadaic acid, on protein phosphatases. Specificity and kinetics. Biochem. J. **256**: 283-290.

141. **Mumby MC and Walter G.** 1991. Protein phosphatases and DNA tumor viruses: transformation through the back door? Cell Regul. **2**: 589-598.

142. **Hofmann K and Dixit VM.** 1998. Ceramide in apoptosis - does it really matter? TIBS. **23**: 374-377.

143. **Jayadev S, Liu B, Bielawski AE, Lee JY, Nazairi F, and Marina Y.** 1995. Role for ceramide in cell cycle arrest. J. Biol. Chem. **270**: 2047-2052.

144. **Zhang H, Desai NN, Murphy JM, and Spiegel S.** 1990. Increases in phosphatidic acid levels accompany sphingosine-stimulated proliferation of quiescent Swiss 3T3 cells. J. Biol. Chem. **265**: 21309-21316.

145. **Zhang H, Buckley NE, Gibson K, and Spiegel S.** 1990. Sphingosine stimulates cellular proliferation via a protein kinase C-independent pathway. J. Biol. Chem. **265**: 76-81.

146. **Kronke M.** 1999. Involvement of sphingomyelinases in TNF signaling pathways. Chem. Phys. Lipids. **102**: 157-166.

147. **Mizutani Y, Tamiya-Koizumi K, Irie F, Hirabayashi Y, Miwa M, and Yoshida S.** 2000. Cloning and expression of rat neutral sphingomyelinase: enzymological characterization and identification of essential histidine residues. **1485**: 236-246.

148. **Hofmann K, Tomiuk S, Wolff G, and Stoffel W.** 2000. Cloning and characterization of the mammalian brain-specific Mg^{+2}-dependent neutral sphingomyelinase. Proc. Natl. Acad. Sci. USA. **97**: 5895-5900.

149. **Chatterjee S, Han H, Rollins S, and Cleveland T.** 1999. Molecular cloning, characterization, and expression of a novel human neutral sphingomyelinase. J. Biol. Chem. **274**: 37407-37412.

150. **Tani M, Okino N, Mori K, Tanigawa T, Izu H, and Ito M.** 2000. Molecular cloning of the full-length cDNA encoding mouse neutral ceramidase. A novel

but highly conserved gene family of neutral/alkaline ceramidases. J. Biol. Chem. **275**: 11229-11234.

151. **Strelon A, Bernardo K, Adam-Kiages S, Linke T, Sandhoff K, Kronke M, and Adam D.** 2000. Overexpression of acid ceramidase protects from tumor necrosis factor-induced cell death. **192**: 601-012.

152. **Nava VE, Lacana E, Poulton S, Liu H, Sugiura M, Kono K, Milstein S, Kohama T, and Spiegel S.** 2000. Functional characterization of human sphingosine kinase-1. FEBS Lett. **473**: 81-84.

153. **Liu H, Sugiura M, Nava VE, Edsall LC, Kono K, Poulton S, Milstein S, Kohama T, and Spiegel S.** 2000. Molecular cloning and functional characterization of a novel mammalian sphingosine kinase type 2 isoform. J. Biol. Chem. **275**: 19513-19520.

154. **Spiegel S.** 1999. Sphingosine-1-phosphate: a prototype of a new class of second messengers. J. Leukoc. Biol. **65**: 341-344.

155. **Hinkovska-Galcheva VT, Boxer LA, Mansfield PJ, Harsh D, Blackwood A, and Shayman JA.** 1998. The formation of ceramide-1-phosphate during neutrophil phagocytosis and its role in liposome fusion. J. Biol. Chem. **273**: 33203-33209.

156. **Mendelson CR.** 2000. Role of transcription factors in fetal lung development and surfactant protein gene expression. Ann. Rev. Physiol. **62**: 875-915.

157. **Castranova V, Rabovsky J, Tucker JH, and Miles PR.** 1988. The alveolar type II epithelial cell: a multifunctional pneumocyte. Toxicol. Appl. Pharm. **93**: 472-483.

158. **Rooney SA, Young SL, and Mendelson CR.** 1994. Molecular and cellular processing of lung surfactant. FASEB J. **8**: 957-967.

159. **Rice WR, Burton FM, and Fiedeldey DT.** 1995. Cloning and expression of the alveolar type II cell P_{2u}-purinergic receptor. Am. J. Respir. Cell Mol. Biol. **12**: 27-32.

160. **Mason RJ and Voelker DR.** 1998. Regulatory mechanisms of surfactant secretion. Biochim. Biophys. Acta. **1408**: 226-240.

161. **Griese M, Gobran LI, and Rooney SA.** 1993. Signal-transduction mechanisms of ATP-stimulated phosphatidylcholine secretion in rat type II

pneumocytes: interactions between ATP and other surfactant secretagogues. Biochim. Biophys. Acta. **1167**: 85-93.

162. **Griese M, Gobran LI, and Rooney SA.** 1991. ATP-stimulated inositol phospholipid metabolism and surfactant secretion in rat type II pneumocytes. Am. J. Physiol. **260**: L586-L593.

163. **Gobran LI, Xu Z-X, Lu Z, and Rooney SA.** 1994. P_{2u} purinoceptor stimulation of surfactant secretion coupled to phosphatidylcholine hydrolysis in type II cells. Am. J. Physiol. **267**: L625-L633.

164. **Rooney SA and Gobran LI.** 1993. Activation of phospholipase D in rat type II pneumocytes by ATP and other surfactant secretagogues. Am. J. Physiol. **264**: L133-L140.

165. **Gobran LI, Xu Z-X, and Rooney SA.** 1998. PKC isoforms and other signaling proteins involved in surfactant secretion in developing rat type II cells. Am. J. Physiol. **274**: L901-L907.

166. **Griese M, Gobran LI, and Rooney SA.** 1992. Ontogeny of surfactant secretion in type II pneumocytes from fetal, newborn, and adult rats. Am. J. Physiol. **262**: L337-L343.

167. **Gobran LI and Rooney SA.** 1999. Surfactant secretagogue activation of protein kinase C isoforms in cultured rat type II cells. Am. J. Physiol. **277**: L251-L256.

168. **Adamson IYR, Hedgecock C, and Bowden DH.** 1990. Epithelial cell-fibroblast interactions in lung injury and repair. Am. J. Pathol. **137**: 385-392.

169. **Smith BT and Post M.** 1989. Fibroblasts pneumocyte factor. Am. J. Physiol. **257**: L174-L178.

170. **Leslie CC, McCormick-Shannon K, Shannon JM, Garrick B, and Damm D, Abraham JA, and Mason RJ.** 1997. Heparin-binding EGF-like growth factor is a mitogen for rat alveolar type II cells. J. Respir. Cell Mol. Biol. **16**: 379-387.

171. **Bui KC, Wu F, Buckley S, Wu L, Williams R, Carbonara-Hall D, Hall FL, and Warbuton D.** 1993. Cyclin A expression in normal and transformed alveolar epithelial cells. Am. J. Respir. Cell Mol. Biol. **9**: 115-125.

172. **Bui KC, Buckley S, Wu F, Uhal B, Joshi I, Liu J, Hussain M, Makhoul I, and Warbuton D.** 1995. Induction of A- and D-type cyclins and cdc2 kinase activity

during recovery from short-term hyperoxic lung injury. Am. J. Physiol. **268**: L625-L635.

173. **Wu F, Buckley S, Bui KC, and Warbuton D.** 1995. Differential expression of cyclin D2 and cdc2 genes in proliferating and nonproliferating alveolar epithelial cells. Am. J. Respir. Cell Mol. Biol. **12**: 95-103.

174. **Fine A, Janssen-Heininger Y, Soultanakis RP, Swisher SG, and Uhal BD.** 2000. Apoptosis in lung pathophysiology. Am. J. Physiol. **279**: L423-L427.

175. **De Paepe ME, Rubin LP, Lude C, Lesieur-Brooke AM, Mills DR, and Luks FI.** 2000. Fas ligand expression coincides with alveolar cell apoptosis in late-gestation fetal lung development. Am. J. Physiol. **279**: L967-L976.

176. **Mallampalli RK, Peterson EJ, Carter AB, Salome RG, Mathur SN, and Koretzky GA.** 1999. TNF-α increases ceramide without inducing apoptosis in alveolar type II epithelial cells. Am. J. Physiol. **276**: L481-L490.

177. **Chan C and Goldkorn T.** 2000. Ceramide path in human lung cell death. Am. J. Respir. Cell Mol. Biol. **22**: 460-468.

178. **Lee SD, Lee BD, Han JM, Kim JH, Kim Y, Suh PG, and Ryu SH.** 2000. Phospholipase D2 activity suppresses hydrogen peroxide-induced apoptosis in PC12 cells. J. Neurochem. **75**: 1053-1059.

Chapter 2

Characterization of the Pulmonary N-Ethylmaleimide-Insensitive Lipid Phosphate Phosphohydrolase

[1] A version of this chapter has been published

Nanjundan, M and Possmayer F. 2000. Characterization of Pulmonary NEM-Insensitive Phosphatidate Phosphohydrolase. Experimental Lung Research, **26**: 361-381, 2000.

2.1 Introduction

Phosphatidate phosphohydrolase (PAPase) was first described in plants by Kates in 1955 (1). In the early 1960's, the characterization of this enzyme was initiated in a number of mammalian tissues including brain, kidney, intestine, and erythrocytes (2). However, PAPase activity in lung tissues was initially shown using a histochemical approach which localized this enzyme to inclusion bodies within the granular pneumocyte (3). Further studies demonstrated that the specific activity of the pulmonary enzyme increased in fetal rabbit lung during development (4) as well as after induction of pulmonary maturation by glucocorticoids (5). This activity has also been reported to increase with the appearance of lamellar bodies in the fetal rabbit lung (6). Furthermore, the observation that an increase in PAPase occurs 24 hours prior to a rise in phosphatidylcholine (PC) in lung (4, 7) led to the suggestion that PAPase could be involved in the regulation of the production of diacylglycerol for pulmonary surfactant PC.

There exist two different forms of pulmonary PAPases, namely PAP1 and lipid phosphate phosphohydrolase (LPP, previously named PAP2). Walton and Possmayer (8) have demonstrated that the former enzyme is magnesium-dependent and heat labile. It was found to have a predominantly cytosolic location although it could translocate to the endoplasmic reticulum where it would become metabolically functional (9). PAP1 has been shown to be involved in phospholipid biosynthesis (10). The initial step in the production of phosphatidylcholine (PC) and dipalmitoylphosphatidylcholine (DPPC) is the formation of phosphatidic acid (PA).

This lipid undergoes hydrolysis to diacylglycerol (DAG) prior to formation of PC by cholinephosphotransferase (CPT).

In contrast, pulmonary LPP was shown to be magnesium-independent, heat stable, and to possess a membrane location (11). However, its function in lung remains undefined. Recent studies indicating the presence of LPP in both rat liver (12) and porcine thymus (13) plasma membranes and evidence of "cross-talk" between the glycerolipid and sphingolipid signaling pathways (14) are suggestive of a potential role in signal transduction. Thus PAP could act to hydrolyze PA arising in the plasma membrane from phospholipase D (PLD) (15) or from DAG kinase (16) thereby regulating the levels of PA in the plasma membrane. In the alveolar type II cells, transient elevations in DAG levels arising through PLC degradation of PIP_2 can be extended through the stimulation of the PLD and PAP pathway (17).

Brindley and colleagues have recently developed an assay for distinguishing the PAP1 and LPP enzymic activities based on the use of NEM, a sulfhydryl group reagent (12). In order to provide insight into the function of pulmonary LPP, this assay was applied to rat lung microsomal fractions and characterized with respect to the effects of various ions, a non-ionic detergent, sphingoid bases, amphiphilic amines, other lipids, and substrate analogs. We also sought to establish whether LPP activity was localized to lung plasma membranes. The distribution of LPP between type II cells and fibroblasts was investigated as a preliminary step toward studying the role of this enzyme in pulmonary cellular signaling.

2.2 Materials and Methods

2.2.1 Materials

All radioactive isotopes were obtained from Amersham. Percoll was obtained from Pharmacia. 1-Palmitoyl-2-oleoyl-phosphatidylcholine and lysophosphatidic acid were purchased from Avanti Polar Lipids. Diacylglycerol kinase, sphingosine-1-phosphate, ceramide-1-phosphate, N-acetyl ceramide, and sphingosine were purchased from Calbiochem. Phospholipase D was from Toyo Joso Limited. All solvents were purchased from Caledon. Lactate dehydrogenase was purchased from Boehringer Mannheim. N-hexanoyl ceramide was purchased from Sigma. Porcine elastase was obtained from Worthington Biochemicals. Other tissue culture materials were obtained from Gibco BRL.

2.2.2 Preparation of Subcellular Fractions from Rat Lung

Female Sprague-Dawley rats (150-300g) were sacrificed by decapitation or by injection with nembutanol. The thorax was opened and the lungs were perfused into the right ventricle with ice-cold saline (0.9%) with the left ventricle bisected to provide drainage. After excision and trimming of large vessels and airways, the lungs were weighed and chopped into $1mm^3$ using a McIlwain tissue chopper. The preparation of microsomes was followed according to the procedure of Walton and Possmayer (8). Briefly, the lungs were homogenized in 9 volumes of ice-cold Buffer A (0.25M sucrose, 0.1mM EDTA, 1mM HEPES, pH 7.4) using five strokes with a loose fitting pestle with a Potter Elvehjem homogenizer (Heidolph) followed by ten strokes with a tight-fitting pestle. The homogenate was then initially centrifuged at 1,450g for 5 min resulting in a nuclear pellet and a supernatant. The latter was

centrifuged at 10,000g for 15 min yielding a mitochondrial pellet and a supernatant. The supernatant was centrifuged at 100,000g for 60 min providing a microsomal pellet and a cytosolic supernatant. The fractions were aliquoted and frozen at -70^{0}C. Various fractions were retained for analysis throughout the isolation procedure.

2.2.3 Preparation of Plasma Membranes from Rat Lung

Plasma membranes were prepared according to Chander and Wu (18). Briefly, the minced lung was homogenized for 30 seconds using a Polytron set at 2.4 in 10 volumes of Buffer B (10mM phosphate buffer containing 0.32M sucrose, 1mM $MgCl_2$, 30mM NaCl, 5μM Pefabloc, 10μg/ml DNAse) followed by a 2 min homogenization with a Potter Elvehjem homogenizer. The homogenate was filtered through 2 layers of cheesecloth. The filtrate (12 ml) was layered over a discontinous sucrose gradient consisting of 5 ml each of 1.2M sucrose, 1M sucrose, 0.9M sucrose, 0.7M sucrose, and 0.5M sucrose. The gradient was centrifuged at 95,000g for 60 min using a swinging bucket rotor (SW28). The enriched plasma membrane fractions occurred between 0.9M and 1.2M sucrose. This interface was diluted to 0.2M sucrose with ice-cold double distilled water and subsequently centrifuged at 95,000g for 30 min. The pellet was then resuspended in a minimal volume of Buffer C (10mM Tris-HCl, pH 7.4, containing 0.3M sucrose). The suspension was layered onto a Percoll mixture consisting of Percoll, Buffer D (2M sucrose in 80mM Tris-8mM EDTA, pH 7.4) and Buffer E (0.25M sucrose in 10mM Tris-2mM EDTA, pH 7.4) in a ratio of 7:1:32 respectively. The mixture was centrifuged at 10,000g for 15 min in a fixed angle rotor resulting in plasma membranes banding at 0.5cm below

the top of the surface. This band was diluted five-fold with Buffer F (0.15M NaCl, 10mM Tris-HCl, 1mM EDTA, pH 7.4) and centrifuged. This wash resulted in a Percoll pellet with the plasma membranes floating over it. The protein was removed and diluted five-fold with Buffer F and again centrifuged as before. This step was performed six times in order to eliminate Percoll. The plasma membranes, which appeared as white sheets, were finally diluted in Buffer B and centrifuged at 100,000g for 60 min. The pellet was resuspended in 3 ml of Buffer B and stored at -70^0C.

2.2.4 Preparation of Alveolar Type II Cells and Fibroblasts

The procedure for the preparation of type II cells was followed according to Dobbs *et al.* (19). Female Sprague-Dawley rats (150-200g) were anesthetized with nembutanol. The trachea was cannulated; the left atrium was bisected; and the lungs were perfused with solution I (140mM NaCl, 5mM KCl, 2.5mM phosphate buffer, 10mM HEPES, 6mM glucose, 2mM $CaCl_2$, and 1.3mM $MgSO_4$) through the right vena cava until the lungs became white. The lungs were removed intact with trachea attached and lavaged to total lung capacity 8 times with solution II (140mM NaCl, 5mM KCl, 2.5mM phosphate buffer, 10mM HEPES, 6mM glucose, 0.2mM EGTA, pH 7.4). For the preparation of alveolar type II cells, 10 ml of elastase (total activity ~172U/rat) was instilled into the trachea followed by another 30 ml of elastase (10ml every 5 minutes). The lungs were then dissected carefully and minced into a fine suspension in the presence of DNase I (0.25mg/ml). The elastase reaction was then terminated with the addition of fetal bovine serum and shaking

in an Erlenmeyer flask at 37^{0}C for 2 minutes. The cell suspension was then filtered sequentially through 2 and 4 layers of gauze and 20μ Nytex membrane. The cells were then centrifuged at 130g for 10 min at 4^{0}C. The pellet was then resuspended in minimal essential media (MEM) with gentamycin and plated on IgG covered petri dishes. The plates were incubated for 1 hour in a 5% CO_2 incubator and the suspension was recovered and centrifuged as before. The pellet was resuspended in MEM (10% FBS) with gentamycin and plated on tissue culture plastic overnight. The following day, the cells were scraped from the plates and homogenized using a probe sonicator for 20 seconds three times at maximal output followed by centrifugation at 313,000g for 15 min to obtain a membrane fraction.

For the preparation of fibroblasts, the lungs were dissected carefully following lavage and minced in MEM containing collagenase (1mg/ml), trypsin (2.5mg/ml), and DNAse I (2mg/ml). These tissue fragments were digested for 1 hour followed by filtration through 2 layers of gauze. The cells were then centrifuged at 420g for 5 min and the pellet was resuspended in MEM (10% FBS) and plated for 5 days. The cells were harvested by trypsinization and total membrane fractions were prepared as described above.

2.2.5 Preparation of ^{32}P-labelled Phosphatidic acid (PA), Lysophosphatidic Acid (LPA), and Sphingosine-1-Phosphate (S-1-P)

The incubation mixture contained the substrate (1,2-diacylglycerol, monoacylglycerol, or ceramide), HEPES (pH 7.0), Triton X-100, $MgCl_2$, [γ-^{32}P]-ATP,

and DAG Kinase in a total volume of 1.5 ml. The mixture was incubated for 2-3 hours at 37^{0}C in a shaking water bath. The reaction was terminated with chloroform/methanol (1:1) and a biphasic system was obtained with the addition of 3 ml of 0.9% NaCl. The chloroform phase was retained, dried under N_2 to complete dryness, and resuspended in a small volume of chloroform. For lysophosphatidic acid and phosphatidic acid (8), the lipids were streaked onto silica gel G thin layer chromatography plates (0.5mm) impregnated with 0.35N oxalic acid and 1% magnesium acetate (w/v). These chromatograms were developed in light petroleum ether/acetone/formic acid (154:46:0.5, v/v/v) and the radiolabelled lipids were then located by X-ray film detection. The radiolabelled PA and LPA bands were isolated and the lipids were extracted with chloroform/methanol (1:1, v/v). For the preparation of S-1-P (20), the ceramide-1-phosphate (C-1-P) was resolved by TLC using silica gel G plates (60Å) with chloroform/methanol/acetic acid (65:15:5, v/v/v). The radioactive lipid, C-1-P, was isolated, eluted from the silica with chloroform/methanol (1:1, v/v), and dried down under nitrogen. The lipids were then treated with butanol/6N HCl (1:1, v/v) for 1 hour at 100^{0}C to produce radiolabelled S-1-P which was further purified by TLC using 1-butanol/acetic acid/water (3:1:1, v/v/v).

2.2.6 Preparation of Unlabelled Phosphatidic Acid (PA)

Nonlabelled PA was prepared enzymatically from 1-palmitoyl-2-oleoyl-phosphatidylcholine (1-POPC) according to Walton and Possmayer (8) using PLD. Briefly, the reaction mixture contained 500mg of 1-POPC dissolved in 10 ml of

diethyl ether, 10 ml of 0.1M sodium acetate (pH 5.6) containing 0.1M $CaCl_2$, and 10mg of PLD. The incubation vial was flushed with nitrogen, stoppered, and shaken overnight at room temperature with a Burrel wrist action shaker. The lipids were extracted and dried down using a rotary evaporator. The lipids were then resuspended in 50 ml of chloroform/methanol/water (5:4:1, v/v/v) and were subsequently passed through a Chelex 100 column four times to remove calcium. The lipids were extracted, dried down in a rotary evaporator, and dissolved in 50 ml of chloroform/methanol/ammonia (70:30:4) and applied to a silica gel column. Subsequently, 20 ml of chloroform/methanol/water (70:30:0.5, v/v/v) was added. Fractions were collected after the addition of 50 ml of chloroform/methanol/formic acid/water (70:30:2:0.5, v/v/v/v) to the column. The fractions were combined and the lipids were extracted. After washing with 0.1M sodium phosphate buffer (pH 7.4), the lower phase was evaporated to complete dryness, resuspended in 50 ml of chloroform containing 5% methanol, and stored at -20^{0}C under nitrogen.

2.2.7 Assaying PAP1 and LPP Activities

PAP1 activity was assayed according to Walton and Possmayer (8). Previous studies by Walton and Possmayer have demonstrated that over 88% of the radioactivity in the aqueous phase is associated with P^{32}-P_i.

LPP activity was assayed in a reaction mixture containing 100mM Tris-Maleate buffer, pH 6.5, 0.6mM PA (0.4mCi/mmol), 0.5mM EDTA, 0.5mM EGTA, pH 7.0, 0.2mg of essentially fatty acid free albumin, and 1mM DTT in final reaction volume of 0.1 ml (12). Incubation times were 60 minutes in duration at 37^{0}C. The

protein was preincubated at 37^0C for 10 min with 4.2mM NEM to eliminate any interference by PAP1 activity. The reactions were terminated by the addition of 1.5 ml of chloroform/methanol (1:1). The phases were broken with 0.75 ml of 0.1N HCl and a sample of the upper aqueous phase was taken for scintillation counting to determine the P^{32}-inorganic phosphate released.

2.2.8 Assays for Marker Enzymes

Enzyme activities for alkaline phosphatase, acid phosphatase, 5'-nucleotidase, monoamine oxidase, and cholinephosphotransferase were assayed according to Possmayer *et al.* (21). Enzyme activity for Na^+K^+-ATPase was assayed according to Chander *et al.* (22). Reaction rates were linear over the range of time and protein used. Normally, 10-50μg of protein was utilized in these assays.

2.2.9 Other Methods

Protein was determined by the method of Lowry *et al.* (23) in the presence of 2mM SDS using bovine serum albumin as a standard. Phosphorous was determined by the method of Rouser (24) using KH_2PO_4 as the standard phosphorous solution.

Experiments were done at least twice each in triplicate and the results are shown as the mean and the standard error.

2.3 Results

2.3.1 Establishment of the LPP assay

Initially, the effect of NEM on both pulmonary PAP1 and LPP was investigated. PAP1 activity was completely inhibited with 2mM NEM, whereas, NEM, up to 8mM, had little effect on LPP activity (Figure 2.1). For subsequent experiments, the protein was always preincubated with NEM for 10 min to exclude any possible interference from PAP1 activity when measuring the LPP activity. Various subcellular fractions were analyzed for enzyme markers and LPP activities to determine the fraction that contained the highest LPP specific activity for optimization of the assay. As shown in Figure 2.2, the microsomal fraction is noted to have over three-fold specific activity over the homogenate in both LPP and cholinephosphotransferase, an endoplasmic reticulum marker. Therefore, the microsomal fraction was used as the protein source for further characterization. The specific activities (nmol/min/mg) of the various enzymic activities in the whole homogenate are: 16.5±1.0 (5'-nucleotidase), 7.2±0.2 (alkaline phosphatase), 6.5±0.6 (acid phosphatase), 0.11±0.02 (monoamine oxidase), 0.8±0.1 (cholinephosphotransferase), 0.052±0.014 (Na^+K^+-ATPase), and 3.6±0.3 (PAP2). These specific activities did not vary by more than 30% in different preparations reported in these studies.

An incubation period of 60 min was used for measuring LPP activity as this was found to be within the linear range. Figure 2.3A shows a linear protein curve until 75μg and, hence, 10-50μg of microsomal protein was used for subsequent experiments. The effect of Triton X-100 on LPP activity, as illustrated in Figure 2.3B, was investigated using pure PA or mixed PA:PC (1:1) as substrate. Addition of PC

Figure 2.1. The effect of NEM on PAPase activities in rat lung microsomal fractions. The fractions were preincubated with varying concentrations of NEM. LPP activities were measured using pure phosphatidate (●) and PAP1 activities were also performed and are indicated by the circles (○). The specific activities of PAP1 and LPP at 0mM NEM are 1.61±0.14 and 8.68±0.27 nmol/min/mg, respectively.

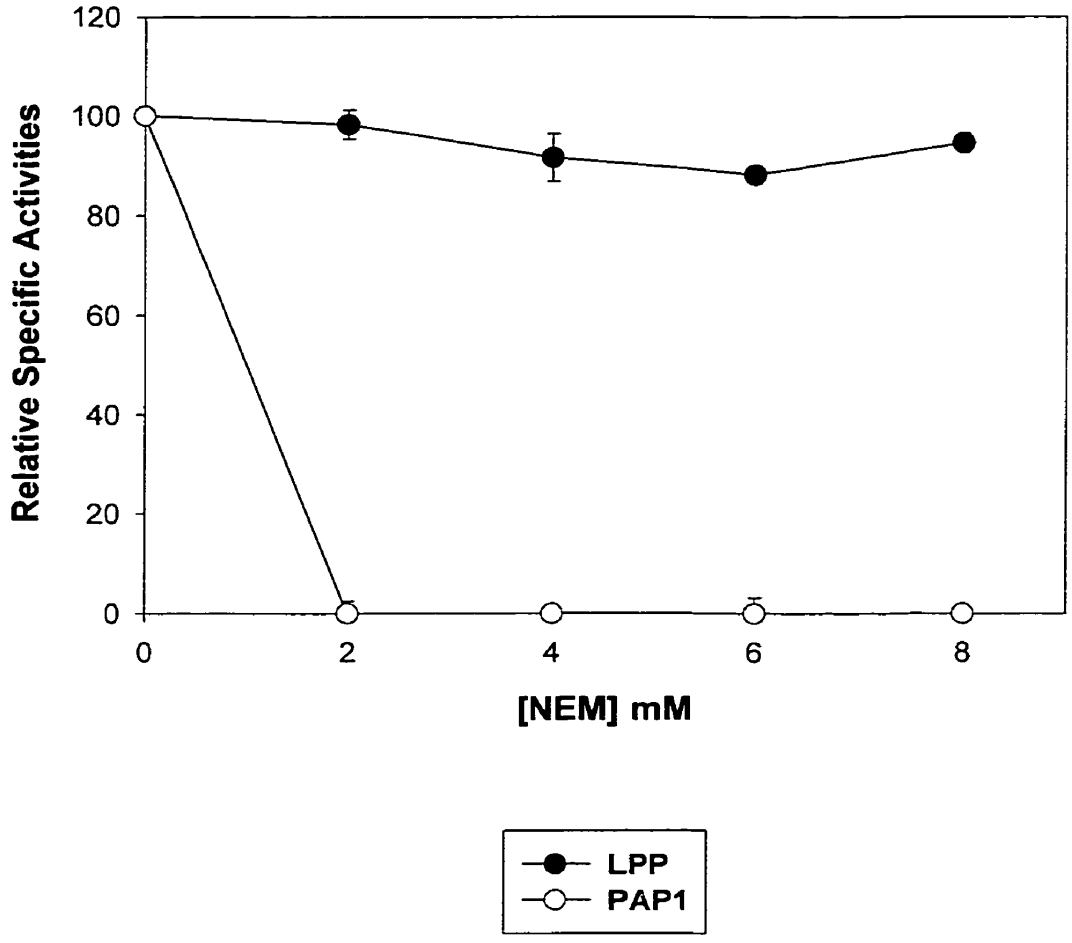
120
100
80
60
40
20
0
Relative Specific Activities
0
2
4
6
8
[NEM] mM
LPP
PAP1

Figure 2.2. Relative specific activities of various enzyme markers in rat lung subcellular fractions. Various subcellular fractions were incubated for 30 minutes at 37^0C for all enzyme assays with the exception of LPP in which the incubation time was 60 minutes (n=3) where C is cytosol, N is nuclear fraction, M is mitochondrial fraction and P is microsomal fraction. A, PAP2; B, CPT (cholinephosphotransferase); C, MAO (monoamine oxidase); D, acid phosphatase; E, Na^+K^+-ATPase; F, alkaline phosphatase; and G, 5'-nucleotidase are shown as relative specific activities. The specific activities (nmol/min/mg) of the various enzymic activities in the whole homogenate are: 16.5±1.0 (5'-nucleotidase), 7.2±0.2 (alkaline phosphatase), 6.5±0.6 (acid phosphatase), 0.11±0.02 (monoamine oxidase), 0.8±0.1 (cholinephosphotransferase), 0.052±0.014 (Na^+K^+-ATPase), and 3.6±0.3 (PAP2).

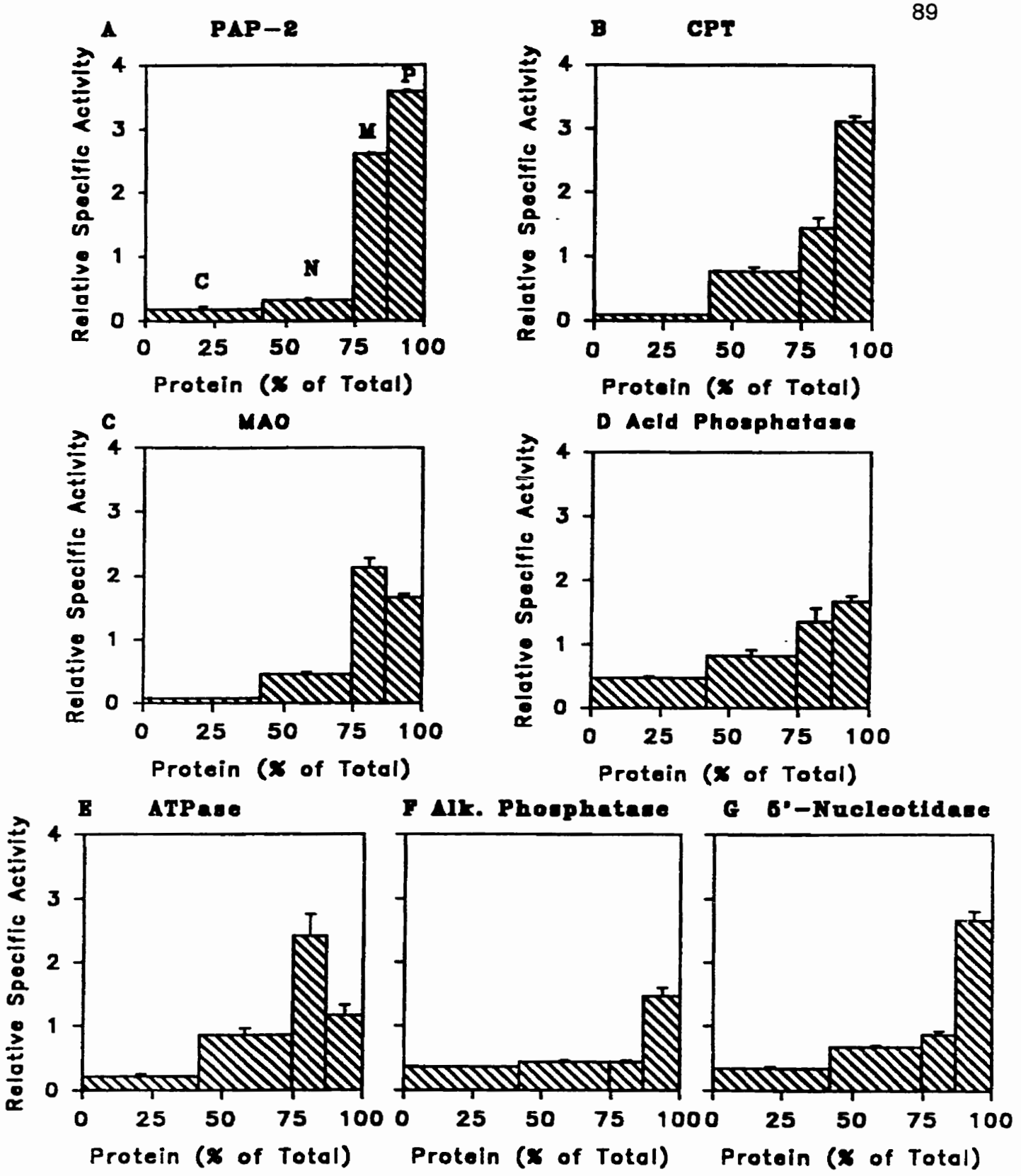
A PAP-2
B CPT
C MAO
D Acid Phosphatase
E ATPase
F Alk. Phosphatase
G 5'-Nucleotidase
Relative Specific Activity
Protein (% of Total)
C
N
M
P
0
1
2
3
4
0
25
50
75
100

Figure 2.3. The effect of varying microsomal protein, Triton X-100, substrate concentration, and pH on LPP activity. In A, various amounts of microsomal fractions were preincubated with 4.2mM NEM using 0.6mM of pure PA as the substrate. The effect of varying the concentration of Triton X-100 on the LPP activity is shown in B and was measured using 50 μg of microsomes with 0.3mM PA (●) or with a mixture of PC and PA (○). In C, the effect of varying the amount of pure PA as substrate in the assay medium for the LPP activity is shown. The activity of LPP was measured using microsomal fractions. In D, the effect of varying the amount of the substrate, PC and PA with Triton X-100 (▽), is shown. The effect of varying the pH on the LPP activity is shown in E and F. LPP activity was measured either using the PA alone (E) or in combination with PC and Triton X-100 (F).

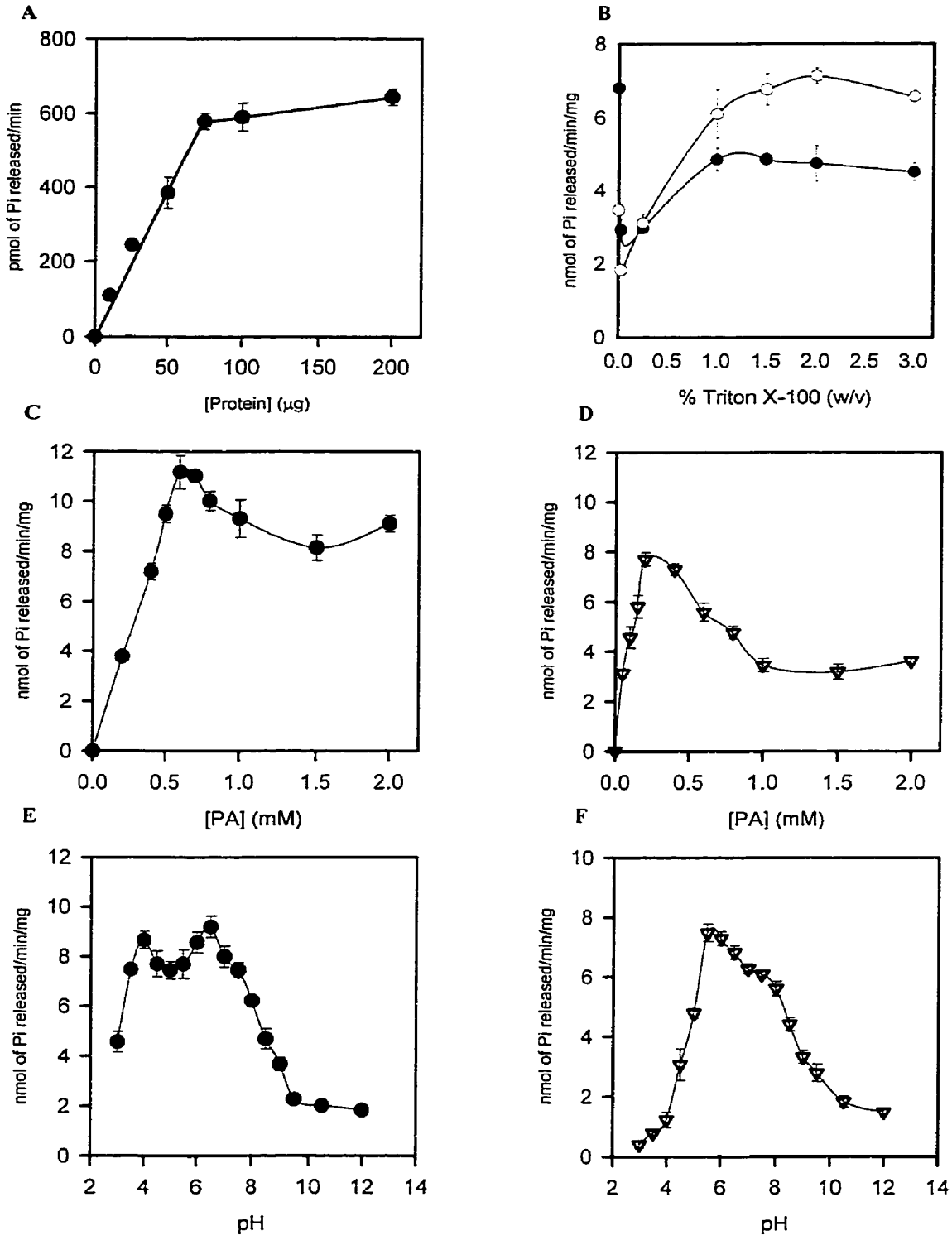
A
pmol of Pi released/min
800
600
400
200
0
0
50
100
150
200
[Protein] (µg)
B
nmol of Pi released/min/mg
8
6
4
2
0
0.0
0.5
1.0
1.5
2.0
2.5
3.0
% Triton X-100 (w/v)
C
nmol of Pi released/min/mg
12
10
8
6
4
2
0
0.0
0.5
1.0
1.5
2.0
[PA] (mM)
D
nmol of Pi released/min/mg
12
10
8
6
4
2
0
0.0
0.5
1.0
1.5
2.0
[PA] (mM)
E
nmol of Pi released/min/mg
12
10
8
6
4
2
0
2
4
6
8
10
12
14
pH
F
nmol of Pi released/min/mg
10
8
6
4
2
0
2
4
6
8
10
12
14
pH

to the pure substrate reduced LPP specific activity by 49%. However, the addition of Triton X-100, a non-ionic detergent, appeared to relieve this inhibition with an optimum at 1%, which is 1.5-fold greater than the activity with pure PA at 1% detergent. Therefore, either pure PA without detergent or mixed PA:PC (1:1) with 1% Triton X-100 were utilized for further characterization (Figure 2.3C and 2.3D). Substrate concentration curves resulted in optimal specific activities of 0.6mM and 0.3mM for the pure and mixed substrates, respectively. Furthermore, the optimal pH for LPP measured using the pure and mixed substrates was determined to be 6.5 and 6.0, respectively (Figure 2.3E and 2.3F). Experiments where microsomes were heated to 55^0C showed that LPP activity was not seriously affected after 20 minutes of heating and, hence, is quite heat stable. DTT had no effect on the enzyme activity at 55^0C, indicating that disulfide bonds are most likely not present in the active site.

2.3.2 Effect of Various Ions on LPP Activities

In contrast to PAP1, which is Mg^{+2}-dependent, LPP activity showed a slight 10-20% inhibition over 15mM magnesium chloride with either substrate (Figure 2.4A). Calcium, another bivalent cation, produced an inhibition of 60% by 10mM with the pure substrate alone (Figure 2.4B) while fluoride, a known phosphatase inhibitor, markedly inhibited the activity with the mixed but not pure substrate (Figure 2.4C).

2.3.3 Effect of amphiphilic amines and sphingoid bases on microsomal

Figure 2.4. The effect of various ions on the LPP activity in the microsomal fractions of rat lung. LPP activities were measured either using PA alone (●) or as a mixture with PC and Triton X-100 (○). The effect of magnesium chloride is shown in A. The effect of calcium chloride in shown in B. The effect of sodium fluoride is shown in C.

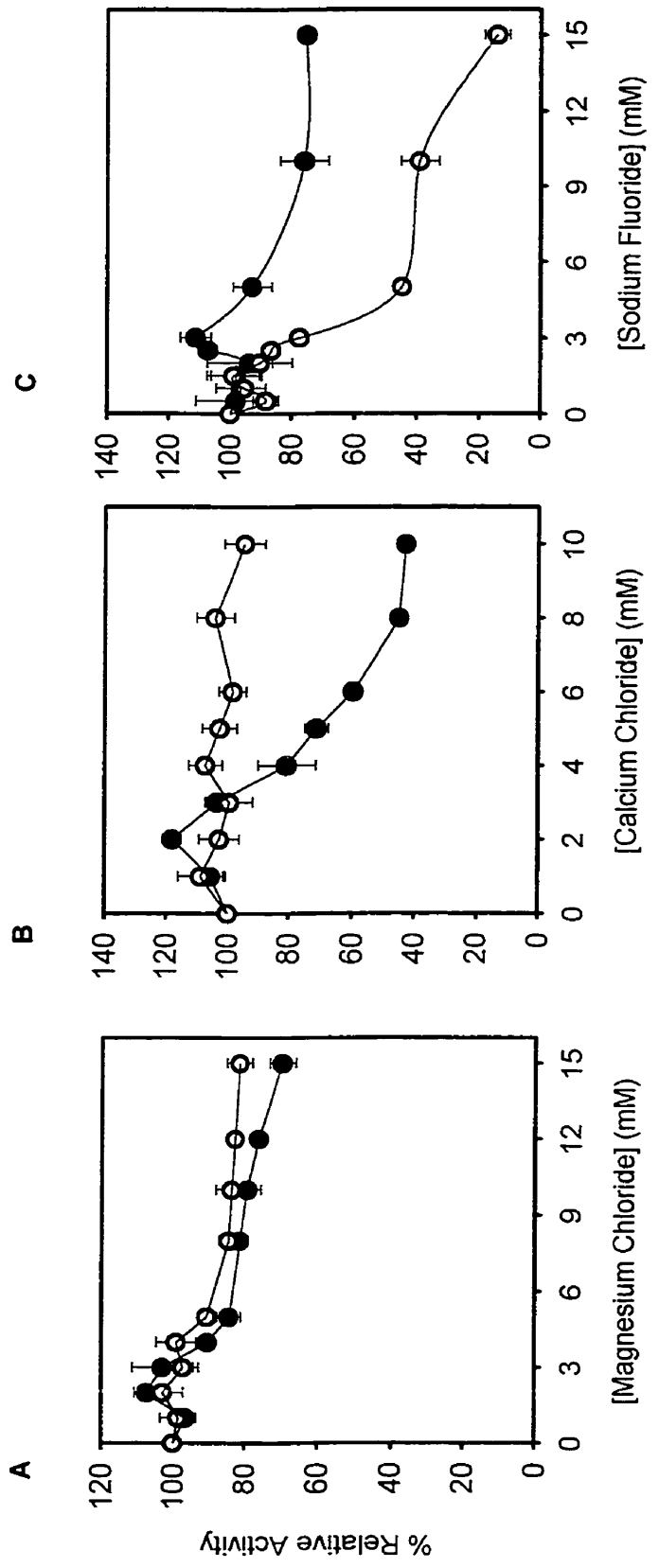
A
B
C
% Relative Activity
[Magnesium Chloride] (mM)
[Calcium Chloride] (mM)
[Sodium Fluoride] (mM)

LPP Activities

Amphiphilic cationic amines inhibit glycerolipid synthesis and interfere with the PLD pathway at the level of PAP in liver tissues (12, 14). Chlorpromazine, spermine, and spermidine trihydrochloride, the latter two of which are naturally occurring polyamines involved in the packaging of DNA in the nucleus (12), inhibited the LPP activity measured using the pure substrate (Figure 2.5A, 2.5B, and 2.5C). At an equimolar concentration of substrate, these cationic compounds induced 55% inhibition with chlorpromazine, 55% with spermine, and 7% with spermidine. However, with the mixed substrate, little of no effect was observed with these amphiphilic amines indicating the mechanism of inhibition could possibly be due to an interaction between the negatively charged substrate and the positively charged amine forming a substrate-inhibitor complex. As observed previously with PC, also a positively charged amphiphile, addition of the non-ionic detergent relieves this inhibition.

It has been known for sometime that agonist-induced breakdown of sphingomyelin has an important role in signal transduction in certain cells (14, 25, 26). The immediate breakdown product of sphingomyelin, ceramide, can cross-talk with signalling via phosphatidic acid by inhibiting the activation of PLD (12, 14). The deacylation product of ceramide, sphingosine, can activate PLD in some cell types (12, 14). Figure 2.6 shows the effect of these sphingoid bases on LPP activity with pure and mixed substrates. At an equimolar substrate concentration with the pure substrate, there was 72% inhibition with sphingomyelin and 93% with sphingosine. At an equimolar concentration with the mixed substrate, there was no effect with

Figure 2.5. The effect of amphiphilic amines and sphingoid bases on the LPP activity in rat lung microsomes. The LPP activity was determined with either PA alone (●) or as a mixture with PC and Triton X-100 (○) using microsomal fractions. The effect of chloropromazine on the LPP activity is shown in A. The effect of spermine on the LPP activity is shown in B. The effect of spermidine trihydrochloride on the LPP activities is shown in C.

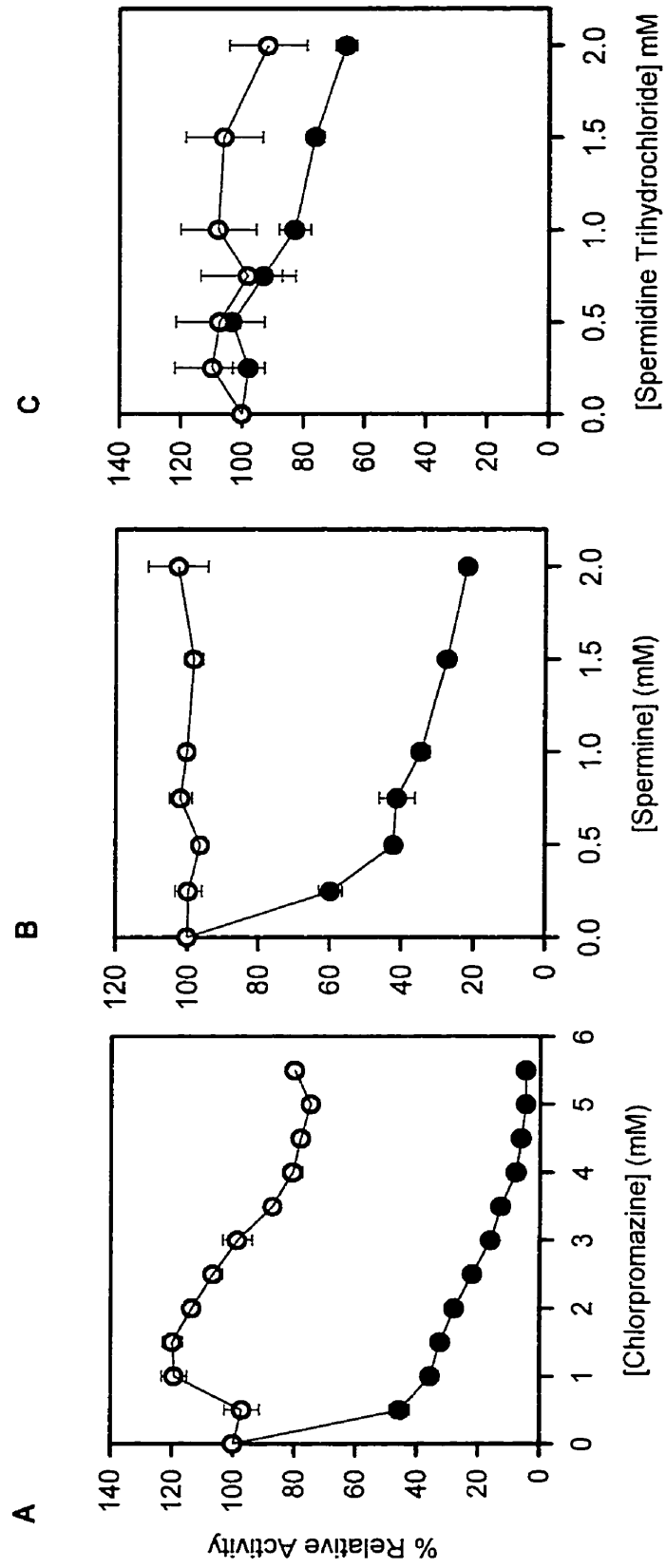
A
B
C
% Relative Activity
[Chlorpromazine] (mM)
[Spermine] (mM)
[Spermidine Trihydrochloride] mM

Figure 2.6. The effect of sphingoid bases on the NEM-insensitive PAP activity of rat lung. The LPP activity was determined with either PA alone (●) or as a mixture with PC and Triton X-100 (○) using microsomal fractions. The effect of sphingomyelin on the LPP activity is shown in A. The effect of sphingosine on the LPP activity is shown in B.

A

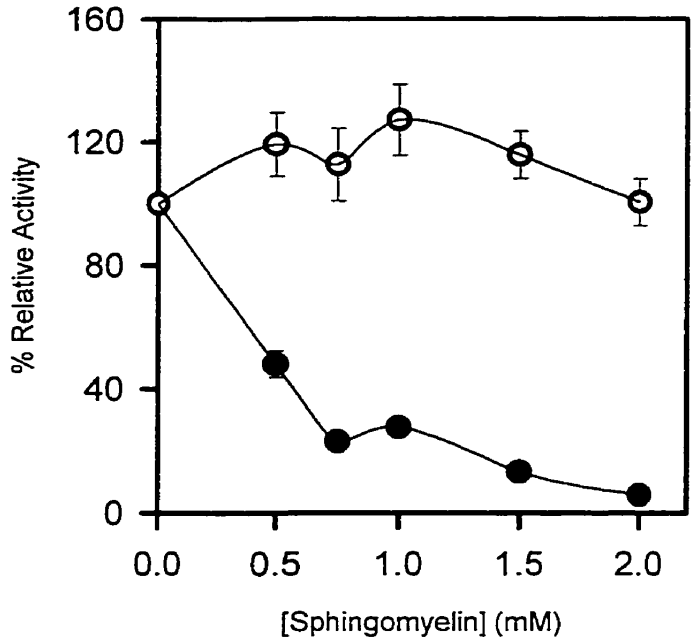
160
120
80
40
0
% Relative Activity
0.0
0.5
1.0
1.5
2.0
[Sphingomyelin] (mM)

B

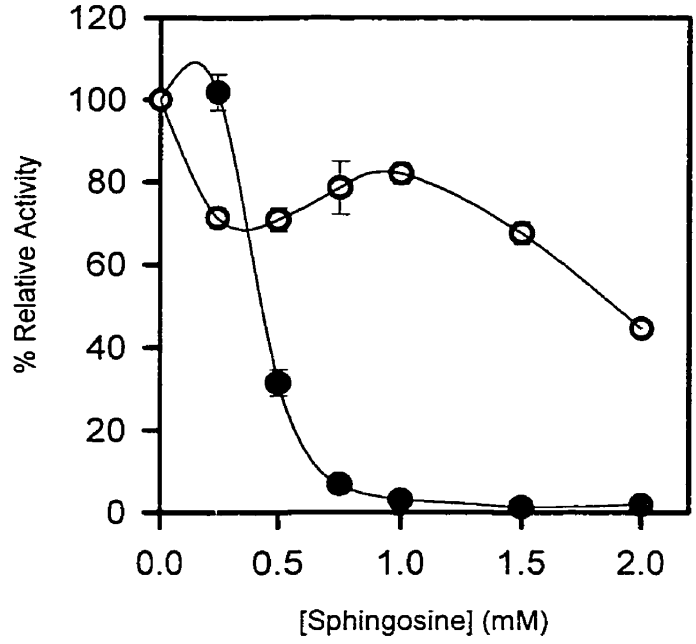
120
100
80
60
40
20
0
% Relative Activity
0.0
0.5
1.0
1.5
2.0
[Sphingosine] (mM)

sphingomyelin and 29% inhibition with sphingosine. The effects of ceramides were also investigated and only small 15-20% inhibitions were observed with N-acetyl ceramide (pure substrate) and N-hexanoyl ceramide (mixed), and with N-acetyl ceramide (mixed).

2.3.4 Effects of Other Lipids & Potential Substrates on Microsomal LPP Activities

It was of interest to examine whether potential lipid signaling molecules or similar lipids affected LPP activity. As shown in Figure 2.7, at equimolar substrate concentrations, DAG affected the enzyme activity by 45% and monoacylglycerol (MAG) inhibited the enzymatic activity by 21% using the mixed substrate. These results may indicate some form of regulation by the products of the LPP enzyme. With the pure substrate, little or no effect was observed. As neither LPP activity was inhibited by triacylglycerol (TAG) (Figure 2.7), these effects cannot be explained by nonspecific interactions with acylglycerols. Furthermore, the effect of LPA, S-1-P, and C-1-P was examined as shown in Figure 2.8A, 2.8B, and 2.8C. At equimolar substrate concentrations using the mixed substrate, there was 24% inhibition with LPA and little or no inhibition with S-1-P. With the pure substrate, there was an 85% inhibition with both LPA and C-1-P and less than 25% inhibition with S-1-P. These results suggest that LPA as well as C-1-P may be good substrates for the LPP enzyme and they could act as competitive inhibitors as shown by others (20) whereas the S-1-P would appear to be a poor substrate.

It has been previously demonstrated that rat liver LPP has a broad substrate

Figure 2.7. The effects of other lipids on LPP activity. The LPP activity was determined with either PA alone (●) or as a mixture with PC and Triton X-100 (○) using microsomal fractions. In A, the effect of MAG is shown. In B, the effect of DAG is shown. In C, the effect of TAG is shown.

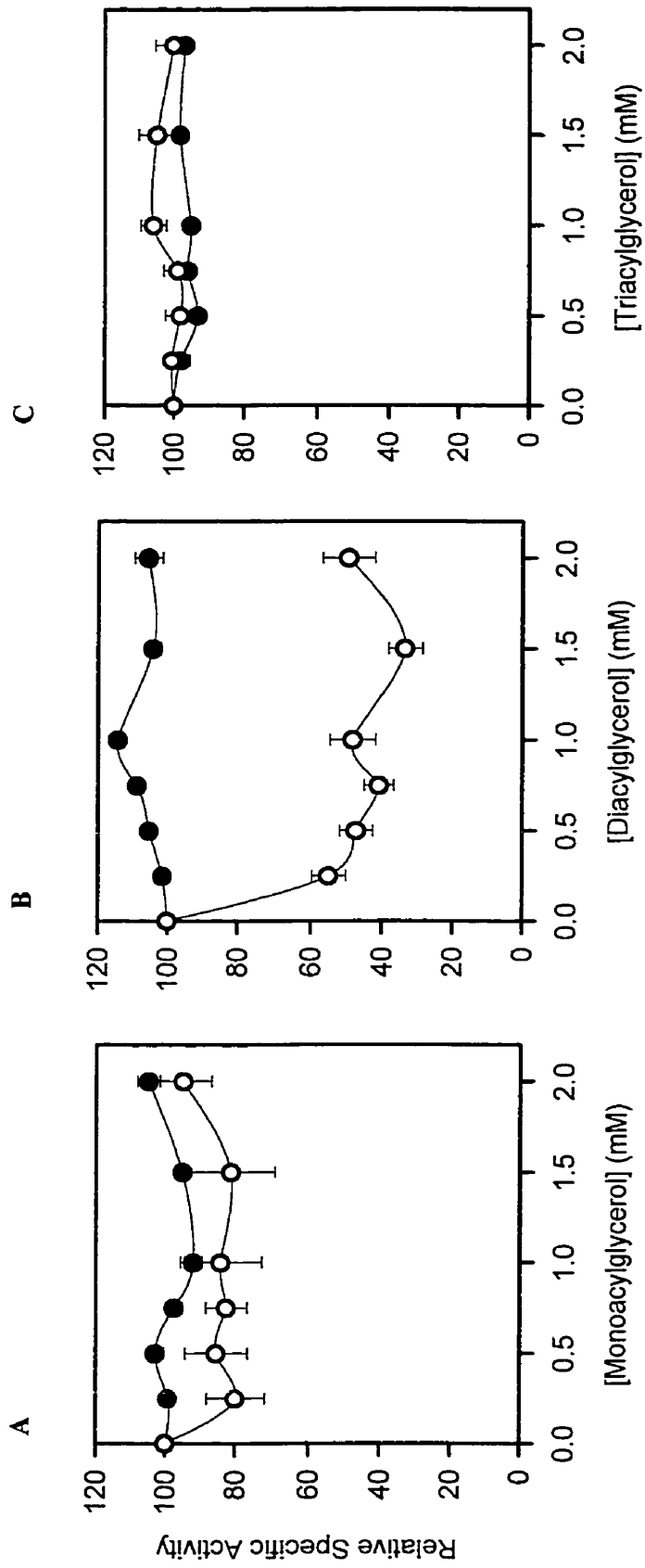
A
B
C
Relative Specific Activity
120
100
80
60
40
20
0
0.0
0.5
1.0
1.5
2.0
[Monoacylglycerol] (mM)
[Diacylglycerol] (mM)
[Triacylglycerol] (mM)

Figure 2.8. The effect of substrate analogs on LPP activity. The LPP activity was determined with either PA alone (●) or as a mixture with PC and Triton X-100 (○) using microsomal fractions. In A, the effect of lysophosphatidic acid (LPA) is shown. In B, the effect of ceramide-1-phosphate (C-1-P) is shown. In C, the effect of sphingosine-1-phosphate (S-1-P) is shown where the pure substrate is represented by black fill and the mixed substrate is represented by crosshatched lines.

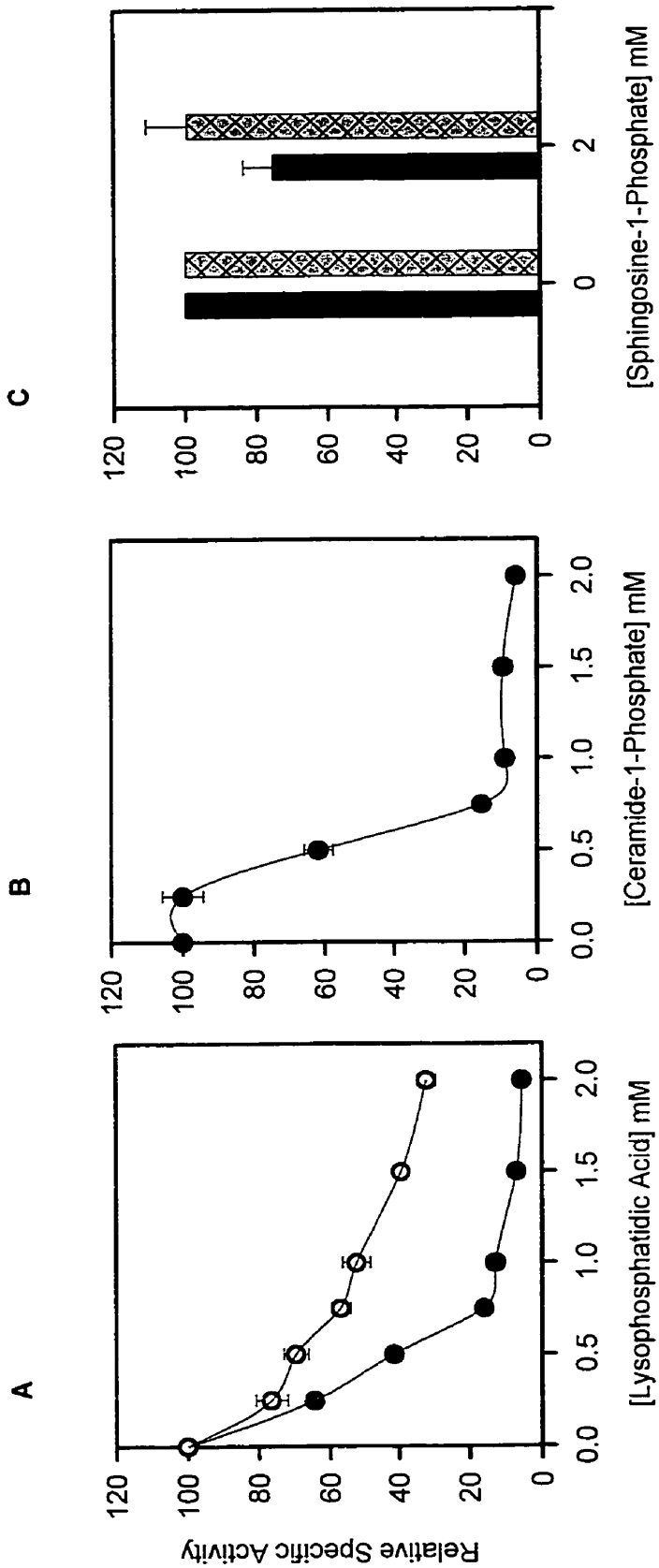
A
B
C
Relative Specific Activity
120
100
80
60
40
20
0
0.0
0.5
1.0
1.5
2.0
[Lysophosphatidic Acid] mM
[Ceramide-1-Phosphate] mM
0
2
[Sphingosine-1-Phosphate] mM

specificity utilizing not only PA but also LPA, C-1-P, and S-1-P (20). Kanoh and colleagues have also examined substrate specificity of LPP1 and LPP3 transfected in HEK 293 cells (27). They found that LPP1 had strong activity towards PA and LPA but weak activity towards C-1-P and no activity towards S-1-P (27). LPP3 had strong activity toward PA and S-1-P but displayed weak activity toward C-1-P and LPA (27). Moreover, another recently discovered novel isoform, namely LPP2, is able to hydrolyze PA and also LPA in HEK 293 cells (28). Substrate concentration curves were performed using both pure and mixed substrates for both LPA and S-1-P (Figure 2.9). For the pure substrates, 0.6mM and 1.5mM were used for LPA (17.6±0.2 nmol/mg/min) and S-1-P (1.4±0.1 nmol/mg/min), respectively, for further experiments. With the mixed substrates, 2mM was used for both LPA (9.6±0.1 nmol/mg/min) and S-1-P (0.8±0.3 nmol/mg/min), respectively, for further experiments. These specific activities can be compared to LPP assays utilizing PA as substrate where at 0.6mM of pure substrate, the specific activity was 11.2±0.7 nmol/min/mg and at 0.3mM of mixed substrate, the specific activity was 7.3±0.2 nmol/min/mg. At these optimal specific activities for the pure substrates, LPA gives 1.6-fold higher specific activity over PA as substrate and S-1-P is only an eighth the specific activity of PA. For the mixed substrates, LPA gives 1.3-fold higher specific activity over PA as substrate and S-1-P is only a fifteenth the specific activity of PA. This suggests that pulmonary LPP activity reflects mainly the specificity of LPP1 although northern blot analysis would suggest the presence of both pulmonary LPP1 and LPP3 isoforms (Chapter 3).

Figure 2.9. Substrate concentration curves for microsomal LPP with lysophosphatidic acid (LPA) and sphingosine-1-phosphate (S-1-P) as substrates. Assays performed with pure LPA is shown as ●, mixed (mixture with PC and Triton X-100) LPA is shown as ○, pure S-1-P is shown as ▼, and mixed S-1-P is shown as ▽.

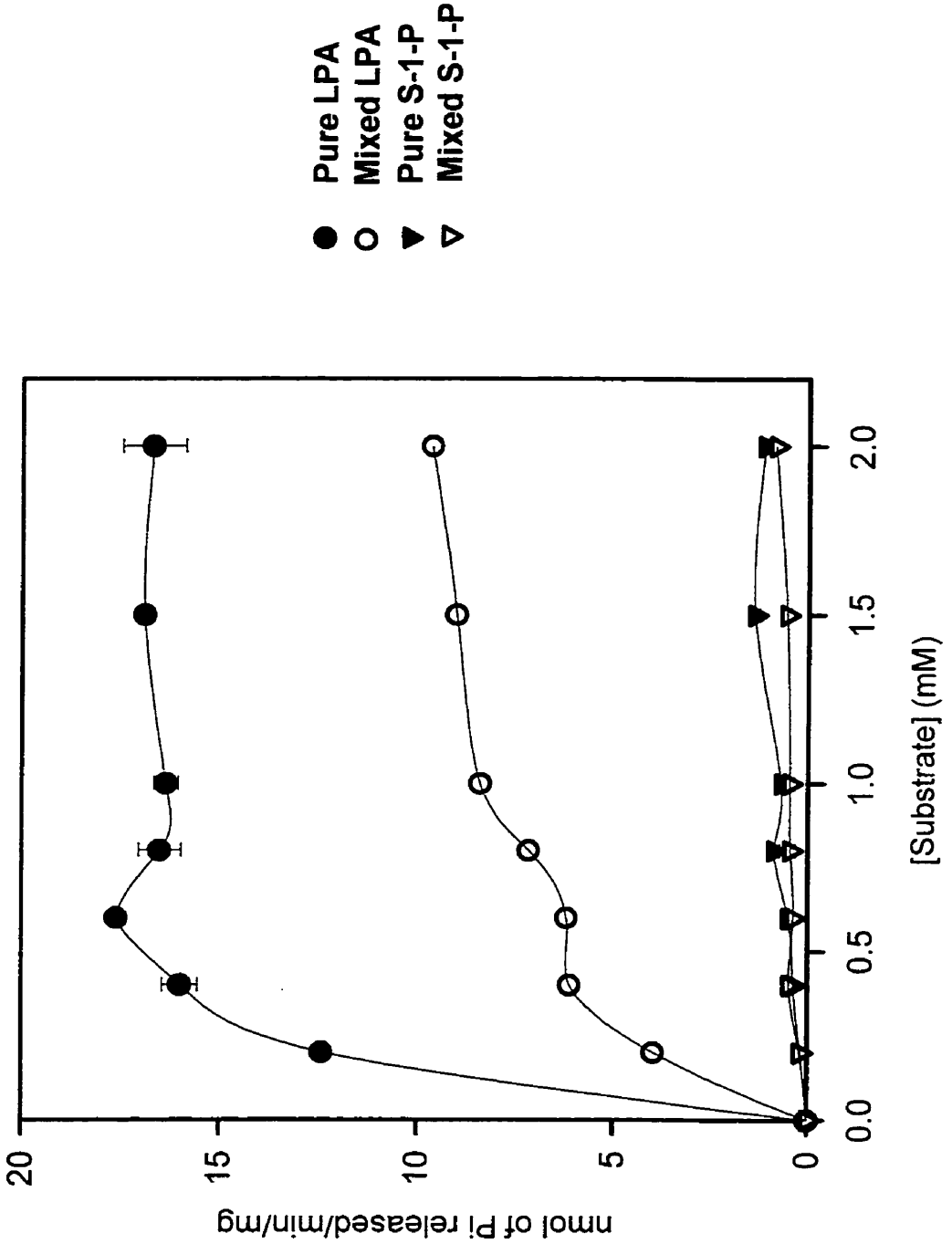
Pure LPA
Mixed LPA
Pure S-1-P
Mixed S-1-P
nmol of Pi released/min/mg
0
5
10
15
20
0.0
0.5
1.0
1.5
2.0
[Substrate] (mM)

2.3.5 LPP Activity in Purified Plasma Membranes from Rat Lung Tissue

Subcellular fractionation revealed that pulmonary LPP was found specifically associated with highly purified plasma membranes prepared by sucrose density and Percoll gradient centrifugations (Figure 2.10). The specific activity of LPP was found to be 6.9±1.6-fold higher over the homogenate, which is between the enrichment for 5'-nucleotidase (14.7±0.3), the apical plasma membrane marker, and for Na^+K^+-ATPase (4.0±0.2), the basolateral plasma membrane marker. Furthermore, the LPP activity profile was similar to 5'-nucleotidase and to a lesser extent Na^+K^+-ATPase and did not follow the endoplasmic reticulum (cholinephosphotransferase), mitochondrial (monoamine oxidase) or lysosomal (acid phosphatase) markers. Alkaline phosphatase showed a similar pattern. The presence of LPP in lung tissue plasma membranes shows that this enzymatic activity is appropriately located to participate in signal transduction. However, only 0.5±0.1% of the total protein was obtained and 3.3±0.8% and 7.5±1.6% of the total activities of LPP and 5'-nucleotidase, respectively, were recovered in the purified plasma membrane fraction. LPP activity using LPA and S-1-P as substrates was also examined and compared to the activities measured in whole lung homogenate, and both the microsomal and mitochondrial fractions (Figure 2.11). The relative specific activities for PA and LPA are very similar and are enriched in the Percoll purified plasma membranes. In contrast, when the S-1-P is used as substrate, the pattern is different and suggests that the LPP isoform in the plasma membrane does not hydrolyze this substrate.

Figure 2.10. Relative specific activities of various enzyme markers in rat lung plasma membranes. 10μg of various fractions were incubated at 37^0C (n=3) where, on the x-axis, A represents the control; B, sucrose gradient fraction 1; C, sucrose gradient fraction 2; D, sucrose gradient fraction 3; E, sucrose gradient fraction 4; F, purified plasma membranes; G, sucrose gradient fraction 5; and H, sucrose gradient pellet fraction. A, PAP2; B, Na^+K^+-ATPase; C, 5'-nucleotidase; D, alkaline phosphatase; E, CPT (cholinephosphotransferase); F, MAO (monoamine oxidase); and G, acid phosphatase are shown as relative specific activities.

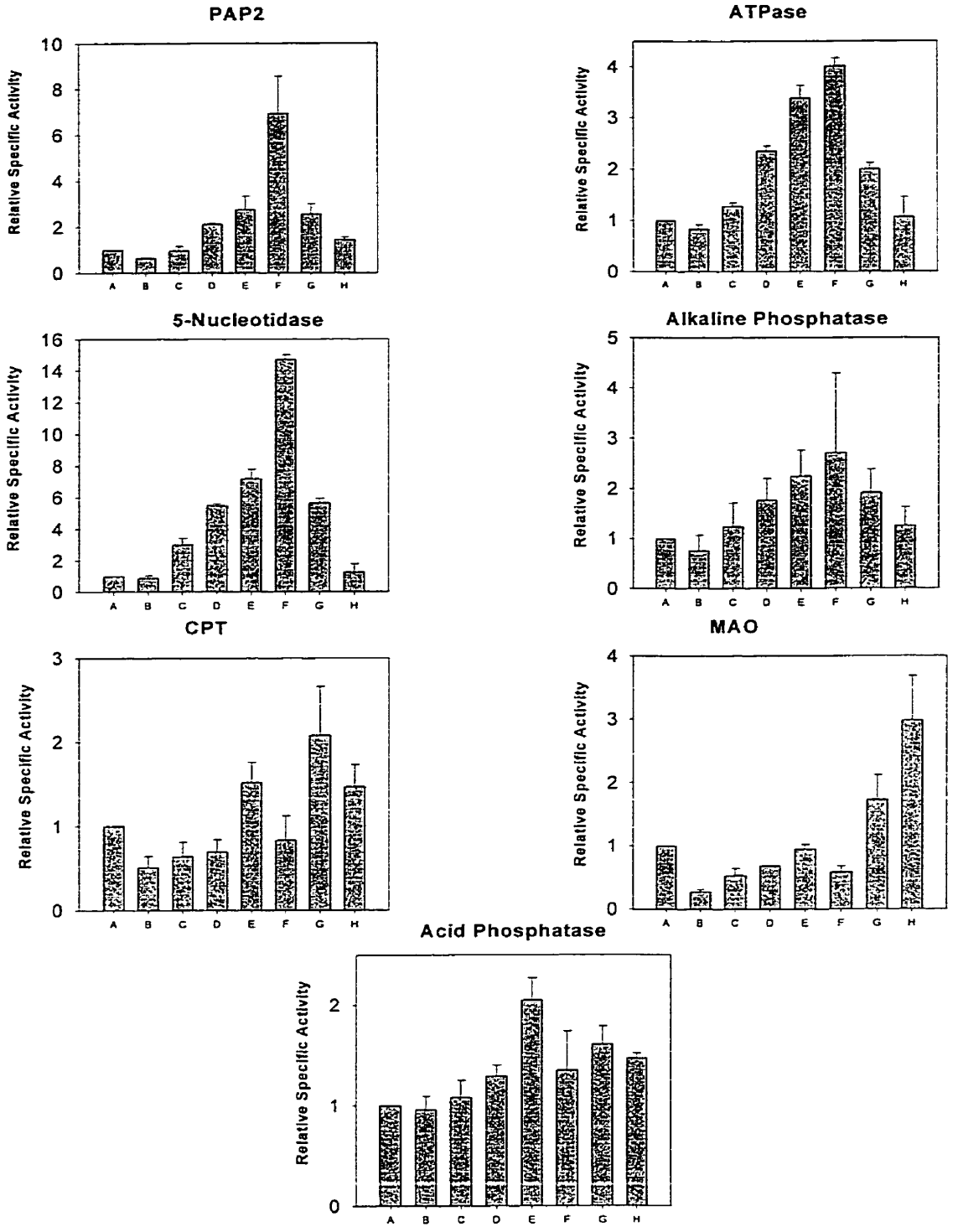
PAP2
Relative Specific Activity
10
8
6
4
2
0
A B C D E F G H
ATPase
Relative Specific Activity
4
3
2
1
0
A B C D E F G H
5-Nucleotidase
Relative Specific Activity
16
14
12
10
8
6
4
2
0
A B C D E F G H
Alkaline Phosphatase
Relative Specific Activity
5
4
3
2
1
0
A B C D E F G H
CPT
Relative Specific Activity
3
2
1
0
A B C D E F G H
MAO
Relative Specific Activity
4
3
2
1
0
A B C D E F G H
Acid Phosphatase
Relative Specific Activity
2
1
0
A B C D E F G H

Figure 2.11. PAP2 specific activities in microsomes, mitochondria, and plasma membranes utilizing different substrates as indicated. Mixed substrate involves substrate:PC (1:1) with 1% Triton X-100.

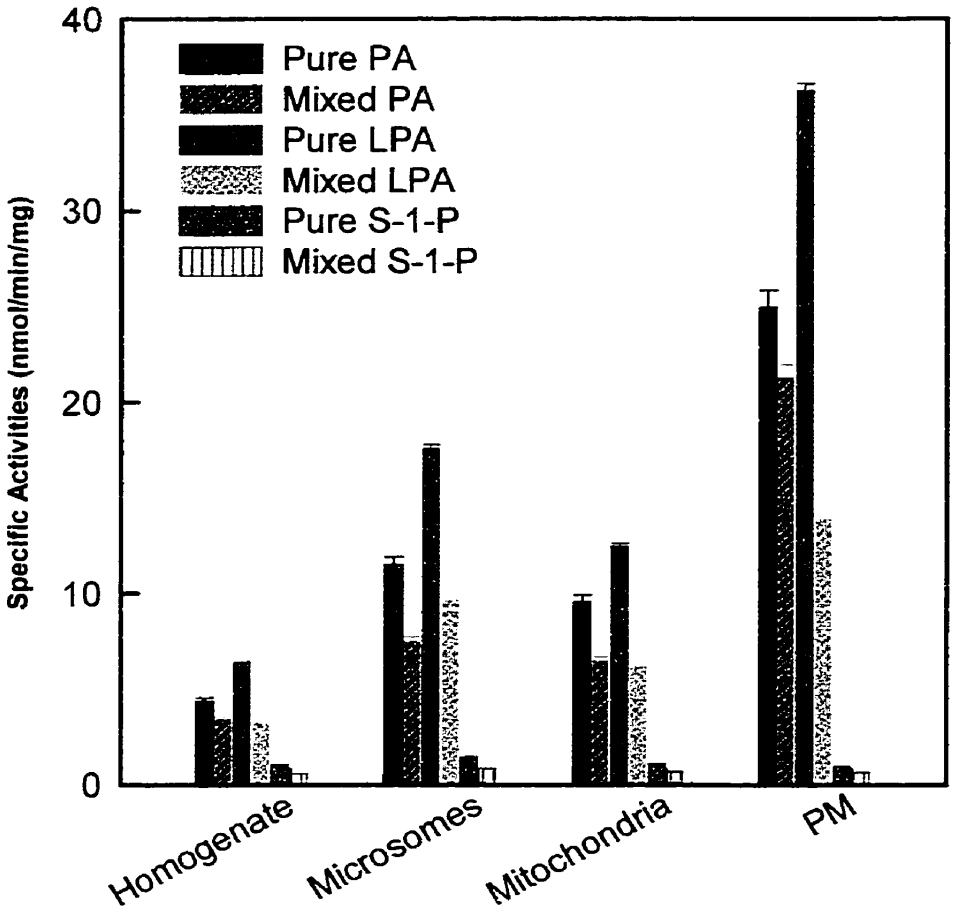
40
30
20
10
0
Specific Activities (nmol/min/mg)
Pure PA
Mixed PA
Pure LPA
Mixed LPA
Pure S-1-P
Mixed S-1-P
Homogenate
Microsomes
Mitochondria
PM

2.3.6 LPP Activity in Alveolar Type II cells and Fibroblasts

LPP activity was slightly enriched (1.2-fold over whole lung homogenate) in type II cells (Figure 2.12). Interestingly, cholinephosphotransferase (CPT), the terminal enzyme in PC synthesis was not enriched in type II cells. Comparison of the relative specific activity profile with type II cells revealed higher proportion of LPP than CPT activity, which remained associated with the high speed supernatant. This suggests that plasma membrane fragments remained in this "cytosolic" fraction. Type II cells were 2-fold enriched in the mitochondrial marker, monoamine oxidase, relative to whole lung homogenate. In contrast lung fibroblasts showed relatively low LPP activity. CPT activity in fibroblasts was similar to that shown in type II cells and whole lung but monoamine oxidase (MAO) activity was relatively low.

2.4 Discussion

Subcellular distribution studies showed that lung microsomes had the highest specific activity of LPP and this fraction was used to characterize the enzyme. Further studies revealed that the enzyme had a distribution similar to the plasma membrane markers, 5'-nucleotidase and Na^+K^+-ATPase. The relative specific activity in the percoll-purified plasma membrane was 6.9±1.6 which was 1.9-fold greater than the relative specific activity in microsomes. Previous investigations have shown that DAG generated by LPP is not available to CPT, a recognized endoplasmic reticulum marker (8, 10). The yield for plasma membranes is very low (0.5%) compared to microsomes (12.5%). For this reason, it was decided not to

Figure 2.12. Relative specific activities of PAP2, CPT and MAO in isolated type II cells (A, B, C) and fibroblasts (D, E, F) are shown. The specific activities in the type II cell sonicate are (nmol/min/mg): 4.4±0.8 (PAP2), 0.9±0.1 (CPT), and 0.25±0.03 (MAO). The specific activities in the fibroblast sonicate are (nmol/min/mg): 0.50±0.01 (PAP2), 0.75±0.09 (CPT) and 0.09±0.01(MAO). Abbreviations: TIIH, type II cell sonicates; Fibroblasts H, fibroblast sonicates; M, total membranes; C, cytosol; and WLH, whole lung homogenate.

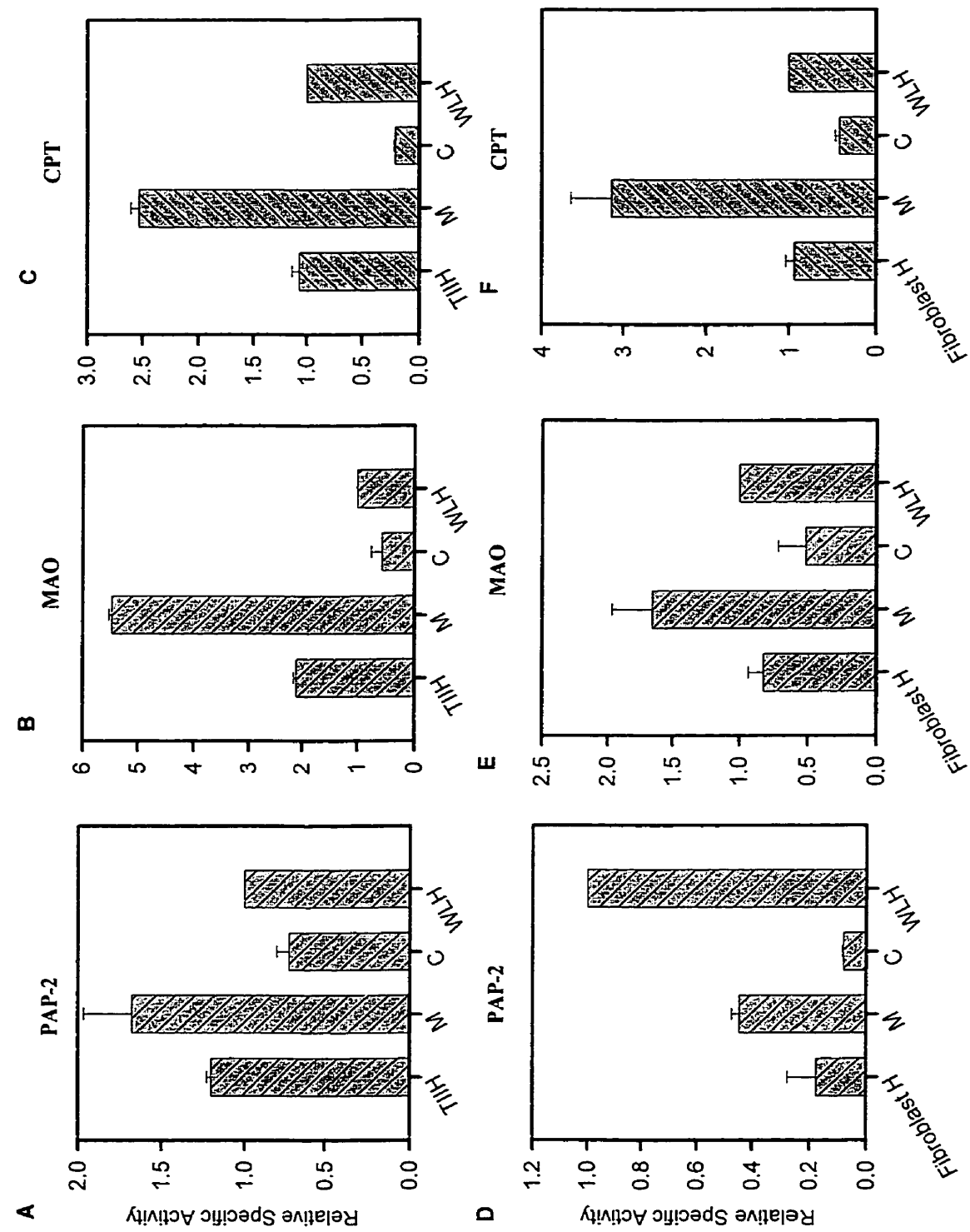
A
PAP-2
Relative Specific Activity
2.0
1.5
1.0
0.5
0.0
THH
M
C
WLH
B
MAO
6
5
4
3
2
1
0
C
CPT
3.0
2.5
2.0
1.5
1.0
0.5
0.0
D
PAP-2
Relative Specific Activity
1.2
1.0
0.8
0.6
0.4
0.2
0.0
Fibroblast H
E
MAO
2.5
2.0
1.5
1.0
0.5
0.0
F
CPT
4
3
2
1
0

repeat the characterization studies using purified plasma membranes.

The studies presented in this chapter show that differential inhibition by NEM readily distinguishes pulmonary LPP from PAP1 activity. As with hepatic PAP1 (12), pulmonary LPP is inhibited by a variety of amphiphilic amines such as chlorpromazine, by sphingoid derivatives such as sphingosine, and by lipids including DAG and MAG. Inhibition by amphiphiles was relieved by presenting the substrate with equimolar PC in the presence of Triton X-100.

Pulmonary LPP activity shows considerable similarity to the corresponding activities in porcine thymus (13), rat liver (12, 20, 29), and human HEK 293 cells (27, 28) but more importantly a few interesting differences were noted. LPP activity from porcine thymus membranes (13) was more specific for PA, since in contrast to the pulmonary activity, it was not inhibited by LPA or MAG and was less susceptible to DAG inhibition. Pulmonary LPP also showed differences compared to the rat liver activity such as a lower susceptibility to calcium chloride (20% versus 80% inhibition at 4mM calcium chloride) and sodium fluoride (no effect versus 60% inhibition at 2mM) with pure substrate (12). In addition, hepatic LPP activity is stimulated rather than inhibited at low Triton X-100 (12). It has been reported that antibodies generated against purified rat liver, LPP did not show cross reactivity with the pulmonary enzyme (30). Rat liver LPP activity shows a higher reactivity towards S-1-P (20) compared with the lung activity.

Recent investigations have demonstrated the presence of three human isoforms, namely LPP1, LPP2, and LPP3, and northern blotting indicates the presence of LPP1 and LPP3 but not LPP2 in lung (27, 28, 31, 32, 33, 34). The

observation that pulmonary LPP hydrolyzes PA and LPA but not S-1-P suggests that LPP1 activity predominates although northern blotting reveals the presence of LPP1 and LPP3 in lung tissues.

The 6.9±1.6-fold enrichment of LPP activity observed with purified plasma membranes was intermediate between the plasma membrane markers, 5'-nucleotidase (14.7±0.3) and Na^+K^+-ATPase (4.0±0.2). These results indicate that the purification procedure resulted in greater apical membrane enrichment as opposed to basolateral plasma membrane. The subcellular distribution study depicted in Figure 2 reveals the LPP activity profile does not resemble that for either 5'-nucleotidase or Na^+K^+-ATPase but calculations show a closer relationship with the profile generated for combined 5'-nucleotidase and ATPase activities. This would suggest LPP activity could be present in both apical and basolateral locations. The plasma membrane localization for pulmonary LPP is consistent with the subcellular localization reported previously for liver, thymus, and kidney membranes (12, 13, 33). The plasma membrane localization indicated by our studies is appropriate for the previously suggested role of pulmonary LPP in signal transduction (35, 36). Ecto- LPP activities, which can hydrolyze PA and LPA supplied to the cells' surface, have been reported for neutrophils and keratinocytes (37) but further work will be required to establish whether pulmonary LPP functions with substrates localized in the inner or outer leaflet of the plasma membrane. Furthermore, while its presence in lung plasma membranes appears established, the possible presence of functional LPP in other membraneous subcellular organelles is not excluded by our studies. In this context, Dri 42, a rat LPP3 isoform

was found localized in endoplasmic reticulum in rat intestine by immunohistochemistry (32). As lung develops as an outcropping of the foregut, this observation is relevant to our subcellular distribution studies.

The potential presence of LPP activity in type II alveolar cells has been postulated from observations indicating that ATP and UTP promotion of surfactant secretion via P_2-receptor activation of phosphatidylinositol-specific phospholipase C (PLC) results in only a transient release of a inositol-trisphosphate (IP_3) and DAG. The continued liberation of DAG required for surfactant secretion likely arises through the action of phospholipase D (PLD) which has been demonstrated in type II cells by transphosphatidylation reactions with radioactive phosphatidylethanol (17, 35, 36). The presence of LPP activity in rat lung plasma membranes and in type II cells could be involved in PA hydrolysis thereby providing DAG for protein kinase C activation. Since PKC can activate PLD, this would provide a mechanism for perpetuating a PLD/ LPP pathway resulting in prolonged DAG elevation, PKC activation allowing for type II cells to continuously secrete surfactant for considerable periods. The present studies, although consistent with this hypothesis (17) requires further experimental support.

2.5 Acknowledgements

We would like to express our gratitude to Dr. A. Chander (Jefferson Medical School, Philadelphia) for his advice on the preparation of plasma membranes. We are also grateful to Dr. D. Brindley (University of Alberta, Edmonton) for stimulating discussions. We also thank Kevin Inchley and Anne Brickenden for their invaluable

technical advice. This work was supported by a group grant from the Medical Research Council of Canada (M268C7).

2.6 References

1. **Kates M.** 1955. Hydrolysis of lecithin by plant plastid enzymes. Can. J. Biochem. **35**: 575-589.

2. **Hubscher, G.** 1970. Glyceride Metabolism. In: Wakil SJ, ed. Lipid Metabolism. New York: Academic Press; 270-370.

3. **Meban C.** 1972. Localization of phosphatidic acid phosphatase activity in granular pneumonocytes. J. Cell. Biol. **53**:249-252.

4. **Schultz FM, Jimenez JM, MacDonald PC, and Johnston JM.** 1974. Fetal lung maturation. I. Phosphatidic acid phosphohydrolase in rabbit lung. Gynecol. Invest. **5**: 222-229.

5. **Brehier A, Benson BJ, Williams MC, Mason RJ, and Ballard PL.** 1977. Corticosteroid induction of phosphatidic acid phosphatase in fetal rabbit lung. Biochem. Biophys. Res. Commun. **77**: 883-890.

6. **Douglas WHJ, Sommers-Smith SK, and Johnston JM.** 1983. Phosphatidate phosphohydrolase activity as a marker for surfactant synthesis in organotypic cultures of type II alveolar pneumonocytes. J. Cell. Sci. **60**: 199-207.

7. **Gluck L, Sribney M, and Kulovich MV.** 1967. The biochemical development of surface activity in mammalian lung. II The biosynthesis of phospholipids in the lung of the developing rabbit fetus and newborn. Pediatr. Research. **1**: 247-265.

8. **Walton PA and Possmayer F.** 1985. Mg^{+2}-dependent phosphatidate phosphohydrolase of rat lung: development of an assay employing a defined chemical substrate which reflects the phosphohydrolase activity measured using membrane-bound substrate. Anal. Biochem. **151**: 479-486.

9. **Walton PA and Possmayer F.** 1986. Translocation of Mg^{+2}-dependent phosphatidate phosphohydrolase between cytosol and endoplasmic reticulum in a permanent cell line from human lung. Biochem. Cell Biol. **64**: 1135-1140.

10. **Walton PA and Possmayer F.** 1984. The role of Mg^{+2}-dependent

phosphatidate phosphohydrolase in pulmonary glycerolipid biosynthesis. Biochim. Biophys. Acta. **796**: 364-372.

11. **Yeung A, Casola P, Wong C, Fellows JF, and Possmayer F.** 1979. Pulmonary phosphatidic acid phosphatase. A comparative study of the aqueously dispersed phosphatidate-dependent and membrane bound phosphatidate-dependent phosphatidic acid phosphatase activities of rat lung. Biochim. Biophys. Acta. **574**: 226-239.

12. **Jamal Z, Martin A, Gomez-Munoz A, and Brindley DN.** 1991. Plasma membrane fractions from rat liver contain a phosphatidate phosphohydrolase distinct from that in the endoplasmic reticulum and cytosol. J. Biol. Chem. **266**: 2988-2996.

13. **Kanoh H, Imai S, Yamada K, and Sakane F.** 1992. Purification and properties of phosphatidic acid phosphatase from porcine thymus membranes. J. Biol. Chem. **267**: 25309-25314.

14. **Brindley DN and Waggoner DW.** 1996. Phosphatidate phosphohydrolase and signal transduction. Chem. Phys. Lipids. **80**: 45-57.

15. **Rooney SA.** 1985. The surfactant system and lung phospholipid biochemistry. Am. Rev. Respir. Dis. **131**: 439-460.

16. **Ide H and Weinhold PA.** 1982. Properties of diacylglycerol kinase in adult and fetal rat lung. Biochim. Biophys. Acta. **713**: 547-554.

17. **Rooney SA and Gobran LI.** 1991. Activation of phospholipase D in rat type II pneumocytes by ATP and other surfactant secretagogues. Am. J. Physiol. **264**: L133-L140.

18. **Chander A and Wu R.** 1991. In vitro fusion of lung lamellar bodies and plasma membrane is augmented by lung synexin. Biochim. Biophys. Acta. **1086**: 157-166.

19. **Dobbs L.** 1990. Isolation and culture of alveolar type II cells. Am. J. Physiol. **258**: L134-L147.

20. **Waggoner DW, Gomez-Munoz A, Dewald J, and Brindley DN.** 1996. Phosphatidate phosphohydrolase catalyzes the hydrolysis of ceramide-1-phosphate, lysophosphatidate, and sphingosine-1-phosphate. J. Biol. Chem. **271**: 16506-16509.

21. **Possmayer F, Klein L, Duwe G, Stewart-Dehaan PJ, Wong T, MacPherson**

CF, and Harding PG. 1979. Differences in the subcellular and subsynaptosomal distribution of the putative endoplasmic reticulum markers, NADPH-cytochrome c reductase, estrone sulfate sulfhydrolase, and CDP-choline-diacylglycerol cholinephosphotransferase in rat brain. J. Neurochem. **32**: 889-906.

22. **Chander A.** 1992. Dicyclohexylcarbodiimide and vanadate sensitive ATPase of lung lamellar bodies. Biochem. Biophys. Acta. **1123**: 198-206.

23. **Lowry OH, Rosebrough HJ, Farr AL, and Randall RJ.** 1951. Protein measurement with the folin phenol reagent. J. Biol. Chem. **193**: 265-275.

24. **Rouser G, Fleisher S, and Yamamoto A.** 1970. Two dimensional thin layer chromatographic separation of polar lipids and determination of phospholipids by phosphorous analysis of spots. Lipids. **5**: 494-496.

25. **Merill AH (Jr.) and Stevens VL.** 1989. Modulation of protein kinase C and diverse cell functions by sphingosine- a pharmacologically interesting compound linking sphingolipids and signal transduction. Biochim. Biophys. Acta. **1010**: 131-139.

26. **Hannun YA.** 1991. The sphingomyelin cycle and the second messenger function of ceramide. J. Biol. Chem. **269**: 3125-3128.

27. **Kai M, Wada I, Imai S, Sakane F, and Kanoh H.** 1997. Cloning and characterization of two human isozymes of Mg^{+2}-independent phosphatidic acid phosphatases. J. Biol. Chem. **270**: 24572-24578.

28. **Hooks SB, Ragan SP, and Lynch KR.** 1998. Identification of a novel human phosphatidic acid phosphatase type 2 isoform. FEBS Lett. **427**: 188-192.

29. **Fleming IN and Yeaman SJ.** 1995. Purification and characterization of N-ethylmaleimide-insensitive phosphatidic acid phosphohydrolase (PAP2) from rat liver. Biochem. J. **308**: 983-989.

30. **Waggoner DW, Martin A, Dewald J, Gomez-Munoz A, and Brindley DN.** 1995. Purification and characterization of a novel plasma membrane phosphatidate phosphohydrolase from rat liver. J. Biol. Chem. **270**: 19422-19429.

31. **Barila D, Murgia C, Nobili F, Gaetani S, and Perozzi G.** 1994. Subtractive hybridization cloning of novel genes differentially expressed during intestinal development. Eur. J. Biochem. **223**: 701-709.

32. **Barila D, Plateroti M, Nobili F, Muda AO, Xie Y, Morimoto T, and Perozzi G.** 1996. The Dri42 gene, whose expression is up-regulated during epithelial differentiation, encodes a novel endoplasmic reticulum resident transmembrane protein. J. Biol. Chem. **271**: 29928-29936.

33. **Kai M, Wada I, Imai S, Sakane F, and Kanoh H.** 1996. Identification and cDNA cloning of 35kDa phosphatidic acid phosphatase (type 2) bound to plasma membranes. J. Biol. Chem. **271**: 18931-18938.

34. **Leung DW, Tompkins CK, and White T.** 1998. Molecular cloning of two alternatively spliced forms of human phosphatidic acid phosphatase cDNAs that are differentially expressed in normal and tumor cells. DNA and Cell Biol. **17**: 377-385.

35. **Griese M, Gobran LI, and Rooney SA.** 1991. ATP-stimulated inositol phospholipid metabolism and surfactant secretion in rat type II pneumocytes. Am. J. Physiol. **260**: L586-L593.

36. **Griese M, Gobran LI, Rooney SA.** 1993. Potentiation of A_2 purinoceptor-stimulated surfactant phospholipid secretion in primary cultures of rat type II pneumonocytes. Lung. **171**: 75-86.

37. **English D, Martin M, Harvey KA, Akard LP, Allen R, Widlanski TS, Garcia JGN, and Siddiqui RA.** 1997. Characterization and purification of neutrophil ecto-phosphatidic acid phosphohydrolase. Biochem. J. **324**: 941-950.

Chapter 3

Molecular Cloning and Expression of Pulmonary Lipid Phosphate Phosphohydrolases

[1] A version of this chapter has been submitted for publication.

Nanjundan M and Possmayer F. Molecular cloning and expression of pulmonary lipid phosphate phosphohydrolases. Submitted to Am. J. Physiol. Lung.

3.1 Introduction

There exist two forms of pulmonary phosphatidic acid phosphohydrolases (PAPases), namely PAP1 and LPP (formerly called PAP2). The former is a Mg^{+2}-dependent, N-ethylmaleimide (NEM)-sensitive, cytosolic enzyme (1). Cytosolic PAP1 can translocate to the endoplasmic reticulum where it becomes metabolically functional in glycerolipid biosynthesis (1). In contrast, pulmonary LPP is a NEM-insensitive, Mg^{+2}-independent, membrane-bound enzyme primarily localized to the plasma membrane (2). Both PA and LPA were excellent substrates for LPP in purified rat lung plasma membranes whereas S-1-P was a relatively poor substrate. This contrasts with liver LPP whose activity hydrolyzes PA, LPA, ceramide-1-phosphate (C-1-P), and S-1-P to similar extents (3).

Recent studies indicate a potential role for LPP in signal transduction. LPP could act to hydrolyze PA arising in the plasma membrane from diacylglycerol (DAG) kinase (4) and phospholipase D (PLD) (5) thereby regulating the levels of PA in the plasma membrane. It has been suggested that transient elevations in DAG levels arising through PLC degradation of phosphatidylinositol bisphosphate (PIP_2) in alveolar type II cells can be extended through the stimulation of the PLD/ LPP pathway (5). LPP activity exists in isolated type II cells and plasma membrane preparations (2) and a proposed function is in the regulation of surfactant phospholipid secretion. The signaling pathway would involve a plasma membrane localized LPP which would act sequentially to PLD in the purinergic P_{2u} receptor cascade where it would generate DAG from phosphatidylcholine (PC)-derived PA,

thereby sustaining protein kinase C (PKC) activation and surfactant secretion (5). Another proposed function of LPP may be in controlling cell growth where recovery from lung injury would involve type II cell proliferation and migration to restore the damaged type I cell population (6). Subsequently, the type II cells undergo a transdifferentiation process in order to re-establish the alveolar epithelium. These latter processes may require elevated DAG levels, generated by LPP for PKC activation leading to expression of specific genes required for this process.

To further our understanding of the role of LPP in lung, pulmonary LPP isoforms were cloned by reverse transcriptase-polymerase chain reaction (RT-PCR) using RNA from adult rat lung and type II cells. The RT-PCR generated LPP1, three LPP1 variants, and LPP3 cDNAs. The three LPP1 variants include LPP1a and two novel isoforms, LPP1b and LPP1c. The latter isoform was rare but LPP1b was present at similar levels to LPP1/1a. A rat tissue profile was screened with isoform-specific primers to investigate whether the novel LPP1 variants are tissue-specific. Transient expression of LPP1, LPP1a, and LPP3 in HEK 293 cells was performed to verify that these cloned cDNAs encode magnesium-independent, NEM-insensitive PAP activity.

3.2 Materials and Methods

3.2.1 Materials

Trizol reagent, Superscript^{TM} preamplification kit, DNAse I (amplification grade), isopropylthio-β-D-galactoside (IPTG), Xgal, and tissue culture media were

obtained from Gibco BRL. Fetal bovine serum was obtained from CanSera. Porcine elastase was obtained from Worthington Biochemicals. RNAse H and restriction enzymes were purchased from Pharmacia Biotech. The Advantage cDNA PCR kit was obtained from Clontech Laboratories. Mineral oil and herring sperm DNA were obtained from Sigma. pGEM-3Zf(+) was obtained from Promega. XL1-blue cells and QuikHyb solution were obtained from Stratagene. [α-^{32}P]-dCTP and [γP^{32}]-ATP was purchased from Amersham. 1-Palmitoyl-2-oleoyl-phosphatidylcholine was purchased from Avanti Polar Lipids. DAG kinase was purchased from Calbiochem. LPP1 antibody was kindly provided by Dr. David Brindley (University of Alberta, Edmonton, Canada). LPP3 antibody was kindly provided by Dr. Andrew Morris (Department of Pharmacological Sciences, Stony Brook Health Sciences Center, USA).

3.2.2 Cloning and Sequencing of LPPs from Rat Lung and Rat Type II Cells

The isolation of alveolar type II cells was followed according to Dobbs et al. (7). Lungs were perfused with 0.9% saline as previously described (2). Total RNA was prepared using Trizol reagent. The RNA was DNAse-treated prior to first strand cDNA synthesis. The reverse transcriptase reaction was performed using oligo $(dT)_{12\text{-}18}$ as the primer and Superscript H$^-$-Reverse transcriptase. The cDNA was then RNAse-treated prior to the PCR reaction. PCR primers for amplification of LPP1, LPP2, LPP3 were based on GenBank sequences (U90556, AA734786, Y07783, respectively). The primers for LPP1 span the start and stop codon and contain BglII

and SalI sites (underlined):

5'-GAGAGATCTGTGACC**ATG**TTCGACAAGCC (5'-primer)

5'-GAGGTCGACCCCT**TCA**GGGCTCGTGATTA (3'-primer)

The primers for LPP2 span the start and an internal region (3rd domain of active site) and contain an EcoRI site:

5'- CCGGAATTCGACC**ATG**GAGAGGA (5'-primer)

5'-GCTCCAGTGGTGTTTGTAATCA (3'-primer)

The primers for LPP3 also span the start and 3'-adjacent to stop codon and contain BamHI sites:

5'-CTCGGATCCGCCAGCGCC**ATG**CAAACGTA (5'-primer)

5'-TTCGGATCCAGTGCTCTGGAGGCCGCAGC (3'-primer)

The reaction mixture (100μl) contained 1XClontech Buffer (containing 3.25mM Mg^{+2}), dNTPs (0.4mM each), primers (0.4μM), and cDNA (2μl). The Clontech proofreading enzyme polymerase mixture (0.5 U) was added and then the samples were overlaid with light mineral oil. The incubation conditions were 94^0C for 5 minutes followed by 30 cycles of 2 minutes at 94^0C, 2 minutes at 62^0C, and 2 minutes at 72^0C. PCR products were subjected to electrophoresis on 1.2% agarose gels in 40mM Tris-borate containing 1mM EDTA and 0.001mg/ml ethidium bromide.

The LPP1 PCR product was restriction enzyme digested with BglII and SalI overnight at 37^0C and ligated into pGEM-3Zf (+) which was gel-purified after overnight restriction enzyme digestion. The LPP3 PCR product was restriction enzyme digested with BamHI overnight at 37^0C and ligated into pGEM-3Zf (+),

which was dephosphorylated with calf intestinal phosphatase after overnight restriction enzyme digestion. Competent XL1-Blue cells were transformed with the ligation products and positive colonies were selected by performing blue-white colony screening.

Nucleotide sequencing of the various LPP clones was performed using fluorescent dye primer extensions with an automated DNA sequencer (Robarts Research Institute, DNA Sequencing Facility). The LPP sequences were analyzed using the BLAST and Dialign2 programs.

3.2.3 Verification of LPP1 Variants

The LPP variants were verified by using a combination of primers that were designed to be isoform-specific. The PCR products were cloned into the pGEM-3Zf (+) vector and sequenced.

The primers for LPP1/LPP1a, LPP1b, and LPP1c (primer set A):

5'-GAGAGATCTGTGACC**ATG**TTCGACAAGCC (5'-primer) (start)

5'-GAGGTCGACGGCCGCAGTCTGCCTATACGA (3'-primer) (383 to 365bp)

The primers for LPP1 and LPP1a (primer set B):

5'-GCTGGCTGGATTGCCTTATATA (5'-primer) (60-87bp)

5'-AACAGCGTGAAGTACCCGTACC (5'-primer) (130-151bp)

5'-GAGGTCGACGGCCGCAGTCTGCCTATAGA (3'-primer) (386-365bp)

The primers for region IIB (see Fig.3.2) of LPP1 (primer set C):

5'-GCTGGCTGGATTGCCTTATATA (5'-primer) (68-81bp)

5'-TCCACCTAATAACGCATAAGGG (3'-primer) (196-175bp)

The primers for region IIA (see Fig.3.2) of LPP1a (primer set D):

5'-TTCCATGCCTATGGCTGTTGTA (5'-primer) (57-78bp)

5'-CAAGCCCCACTAGGACGAGTAC (3'-primer) (186-165bp)

3.2.4 Southern Analysis of Tissue Profile

RNA was isolated from tissues obtained from 150-200g Sprague-Dawley rats. As described above, RT-PCR was performed and the products were run on a 2% agarose gel. The gel was denatured in denaturing buffer (0.5M NaOH, 1.5M NaCl) for 30 minutes at room temperature. Subsequently, the gel was transferred to neutralizing buffer (0.5M Tris-HCl (pH 7.0), 1.5M NaCl) and slowly shaken for 30 minutes at room temperature. The gel was soaked in 20XSSC transfer buffer for 30 minutes and then transferred to nylon membrane using the Turboblotter Rapid Downward Transfer System (Schleicher & Schull). The blots were probed with LPP1.

3.2.5 Northern Analysis of Tissue Profile

A 1% agarose-RNA formaldehyde gel containing total RNA from tissues (20μg/lane) was transferred to Nylon membranes. Prehybridization for 20 minutes at 68^0C in QuikHyb solution was followed by hybridization with the appropriate probe with 100μl of denatured herring sperm DNA for 1 hour at 68^0C. For LPP3, the blots were washed for 1 hour at 60^0C in 2XSSC and 0.1% SDS followed by a 30 minutes wash in 0.1XSSC and 0.1% SDS at room temperature. For LPP1, the blots

were washed in 0.1XSSC and 0.1% SDS at room temperature for 6 hours. LPP1 and LPP3 probes were prepared by random prime labeling using [α-^{32}P]-dCTP. The membranes were exposed to X-ray film between 24-72 hours for the LPP3 probe and up to 1 week for the LPP1 probe.

3.2.6 Transient Expression of LPPs in HEK 293 Cells

HEK 293 cells were maintained in Dulbecco's Modified Eagle's Medium (high glucose) containing 10% fetal bovine serum. LPP1 and LPP1b were first digested from pGEM-3Zf (+) with SalI, blunt-ended with Klenow Fragment, and KpnI digested. LPP1a was digested from pGEM-3Zf (+) with HindIII, blunt-ended with Klenow Fragment, and KpnI digested. LPP3 was digested from pGEM-3Zf (+) with BamHI and blunt-ended with Klenow Fragment. These LPP1/1a/1b inserts were then subcloned into the KpnI and XbaI (blunt-ended) sites and for LPP3 cDNAs, into the XbaI (blunt-ended) site of the mammalian expression vector, pTracer-CMV2 (Invitrogen). The orientation was verified by a combination of restriction enzyme digestion and sequencing. Transfection quality plasmid DNA was obtained using a Maxi Plasmid Preparative kit (Qiagen). Transient expression of LPP1, LPP1b, and LPP3 was obtained using 1μg of DNA and Effectene transfection reagent (Qiagen). Transient expression of LPP1a was obtained using 2μg of DNA. Cells were harvested 36 - 48 hours post-transfection, sonicated for 10 seconds (three bursts), and then centrifuged at 100,000g for 1 hour at 4^{0}C in a Ti70.1 rotor to obtain total membranes.

3.2.7 LPP Assays

The activity was assayed using pure PA as substrate. Unlabelled PA and P^{32}-labelled PA were prepared as described previously (2). Reaction mixtures contained 100mM Tris-Maleate buffer, pH 6.5, 0.6mM PA (0.4mCi/mmol), 0.5mM EDTA, 0.5mM EGTA, pH 7.0, 0.2mg of essentially fatty acid free albumin and 1mM DTT in a final reaction volume of 0.1 ml. Incubation times were 60 minutes in duration at 37^0C. The protein was preincubated at 37^0C for 10 minutes with 4.2mM N-ethylmaleimide (NEM). Reactions were terminated by the addition of 1.5 ml of chloroform: methanol (1:1). The phases were broken with 0.75ml of 0.1N HCl and a sample of the upper aqueous phase was taken for scintillation counting to determine the P^{32} inorganic phosphate released (2).

3.2.8 Other Assays

Protein was determined by the method of Lowry *et al.* (8) in the presence of 2mM SDS using bovine serum albumin as the standard.

3.3 Results

3.3.1 The Cloning of Pulmonary LPPs and Variants

LPP isoforms were cloned from perfused rat lung and isolated alveolar type II cells that were maintained on tissue culture plastic overnight. Primers were designed to amplify the entire coding sequence of LPP1, LPP3, and a partial region

of LPP2. RT-PCR products were cloned and sequenced revealing the presence of mRNA for LPP1 and its variants in lung (LPP1a, 1b, and 1c) and type II cells (LPP1b). Meanwhile, LPP2 mRNA was detected in brain but was absent in lung. LPP3 was present in lung and type II cells.

The LPP1 PCR products, when sequenced, revealed multiple products including LPP1, LPP1a, LPP1b, and LPP1c. Figures 3.1A and 3.2, respectively, show the nucleotide sequence alignment and a graphical view of the LPP1 variants. The LPP1 products (LPP1, 1a, and 1b) were confirmed using other combinations of primers whose products were verified by sequencing. The LPP3 cDNA sequence is displayed in Figure 3.1B. The LPP1 and LPP3 isoforms are identical to the previously cloned rat liver (9) and intestinal isoforms (10), respectively. The LPP1a isoform is homologous to the human (11) and guinea pig (12) isoforms. The LPP1b and LPP1c isoforms are novel but contain nucleotide insertions/deletions (as indicated in bold in Figure 3.1 and 3.2) that result in a frameshift leading to early termination of the polypeptide. A homolog of the LPP1b isoform was recently identified in the database of expressed sequence tags (dbEST) that was cloned from Bovine Taurus cartilage fetus (Genbank Accession # AV595831).

3.3.2 Sequence Analysis of Pulmonary LPP Isoforms

Hydropathy plot analysis of LPP1, LPP1a, and LPP3 based on the Kyte and Doolittle algorithm suggests that each have six membrane-spanning regions (Figure 3.3) while the truncated isoforms may have one or two transmembrane domains. These full-length proteins contain an active site comprised of three domains (Figure

Figure 3.1. In A, nucleotide sequence alignment of the LPP1 isoforms from lung tissue. The sequences were aligned using the DiAlign2 program. The dashes denote the absence of bases. RL is an abbreviation for rat lung. The bold and underlined letters indicate insertions or deletions in the novel isoforms as well as the stop codons in the novel isoforms. In B, nucleotide and amino acid sequence alignment for rat lung LPP3.

```
RLLPP1      1  ATGTTCGACA AGCCGCGGCT GCCGTACGTG GTCCTCGATG TGATTTGCGT GTTGCTGGCT ---------- ---------- ---------- ----------
RLLPP1A     1  ATGTTCGACA AGCCGCGGCT GCCGTACGTG GTCCTCGATG TGATTTGCGT GTTGCTGGCT TCCATGCCTA TGGCTGTTGT AAATTTGGGC CAAATATATC
RLLPP1B     1  ATGTTCGACA AGCCGCGGCT GCCGTACGTG GTCCTCGATG TGATTTGCGT GTTGCTGG-- ---------- ---------- ---------- ----------
RLLPP1C     1  ATGTTCGACA AGCCGCGGCT GCCGTACGTG GTCCTCGATG TGATTTGCGT GTTGCTGGCT TCCATGCCTA TGGCTGTTGT AAATTTGGGC CAAATATATC

RLLPP1     61  ---------- ---------- ---------- ---------- ---------- ---------- ---------- ---------- ---------- ----------
RLLPP1A   101  CATTTCAGAG AGGCTTTTTC TGTTCTGACA ACAGCGTGAA GTACCCGTAC CATGACAGTA CCGTCACAAC CAGTGTACTC GTCCTAGTGG GGCTTGGCAT
RLLPP1B    59  ---------- ---------- ---------- ---------- ---------- ---------- ---------- ---------- ---------- ----------
RLLPP1C   101  CATTTCAGAG AGGCTTTTTC TGTTCTGACA ACAGCGTGAA GTACCCGTAC CATGACAGTA CCGTCACAAC CAGTGTACTC GTCCTAGTGG GGCTTGGCAT

RLLPP1     61  ---------- -----GGATT GCCTTATATA ATTCTTACTT CAAGGCATAC CCCCTTCCAA CGAGGAGTGT TCTGTACTGA TGAGTCCATC AAGTACCCTT
RLLPP1A   201  ACCCATTTTC TC-------- ---------- ---------- ---------- ---------- ---------- ---------- ---------- ----------
RLLPP1B    59  ---------- ---------- ---------- ---------- ---------- ---------- ---------- ---------- ---------- ----------
RLLPP1C   201  ACCCATTTTC TCTCTGGATT GCCTTATATA ATTCTTACTT CAAGGCATAC CCCCTTCCAA CGAGGAGTGT TCTGTACTGA TGAGTCCATC AAGTACCCTT

RLLPP1    146  ACAGAGAAGA CACCATCCCT TATGCGTTAT TAGGTGGAAT AGTCATTCCA TTCTGTATTA TCGTTATGAC TACTGGAGAA ACTCTGTCTG TTTACTTTAA
RLLPP1A   213  ---------- ---------- ---------- ---------- ---------- ---------- ----TATGAT TACTGGAGAA ACTCTGTCTG TTTACTTTAA
RLLPP1B    59  ---------- ---------- ---------- ---------- ---------- ---------- -----ATGAT TACTGGAGAA ACTCTGTCTG TTTACTTTAA
RLLPP1C   301  ACAGAGAAGA CACCATCCCT TATGCGTTAT TAGGTGGAAT AGTCATTCCA TTCTGTATTA TCGATATGAT TACTGGAGAA ACTCTGTCTG TTTACTTTAA

RLLPP1    246  TGTCTTGCAT TCAAATTCCT TTGTCAGCAA TCACTATATA GCCACCATTT ACAAAGCCGT TGGAGCCTTT TTGTTTGGAG CCTCAGCCAG TCAGTCCCTG
RLLPP1A   249  TGTCTTGCAT TCAAATTCCT TTGTCAGCAA TCACTATATA GCCACCATTT ACAAAGCCGT TGGAGCCTTT TTGTTTGGAG CCTCAGCCAG TCAGTCCCTG
RLLPP1B    94  TGTCTTGCAT TCAAATTCCT TTGTCAGCAA TCACTATATA GCCACCATTT ACAAAGCCGT TGGAGCCTTT TTGTTTGGAG CCTCAGCCAG TCAGTCCCTG
RLLPP1C   401  TGTCTTGCAT TCAAATTCCT TTGTCAGCAA TCACTATATA GCCACCATTT ACAAAGCCGT TGGAGCCTTT TTGTTTGGAG CCTCAGCCAG TCAGTCCCTG

RLLPP1    346  ACTGACATTG CTAAGTACTC TATAGGCAGA CTGCGGCCTC ACTTCCTGGC TGTCTGTAAC CCAGACTGGT CAAAAATCAA CTGCAGCGAT GGCTACATTG
RLLPP1A   349  ACTGACATTG CTAAGTACTC TATAGGCAGA CTGCGGCCTC ACTTCCTGGC TGTCTGTAAC CCAGACTGGT CAAAAATCAA CTGCAGCGAT GGCTACATTG
RLLPP1B   194  ACTGACATTG CTAAGTACTC TATAGGCAGA CTGCGGCCTC ACTTCCTGGC TGTCTGTAAC CCAGACTGGT CAAAAATCAA CTGCAGCGAT GGCTACATTG
RLLPP1C   501  ACTGACATTG CTAAGTACTC TATAGGCAGA CTGCGGCCTC ACTTCCTGGC TGTCTGTAAC CCAGACTGGT CAAAAATCAA CTGCAGCGAT GGCTACATTG

RLLPP1    446  AGAACTTCGT ATGTCAAGGG AATGAACAGA AGGTCAGGGA AGGCAGGTTG TCCTTCTACT CGGGGCACTC CTCATTCTCT ATGTACTGCA TGCTGTTTGT
RLLPP1A   449  AGAACTTCGT ATGTCAAGGG AATGAACAGA AGGTCAGGGA AGGCAGGTTG TCCTTCTACT CGGGGCACTC CTCATTCTCT ATGTACTGCA TGCTGTTTGT
RLLPP1B   294  AGAACTTCGT ATGTCAAGGG AATGAACAGA AGGTCAGGGA AGGCAGGTTG TCCTTCTACT CGGGGCACTC CTCATTCTCT ATGTACTGCA TGCTGTTTGT
RLLPP1C   601  AGAACTTCGT ATGTCAAGGG AATGAACAGA AGGTCAGGGA AGGCAGGTTG TCCTTCTACT CGGGGCACTC CTCATTCTCT ATGTACTGCA TGCTGTTTGT

RLLPP1    546  CGCACTTTAT CTTCAAGCCA GGATGAAAGG AGATTGGGCA AGACTCTTAC GACCCATGCT ACAGTTTGGG CTTGTTGCTT TATCCATATA TGTGGGCCTG
RLLPP1A   549  CGCACTTTAT CTTCAAGCCA GGATGAAGGG AGATTGGGCA AGACTCTTAC GACCCATGCT ACAGTTTGGG CTTGTTGCTT TATCCATATA TGTGGGCCTG
RLLPP1B   394  CGCACTTTAT CTTCAAGCCA GGATGAAGGG AGATTGGGCA AGACTCTTAC GACCCATGCT ACAGTTTGGG CTTGTTGCTT TATCCATATA TGTGGGCCTG
RLLPP1C   701  CGCACTTTAT CTTCAAGCCA GGATGAAGGG AGATTGGGCA AGACTCTTAC GACCCATGCT ACAGTTTGGG CTTGTTGCTT TATCCATATA TGTGGGCCTG

RLLPP1    646  TCTCGAGTTT CTGATTACAA ACACCACTGG AGCGACGTGT TAATTGGCCT CATTCAAGGA GCTGTTGTGG CAATATTAGT GGTTTTGTAT GTAACTGATT
RLLPP1A   649  TCTCGAGTTT CTGATTACAA ACACCACTGG AGCGACGTGT TAATTGGCCT CATTCAAGGA GCTGTTGTGG CAATATTAGT GGTTTTGTAT GTAACTGATT
RLLPP1B   494  TCTCGAGTTT CTGATTACAA ACACCACTGG AGCGACGTGT TAATTGGCCT CATTCAAGGA GCTGTTGTGG CAATATTAGT GGTTTTGTAT GTAACTGATT
RLLPP1C   801  TCTCGAGTTT CTGATTACAA ACACCACTGG AGCGACGTGT TAATTGGCCT CATTCAAGGA GCTGTTGTGG CAATATTAGT GGTTTTGTAT GTAACTGATT

RLLPP1    746  TCTTCAAGAC CACAGAGTCT AACAAAGAAA GAAAAGAGGA CTCACATACG ACTCTACACG AAACCACCAA CAGACAGAGC TACGCAAGGA ATCACGAGCC
RLLPP1A   749  TCTTCAAGAC CACAGAGTCT AACAAAGAAA GAAAAGAGGA CTCACATACG ACTCTACACG AAACCACCAA CAGACAGAGC TACGCAAGGA ATCACGAGCC
RLLPP1B   594  TCTTCAAGAC CACAGAGTCT AACAAAGAAA GAAAAGAGGA CTCACATACG ACTCTACACG AAACCACCAA CAGACAGAGC TACGCAAGGA ATCACGAGCC
RLLPP1C   901  TCTTCAAGAC CACAGAGTCT AACAAAGAAA GAAAAGAGGA CTCACATACG ACTCTACACG AAACCACCAA CAGACAGAGC TACGCAAGGA ATCACGAGCC

RLLPP1    846  CTGA
RLLPP1A   849  CTGA
RLLPP1B   694  CTGA
RLLPP1C  1001  CTGA
```

```
 M  Q  S  Y  K  Y  D  K  A  I  V  P  E  S  K  N  G  G     18
ATG CAA AGC TAC AAG TAC GAC AAG GCG ATC GTC CCT GAG AGT AAG AAC GGC GGC    54

 S  P  A  L  N  N  N  P  R  K  G  G  S  K  R  V  L  L     36
AGC CCG GCG CTC AAC AAC AAC CCG AGG AAA GGC GGC AGC AAG CGG GTG CTG CTC   108

 I  C  L  D  L  F  C  L  F  M  A  A  L  P  F  L  I  I     54
ATC TGC CTC GAC CTC TTC TGC CTC TTC ATG GCG GCT CTG CCC TTC CTC ATC ATC   162

 E  T  S  T  I  K  P  Y  R  R  G  F  Y  C  N  D  E  S     72
GAG ACA AGC ACC ATT AAG CCT TAT CGT CGA GGG TTT TAC TGC AAC GAC GAG AGC   216

 I  K  Y  P  L  K  V  S  E  T  I  N  D  A  V  L  C  A     90
ATC AAG TAC CCC CTG AAA GTC AGC GAG ACT ATA AAC GAC GCC GTG CTC TGT GCG   270

 V  G  I  V  I  A  I  L  A  I  I  T  G  E  F  Y  R  I    108
GTG GGG ATC GTC ATC GCC ATC CTG GCG ATC ATC ACG GGG GAA TTC TAC CGG ATC   324

 Y  Y  L  K  E  K  S  R  S  T  I  Q  N  P  Y  V  A  A    126
TAT TAC CTC AAG GAG AAG TCC CGA TCC ACC ATT CAG AAC CCT TAT GTG GCC GCT   378

 L  Y  K  Q  V  G  C  F  L  F  G  C  A  I  S  Q  S  F    144
CTC TAT AAG CAA GTG GGA TGC TTC CTT TTC GGT TGT GCC ATC AGC CAG TCC TTC   432

 T  D  I  A  K  V  S  I  G  R  L  R  P  H  F  L  S  V    162
ACA GAC ATC GCC AAA GTG TCC ATT GGG CGC CTG AGG CCT CAC TTC CTC AGC GTC   486

 C  D  P  D  F  S  Q  I  N  C  S  E  G  Y  I  Q  N  Y    180
TGT GAC CCT GAT TTC AGT CAG ATC AAT TGC TCC GAG GGC TAC ATT CAG AAC TAC   540

 R  C  R  G  E  D  S  K  V  Q  E  A  R  K  S  F  F  S    198
AGG TGC CGA GGA GAA GAC AGC AAA GTA CAG GAG GCC AGG AAA TCC TTC TTC TCG   594

 G  H  A  S  F  S  M  F  T  M  L  Y  L  V  L  Y  L  Q    216
GGC CAC GCC TCC TTC TCC ATG TTC ACA ATG CTG TAT CTG GTG CTT TAT CTA CAG   648

 A  R  F  T  W  R  G  A  R  L  L  R  P  L  L  Q  F  T    234
GCC CGC TTC ACC TGG CGT GGG GCC CGG CTC CTC CGC CCC CTC CTG CAG TTC ACT   702

 L  L  M  M  A  F  Y  T  G  L  S  R  V  S  D  Y  K  H    252
TTG CTC ATG ATG GCC TTC TAC ACG GGA TTG TCA CGT GTA TCT GAC TAC AAA CAC   756

 H  P  S  D  V  L  A  G  F  A  Q  G  A  L  V  A  C  C    270
CAT CCT AGC GAT GTC CTG GCA GGA TTT GCC CAA GGA GCT CTG GTG GCC TGC TGC   810

 I  V  F  F  V  S  D  L  F  K  T  K  T  T  L  S  L  P    288
ATA GTG TTC TTC GTG TCT GAC CTC TTC AAG ACT AAG ACG ACC CTC TCA CTG CCT   864

 A  P  A  I  R  R  E  I  L  S  P  V  D  I  M  D  R  S    306
GCC CCC GCG ATC AGG AGA GAG ATC CTG TCT CCT GTA GAC ATC ATG GAC AGG AGC   918

 N  H  H  N  M  V  *                                    313
AAT CAC CAC AAC ATG GTG TAG                             939
```

Figure 3.2. Graphical view of the cDNA to protein alignment of LPP1 and its variants. The cDNA for LPP1 and LPP1a are divided into three regions: I, IIA or IIB, and III. LPP1 and LPP1a diverge at region II. The protein alignment is shown below the cDNA. The red boxes represent transmembrane domains and the violet regions represent the domains of the active site. The asterix indicates an N-linked glycosylation site. The cDNA for LPP1b contains an extra "G" nucleotide (shown in yellow with asterix) leading to a frameshift and is lacking region II. Likewise, LPP1c contains both region IIA and IIB with a nucleotide deletion leading to a frameshift. The bases at the edges of these regions are shown above each region to illustrate the frameshifts which occur in the novel LPP isoforms.

cDNA
cDNA
Protein -
282 & 283 aa
cDNA
Protein -30aa
cDNA
Protein -76 aa

Figure 3.3. Hydropathy plot analyses for the cloned full-length pulmonary LPPs. These plots were generated using a program based on the Kyte and Doolittle algorithm (Expasy).

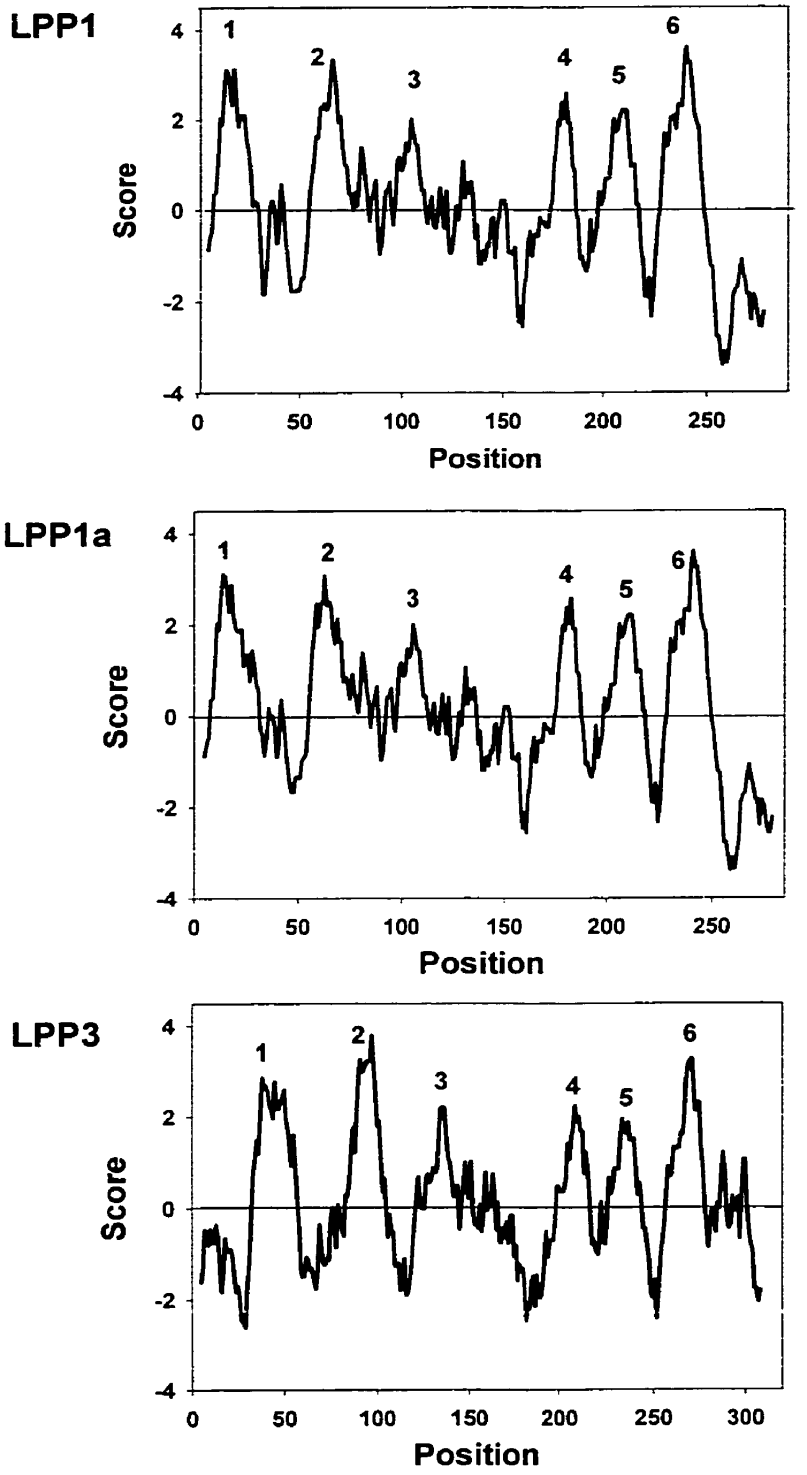
LPP1
Score
Position
1
2
3
4
5
6
LPP1a
Score
Position
LPP3
Score
Position

3.4), which is part of a novel phosphatase superfamily (13). They each contain a potential N-linked glycosylation site at amino acid positions 142, 143, and 171 (LPP1, LPP1a, and LPP3, respectively). The principle divergent regions among these LPPs include the N- and C-termini. Regions of divergence between LPP1 and LPP1a include the end of transmembrane region 1 (TM1) and the beginning of transmembrane region 2 (TM2) as well as certain residues in the first extracellular loop (Figure 3.4). The LPP1 and LPP1a isoforms are most probably derived from alternative splicing. The expected molecular weights of the full-length LPPs are 31.9 kDa (LPP1), 32.0 kDa (LPP1a), and 35.2 kDa (LPP3).

The LPP1b isoform contains a G nucleotide insertion, which would predict a peptide of 30 amino acids (3.61 kDa). Likewise, the LPP1c isoform contains a nucleotide deletion, which would predict a peptide of 76 amino acids (8.55 kDa). Their predicted sequences are shown in Figure 3.5. If proteins are expressed, these isoforms would be catalytically inactive since they would not possess the active site. Furthermore, they would both lack the N-linked glycosylation site. Three different preparations of lung RNA were used for the RT-PCR resulting in the consistent appearance of LPP1b whereas LPP1c was much rarer. The LPP1b isoform was not generated in reactions without cDNA.

3.3.3 Overexpression of Rat Pulmonary LPPs in HEK 293 Cells

Transient transfection of rat lung LPP1, LPP1a, and LPP3 cDNAs in human embryonic kidney cells resulted in an 8.7-fold, 2.4-fold, and 16.9-fold increase in membrane-bound LPP enzyme activity, respectively (Figure 3.6A). The activity of

Figure 3.4. Amino acid sequence alignment of pulmonary LPP1, LPP1a, and LPP3. The predicted rat lung amino acid sequences are aligned with those of the human sequences (Genbank sequences AB000888 (LPP1), AF014402 (LPP1a), and AF056083 (LPP2)). Alignment was performed using the DiAlign2 program. The predicted membrane-spanning regions are denoted TM-1 through TM-6 and the active sites are shown highlighted in yellow.

AMINO ACID SEQUENCE ALIGNMENTS OF LIPID PHOSPHATE PHOSPHOHYDROLASES

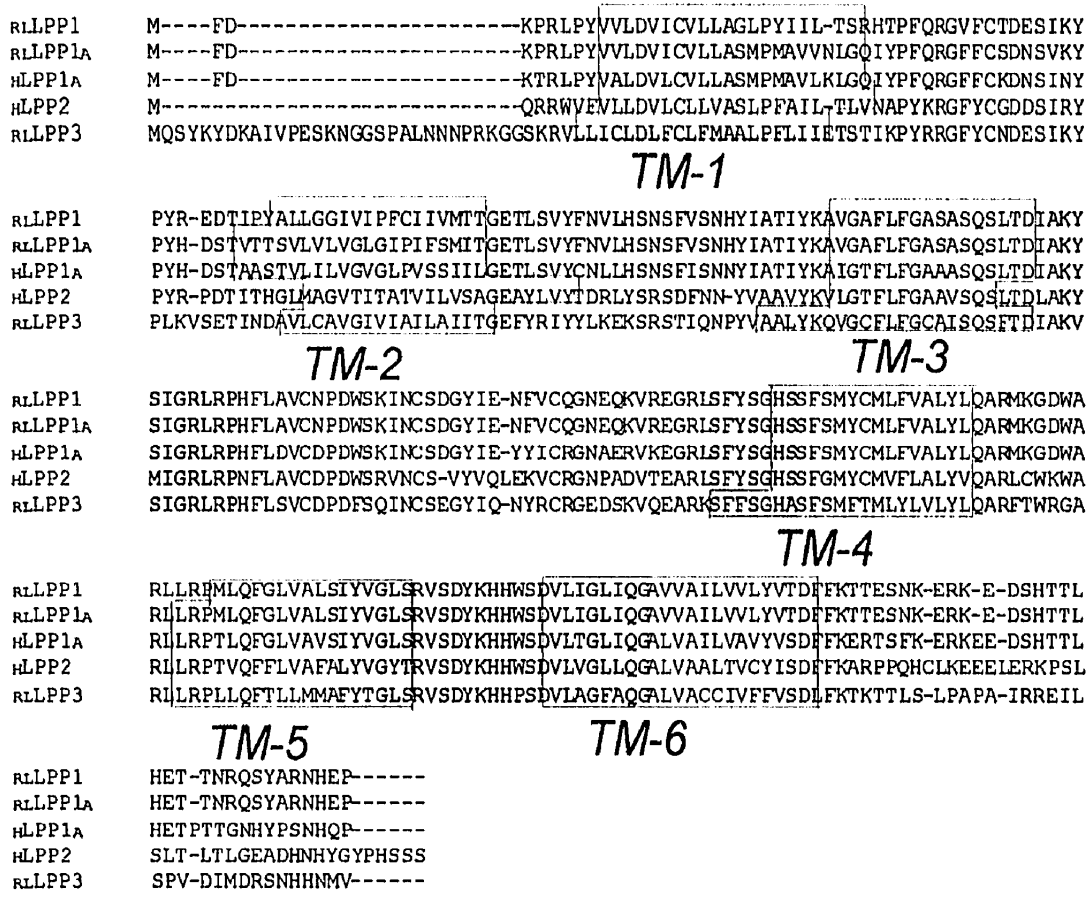

Figure 3.5. Amino acid sequences of the novel truncated LPP1 isoforms. The cDNA sequences were translated using a DNA sequence translator program (Infobiogen, France).

```
LPP1B MRDKPRLPYV VLDVICVLLD DYWRNSVCLL

LPP1C MFDKPRLPYV VLDVICVLLA SMPMAVVNFG QIYPFQRGFF
      CSDNSVKYPY HDSTVTTSVL VLVGLGIPIF SLDCLL
```

Figure 3.6. Overexpression of pulmonary LPPs in HEK 293 cells. In A, Transient transfections of LPP cDNAs and empty vector was performed using Effectene reagent. Cells were harvested 48 hours post-transfection and 10μg of total membranes and sonicates were analyzed for NEM-insensitive PAP enzyme activity using PA as substrate in the absence of magnesium. In B, SDS-PAGE of10μg of total membrane protein/lane and immunoblot analysis with LPP3 antibody. Lane 1, 36 hours control vector, 2 and 3, 48 hours control vector, 4, 36 hours LPP1 transfectants, 5 and 6, 48 hours LPP1 transfectants, 7, 36 hours LPP3 transfectants, 8 and 9, 48 hours LPP3 transfectants.

A

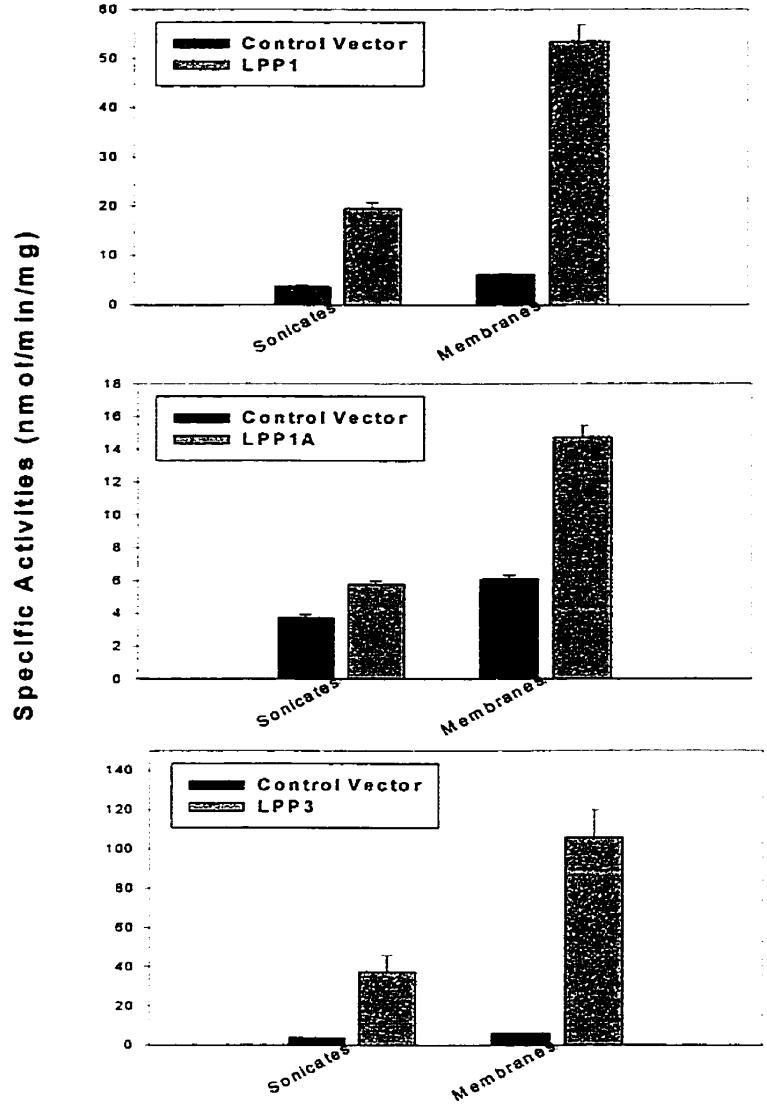
Specific Activities (nmol/min/mg)
Control Vector
LPP1
Sonicates
Membranes
Control Vector
LPP1A
Sonicates
Membranes
Control Vector
LPP3
Sonicates
Membranes

B

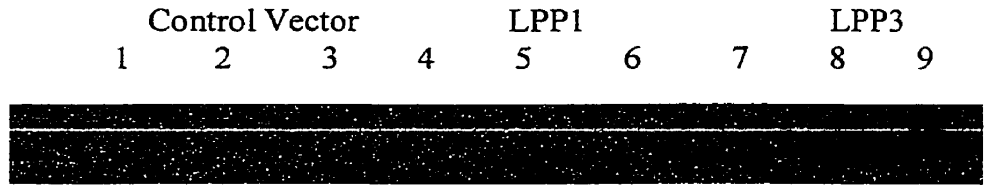
Control Vector
LPP1
LPP3
1 2 3 4 5 6 7 8 9

the three LPP isoforms was assayed using phosphatidate as substrate in the presence of NEM and without magnesium. Therefore, these rat lung cDNAs encode functional NEM-insensitive, magnesium-independent phosphatidate phosphatases. An antibody against LPP3 allowed detection of overexpressed rat LPP3 in HEK 293 cells (Figure 3.6B). Available antibodies against LPP1/1a isoforms failed to immunoreact with the rat isoforms. As expected, transient expression of the LPP1b isoform did not affect the LPP activity since it was predicted to lack the three domains of the active site. Transient expression of these cDNAs was initially attempted in SV-40 large T antigen transformed mouse type II-like lung epithelial cell lines (MLE12 and MLE15) to investigate the role of LPP in surfactant secretion. However, transient transfections were without success. These cell lines have high endogenous LPP enzyme activity and thus, stable expression of various LPPs including LPP1b was attempted. However, cell death resulted with the MLE12 cell line and increases in LPP enzyme activity were not detected in the MLE15 cell line using an inducible tetracycline system.

3.3.4 Analysis of LPP Isoforms Across a Rat Tissue Profile

Northern analysis of a tissue profile is shown in Figure 3.7A. Tissues that were investigated include the lung, liver, intestine, kidney, spleen, uterus, heart, and brain. The LPP1 RNA is highly expressed in lung and intestine. The LPP3 RNA levels are high in lung, liver, and brain tissues. As shown in Figure 3.7B, using primers designed to distinguish between LPP1/LPP1a and LPP1b (~400bp and ~250bp products), LPP1b appears to be in equal abundance to the LPP1/1a

Figure 3.7. Expression of LPPs across a rat tissue profile. In A, northern analysis using LPP1 and LPP3 as probes. In B, southern analysis of RT-PCR products of LPP1 variants, LPP1/1a (top band) and LPP1b (lower band). In C, southern analysis of RT-PCR products of LPP1 variants, LPP1 (top band) and LPP1a (lower band). Two separate tissue blots are shown for the southern analysis.

A

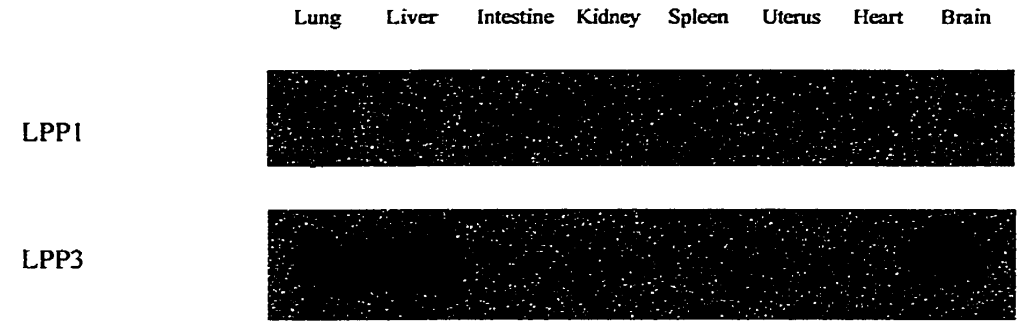
Lung
Liver
Intestine
Kidney
Spleen
Uterus
Heart
Brain
LPP1
LPP3

B


Lung
Liver
Intestine
Kidney
Spleen
Uterus
Heart
Brain
Lung
Intestine
Kidney
Spleen
Uterus
Heart
Brain
Liver
LPP1/1a
LPP1b

C

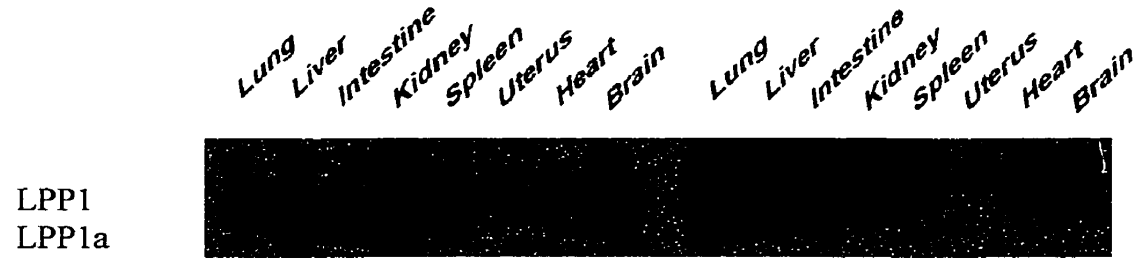
Lung
Liver
Intestine
Kidney
Spleen
Uterus
Heart
Brain
Lung
Liver
Intestine
Kidney
Spleen
Uterus
Heart
Brain
LPP1
LPP1a

isoform in lung and brain tissue. Using primers designed to distinguish between LPP1 and LPP1a, the LPP1a is present in most tissues examined (Figure 3.7C).

3.4 Discussion

3.4.1 LPP Isoforms in Rat Lung and Type II Cells

In lung, we previously showed that PA and LPA were excellent substrates in plasma membranes whereas, S-1-P was a relatively poor substrate (2). This was in contrast to other investigators who have shown that these substrates were used with similar efficiencies (3). In order to investigate the possible presence of novel isoforms, LPPs were cloned by RT-PCR from both adult rat lung and type II cell RNA which generated LPP1, three LPP1 variants (LPP1a, LPP1b, and LPP1c), and LPP3 cDNAs. The LPP2 isoform was absent in lung tissue as determined by RT-PCR.

In intact rat 2 fibroblasts, LPPs were recently shown to be capable of hydrolyzing exogenously presented substrates including LPA, a phospholipid growth factor (14). Furthermore, LPP1 attenuated LPA-mediated effects on cellular proliferation through the Edg2 receptor (15). Both S-1-P and LPA are biologically active lipids, which have been implicated in eliciting various biological responses including cellular proliferation, differentiation, migration, and inhibition of apoptosis (16). Sciorra and Morris (17) have provided evidence that LPP3 can generate DAG sequentially to PLD in HEK 293 cells in caveolin-enriched domains. The substrate specificity of LPP1a, its localization, and its possible functions require further investigation.

3.4.2 Function of LPP1b

LPP1b is a novel isoform which predicts an inactive truncated protein of 30 amino acids. The possibility that LPP1b could be generated by PCR was considered. PCR was performed using three separate preparations of RNA from lung tissue and this isoform was generated in all reactions. Bidirectional sequencing was performed on numerous clones showing the consistent presence of the "G" nucleotide in exactly the same position in all clones sequenced. Tissue profiles show that LPP1b is expressed at high levels in lung and brain and varies across tissues different to that of the LPP1/LPP1a isoforms. Furthermore, LPP1b mRNA, determined by RT-PCR, is present in various human lung epithelial cells, namely human bronchial epithelial cells (HBE) and an adenocarcinoma lung cell line (A549) (Jonathan Faulkner and Fred Possmayer, unpublished observations). Thus, the mRNA for this LPP1 variant is not only present in rat but also in human.

The LPP1b isoform would be inactive if a protein were produced and may possess regulatory functions either at the RNA or protein level. We propose that the LPP1b isoform may be present in an inactive form to control the levels of LPP1 expression and may be a physiological means to keep the activity of this LPP1 isoform to a minimum at the level of RNA splicing. Truncated isoforms, which possess no catalytic activity, also exist for PLD, DAG kinase, and PKC-δ. The PLD2 splice variants cloned from lung and brain are in equal abundance to the full-length protein reported by Steed *et al.* (18) and encode inactive proteins due to the absence of the transphosphatidyl domains. Kai *et al.* (19) have detected expression

of an internally truncated mRNA (not truncated in retina or brain) encoding inactive DAG kinase with both mRNA and protein expression. Moreover, Ueyama *et al.* (20) have cloned a truncated PKC-δ isoform from rat testis which has an 83bp insertion resulting in early termination. The protein is expressed and possesses the regulatory domain without catalytic regions. The authors propose that it may act as a dominant negative against full-length PKC δ thereby modulating signaling. Since the genomic organization for the LPPs is currently unknown, it is still possible that LPP1b may be the product of a pseudogene.

3.4.3 Expression of Pulmonary LPPs

Lung expresses LPP1, LPP1a, LPP1b, and LPP3 mRNAs. The LPP2 isoform was detected in rat brain and absent in lung. Hooks and colleagues (21) have described high tissue specific expression of human LPP2 where it was detected in brain, pancreas, and placenta. The profiles obtained in this study compares similarly to those obtained in the mouse and human (22, 23).

Transient expression of the pulmonary LPP cDNAs in HEK 293 cells confirms that the full-length pulmonary LPPs are, indeed, catalytically active members of the PAP2 superfamily. Meanwhile, expression of the novel LPP1b isoform did not modulate LPP enzyme activity. LPP1b contains a "G" nucleotide resulting in a frameshift and would be expected to produce a catalytically inactive truncated 30 residue protein. The inability to overexpress LPPs in the MLE12 cell line may be due to toxic effects arising from the high constitutive expression from the strong

cytomegalovirus promoter in the pTracer-CMV2 expression vector. Overexpression of lipid signaling enzymes may lead to changes in cell morphology due to membrane damage, which may eventually lead to cell death. It was reported that stable ECV 340 and HEK293 cell lines overexpressing LPP1, LPP1a, and LPP3 had a significant decrease in phosphatidic acid content compared to control cell lines (11, 17).

3.4.4 Other Potential Lipid Phosphate Phosphohydrolases

It is highly probably that there exists other lipid phosphate phosphohydrolases that have yet to be cloned. A S-1-P phosphohydrolase was recently cloned by Spiegel's group (24) which had high homology to the active site of the LPPs but was proposed to contain 8-10 transmembrane domains. Boudker and Futerman (25) have identified an NEM-insensitive, magnesium-independent activity in rat liver plasma membranes that demonstrates specificity towards C-1-P. There also exists a nuclear LPP activity that was characterized by Baker and colleagues (26) in neuronal nuclei which appears to be NEM-insensitive and magnesium-independent. It displayed specificity towards LPA but was inhibited only by S-1-P and not C-1-P and PA. Furthermore, Imai and collaborators (27) have recently described an activity in ovarian cancer cells that is NEM-insensitive, magnesium-independent with activity against LPA that was not inhibited by S-1-P, C-1-P, or PA. Hence, the enzymological properties of these activities including their substrate specificity distinguish them from the presently cloned LPPs.

The cloning of the NEM-sensitive, magnesium-dependent PAP1 and its

substrate specificity has not yet been reported. This enzyme may also be implicated in signaling as reported by various investigators (28, 29). Other NEM-sensitive enzymes may exist including an activity characterized by Frank and Waechter (30) which is unaffected by magnesium and catalyses the hydrolysis of polyisoprenyl phosphate and PA with similar efficiencies.

3.4.5 Summary

We have shown previously that pulmonary LPP activity exists in alveolar type II cells and hydrolyses PA and LPA in purified lung plasma membranes (2). Sphingosine-1-phosphate (S-1-P) was a relatively poor substrate in contrast to purified rat liver LPP which suggested the presence of a novel LPP in lung. Thus, various LPPs were cloned by RT-PCR from both adult rat lung and type II cell RNA generating LPP1, up to three LPP1 variants, and LPP3 cDNAs. The three LPP1 variants include LPP1a and two novel truncated isoforms, LPP1b and LPP1c. The full-length rat lung cDNAs encode functional NEM-insensitive phosphatidate phosphohydrolases. These pulmonary LPPs are proposed to be involved in regulating surfactant phospholipid secretion in alveolar type II cells as well as in controlling cell growth during lung development and injury. The LPP1b and LPP1c isoforms contain frameshifts, which would result in premature termination producing putative catalytically inactive polypeptides of 30 and 76 amino acids, respectively. Further investigation of the LPP1b isoform across a tissue profile revealed that it exists in equal abundance to the LPP1/1a isoform in lung tissue. It is proposed that

LPP1b may have a function in controlling the expression level of LPP1 in order to regulate its activity at the level of RNA splicing.

3.5 Acknowledgements

We would like to express our gratitude to Dr. D. Brindley (University of Alberta, Edmonton) for stimulating discussions. We thank Allan Grolla and Dave Dales for synthesizing the oligonucleotides (London Regional Cancer Centre, London, Ontario). We thank the laboratory of Dr. Stephen Ferguson (Robarts Research Institute) for providing HEK 293 cells for the expression studies. We also thank Anne Brickenden for invaluable technical assistance. This work was supported by a group grant from the Medical Research Council of Canada.

3.6 References

1. **Walton PA and Possmayer F.** 1986. Translocation of Mg^{+2}-dependent phosphatidate phosphohydrolase between cytosol and endoplasmic reticulum in a permanent cell line from human lung. Biochem. Cell Biol. **64**: 1135-1140.

2. **Nanjundan M and Possmayer F.** Characterization of Pulmonary NEM-Insensitive Phosphatidate Phosphohydrolase. 2000. Experimental Lung Research, **26**: 361–381,

3. **Waggoner DW, Gomez-Munoz A, Dewald J, and Brindley DN.** Phosphatidate phosphohydrolase catalyzes the hydrolysis of ceramide-1-phosphate, lysophosphatidate, and sphingosine-1-phosphate. 1996. J. Biol. Chem. **271**: 16506-16509.

4. **Ide H and Weinhold PA.** 1982. Properties of diacylglycerol kinase in adult and fetal rat lung. Biochim. Biophys. Acta. **713**: 547-554.

5. **Rooney SA.** 1985. The surfactant system and lung phospholipid biochemistry. Am. Rev. Respir. Dis. **131**: 439-460.

6. **Castranova V, Robovsky J, Tucker JH, and Miles PR.** 1988. The alveolar type II epithelial cells: a multifunctional pneumocyte. Toxicol. Appl. Pharmacol. **93**: 472-483.

7. **Dobbs, L.** 1990.Isolation and culture of alveolar type II cells. Am. J. Physiol. **258**: L134-L147,

8. **Lowry OH, Rosebrough NJ, Farr AL, and Randall RJ.** 1951. Protein measurement with the folin phenol reagent. J. Biol. Chem. **193**: 265-275.

9. **Brindley D and Wagonner D.** 1998. Mammalian lipid phosphate phosphohydrolases. J. Biol. Chem. **273**: 24281-24284.

10. **Barila D, Plateroti M, Nobili F, Muda AO, Xie Y, Morimoto T, and Perozzi G.** 1996. The Dri42 gene, whose expression is up-regulated during epithelial differentiation, encodes a novel endoplasmic reticulum resident transmembrane protein. J. Biol. Chem. **271**: 29928-29936.

11. **Leung DW, Tompkins CK, and White T.** 1998. Molecular cloning of two alternatively spliced forms of human phosphatidic acid phosphatase cDNAs that are differentially expressed in normal and tumor cells. DNA and Cell Biol. **17**: 377-385.

12. **Tate R, Tolan D, and Pyne S.** 1999. Molecular cloning of magnesium-independent type 2 phosphatidic acid phosphatases from airway smooth muscle. Cell. Signal. **11**: 515-522.

13. **Stukey J and Carman GM.** 1997. Identification of a novel phosphatase sequence motif. Protein Science. **6**: 469-472.

14. **Xu J, Zhang QX, Pilquil C, Berthiaume LG, Waggoner DW, and Brindley DN.** 2000. Related Lipid phosphate phosphatase-1 in the regulation of lysophosphatidate signaling. Ann N Y Acad. Sci. **905**:81-90.

15. **Xu J, Love LM, Singh I, Zhang QX, Dewald J, Wang DA, Fischer DJ, Tigyi G, Berthiaume LG, Waggoner DW, and Brindley DN.** 2000. Lipid phosphate phosphatase-1 and Ca2+ control lysophosphatidate signaling through EDG-2 receptors. J. Biol. Chem.

16. **An S.** 2000. Identification and characterization of G protein-coupled receptors for lysophosphatidic acid and sphingosine 1-phosphate. Ann N Y Acad. Sci. **905**:25-33.

17. **Sciorra VA and Morris AJ.** 1999. Sequential actions of phospholipase D and

phosphatidic acid phosphohydrolase 2b generate diglyceride in mammalian cells. Mol. Biol Cell. **10**: 3863-3876.

18. **Steed P, Clark K, Boyar W, and Lasala D.** 1998. Characterization of human PLD2 and the analysis of PLD isoform splice variants. FASEB J. **12**: 1309-1317.

19. **Kai M, Sakane F, Imai S, Wada I, and Kanoh H.** 1994. Molecular cloning of a diacylglycerol kinase isozyme predominantly expressed in human retina with a truncated and inactive enzyme expression in most other human cells. J. Biol. Chem. **269**: 18492-18498.

20. **Ueyama T, Ren Y, Ohmori S, Sakai K, Tamaki N, and Saito N.** 2000. cDNA cloning of an alternative splicing variant of protein kinase C delta (PKC deltaIII), a new truncated form of PKCdelta, in rats. Biochem Biophys Res Commun. **269**: 557-563.

21. **Hooks SB, Regan SP, and Lynch KR.** 1998. Identification of a novel human phosphatidic acid phosphatase type 2 isoform. FEBS Lett. **427**: 188-192.

22. **Kai M, Wada I, Imai S, Sakane F, and Kanoh H.** 1996. Identification and cDNA cloning of 35kDa phosphatidic acid phosphatase (type 2) bound to plasma membrane. Polymerase chain reaction amplification of mouse H_2O_2-inducible hic 53 clone yielded the cDNA encoding phosphatidic acid phosphatase. J. Biol. Chem. **271**: 18931-18938.

23. **Kai M, Wada I, Imai S, Sakane F, and Kanoh H.** 1997. Cloning and characterization of two human isozymes of Mg^{+2}-independent phosphatidic acid phosphatase. J. Biol. Chem. **272**: 24572-24578.

24. **Mandala SM, Thornton R, Galve-Roperh I, Poulton S, Peterson C, Olivera A, Bergstrom J, Kurtz MB, and Spiegel S.** 2000. Molecular cloning and characterization of a lipid phosphohydrolase that degrades sphingosine-1-phosphate and induces cell death. Proc Natl Acad Sci U S A. **97**:7859-7864.

25. **Boudker O and Futerman AH.** 1993. Detection and characterization of ceramide-1-phosphate phosphatase activity in rat liver plasma membrane. J Biol Chem. **268**: 22150-22155.

26. **Baker RR and Chang HY.** 2000. A metabolic path for the degradation of lysophosphatidic acid, an inhibitor of lysophosphatidylcholine lysophospholipase, in neuronal nuclei of cerebral cortex. Biochim Biophys Acta. **1483:** 58-68.

27. **Imai A, Furui T, Tamaya T, and Mills GB.** 2000. A gonadotropin-releasing hormone-responsive phosphatase hydrolyses lysophosphatidic acid within the plasma membrane of ovarian cancer cells. J Clin Endocrinol Metab. **85**:3370-3375.

28. **Johnson CA, Balboa MA, Balsinde J, and Dennis EA.** 1999. Regulation of cyclooxygenase-2 expression by phosphatidate phosphohydrolase in human amnionic WISH cells. J Biol Chem. **274**:27689-27693.

29. **Jiang Y, Lu Z, Zang Q, and Foster DA.** 1996. Regulation of phosphatidic acid phosphohydrolase by epidermal growth factor. Reduced association with the EGF receptor followed by increased association with protein kinase C epsilon. J Biol Chem. **271**:29529-29532.

30. **Frank DW and Waechter CJ.** 1998. Purification and characterization of a polyisoprenyl phosphate phosphatase from pig brain. Possible dual specificity. J Biol Chem. **273**:11791-11798.

Chapter 4

Developmental Patterns of Lipid Phosphate Phosphohydrolases in Rat Lung and Alveolar Type II Cells

4.1 Introduction

Lipid phosphate phosphohydrolase (LPP) catalyzes the hydrolysis of various lipid phosphates including phosphatidic acid (PA), lysophosphatidic acid (LPA), ceramide-1-phosphate (C-1-P), and sphingosine-1-phosphate (S-1-P) (1). We have shown previously that pulmonary LPP activity exists in surfactant-secreting alveolar epithelial type II cells and hydrolyzes PA and LPA in purified lung plasma membranes (2). Various LPPs were cloned by RT-PCR from both adult rat lung and type II cell RNA generating LPP1, up to three LPP1 variants, and LPP3 cDNAs (3). The three LPP1 variants include LPP1a and two truncated isoforms, namely, LPP1b and LPP1c (3).

Recent studies indicate a potential role for LPP in signal transduction. LPP could act to hydrolyze PA arising in the plasma membrane from diacylglycerol (DAG) kinase (4) and phospholipase D (PLD) (5) thereby regulating the levels of PA in the plasma membrane. It has been suggested that transient elevations in DAG levels arising through phospholipase C (PLC) degradation of phosphatidylinositol bisphosphate (PIP_2) in alveolar type II cells can be extended through the stimulation of the PLD/ LPP pathway (6). Phosphatidylinositol-specific PLC (PI-PLC) will hydrolyze PIP_2 to generate DAG for protein kinase C (PKC) activation. PKC can then stimulate PLD which will hydrolyze the abundant PC to provide substrate for a plasma membrane localized LPP which will generate DAG to sustain PKC activation to maintain surfactant secretion for longer periods. Another proposed function for LPP is in controlling cell growth during lung development and injury which may involve the Edg (endothelial differentiation gene) receptor. Both S-1-P

and LPA are biologically active lipids which have been implicated in eliciting various biological responses including cellular proliferation, differentiation, migration, and inhibition of apoptosis through these receptors (7). The involvement of Edg in lung function has not yet been described.

Lung development is a highly complex process that involves morphogenesis, growth, and differentiation, which is required for transition from an aqueous to an air-breathing environment (8). It was previously shown by Casola and Possmayer (9) that membrane-bound LPP activity in rat lung tissue did not change appreciably in the fetus but increased significantly after birth. However, in rabbit lung, there was a small increase during late gestation followed by a decrease in the adult (10). The specific activity of LPP also was reported to increase with the induction of pulmonary maturation by glucocorticoids and phosphatidylcholine (PC) (11, 12). The increased LPP activity correlated with the appearance of lamellar bodies (stored intracellular surfactant) in the fetal rabbit lung (13). Thus, these changes in LPP activity appear to parallel surfactant production and accumulation.

Pulmonary surfactant, composed of 90% lipid and 10% protein, is essential for normal lung function (14). Its main function is to maintain low surface tensions at the air-liquid interface and to prevent alveolar collapse on expiration (14). In the rat, the production of pulmonary surfactant is initiated when gestation is approximately 80% complete. Increased phosphatidylcholine synthesis occurs between day 20 of gestation and day 1 in the neonate (14). In this species, the levels of PC and disaturated PC increases between days 20 of gestation and day 1 after birth (14). Surfactant secretion also increases as indicated by the levels of

surfactant phospholipids in lung lavage which has been shown to increase during the later stages of fetal development and to a greater extent in the neonate (14).

Surfactant phospholipid secretion by isolated type II cells can be stimulated by a variety of agonists acting by at least three signal transduction mechanisms: β_2 or A_2 receptor leading to the activation of adenylyl cyclase, P_{2u} receptor leading to the activation of calcium-calmodulin, and the activation of PKC (15). Rooney and colleagues have demonstrated differential maturation of the signal transduction pathways mediating surfactant secretion in rat isolated type II cells (16). The response to phorbol ester was lower in fetal cells and reached adult levels by day 1 after birth (16). However, the developmental increase in the response of the cells to ATP, which acts through all three signaling pathways, did not attain maximal levels until day 30 (16). UTP, an agonist which acts only through the P_{2u} receptor, fails to stimulate significant secretion until day 4 (17). Rooney and colleagues identified that the levels of PKCα, βI, βII, and ζ in newborn type II cells were only half the level of adult cells (17). These investigators suggest that the lack of response in the early newborn type II cells to P_{2u} agonists is due possibly to insufficient amounts of one or more of PKC isoforms (17).

As a preliminary step towards investigating the possible functions of the cloned LPP isoforms, we examined the developmental patterns for LPP activity and the mRNA levels of LPP1, LPP1a, LPP1b, and LPP3 in whole lung tissues from male and female rats. The expression of PLD, Edg receptors, and PKC isoforms was also investigated across development. We propose that an LPP isoform(s) may

be involved in phospholipid surfactant secretion acting downstream to P_{2u} receptor activation to provide DAG for prolonged PKC activation. However, type II cells comprise less than 10% of the lung cellular population and thus, any changes in LPP observed in the whole lung profile cannot be extrapolated to this cell type. Therefore, similar studies were also performed in isolated airway epithelial cells or primary type II cells across development to assess the role of LPP(s).

4.2 Materials and Methods

4.2.1 Materials

Trizol reagent, Superscript™ preamplification kit, DNAse I (amplification grade), IPTG, and Xgal were obtained from Gibco BRL. RNAse H and restriction enzymes were purchased from Pharmacia Biotech. The Advantage cDNA PCR kit was obtained from Clontech Laboratories. Mineral oil and herring sperm DNA were obtained from Sigma. pGEM-3Zf(+) was obtained from Promega. XL1-blue cells and QuikHyb solution were obtained from Stratagene. Polyclonal antibodies for PKC-μ and PKC-α were obtained from Santa Cruz Biotechnologies, Santa Cruz, USA. Tissue culture media was obtained from Gibco BRL. Porcine elastase was obtained from Worthington Biochemicals. Fetal bovine serum was obtained from CanSera. 1-Palmitoyl-2-oleoyl-phosphatidylcholine was purchased from Avanti Polar Lipids. DAG kinase was purchased from Calbiochem. [α-^{32}P]-dCTP and [γ–P^{32}]-ATP were purchased from Amersham.

4.2.2 RT-PCR of LPP variants

Rat lung tissue was obtained from Sprague-Dawley and Wistar rats for the whole lung and type II cell developmental profiles, respectively. The LPP variant primers were designed to be isoform-specific. These primers were used for semi-quantitative RT-PCR and for generation of probes for southern and northern analysis. The primers for LPP1/LPP1a and LPP1b (30 cycles):

5'-GAGAGATCTGTGACC**ATG**TTCGACAAGCC (5'-primer) (**start**)

5'-GAGGTCGACGGCCGCAGTCTGCCTATACGA (3'-primer) (383 to 365bp)

The primers for region IIB (see Fig.3.2) of LPP1:

5'-GCTGGCTGGATTGCCTTATATA (5'-primer) (68-81bp)

5'-TCCACCTAATAACGCATAAGGG (3'-primer) (196-175bp)

The primers for region IIA (see Fig.3.2) of LPP1a:

5'-TTCCATGCCTATGGCTGTTGTA (5'-primer) (57-78bp)

5'-CAAGCCCCACTAGGACGAGTAC (3'-primer) (186-165bp)

The primers for LPP3 (Genbank # YO7783) (30 cycles):

5'-CTCGGATCCGCCAGCGCC**ATG**CAAACGTA (5'-primer) (**start)**

5'-TTCGGATCCAGTGCTCTGGAGGCCGCAGC (3'-primer) (adjacent to stop)

The primers for PLD1 (Genbank #2723381) (30 cycles):

5'-ATGGATTAAGCCCCACTTGAA (5'-primer) (1795-1816bp)

5'-ACAAGGTTTCCTTCCAGCTCTG (3'-primer) (2668-2647bp)

The primers for PLD2 (Genbank #2723385) (30 cycles):

5'-TGGCTAGG**ATG**ACTGTAACCCA (5'-primer) (**start**)

5'-CCAAGGTCTGGGATAAAGGAAA (3'-primer) (612-591bp)

The primers for Edg1 (Genbank #8393289) (30 cycles):

5'-TGCTGCTTGATCCTAGAGA (5'-primer) (191-212bp)

5'-TAATGGTCTCTGGATTGTCCCC (3'-primer) (1142-1121bp)

The primers for Edg2 (Genbank #2623061) (30 cycles):

5'-AGATCTGACCAGCCGACTCAC (5'-primer) (65-85bp)

5'-GTTGGCCATCAAGTAATAAATA (3'-primer) (443-422bp)

The primers for β-Actin (Genbank # J00691) (22 cycles):

5'-TTCAACACCCCAGCCATGTA (5'-primer)

5'-ATCTCCTTCTGCATCCTGTC (3'-primer)

4.2.3 Cloning and Sequencing of PLDs and Edg from Adult Rat Lung and Type II Cells

The isolation of alveolar type II cells was followed according to Dobbs *et al* (18). Lungs were perfused with 0.9% saline as previously described (2). Total RNA was prepared using Trizol reagent. The RNA was DNAse-treated prior to first strand cDNA synthesis. The reverse transcriptase reaction was performed using oligo $(dT)_{12\text{-}18}$ as the primer and Superscript H^--Reverse transcriptase. The cDNA was then RNAse-treated prior to the PCR reaction. PCR primers for amplification of PLD1, PLD2, Edg1, and Edg2 are described above.

The reaction mixture (100μl) contained 1XClontech Buffer (containing 3.25mM Mg^{+2}), dNTPs (0.4mM each), primers (0.4μM), and cDNA (2μl). The Clontech proofreading enzyme polymerase mixture (0.5 U) was added and then the

samples were overlaid with light mineral oil. The incubation conditions were 94^0C for 5 minutes followed by 30 cycles of 2 minutes at 94^0C, 2 minutes at 62^0C, and 2 minutes at 72^0C. PCR products were subjected to electrophoresis on 1.2% agarose gels in 40mM Tris-borate containing 1mM EDTA and 0.001mg/ml ethidium bromide.

PCR products were cloned into the pCR-Topo II vector (Stratagene) and transformed into competent XL1-Blue cells. Positive colonies were selected by peforming blue-white colony screening. Nucleotide sequencing of the various PLD and Edg clones was performed using fluorescent dye primer extension with an automated DNA sequencer (Robarts Research Institute, DNA Sequencing Facility). The sequences were analyzed using the BLAST program.

4.2.4 Rat Lung Developmental Profile: RNA and Protein Isolation

For each day, a total of 3 litters of rats (n = 3) were analyzed with the exception of 17 days of gestation, where lungs were isolated from a total of 9 litters and 3 litters were pooled and analyzed (n = 3). Timed pregnant Sprague-Dawley rats were obtained from Charles River Laboratories (Montreal, Canada). Total RNA was isolated using Trizol reagent from male and female rat lung tissues from 17 days of gestation (dg), 19 dg, 21 dg, 22dg, 1 day after birth (D), 2D, 4D, 9D, 16D, and adult. For the preparation of subcellular fractions, the lungs were first chopped and then homogenized in 9 volumes of ice-cold Buffer A (0.25M sucrose, 0.1mM EDTA, 1mM HEPES, pH 7.4, 1mM pefabloc) using ten strokes with a tight fitting pestle with a Potter Elvehjem homogenizer (Heidolph). The homogenate was then initially centrifuged at 1,450g for 5 min resulting in a nuclear pellet and a

supernatant. The latter was centrifuged at 10,000g for 15 min yielding a mitochondrial pellet and a supernatant. The supernatant was centrifuged at 100,000g for 60 min providing a microsomal pellet and a cytosolic supernatant. The fractions were aliquoted and frozen at -70^{0}C. Various fractions were retained for analysis throughout the isolation procedure.

4.2.5 Type II Cell Developmental Profile: RNA and Protein Isolation

Timed pregnant Wistar rats were obtained for these studies. Rat lung tissues from 19 dg, 21 dg, 1 day after birth (D), 6D, and adult were used for isolated of primary alveolar epithelial cells following the methods of Dobbs *et al* (18) and Caniggia *et al* (19). Total RNA was isolated using Trizol reagent. For protein, cells were harvested and homogenized using a probe sonicator for 10 seconds three times in Buffer A and stored at -70^{0}C.

4.2.6 Northern Analysis

A 1% agarose-RNA formaldehyde gel containing total RNA from tissues (20μg/lane) was transferred to Nylon membranes. Prehybridization for 20 minutes at 68^{0}C in QuikHyb solution was followed by hybridization with the appropriate probe with 100μl of denatured herring sperm DNA for 1 hour at 68^{0}C. For 18S and LPP3, the blots were washed for 1 hour at 60^{0}C in 2XSSC and 0.1% SDS followed by a 30 minutes wash in 0.1XSSC and 0.1% SDS at room temperature. For LPP1, the blots were washed in 0.1XSSC and 0.1% SDS at room temperature for 6 hours.

LPP1 and LPP3 probes were prepared by random prime labeling using [α-^{32}P]-dCTP. The membranes were exposed to X-ray film between 8-12 hours for 18S, 24-72 hours for LPP3, and at least 1 week for LPP1.

4.2.7 Southern Analysis

As described above, RT-PCR was performed and the products were run on a 2% agarose gel. The gel was denatured in denaturing buffer (0.5M NaOH, 1.5M NaCl) for 30 minutes at room temperature. Subsequently, the gel was transferred to neutralizing buffer (0.5M Tris-HCl (pH 7.0), 1.5M NaCl) and slowly shaken for 30 minutes at room temperature. The gel was soaked in 20XSSC transfer buffer for 30 minutes and then transferred to nylon membrane using the Turboblotter Rapid Downward Transfer System (Schleicher & Schull).

4.2.8 SDS-PAGE and Western Blot Analysis

The samples were boiled in sample buffer for 5 minutes and cooled on ice before loading onto 8% SDS-PAGE gels. The gel was run at 100 volts and the proteins were electrophoretically transferred onto Immobilon P membranes for 1 hour at 200mA at 4^{0}C. Blots were blocked in 5% nonfat dry milk in TBS with 0.2% Tween-20 (v/v) (TBST) for 1 hour at room temperature. Primary antibody incubations were performed in the same blocking buffer at dilutions of 1:1000 for up to 2 hours at room temperature. The blots were then washed in TBST for 10 minutes three times at room temperature. Secondary antibody incubations were

performed in TBST containing 5% nonfat dry milk at 1:10,000 for 1 hour at room temperature followed by another 30 minutes wash in TBST. Protein bands were visualized by enhanced chemiluminescence (kit from Gibco BRL) and exposed to film.

4.2.9 LPP Assays

The activity was assayed using pure PA as substrate. Unlabelled PA and P^{32}-labelled PA were prepared as described before (2). Reaction mixtures contained 100mM Tris-Maleate buffer, pH 6.5, 0.6mM PA (0.4mCi/mmol), 0.5mM EDTA, 0.5mM EGTA, pH 7.0, 0.2mg of essentially fatty acid free albumin and 1mM DTT in a final reaction volume of 0.1 ml. Incubation times were 60 minutes in duration at 37^0C. The protein was preincubated at 37^0C for 10 minutes with 4.2mM N-ethylmaleimide (NEM). Reactions were terminated by the addition of 1.5 ml of chloroform: methanol (1:1). The phases were broken with 0.75ml of 0.1N HCl and a sample of the upper aqueous phase was taken for scintillation counting to determine the P^{32} inorganic phosphate released (2).

4.2.10 Other Assays

Protein was determined by the method of Lowry *et al.* in the presence of 2mM SDS (20) using bovine serum albumin as the standard.

4.3 Results

4.3.1 mRNA Expression Profiles for LPP Isoforms

In order to obtain insight into the potential function of the previously cloned LPP isoforms (Chapter 3), their mRNA expression patterns were investigated across rat lung development. The profiles for the mRNA levels of LPP1 and LPP3 were determined by northern analysis and the results are shown in Figure 4.1A. LPP1 mRNA levels were determined using a probe designed against region IIB (refer to Chapter 3) which recognizes the LPP1 isoform. The mRNA levels are low at 17 days of gestation but increase slightly in the fetal period (21 and 22 dg). There is a marked increase in LPP1 mRNA expression in the newborn which remains high until day 4. The mRNA expression increases further on day 16 although remaining low compared to that in the newborn and there is also a slight decrease in LPP1 mRNA in the adult. The mRNA levels for LPP3 were low at 17 days of gestation and high at 19 dg with slightly decreased levels in late gestation (21 and 22 dg). The mRNA increased in the early neonate (1D or 2D) and remained fairly constant during the first week of life. The mRNA expression increased during the second week of life (16 days) and in the adult. LPP1a was undetectable by northern blotting and its profile was consequently determined by southern blotting of RT-PCR products using β-actin as a control (Figure 4.1B). The mRNA expression for LPP1a is low at 17 and 19 days of gestation with increased levels of expression in the late fetal period (21 and 22 dg). The LPP1a mRNA increases after birth between 2 and 4 days and remains at a high level of expression into the second week of life and

Figure 4.1. mRNA profiles for LPP isoforms across rat lung development. A, Northern blot analysis of rat lung developmental profiles from 17 dg to adult for LPP1, LPP3, and 18S. The results are from a representative experiment (n = 3). B, Semi-quantitative RT-PCR analysis across rat lung development from 17 dg to adult for LPP1/1a and LPP1b, LPP1, LPP1a, and control β-actin. The results are from a representative experiment (n = 3).

A

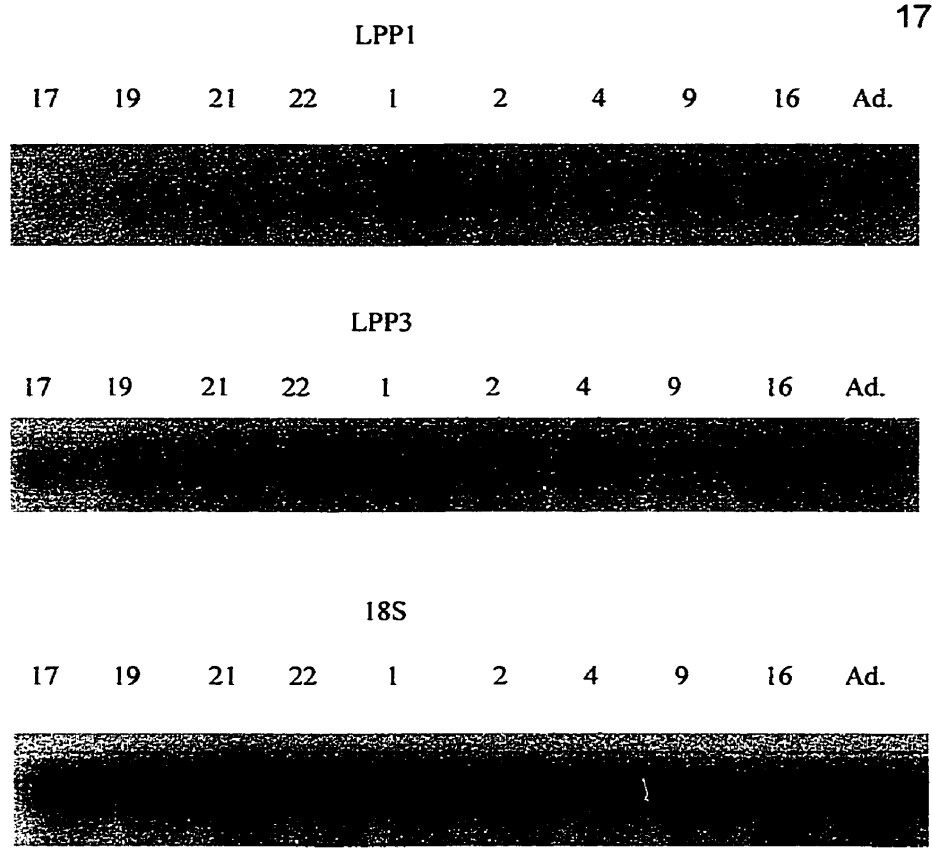
LPP1
17 19 21 22 1 2 4 9 16 Ad.
LPP3
17 19 21 22 1 2 4 9 16 Ad.
18S
17 19 21 22 1 2 4 9 16 Ad.

B

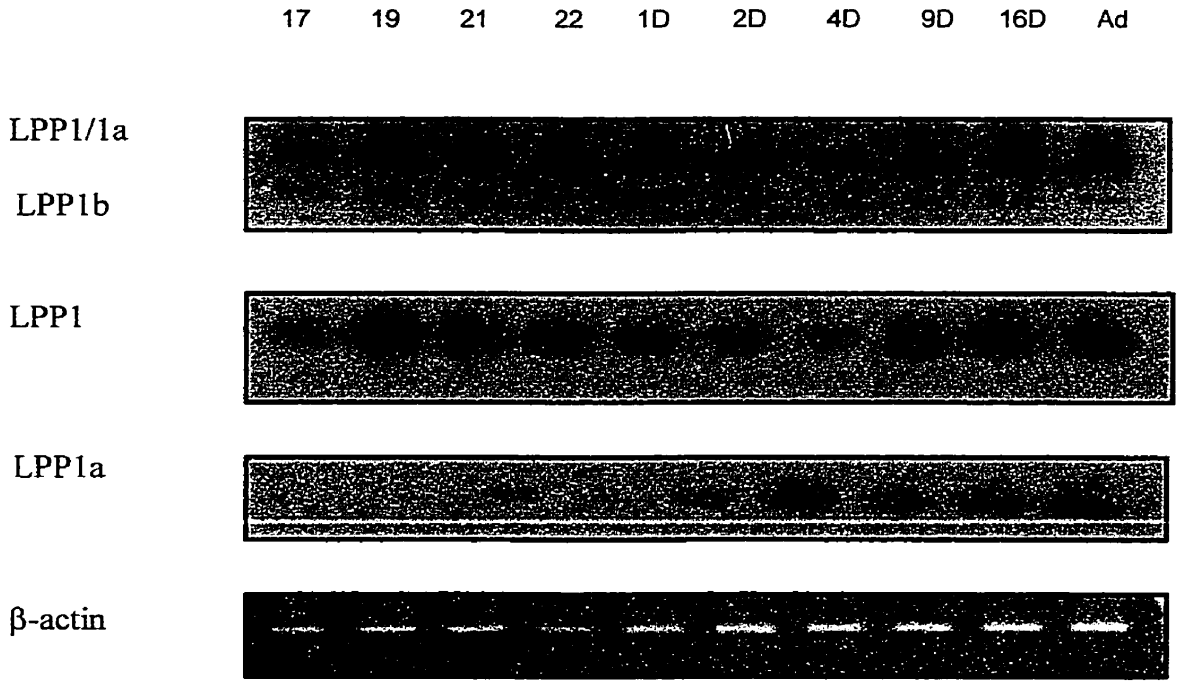
17 19 21 22 1D 2D 4D 9D 16D Ad
LPP1/1a
LPP1b
LPP1
LPP1a
β-actin

in the adult. The mRNA levels for LPP1b, the truncated inactive isoform, determined by RT-PCR, displays a high level of expression in the fetal tissues at 17 dg decreasing steadily in the neonate with low levels at 16 days and in the adult.

4.3.2 LPP Activity during Rat Lung Development

In order to gain some insight with respect to the potential function of LPPs in lung, LPP activity was measured in the microsomal fraction across a rat lung developmental profile (Figure 4.2A). We have previously shown high 5'-nucleotidase and alkaline phosphatase activity in adult rat lung microsomal fractions (Chapter 2) indicating that the LPP activity present within the microsomes could arise from plasma membranes athough its presence in other subcellular organelles cannot be excluded. The profile shows a 2.1-fold increase in membrane-bound LPP activity during the fetal period at 19 days gestation with a further 1.4-fold increase in activity after birth in the neonate. An additional small increase was observed in the adult.

The increases in LPP activity at 19-21 dg corresponds to the late pseudoglandular to canalicular phase of lung development which involves a combination of cellular proliferation and apoptosis to form bronchioles, alveolar ducts, blood vessels, and pre-type II cells enriched in glycogen (8). The increases in the neonate occur during the regression and stasis of the developing pulmonary vasculature, maturation of alveolar ducts, and after the well established marked increases in the synthesis of total PC and disaturated PC in type II cells (8). Thus, LPP, acting sequentially to PLD, could generate DAG to sustain PKC activation for signaling events including the regulation of cell growth and surfactant secretion.

Figure 4.2. LPP activity across rat lung development. The gestational ages investigated are 17 days gestation (dg), 19 dg, 21dg, 22 dg (term), 1 day after birth (D), 2D, 4D, 9D, 16D, and adult. LPP specific activity is shown as nmol of Pi released/min/mg. 10μg of protein was used for each assay. Assays were performed in triplicate for each group of rats (n = 3). The results are shown as the mean ± S.E.M. The dark filled bars represent males and the diagonal filled bars represent females.

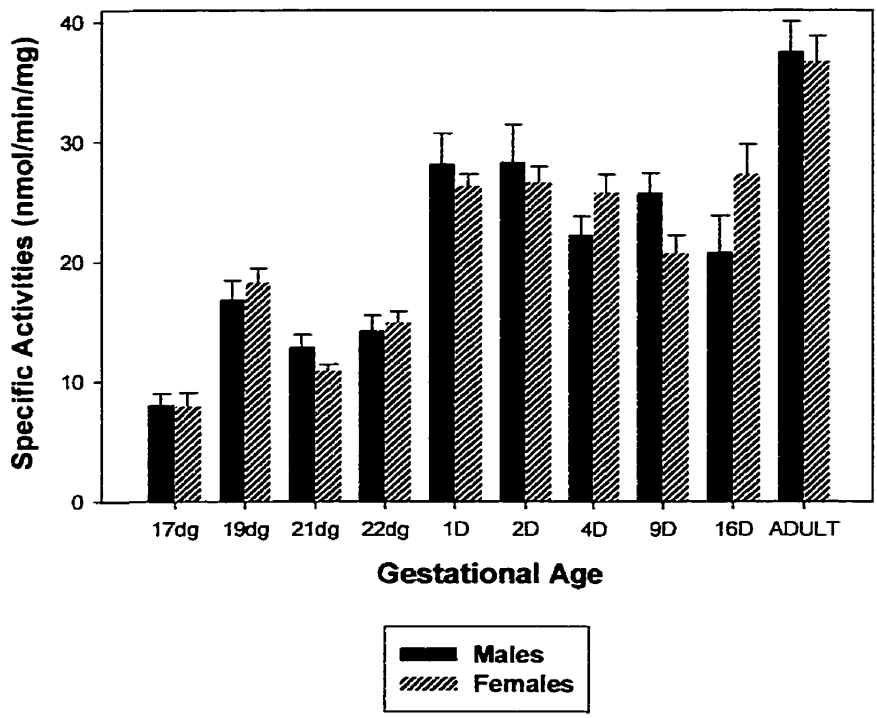
Specific Activities (nmol/min/mg)
40
30
20
10
0
17dg
19dg
21dg
22dg
1D
2D
4D
9D
16D
ADULT
Gestational Age
Males
Females

It is known that human premature male infants are more prone to respiratory distress syndrome (RDS) as there may be a delay in the maturation of their surfactant system (21, 22). This male disadvantage also occurs in rats (23) and rabbits (24) but not in some non-human primates (25). There are reports indicating that this may be due to inhibition of surfactant production in males by androgens (26). In the rabbit, female fetuses contain more pulmonary β-receptors than males and it has been suggested that part of the observed differences may be due to differences in surfactant secretion rather than its synthesis (27). In rat, Rooney and colleagues have addressed the possibility that differences in surfactant phospholipid secretion may account for the increased susceptibility of males to RDS (16). However, they did not observe any significant differences in basal secretion in the response to any secretagogue in type II cells in 30-day old rats (16). We did not observe any differences in LPP activity between males and females across whole lung development. This would suggest that differences in neonatal respiratory distress in the rat cannot be attributed to a lower production of DAG by LPP for PKC activation. However, further studies in type II cells must still be performed.

4.3.3 Edg Receptors, PLD, and PKC Patterns during Rat Lung Development

As it was recently shown that LPP could generate DAG sequentially to PLD (27) as well as being capable of hydrolyzing phospholipid growth factors such as LPA and S-1-P, which mediate their effects through Edg receptors (28), both PLD and Edg mRNA expression patterns were investigated across development. Both subtypes of the Edg receptor (S-1-P (Edg1) and LPA (Edg2)) as well as PLD1 and

PLD2 isoforms were found to be present in lung tissue

As shown in Figure 4.3A, PLD1 mRNA, as determined by RT-PCR, was found to be low during the fetal period and increased postnatally on day 4 to day 9 followed by a decrease in the adult. In contrast, PLD2 mRNA levels were high in fetal tissues, particularly on 21 days of gestation followed by a decrease around term. The mRNA expression increases in the early neonate (2D) and the second week of life. The control, β-actin, appears to increase slightly in the neonate as there are increases in the lung connective tissues.

The Edg1 and Edg2 mRNA expression profiles were determined by northern analysis as shown in Figure 4.3B. Edg1 mRNA is low in the fetal period and is highly expressed in the neonate on Day 4 while decreasing in the adult tissue. The Edg2 mRNA pattern shows high levels of expression in the fetal period (21 dg) and decreases around term. The levels increase after birth and remain high in the neonate (Day 4) followed by decreased levels in the adult.

The profiles for the protein levels of various PKC isoforms are shown in Figure 4.3C. With respect to PKCμ, the protein levels were low at 17 days gestation with a tendency to increase in the fetal period followed by a peak in the newborn. The protein levels remain high during the neonatal period and in the adult. PKCμ appears as a doublet where the top band most likely represents the phosphorylated PKC species. PKCα protein levels were found to increase in the fetal period with highest levels of expression in the neonate and a further increase in the adult.

Figure 4.3. Profiles for PLD, EDG receptors, and PKC isoforms across rat lung development. A, Semi-quantitative RT-PCR analysis across rat lung development from 17 dg to adult for PLD1, PLD2, and control β-actin. The results are from a representative experiment (n = 3). B, Northern blot analysis of rat lung developmental profiles from 17 dg to adult for Edg1 and Edg2. . The results are from a representative experiment (n = 3). C, The results of immunoblot analysis are shown for PKC-α and PKC-μ. The results are from a representative experiment (n = 3).

A

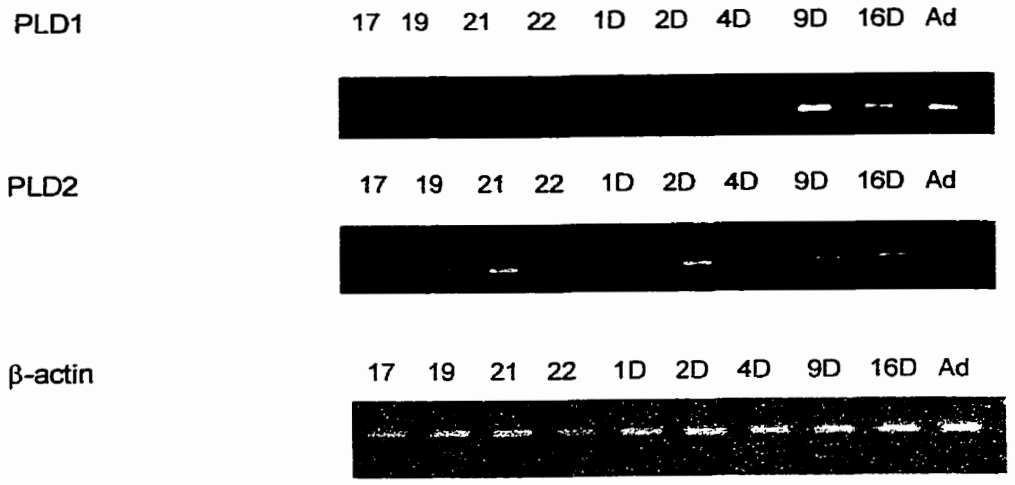
PLD1
17 19 21 22 1D 2D 4D 9D 16D Ad
PLD2
17 19 21 22 1D 2D 4D 9D 16D Ad
β-actin
17 19 21 22 1D 2D 4D 9D 16D Ad

B

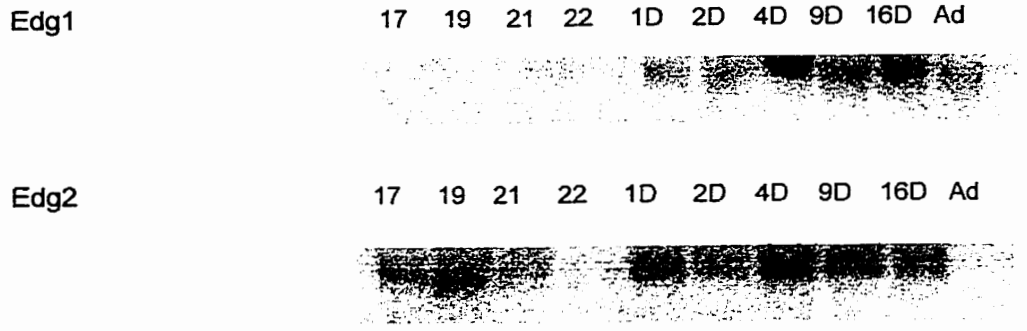
Edg1
17 19 21 22 1D 2D 4D 9D 16D Ad
Edg2
17 19 21 22 1D 2D 4D 9D 16D Ad

C

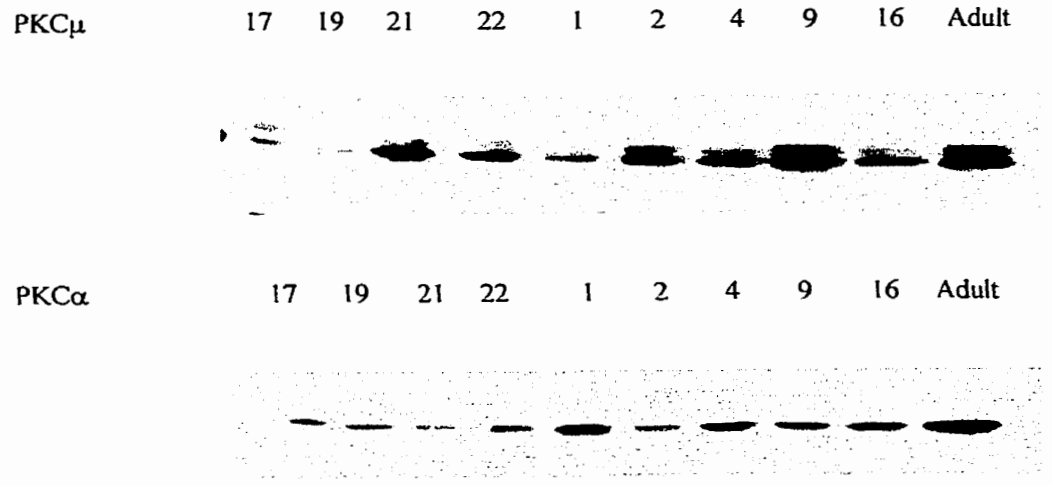
PKCμ
17 19 21 22 1 2 4 9 16 Adult
PKCα
17 19 21 22 1 2 4 9 16 Adult

4.3.4 Alveolar Type II Epithelial Cells Across Development

Since type II cells comprise less than 10% of the lung cellular population, the increases in LPP activity or changes in mRNA levels in the whole rat lung developmental profile cannot be extrapolated to this cell type. We proposed that an LPP isoform(s) may be involved in phospholipid surfactant secretion acting downstream to P_{2u} receptor activation to provide DAG for prolonged PKC activation and, hence, sustain surfactant secretion for a longer period of time (5). Hence, type II cells from 19 dg, 21 dg, 6-day-old, and adult rat lungs were isolated and the profiles for LPP and other lipid signaling enzymes were investigated. As shown in Figure 4.4A, LPP activity in type II cell lysates was found to decrease 1.6-fold in the neonate and adult compared to the relatively high levels in the fetal alveolar epithelial cells. Both PKCα and PKCμ protein decrease dramatically in the neonate and adult from the relatively high levels of expression during the fetal period (Figure 4.4B). Preliminary profiles for the mRNA levels of LPP, PLD, and Edg receptors are shown in Figure 4.5. Relative to β-actin, the levels of these signaling molecules did not appear to change dramatically.

The alveolar epithelial cells from 19 days gestation (100% confluent) were left in culture for 48 hours while the cells from 21 days gestation (60-70% confluent), 6-day-old (sparse), and adult (sparse) were maintained in culture for 24 hours. It is well established that there is increasing communication among cells with increasing density in cell culture and that the specific activity of LPP increases with progression to confluence (28). Moreover, the PI-PLC activity was also observed to increase with

Figure 4.4. Type II cell developmental profile. Type II cells were isolated from 19 dg, 21dg, 6-day-old, and adult Wistar rats. A, The enzyme activity of LPP was assayed using PA as substrate and 10μg of protein. The results are reported as nmol of Pi released/min/mg. Assays were performed in triplicate and the results are shown as the mean ± S.E.M. B, The results of immunoblot analysis are shown for PKC-α and PKC-μ.

A

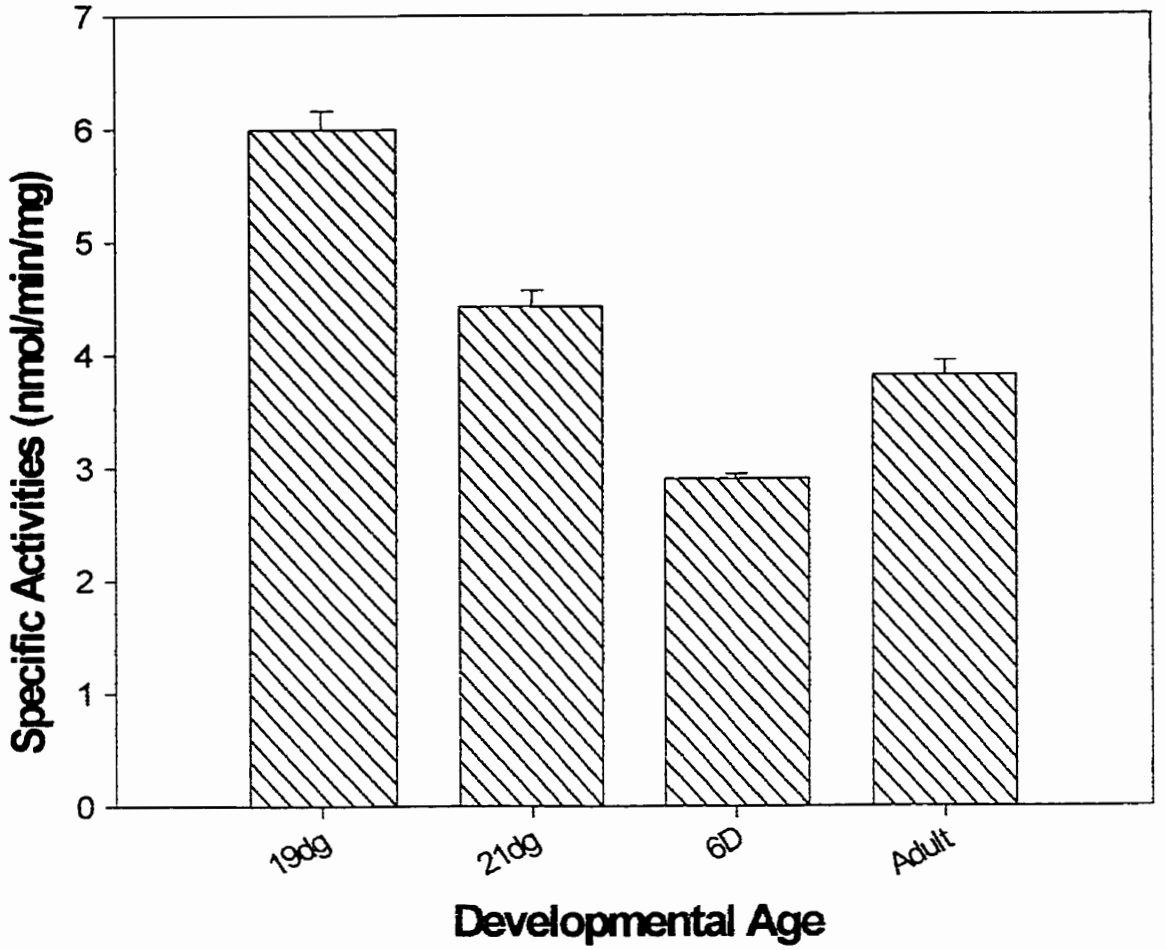
Specific Activities (nmol/min/mg)
0
1
2
3
4
5
6
7
19dg
21dg
6D
Adult
Developmental Age

B

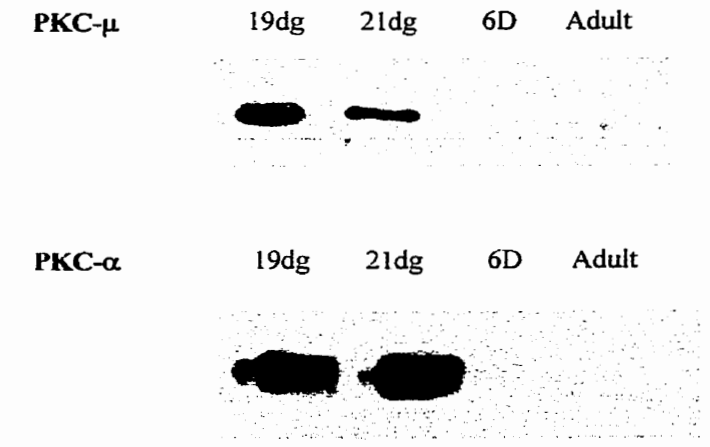
PKC-μ
19dg
21dg
6D
Adult
PKC-α
19dg
21dg
6D
Adult

Figure 4.5. mRNA expression profiles in type II cells during development. Semi-quantitative RT-PCR analysis was performed for LPP1, LPP1a, PLD1, PLD2, Edg1, Edg2, and control β-actin. Lane 1, 19dg; Lane 2, 21dg, and Lane 3, Adult.

LPP1 & LPP1a

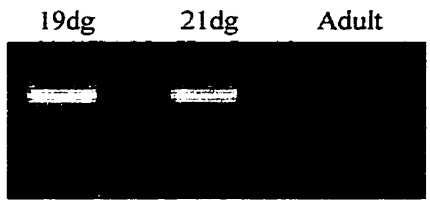

LPP3

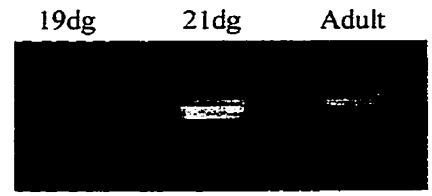

PLD1

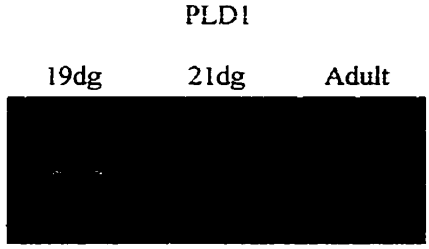

PLD2

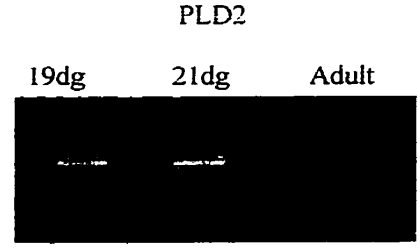

Edg1

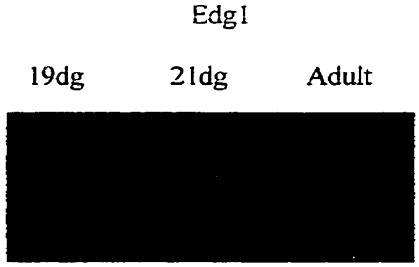

Edg2

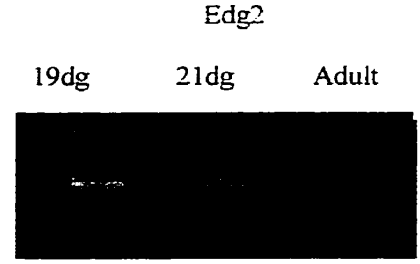

β-actin

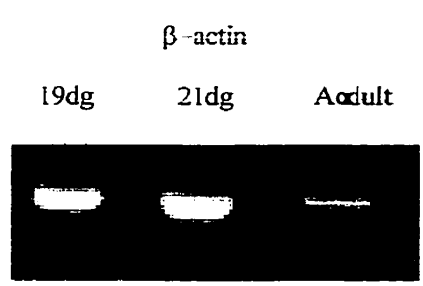

increasing cell density and when the cells become quiescent (29). Cell-cell communication is crucial for signaling in type II cells (fibroblast-type II and type I-type II cell interactions) (30) and is lost upon cellular isolation. The LPP activity and PKC isoform expression in these adult type II cells correlates with the transdifferentiation study presented in Chapter 5 where on day 1, there was undetectable PKC protein which increased dramatically on day 7. However, Rooney and colleagues were able to detect PKC expression in their isolated type II cells after 18-20 hours in culture (30μg of protein) (17). The plating confluency of their isolated type II cells was not reported. The dramatic decrease in the 6-day-old rat and adult PKC protein expression suggests increased turnover as reported to occur for PKC down-regulation (31). The type II cell developmental profile results are inconclusive and require further experimentation to elucidate the role of LPP(s) in the control of surfactant secretion and epithelial cell growth.

4.4 Discussion

4.4.1 Rat Lung Developmental Patterns

In order to obtain insight into the LPP isoforms, the patterns for LPP as well as for various PKC isoforms were examined across a rat lung developmental profile. The profiles show high levels of protein, activity, and mRNA for various LPP and PKC isoforms during the fetal gestation period, at birth, and postnatally. Generally, the LPP and PKC expression is low on 17 days of gestation with the exception of LPP1b which remains high in the fetal period. There is an increase in LPP activity

and mRNA, Edg2 mRNA, and PKCα protein on 19 dg. LPP1, LPP1a, PLD2, PKCα, and PKCμ increase slightly in the late gestation period (21 and 22 dg). These increases correspond to the late pseudoglandular to canalicular phase of development at which time these signaling enzymes could be involved in cellular remodelling, vasculogenesis, and the control of cell growth. At birth, there are marked increases in LPP activity, LPP1 mRNA, LPP3 mRNA, PLD2, Edg2, PKCμ, and PKCα which correlates with increased surfactant secretion. These levels tend to remain fairly constant into the first and second week of life with increases on day 4 (for LPP3, Edg1 and Edg2), day 9 to 16 (for LPP1a, PLD1, PLD2, and PKCμ) where they could be involved in the control of surfactant phospholipid secretion, the development and maturation of alveolar ducts, and the regression and stasis of the pulmonary vasculature.

Lung development is initiated in the embryo as a ventral outpouching of endodermal cells from the anterior foregut into the surrounding mesenchyme (8). There exist three phases of lung development: pseudoglandular, canalicular, and saccular phases. During the pseudoglandular phase (17 to 20 dg), airway construction as well as branching occurs to form bronchioles and alveolar ducts (8). Cyclins and cyclin-dependent kinases were found to be highly expressed in the proliferative stages of lung development (32, 33, 34). During this phase, apoptosis which is known to play a crucial role in the cellular remodeling of the developing lung (35), appears to be restricted to interstitial cells and may contribute to mesenchymal involution and the thinning of the alveolar septa (36). This is followed

by the canalicular phase (21 dg) in which the rapid growth diminishes with differentiation of epithelial cells lining the ducts, and the initiation of capillary growth. Neovascularization, involving vasculogenesis and angiogenesis, is crucial to lung development and is mediated through a variety of angiogenic and antiangiogenic factors (37). From the canalicular to terminal saccular stage (22 dg – after birth), most of the apoptotic activity is detected in epithelial cells (38). Capillaries continue to grow and epithelial cells undergo differentiation during this period of development.

Interactions between epithelial cells and the mesoderm are essential for the effects of growth and differentiation factors as well as hormones in various developmental processes including cellular differentiation, vasculogenesis, and synthesis of surfactant lipids and proteins. Mallampalli and colleagues have shown that sphingomyelin metabolism is developmentally regulated in rat lungs (39). They observed that sphingomyelin, ceramide, and sphingosine levels increase during development reaching their highest levels in the newborn. The rate of sphingomyelin biosynthesis (serine palmitoyltransferase and sphingomyelin synthase) was found to increase in the newborn with a concomitant decrease in the activities involved in sphingomyelin degradation (sphingomyelinase and ceramidase) which have high levels of activity at 19dg and decreasing in the neonate. There may be cross-talk between the glycerolipid (PA, LPA, and DAG) and sphingolipid pathways (ceramide, C-1-P, sphingosine, and S-1-P) during lung development. Both PKC and LPP are inhibited by sphingosine while PLD is activated resulting in increased levels of PA which is a potent mitogen. Both LPA

and S-1-P mediate their effects through the Edg receptors and LPP can hydrolyze these phospholipid growth factors to regulate these effects.

During late gestation (21 dg), the number and size of lamellar bodies increases in type II cells with decreases in glycogen content (6). During this time, there is a prenatal increase in surfactant PC as well as increases in the activities of enzymes involved in fetal lung PC biosynthesis. Choline-phosphate cytidylyltransferase activity was found to increase at the end of gestation and immediately after birth by a combination of increased synthesis and lipid activation (40, 41, 42). There are increases in PAP1 activity between 18 to 21 days of gestation (9), increases in DAG kinase activity between 19 and 21 dg (4), and increases in lung fatty acid biosynthesis during late fetal development (5). The increases in LPP at birth parallels the onset of surfactant phospholipid secretion rather than surfactant phospholipid synthesis.

LPP, acting sequentially to PLD, may be involved in the control of alveolar epithelial cell growth. During late gestation, the type II cells proliferate, undergo programmed cell death, and dedifferentiate into a type I cell. It was observed that type II cell apoptosis increased from the transition from the canalicular to the terminal sac stage in the developing rabbit (36) and there were increases in Fas ligand protein levels, which may be an important regulatory pathway in the control of postcanalicular alveolar differentiation (43). It is well established that epithelial-mesenchymal interactions are important for cellular differentiation when flattened cells, termed type I cells which are involved in gas exchange, arise through mitosis from the cuboidal type II cells.

LPPs may also be involved in the regulation of phospholipid surfactant secretion. Although the response to UTP failed to stimulate secretion until day 4 which appears to involve the production or activation of PKCα, βI, βII, and ζ in newborn type II cells, the response to phorbol esters reached adult levels by day 1 after birth (11). Rooney and colleagues later report that PKCμ may be implicated in the purinergic receptor signaling cascade. However, there did not appear to be any developmental delay in PKCμ protein levels (11). Thus, it is more likely that other signaling molecules such as the P_{2u} receptor, PLD isoforms, or LPP isoforms are not fully expressed or activated until after birth. Further experimental work is required to identify the role of LPP isoform(s) in surfactant secretion and in epithelial cell growth and may be better addressed using the recently described immortalized cell line by deMello and colleagues (44).

We had previously reported that LPP activity in type II cells was equivalent to whole lung homogenate and low in fibroblasts (2), which is indicative of another cellular localization. *In situ* hybridization and immunohistochemistry will provide us with a better understanding of the functional significance of these various LPPs in lung. LPP may serve in regulating the effects of the bioactive lipids, including LPA and S-1-P, through the Edg receptor in the development and maintenance of the lung endothelium. Perozzi and colleagues suggested that LPP3 may be involved in the migration of enterocytes in the intestinal villi during differentiation (45). In brain development, the spatial and temporal pattern for LPP3 suggests a potential function in the neuroepithelial developmental for gliogenesis (46). LPP3 was found

to be highly enriched in the ventricular zone of the brain in which the Edg receptor for LPA had been previously reported (47). Thus, LPP could be involved in controlling phospholipid growth factor mediated effects through the Edg receptors in the control of lung vascularization.

4.4 Acknowledgements

We would like to express our gratitude to Dr. D. Brindley (University of Alberta, Edmonton) for stimulating discussions. We thank Irene Tseu and Dr. Martin Post for generously providing fetal alveolar type II cells. We thank Anne Brickenden and Dr. K Rodriguez-Capote for invaluable assistance with the tissue isolation. We are also grateful to Maureen Mollard and Lisa Barry for their assistance with the animal work. This work was supported by a group grant from the Medical Research Council of Canada.

4.5 References

1. **Waggoner DW, Gomez-Munoz A, Dewald J, and Brindley DN.** Phosphatidate phosphohydrolase catalyzes the hydrolysis of ceramide-1-phosphate, lysophosphatidate, and sphingosine-1-phosphate. 1996. J. Biol. Chem. **271**: 16506-16509.

2. **Nanjundan M and Possmayer F.** Characterization of Pulmonary NEM-Insensitive Phosphatidate Phosphohydrolase. 2000. Experimental Lung Research, **26**: 361–381.

3. **Nanjundan M and Possmayer F.** Cloning and expression of pulmonary lipid phosphate phosphohydrolase. Manuscript submitted.

4. **Ide H and Weinhold PA.** 1982. Properties of diacylglycerol kinase in adult and fetal rat lung. Biochim. Biophys. Acta. **713**: 547-554.

5. **Rooney SA.** 1985. The surfactant system and lung phospholipid biochemistry. Am. Rev. Respir. Dis. **131**: 439-460.

6. **Rooney SA.** Regulation of Surfactant-Associated Phospholipid Synthesis and Secretion. Chapter 117, p.1283-1299.

7. **An S.** 2000. Identification and characterization of G protein-coupled receptors for lysophosphatidic acid and sphingosine 1-phosphate. Ann N Y Acad. Sci. **905**:25-33.

8. **Mendelson CR.** 2000. Role of transcription factors in fetal lung development and surfactant protein gene expression. Ann. Rev. Physiol. **62**: 875-915.

9. **Casola PG and Possmayer F.** 1981. Pulmonary phosphatidic acid phosphohydrolase developmental patterns in rat lung. Biochim Biophys Acta. **665**: 177-185.

10. **Casola PG and Possmayer F.** 1981. Pulmonary phosphatidic acid phosphohydrolase. Developmental patterns in rabbit lung. Biochim. Biophys. Acta. **665**: 186-194.

11. **Brehier A, Benson BJ, Williams MC, Mason RJ, and Ballard PL.** 1977. Corticosteroid induction of phosphatidic acid phosphatase in fetal rabbit lung. **77**: 883-890.

12. **Possmayer F, Duwe G, Metcalfe R, Stewart-DeHaan PJ, Wong C, Heras JL, and Harding PG.** 1977. Cortisol induction of pulmonary maturation in the rabbit foetus. Its effects on enzymes related to phospholipid biosynthesis and on marker enzymes for subcellular organelles. Biochem J. **166**:485-494.

13. **Douglas WHJ, Sommers-Smith SK, and Johnston JM.** 1983. Phosphatidate phosphohydrolase activity as a marker for surfactant synthesis in organotypic cultures of type II alveolar pneumocytes. J. Cell Sci. **60**: 199-207.

14. **Cockshutt AM and Possmayer F.** 1992. Metabolism of surfactant lipids and proteins in the developing lung. Ed: Robertson, van Golde LMG, and Batenburg JJ. Chapter 16, p339-397.

15. **Rooney SA, Young SL, and Mendelson CR.** 1994. Molecular and cellular processing of lung surfactant. FASEB J. **8**: 957-967.

16. **Griese M, Gobran LI, and Rooney SA.** 1992.Ontogeny of surfactant secretion in type II pneumocytes from fetal, newborn, and adult rats. Am. J. Physiol. **262**:

L337-L343.

17. **Gobran LI, Xu ZX, and Rooney SA.** 1998. PKC isoforms and other signaling proteins involved in surfactant secretion in developing rat type II cells. Am J Physiol. **274**: L901-L907.

18. **Dobbs L.** 1990.Isolation and culture of alveolar type II cells. Am. J. Physiol. **258**: L134-L147.

19. **Caniggia I, Tseu I, Rolland G, Edelson J, Tanswell AK, and Post M.** 1995. Inhibition of fibroblast growth by epithelial cells in fetal rat lung. Am. J. Respir. Cell Mol. Biol. **13**: 91-98.

20. **Lowry OH, Rosebrough NJ, Farr AL, and Randall RJ.** 1951.Protein measurement with the folin phenol reagent. J. Biol. Chem. **193**: 265-275.

21. **Perelman RH, Palta M, Kirby R, and Farrell PM.** 1986. Discordance between male and female deaths due to the respiratory distress syndrome. Pediatrics. **78**: 238-244.

22. **Torday JS, Nielsen HC, Fencl M de M, and Avery ME.** 1981. Sex differences in fetal lung maturation. Am Rev Respir Dis. **123**: 205-208.

23. **Nielsen HC and Torday JS.** 1981. Sex differences in fetal rabbit pulmonary surfactant production. Pediatr Res. **15**: 1245-1247.

24. **Adamson IY and King GM.** 1984. Sex-related differences in cellular composition and surfactant synthesis of developing fetal rat lungs. Am Rev Respir Dis. **129**: 130-134.

25. **Perelman RH, Engle MJ, Palta M, Kemnitz JW, and Farrell PM.** 1986. Fetal lung development in male and female nonhuman primates. Pediatr Res. **20**: 987-991.

26. **Nielsen HC, Zinman HM, and Torday JS.** 1982. Dihydrotestosterone inhibits fetal rabbit pulmonary surfactant production. J. Clin. Invest. **69**:611-616.

27. **Padbury JF, Hobel CJ, Lam RW, and Fisher DA.** 1981. Sex differences in lung and adrenal neurosympathetic development in rabbits. Am J Obstet Gynecol. **141**: 199-204.

28. **Sciorra VA and Morris AJ.** 1999. Sequential actions of phospholipase D and phosphatidic acid phosphohydrolase 2b generate diglyceride in mammalian cells. Mol. Biol Cell. **10**: 3863-3876.

29. **Xu J, Love LM, Singh I, Zhang QX, Dewald J, Wang DA, Fischer DJ, Tigyi G, Berthiaume LG, Waggoner DW, and Brindley DN.** 2000. Lipid phosphate phosphatase-1 and Ca2+ control lysophosphatidate signaling through EDG-2 receptors. J. Biol. Chem. **275**: 27520-27530.

30. **Martin A, Gomez-Munoz A, Waggoner DN, Stone JC, and Brindley DN.** 1993. Decreased activities of phosphatidic acid phosphohydrolase and phospholipase D in ras and tyrosine kinase (fps) transformed fibroblasts. J. Biol. Chem. **268**: 23924-23932.

31. **Ting AE and Pagano RE.** 1991. Density-dependent inhibition of cell growth is correlated with the activity of a cell surface phosphatidylinositol-specific phospholipase C. Eur. J. Cell Biol. **56**: 401-406.

32. **Adamson IYR, Hedgecock C, and Bowden DH.** 1990. Epithelial cell-fibroblast interactions in lung injury and repair. Am. J. Pathology. **137**: 385-392.

33. **Liu JP.** 1996. Protein kinase C and its substrates. Mol. Cell Endocrinology. **116**: 1-29.

34. **Bui KC, Wu F, Buckley S, Wu L, Williams R, Carbonaro-Hall D, Hall FL, and Warburton D.** 1993. Cyclin A expression in normal and transformed alveolar epithelial cells. Am J Respir Cell Mol Biol. **9**:115-125.

35. **Bui KC, Buckley S, Wu F, Uhal B, Joshi I, Liu J, Hussain M, Makhoul I, and Warbuton D.** 1995. Induction of A- and D-type cyclins and cdc2 kinase activity during recovery from short-term hyperoxic lung injury. Am. J. Physiol. **268**: L625-L635.

36. **Wu F, Buckley S, Bui KC, and Warbuton D.** 1995. Differential expression of cyclin D2 and cdc2 genes in proliferating and nonproliferating alveolar epithelial cells. Am. J. Respir. Cell Mol. Biol. **12**: 95-103.

37. **Fine A, Janssen-Heininger Y, Soultanakis RP, Swisher SG, and Uhal BD.** 2000. Apoptosis in lung pathophysiology. Am. J. Physiol. **279**: L423-L427.

38. **Fehrenbach H, Kasper M, Tschering J, Pan T, Schuh D, Shannon JM, Muller M, and Mason RJ.** 1999. Keratinocyte growth factor-induced hyperplasia of rat alveolar type II cells in vivo resolved by differentiation into type I cells and by apoptosis. Eur. Respir. J. **14**: 534-544.

39. **Longo CA, Tyler D, and Mallampalli RK.** 1997. Sphingomyelin metabolism is developmentally regulated in the rat lung. Am. J. Respir. Cell Mol. Biol. **16**:

605-612.

40. **Zimmermann LJ, Hogan M, Carlson KS, Smith BT, and Post M.** 1993. Regulation of phosphatidylcholine synthesis in fetal type II cells by CTP:phosphocholine cytidylyltransferase. Am. J. Physiol. **264**: L575-L580.

41. **Hogan M, Zimmerman LJ, Wang J, Kuliczewski M, Liu J, and Post M.** 1994. Increased expression of CTP:phosphocholine cytidyldyltransferase in maturing type II cells. Am. J. Physiol. **267**: L25-L32.

42. **Zimmermann LJ, Lee W-S, and Post M.** 1995. Regulation of CTP:phosphocholine cytidylyltransferase by cytosolic lipids in rat type II pneumocytes during development. Pediatric Res. **38**: 864-869.

43. **De Paepe ME, Rubin LP, Lude C, Lesieur-Brooke AM, Mills DR, and Luks FI.** 2000. Fas ligand expression coincides with alveolar cell apoptosis in late-gestation fetal lung development. Am. J. Physiol. **279**: L967-L976.

44. **Barila D, Murgia C, Nobili F, Gaetani S, and Perozzi G.** 1994. Subtractive hybridization cloning of novel genes differentially expressed during intestinal development. Eur J Biochem. **223**: 701-709.

45. **Suzuki R, Sakagami H, Owada Y, Handa Y, and Kondo H.** 1999. Localization of mRNA for Dri 42, subtype 2b of phosphatidic acid phosphatase, in the rat brain during development. Brain Res Mol Brain Res. **66**: 195-199.

46. **Hecht JH, Weiner JA, Post SR, and Chun J.** 1996. Ventricular zone gene-1 (vzg-1) encodes a lysophosphatidic acid receptor expressed in neurogenic regions of the developing cerebral cortex. J Cell Biol. **135**: 1071-1083.

47. **deMello DE, Mahmoud S, Padfield PJ, and Hoffmann JW.** 2000. Generation of an immortal differentiated lung type-II epithelial cell line from the adult H-2K(b)tsA58 transgenic mouse. In Vitro Cell Dev Biol Anim. **36**:374-382.

Chapter 5

Pulmonary Lipid Phosphate Phosphohydrolase in Plasma Membrane Signaling Platforms

[1] A version of this chapter has been submitted for publication.

Nanjundan M and Possmayer F. Pulmonary lipid phosphate phosphohydrolase in signaling platforms. Submitted to Biochemical Journal.

5.1 Introduction

Phosphatidate phosphohydrolase (PAP) is a key enzyme in glycerolipid synthesis where it converts phosphatidic acid (PA) to diacylglycerol (DAG). There exists two different forms of pulmonary PAPases, namely PAP1 and LPP (formerly called PAP2). The former enzyme is magnesium-dependent and NEM-sensitive (1). It was reported to have a predominantly cytosolic location although it could translocate to the endoplasmic reticulum where it would become metabolically functional in phospholipid biosynthesis (2, 3). In contrast, pulmonary LPP was shown to be magnesium-independent, NEM-insensitive, and enriched in lung plasma membranes (4). It has been proposed that one function in lung, specifically in alveolar type II cells, is to act sequentially to phospholipase D (PLD) to provide DAG to sustain protein kinase C (PKC) activation and thus, maintain surfactant secretion (5).

A number of isoforms have been recently cloned including LPP1, LPP1a, LPP2, and LPP3. Hydropathy plot analysis indicates that each have six membrane-spanning regions (6, 7). These proteins also contain an active site comprised of three domains which is consistent with other members of a novel phosphatase superfamily which includes glucose-6-phosphatase (6, 7). Furthermore, all LPP's contain an N-linked glycosylation site (6, 7). The divergent regions among these isoforms include the N- and C-termini, which contain a number of potential PKC phosphorylation sites.

LPPs are reported to possess broad substrate specificity hydrolyzing lyso-PA (LPA), ceramide-1-phosphate (C-1-P), and sphingosine-1-phosphate (S-1-P) in

addition to PA (6). The enzymes' active site appears to be on the same side of the plasma membrane as the N-linked glycosylation site. Moreover, LPPs were recently shown to be capable of hydrolyzing exogenously presented substrates including lyso-PA, a phospholipid growth factor, in intact cells (8, 9). LPP1 overexpressed in rat 2 fibroblasts attenuated LPA-mediated effects on cellular proliferation through the Edg2 receptor (10). Both S-1-P and LPA are biologically active lipids which have been implicated in eliciting various biological responses including cellular proliferation, differentiation, migration, and inhibition of apoptosis (11). These responses are well recognized to be mediated through Edg (endothelial differentiation gene) receptors which belong to a superfamily of G-protein coupled receptors, of which there are 8 subtypes.

Caveolae are non-clathrin-coated "vesicular" invaginations of the plasma membrane with a characteristic flask-like shape and a diameter in the range of 50-100nm (12). Large numbers of caveolae have been reported in endothelial cells, adipocytes, smooth muscle cells, fibroblasts, and type I pneumocytes (12). The caveolae are attached to the plasma membrane via a short neck, but they may also appear as flat pits, which could be early invagination stages (12). They are dynamic structures that can bud from the plasma membrane and the molecular transport machinery of vesicle budding, docking, and fusion regulates their internalization (13, 14). Many different cellular functions are attributed to caveolae. In capillary endothelial cells, they have a function in clathrin-independent transport of macromolecules across the cell by transcytosis (12). They have also been implicated in signal transduction and contain a number of receptors such as EGF

and PDGF and lipid signaling enzymes such as phosphatidylinositol-specific phospholipase C (PI-PLC), PLD, and PKC (15). Caveolin, the principal structural component of caveolae, can interact directly with these signaling molecules to negatively regulate their activity through a short stretch in its membrane proximal called the caveolin scaffolding domain (CSD) (15). A role for caveolae in potocytosis (receptor-mediated uptake of small molecules and ions) was also proposed (16). Another important proposed function of caveolae is in mediating cholesterol efflux where caveolin-1 expression is upregulated by the sterol regulatory element-binding protein (17).

As recent work demonstrated PLD (18, 19, 20, 21) and Edg1 (22) localization to caveolin-enriched domains, we sought to establish whether LPP activity was also localized to these domains. This paper investigates the localization of LPP in lipid-rich signaling platforms from rat lung, isolated rat type II cells, and mouse lung epithelial cell lines including MLE12 and MLE15 cells. Since PKC is known to affect a variety of signaling pathways including activation and phosphorylation of PLD, the effect of phorbol 12-myristate 13-acetate (PMA) on LPP activity was examined specifically in caveolin-enriched domains isolated from mouse lung cell lines. As caveolin-1 was demonstrated to be absent from isolated type II cells and it is well established that type I cells have large numbers of caveolae (23,24), transdifferentiation studies on isolated rat type II cells were performed to examine the relationship between caveolin-1 expression and LPP activity.

5.2 Materials and Methods

5.2.1 Materials

Polyclonal antibodies for caveolin-1, transferrin receptor, PKC-μ, PKC-α, and PKC-βII were obtained from Santa Cruz Biotechnologies, Santa Cruz, USA. Tissue culture media was obtained from Gibco BRL. Fetal bovine serum was obtained from CanSera. γP^{32}-ATP was obtained from Amersham. LPA was purchased from Avanti Polar Lipids. DAG kinase was purchased from Calbiochem. All solvents were purchased from VWR. Porcine elastase was obtained from Worthington Biochemicals. 25% Polyacrylic acid (average molecular weight 240,000) was purchased from Aldrich Chemical. Metrizamide, monoacylglycerol, and phorbol 12-myristate 13-acetate were obtained from Sigma. Pefabloc was obtained from Roche Biochemicals. Cationic colloidal particles (30%) were kindly provided by Dr. Donna Stolz (Department of Cell Biology and Physiology, University of Pittsburgh, Pittsburgh, USA). LPP1 antibody was kindly provided by Dr. David Brindley (University of Alberta, Edmonton, Canada). LPP3 antibody was kindly provided by Dr. Andrew Morris (Department of Pharmacological Sciences, Stony Brook Health Sciences Center, Stony Brook, USA). PLD1 and PLD2 antibodies were kindley provided by Dr. Sylvain Bourgoin (University of Laval, Montreal, Quebec).

5.2.2 Cell Culture

MLE12 and MLE15 cells were obtained from Dr. J. Whitsett (Divisions of Neonatology and Pulmonary Biology, Children's Hospital Medical Center, Cincinnati, Ohio) and were cultured in HITES (RPMI 1640 containing insulin, transferrin,

sodium selenite, hydrocortisone, β-estradiol, HEPES, glutamine, and 2% FBS (25) and RPMI 1640 (5% FBS), respectively. These cells are transformed with the large T antigen and contain some surfactant proteins but lack distinct lamellar bodies. They were maintained in 75-cm^2 flasks and subcultured at 4 to 5-day intervals. For the experiments described herein, MLE12 cells were used between passages 23 and 27 and the MLE15 cells were used between passages 16-20. Rat type II cells were isolated according to the method of Dobbs *et al.* (26). For the transdifferentiation studies, the isolated cells were maintained on tissue culture plastic for up to 7 days on 60mm dishes.

5.2.3 Isolation of Caveolin-Enriched Domains from Rat Lung by the Detergent Method

This isolation was performed according to Lisanti *et al.* (27). Female Sprague-Dawley rats (150-300g) were killed by injection with nembutanol. The thorax was opened and the lungs were perfused into the right ventricle with ice-cold saline (0.9%) with the left ventricle bisected to provide drainage. Lungs became white immediately upon washing. After excision and trimming of large vessels and airways, the lungs were minced. One gram was homogenized in 6ml of MBS (morpholinoethanesulfonic acid-buffered saline 25mM, pH 6.8, 0.15mM NaCl) containing 1% Triton X-100 and 1mM pefabloc with 10 strokes of a Potter Elvehjem (Heidolph) followed by 3 bursts of 10 seconds with a polytron. The homogenate was adjusted to 40% sucrose by adding an equal volume of 80% sucrose in MBS. This

was placed at the bottom of an ultracentrifuge tube and a 5-30% sucrose density gradient (in MBS without Triton X-100) was layered above the homogenate. Centrifugation was carried out at 25,000 rpm for 20 hours using an SW28 rotor at 4°C. After centrifugation, 3ml fractions from the top of tube were harvested and stored at -60°C.

5.2.4 Isolation of Caveolin-Enriched Domains from Type II Cell Lines by the Detergent Method

This procedure was followed according to Czarny *et al.* (20). MLE12 and MLE15 cells were grown to confluence in 75-cm^2 flasks. Cells were washed twice in phosphate buffered saline (PBS) and scraped into 2ml of MBS containing 1% Triton X-100 and 1mM pefabloc. The cell suspension was homogenized using 10 strokes of a Potter Elvehjem homogenizer and subjected to sonication using a Branson Sonifier with a microprobe (three 10 seconds bursts). The homogenate was then adjusted to 45% sucrose by addition of an equal volume of 80% sucrose prepared in MBS buffer and placed at the bottom of an ultracentrifuge tube. A 5-35% discontinuous sucrose gradient was layered on and the sample centrifuged at 39,000 rpm for 16 hours with a SW-40 rotor at 4°C. After centrifugation, 1ml fractions from the top of the tube were harvested and stored at -60°C.

5.2.5 Isolation of Caveolae from Other Lipid-Rich Microdomains in MLE15 Cells

This isolation was performed according to the procedures of Stolz *et al.* (28) and Schnitzer *et al.* (29, 30). Briefly, MLE15 cells were trypsinized and allowed to re-express plasma membrane proteins by a 1 hour incubation at 37°C. Cells from fifteen T75 flasks (one preparation) were pelleted at 1000 rpm for 5 minutes in a Beckman J6-B centrifuge at 4°C and gently resuspended in 1ml PMCB (20mM MES, 150mM NaCl, 280mM sorbitol, pH 5.3). The cell suspension was added dropwise to 5ml of 1% cationic colloidal silica in PMCB. The silica-coated cells were sedimented and washed twice by resuspending in 20ml PMCB and centrifugation. The silica-coated cells were added to 5ml of polyacrylic acid in PMCB (5ml of 1mg/ml) and diluted up to 20ml with PMCB and sedimented/washed twice. The cells were then resuspended in 1ml of lysis buffer (2.5mM imidazole, pH 7.0) and incubated at 4°C for 30 minutes. The cells were then lysed using a Dounce homogenizer (12 strokes) and centrifuged at 1000rpm for 5 minutes. The pellet (silica-coated membranes plus nuclei (TM)) was resuspended in 8ml of lysis buffer and fractionated using a cushion of 70% Metrizamide and centrifuging at 15,000 rpm for 30 minutes in a SW41 rotor. The resulting pellet containing silica-coated plasma membranes (P) was resuspended in 1ml of MBS and washed three times by centrifugation. Cold 10% (v/v) Triton X-100 was added to this suspension (final 1%). This mixture was mixed for 10 minutes at 4°C and homogenized using a Potter Elvehjem homogenizer (10 strokes). The sucrose concentration was brought up to 60% containing 20mM KCl and a 5-30% gradient was then layered in 20mM KCl and centrifuged at 39,000 rpm for 16 hours in a SW-40 rotor at 4°C. The caveolae (V), which floated to the 30% interface, were collected. The silica-coated membrane

pellet (P-V) was resuspended in 20mM MES with 125mM NaCl to which an equal volume of 4M K_2HPO_4 and 0.2% polyacrylate (pH 9.5) was added. This suspension was sonicated (10-10s bursts) on ice and mixed on a rotator for 8 hours at room temperature followed by another sonication (15-10s bursts) on ice. Triton X-100 was added to 1% and mixed for 10 minutes at 4°C and homogenized using a Potter Elvehjem homogenizer. Discontinuous sucrose density centrifugation was performed and the remaining floating detergent-insoluble membranes were harvested (LR).

5.2.6 SDS-PAGE and Western Blot Analysis

Equal volumes of fractions were analyzed with 8% SDS-PAGE gels. The samples were boiled in sample buffer for 5 minutes and cooled on ice before loading onto the gel. The gel was run at 100 volts and the proteins were electrophoretically transferred onto Immobilon P membranes for 1 hour at 100 volts at 4°C. Blots were blocked in 5% nonfat dry milk in Tris-buffered saline (TBS, pH 7.4) with 0.2% Tween-20 (v/v) (TBST) for 1 hour at room temperature. Primary antibody incubations were performed in the same blocking buffer at dilutions of 1:1000 (1:5000 for LPP3) for up to 2 hours at room temperature. The blots were then washed in TBST for 10 minutes three times at room temperature. Secondary antibody incubations were performed in TBST containing 5% nonfat dry milk at 1:10,000 for 1 hour at room temperature followed by another 30 minutes wash in TBST. Protein bands were visualized by enhanced chemiluminescence and exposed to x-ray film.

5.2.7 LPP Assays

The activity was assayed using either pure PA or LPA as substrate. Unlabelled PA and P^{32}-labelled PA and LPA were prepared as described before (4). Reaction mixtures contained 100mM Tris-maleate buffer, pH 6.5, 0.6mM PA (0.4mCi/mmol), 0.5mM EDTA, 0.5mM EGTA, pH 7.0, 0.2mg of essentially fatty acid free albumin and 1mM DTT in a final reaction volume of 0.1 ml. Incubation times were 60 minutes in duration at 37^0C. The protein was preincubated at 37^0C for 10 minutes with 4.2mM N-ethylmaleimide (NEM). Reactions were terminated by the addition of 1.5 ml of chloroform: methanol (1:1). The phases were broken with 0.75ml of 0.1N HCl and a sample of the upper aqueous phase was taken for scintillation counting to determine the P^{32} inorganic phosphate released (4).

5.2.8 Co-Immunoprecipitation of LPP Activity with Caveolin-1

MLE15 cell caveolin-enriched domains (60μl) were diluted in OG buffer (50mM Tris-HCl (pH 7.4), 60mM n-octyl β-glucopyranoside, 125mM NaCl, 2mM dithiothreitol, 0.1mM EGTA). These domains were then incubated with 1μg of anti-caveolin antibody for 1 hour at 4°C. This was followed by another 1 hour incubation at 4°C with 50μl of protein A-Sepharose. The beads were then washed extensively with OG buffer. The pellet and supernatant were then assayed for LPP activity. Proteins were eluted from the beads, resolved by SDS-PAGE, and subjected to western blot analysis.

5.2.9 Other Assays

Protein was determined by the method of Lowry *et al.* in the presence of 2mM SDS (31) using bovine serum albumin as the standard. Quantitation of phospholipid was determined using a kit obtained from Boehringer Mannheim which employs choline oxidase to measure choline released from phosphatidylcholine (PC) and sphingomyelin (SM) by PLD. Total cholesterol content was measured using a kit obtained from Boehringer Mannheim which measures the released hydrogen peroxide from cholesterol oxidase. Protocol was followed as for with minor modifications, after incubation for 15 minutes at 37°C for standards and caveolar fractions, the samples were read on an ELISA reader using a 420nm filter. Standard curves were 0 to 10μg for choline chloride and cholesterol.

5.3 Results

5.3.1 Rat Lung Caveolin-Enriched Domains are Enriched in LPP Activity

In order to establish whether LPP activity exists in pulmonary caveolin-enriched domains, lipid rich microdomains were isolated from whole rat lung tissue based on their detergent insolubility in Triton X-100. As shown in Figure 5.1A, the distribution of protein along the gradient indicates a greater percentage in the heavier detergent soluble fractions with less than 5% in the lighter detergent insoluble fraction. Within this 5th fraction, LPP activity is highly enriched where 31.2±0.7% of the total recovered activity resides. An antibody against LPP3 allowed

Figure 5.1. Lung caveolin-enriched domains. Lipid rich microdomains were isolated based on their detergent insolubility in 1% Triton X-100. A, LPP activity in each gradient fraction (1-14, top to bottom), indicated as bars, using equal volumes was measured and calculated as % of total. The protein concentration is indicated as (•) in μg/μl. The result of immunoblot analysis for LPP3 is shown. B, The % of total phosphatidylcholine and sphingomyelin (PC: SM) in each gradient fraction is shown. C, The results of immunoblot analysis are shown for caveolin-1, PKC-α, PKC-βII, and PKC-μ. D, The % of total cholesterol in each gradient fraction is shown. The results are from a representative experiment (n=3). The results are shown as the mean ± S.E.M.

A LPP Activity

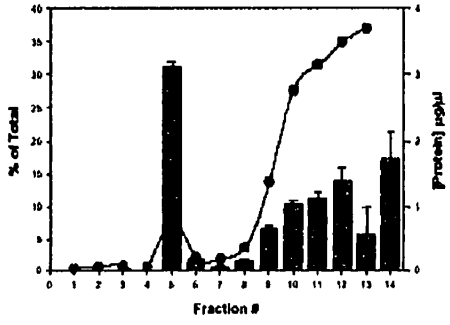

LPP3

B PC: SM

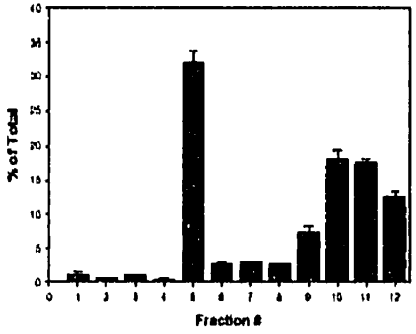

C

1 2 3 4 5 6 7 8 9 10 11 12

caveolin-1

1 2 3 4 5 6 7 8 9 10 11 12 13

PKC-α

PKC-βII

PKC-μ

D Cholesterol

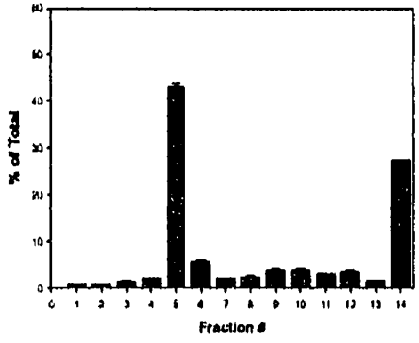

investigation of its localization across the gradient (Figure 5.1A). LPP3 was found to be predominantly localized in the lung CED fraction. There is also 41% of the total LPP activity in the detergent soluble fractions (fractions 10-14) possibly indicating other subcellular localizations (Golgi, endoplasmic reticulum, or plasma membranes). This activity most likely represents another LPP isoform as LPP3 was undetectable in these detergent soluble fractions.

In previous studies, we have shown that LPP is highly enriched in plasma membranes and this would correspond in part to LPP in areas of the plasma membrane excluding caveolae-rafts. The detergent insoluble domains are rich in SM: PC (32.1±1.6% of total) and cholesterol (42.9±0.8% of total) (Figure 5.1B and 5.1D). By western blotting, caveolin-1 localizes predominantly to the detergent insoluble fractions 5 to 8 where a high proportion of LPP is found (Figure 5.1C). Various PKC isoforms including PKCα, PKCμ, and PKCβII localize predominantly to the detergent soluble fraction but there is a small percentage of PKCβII and μ localized to the CEDs. A yield of 2.3±0.4mg (n=3) of CED protein was obtained from 1 gram of tissue which represents 0.23±0.04% of the starting material. Enzyme marker studies indicate that these light microdomains retain plasma membrane markers, alkaline phosphatase and 5'-nucleotidase. These studies indicate that caveolin-enriched domains can be isolated from rat lung tissue where the high proportion of LPP activity, represented by the LPP3 isoform, and a small proportion of PKCβII and μ reside.

5.3.2 Rafts from Isolated Type II Cells Contain LPP Activity

It has been recently shown by transmission electron microscopy that caveolin-1 is localized to the membranes of plasmalemmal invaginations in the alveolar type I cell (23, 24). In contrast, the plasma membrane of surfactant-secreting alveolar type II cells appears to lack such structures (23, 24). Nonetheless, type II cells are fully responsive to agonists such as UTP involved in phospholipid surfactant secretion (5) where LPP would act sequentially to PLD downstream to P_{2u} receptor activation. Other cells lacking in caveolae/caveolin at the cell surface are fully functional in responding to growth factors and, indeed, have microdomains, namely rafts that are resistant to Triton X-100 solubilization (32). Thus, caveolae are not the only type of plasmalemmal subcompartment organized to transduce signaling cascades.

Rafts from Type II cells maintained in culture overnight were isolated based on their detergent insolubility in Triton X-100 and examined for LPP activity. As shown in Figure 5.2, LPP activity (8.1±0.8% of total (PA), 15.6±3.6% of total (LPA), 5.2A), SM: PC (19.0±1.6% of total, 5.2B) and cholesterol (9.7±1.4% of total, 5.2D) were enriched in the detergent-insoluble domains (4^{th} fraction). However, nearly 80% of the total LPP activity partitioned to the detergent soluble fractions. The transferrin receptor, a clathrin-coated pit marker, as well as PKCα localized predominantly to the detergent soluble fractions (Figure 5.2C). Caveolin could not be detected by western blotting in any gradient fraction. These results indicate that LPP is present in rafts in isolated type II cells where it is proposed to act in the

Figure 5.2. Type II Cell lipid rafts. Lipid rafts were isolated based on their detergent insolubility in 1% Triton X-100. A, LPP activity in each gradient fraction (1-13, top to bottom), indicated as bars, using equal volumes was measured and calculated as % of total. The protein concentration is indicated as (•) in μg/μl. B, The % of total phosphatidylcholine and sphingomyelin (PC: SM) in each gradient fraction is shown. C, The results of immunoblot analysis are shown for transferrin receptor (Ttf) and PKC-α. D, The % of total cholesterol in each gradient fraction is shown. The results are from a representative experiment (n=3). The results are shown as the mean ± S.E.M.

A LPP Activity

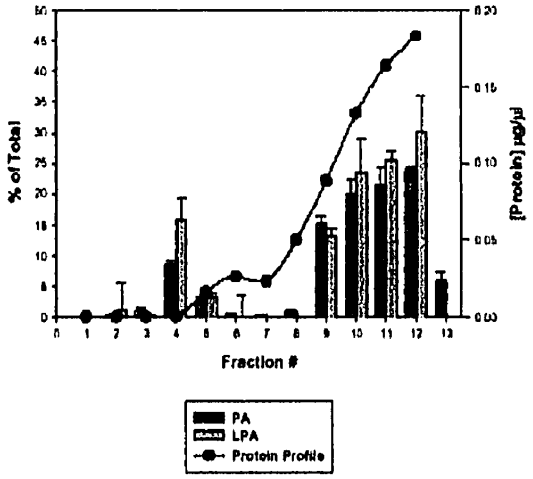

B PC: SM

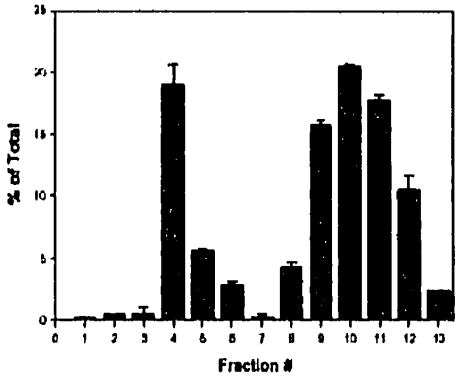

C

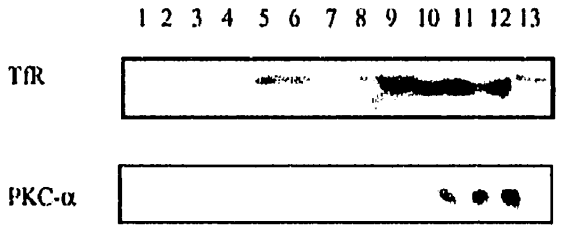

D Cholesterol

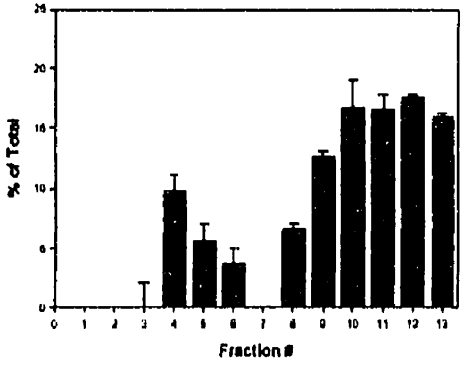

PLD/LPP pathway in surfactant phospholipid secretion.

5.3.3 Transdifferentiation of Isolated Rat Alveolar Type II Cells

It is well recognized that when isolated type II cells are cultured on tissue culture plastic, they lose their characteristic cuboidal morphology, lamellar bodies, surfactant proteins and acquire a type I-like phenotype. Interestingly, it was recently reported that caveolin-1 expression and caveolae biogenesis increase as the type II cells transdifferentiate to a type I-like cell (24). Thus, to determine whether any correlation exists between LPP and caveolin-1, type II cells were isolated and maintained on tissue culture plastic for up to 7 days allowing the cells to transdifferentiate into a type I-like cell. On day 1, caveolin-1 levels were almost undetectable by western blotting. As shown in Figure 5.3, the specific activity of LPP increased four-fold after 7 days in culture. Moreover, the protein levels of caveolin-1, PLD2, PKC isoforms increased dramatically. In contrast, alkaline phosphatase, enriched in type II cells, was found to decrease upon cellular transdifferentiation. Therefore, it is evident that during dedifferentiation of type II cells, LPP activity and protein levels of caveolin-1 as well as lipid signaling enzymes increase. Thus, we propose that either LPP is involved in the transdifferentiation of the type II cell to a type I cell or is required for an unidentified type I cell function.

5.3.4 Modulation of LPP activity within CEDs Isolated from MLE12 and MLE15 Cell Lines

Figure 5.3. Transdifferentiation of type II cells. Whole cell lysates were obtained from isolated rat type II cells maintained on tissue culture plastic from 1 to 7 days in culture. A, LPP specific activity is shown as nmol of Pi released per minute per mg measured on whole cell lysates. B, Alkaline phosphatase specific activity is shown as nmol of Pi released per minute per mg measured on whole cell lysates. C, SDS-PAGE and immunoblot analysis on day 1 and day 7 cell lysates was performed (30μg of protein loaded per lane). The immunoblot results are from four experiments (n=4) and the specific activities are shown as the mean ± S.E.M for four independent experiments.

A LPP Activity

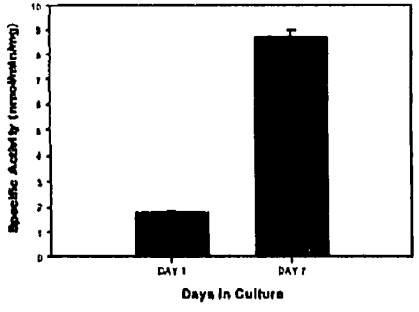

B Alkaline Phosphatase Activity

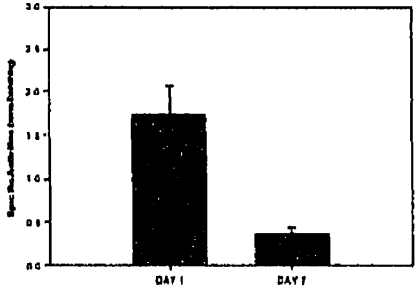

C

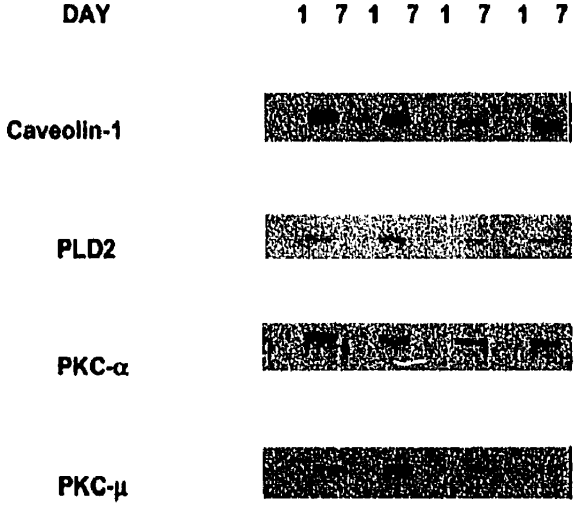

Lipid rich microdomains were isolated from mouse lung epithelial cell lines, namely MLE12 and MLE15. These cells are transformed with the large T antigen and contain some surfactant proteins but are lacking in well-formed lamellar bodies (25). Surprisingly, these cells contain caveolin-1 indicating these cells may be transdifferentiated to some extent although they retained their cuboidal morphology. As shown in Figure 5.4A, MLE12 cell lipid-rich domains were slightly enriched in LPP activity (4.8% of total) as well as PC: SM (21.5% of total). The transferrin receptor was completely detergent soluble (Figure 5.4B). Interestingly, LPP3 was also detergent soluble, which was different to results obtained in HEK293 and NIH 3T3 cells (23). MLE15 cell lipid-rich domains, as shown in Figure 5.4C, were 10-fold more enriched in LPP activity (47.4% of total, 5^{th} and 6^{th} fractions combined) compared to MLE12 cells. They were also more enriched in cholesterol (33.8% of total) and PC: SM (29.9% of total). However, the LPP3 isoform was undetectable in this cell line as determined by western blotting.

The effect of phorbol ester (PMA) treatment, which is known to influence cell signaling, on LPP activity was examined specifically in caveolin-enriched domains isolated from mouse lung cell lines. PMA treatment for 5 minutes promoted PKC-α translocation from the detergent soluble fractions to the detergent insoluble domains, which colocalized with caveolin-1 (Figure 5.4B & 5.4D). Interestingly, in PMA-treated MLE12 cells, the total percent of LPP activity changed from 4.8% to 14.5%. This suggests a potential increase in LPP protein from other subcellular locations since the total LPP activity in the control detergent soluble fractions decreased from 86% to 61.9% with PMA treatment. The specific activity of LPP was

Figure 5.4. Phorbol ester treatment of MLE12 and MLE15 cells. Mouse lung epithelial cell lines were treated with or without PMA (10μM) for 5 minutes. Control cells were treated with 0.1% DMSO for 5 minutes. Lipid rich microdomains were then isolated based on their detergent insolubility in 1% Triton X-100. A, LPP activity in MLE12 cells, shown as % of total, is indicated as light and dark colored bars for the control and PMA-treated gradient fractions, respectively. The protein concentration is indicated as (•) and (▽) in μg/μl for control and treated cells, respectively. The results are from a representative experiment (n=3). The results are shown as the mean ± S.E.M. B, The results of immunoblot analysis for MLE12 cells are shown for caveolin-1, transferrin receptor (Ttf), PKC-α (with or without PMA treatment), and LPP3. With PKC, non-specific bands were observed below the PKC-α band. C, LPP activity in MLE15 cells, shown as % of total, is indicated as light and dark colored bars for the control and PMA-treated gradient fractions, respectively. The protein concentration is indicated as (•) and (▽) in μg/μl for control and treated cells, respectively. D, The results of immunoblot analysis for MLE15 cells are shown for caveolin-1, transferrin receptor (Ttf), and PKC-α (with or without PMA treatment). The results are from a representative experiment (n=2). The results are shown as the mean ± S.E.M.

A MLE12 LPP Activity

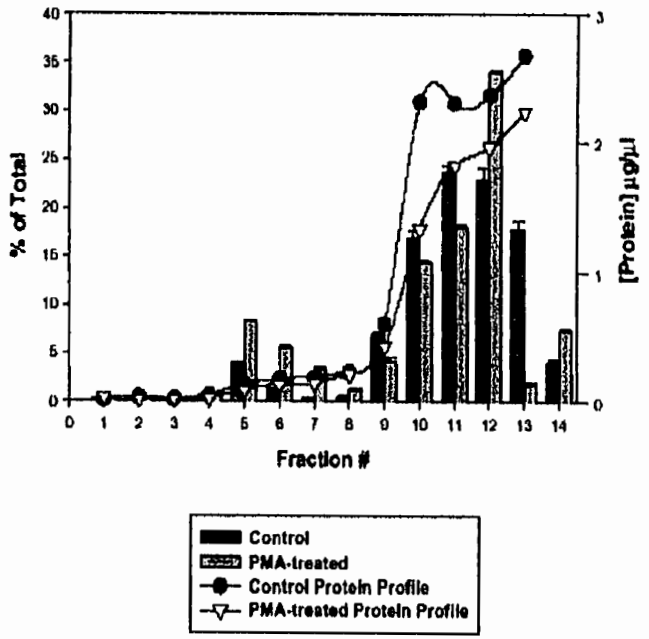

B

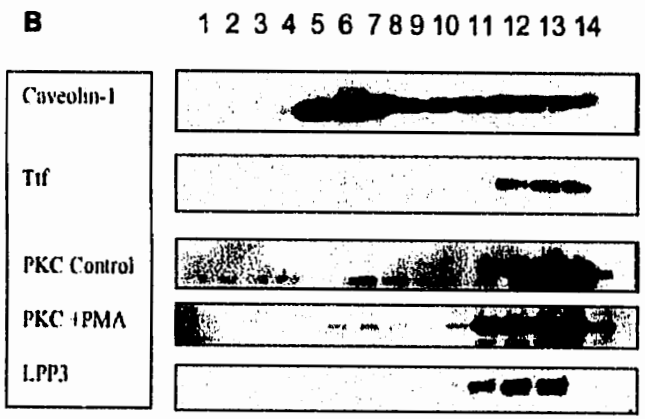

C MLE15 LPP Activity

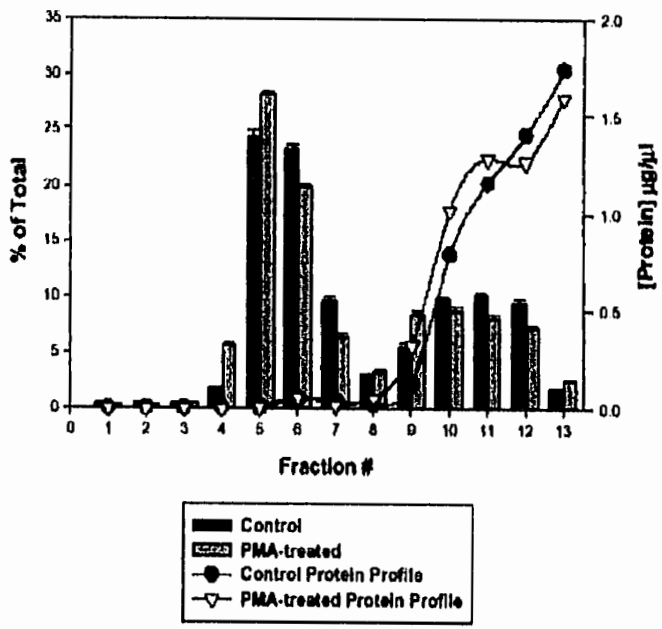

D

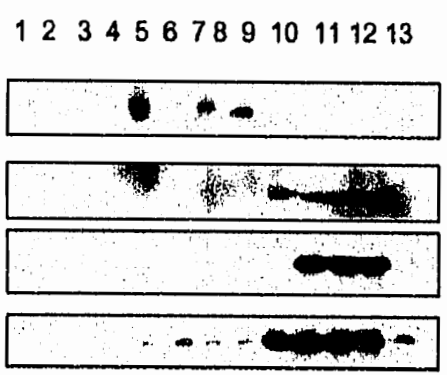

found to increase 3.8-fold in the CED fraction in the PMA-stimulated MLE12 cells (Figure 5.5). These results suggest a redistribution of LPP from the plasma membrane to the CEDs although the results could be explained by selective activation of LPP activity (through phosphorylation) in these domains with a corresponding inactivation in the bulk plasma membrane. The ability of PMA to increase the LPP enzymatic activity in the CED fraction emphasizes the dynamic properties of caveolae and rafts in the plasma membrane.

The effect of saponin was also investigated, as it is known to sequester cholesterol thereby destabilizing the lipid-rich microdomain structure and rendering them sensitive to solubilization by nonionic detergents. The addition of saponin to MLE15 cells resulted in a redistribution of caveolin-1 and LPP activity from the 5^{th} and 6^{th} fractions (from 47.3% to 11.7% of total) to the 9^{th} and 10^{th} fractions (from 15.4% to 51.1% of total) (Figure 5.6A & 5.6C). Furthermore, there was a corresponding redistribution in cholesterol and PC: SM (Figure 5.6B & 5.6D, respectively) from the 5^{th} and 6^{th} fractions (from 33.8% to 13.3% and from 30% to 20.5%, respectively) to the 9^{th} and 10^{th} fractions (from 20% to 45% and from 26.3% to 42%, respectively). Thus, saponin treatment resulted in a redistribution of LPP activity indicating that when cholesterol was removed from the CEDs, LPP association with the light microdomains was disrupted.

5.3.5 Separation of Caveolae from Other Lipid-Rich Microdomains in MLE15 Cells

Schnitzer and colleagues (33, 34) have developed a protocol utilizing

Figure 5.5. Specific activity of LPP in CED fraction from phorbol ester treated MLE12 cells. LPP activity in MLE12 cells was measured in the 5^{th} and 6^{th} fractions in both control and PMA-treated CED fractions and calculated as nmol of Pi released per minute per mg.

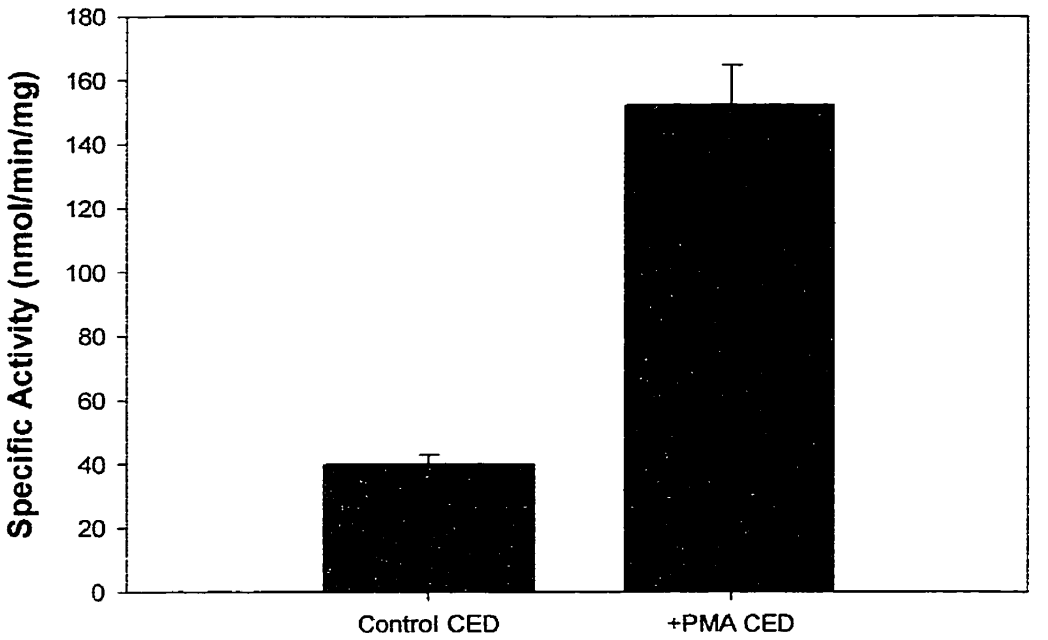
Specific Activity (nmol/min/mg)
180
160
140
120
100
80
60
40
20
0
Control CED
+PMA CED

Figure 5.6. Saponin treatment of MLE15 cells. Mouse lung epithelial cells were treated with or without saponin (0.2%) and lipid rich microdomains were then isolated based on their detergent insolubility in 1% Triton X-100. A, LPP activity in MLE15 cells, shown as % of total, is indicated as light and dark colored bars for the control and saponin-treated gradient fractions, respectively. The protein concentration is indicated as (•) and (▽) in μg/μl for control and treated cells, respectively. B, The % of total phosphatidylcholine and sphingomyelin (PC: SM) in each gradient fraction is shown as light and dark colored bars for the control and saponin-treated gradient fractions, respectively. C, The results of immunoblot analysis are shown for caveolin-1 with or without saponin treatment. D, The % of total cholesterol in each gradient fraction is shown as light and dark colored bars for the control and saponin-treated gradient fractions, respectively. The results are from a representative experiment (n=2). The results are shown as the mean ± S.E.M.

A LPP Activity

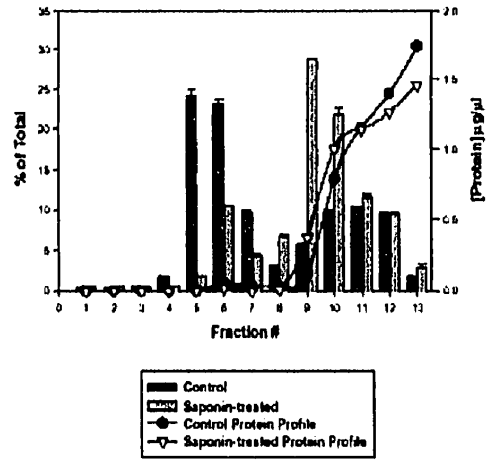

B Cholesterol

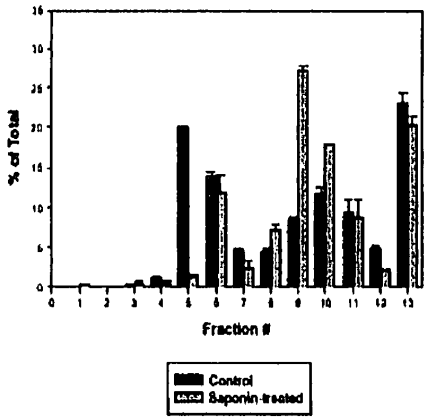

C

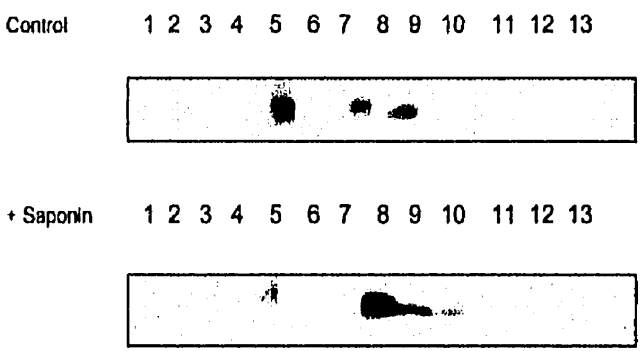

D PC:SM

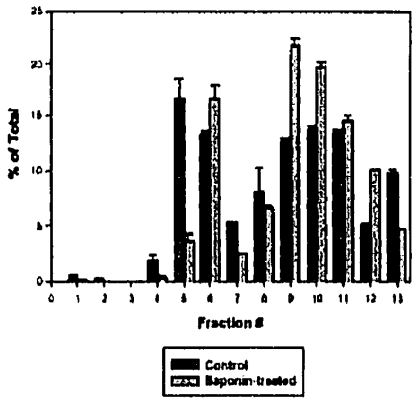

colloidal silica particles to separate caveolae from other Triton-insoluble microdomains including those on the cell surface rich in GPI-anchored proteins, cytoskeletal elements, and intracellular trans-Golgi network (TGN) exocytic vesicles rich in glycolipids and caveolin. This caveolae purification procedure prevents co-isolation of other noncaveolar domains that are very similar to caveolae in their detergent resistance and buoyant densities. The actual coating of the plasma membrane with the silica particles allows isolation to high purity of the plasma membranes, thereby avoiding contamination from other sources (TGN and vesicles), and it stably attaches to the plasmalemma proper and prevents excision of the flat noninvaginated domains that are not caveolar.

In order to determine whether LPP activity exists in caveolae and/or rafts, MLE15 cells were coated sequentially with cationic colloidal silica and polyacrylate allowing the plasma membrane to be purified away from contaminating membranes. Caveolae from the silica-coated plasma membrane (P) were sheared away in 1% Triton X-100. The purified caveolae (V) were enriched in LPP activity as well as caveolin-1 (Figure 5.7A & 5.7C). The 5'-nucleotidase activity was essentially undetectable in the total membrane (TM) fraction as well as in the isolated P and V fractions (Figure 5.7B). The 5'-nucleotidase, whose activity was measured by inorganic phosphate release, may not be able to access its substrate due to the presence of the silica in the P fraction. The raft or other lipid-rich microdomains (LR) were isolated by disruption of the cationic silica from the plasma membrane (P-V) followed by extensive sonication. These detergent insoluble domains that were obtained after gradient centrifugation contained LPP activity and were also enriched

Figure 5.7. Separation of caveolae from lipid rafts in MLE15 cells. As described in the **Methods and Materials** section, caveolae were purified from other lipid-rich microdomains using cationic colloidal silica particles. A, The specific activity of LPP is shown as nmol of Pi released per minute per mg in various membrane fractions: total membranes (TM), plasma membrane (P), caveolae (V), plasma membrane minus sheared caveolae (P-V), and other lipid-rich raft microdomains (LR). B, The specific activity of 5'-nucleotidase is shown as nmol of Pi released per minute per mg in various membrane fractions: TM, P, V, P-V, and LR. C, SDS-PAGE and immunoblot analysis was performed with caveolin-1 (1μg of protein loaded per fraction). D, immunoblot analysis with LPP1 (1μg of protein loaded per fraction). Ct represents 50μg of MLE15 total membranes. E, immunoblot analysis with LPP3 (1μg of protein loaded per fraction). Ct represents 10μg LPP3 overexpressed - Sf9 insect cell detergent extracts. The results are from a representative experiment (n=2). The results are shown as the mean ± S.E.M.

A LPP Activity

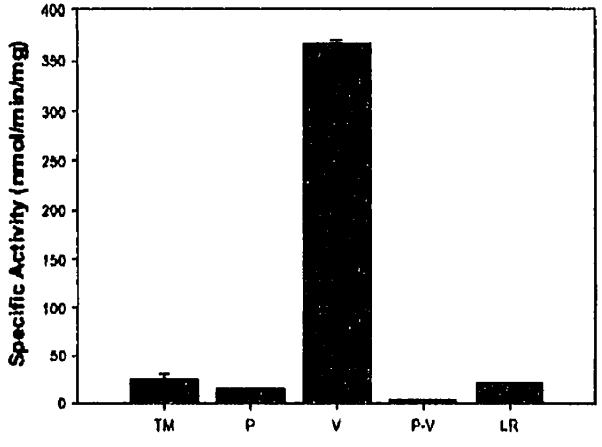

B 5'-Nucleotidase Activity

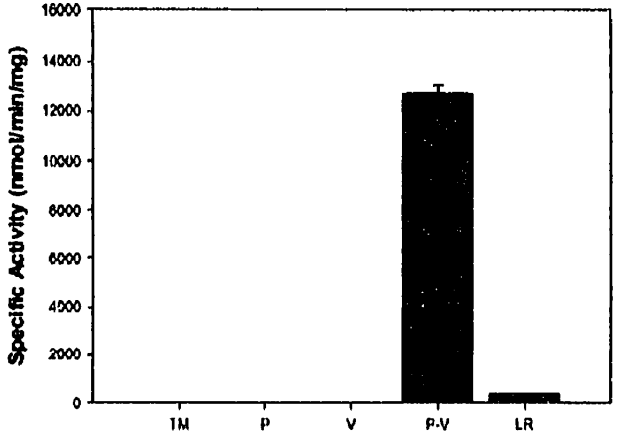

C

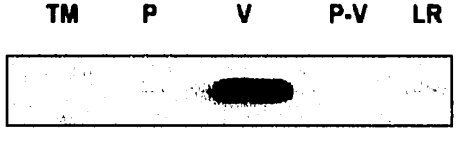

D

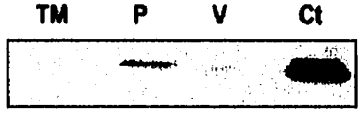

E

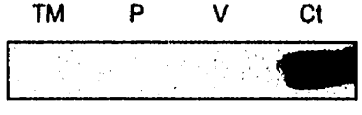

in 5'-nucleotidase activity (Figure 5.7B). The P-V fraction may contain domains which are non-invaginated but contain some caveolin-1. Caveolae are dynamic membrane structures which appear to cycle between flat, invaginated, and vesicularized forms. However, the P-V fraction was not enriched in LPP activity or caveolin-1 protein suggesting that, in MLE15 cells, the majority of the active LPP appears to be associated with invaginated caveolae. The LR or lipid raft fraction contains 5'-nucleotidase as well as some LPP activity. Some caveolin-1 was present in the LR fraction although this could be the result of contamination.

The LPP isoform present within the purified caveolae was investigated using LPP1/1a and LPP3 mouse-reactive antibodies. As shown in Figure 5.7D, LPP1/1a was detected in purified caveolae although the protein level was more abundant in the total plasma membranes. The LPP3 isoform was undetectable in any of the MLE15 cell fractions (Figure 5.7E). Thus, LPP activity is much more highly enriched in caveolae compared to the plasma membrane and lipid rafts. Furthermore, LPP1/1a is present within caveolae where it may be in an activated form.

5.3.6 Lack of Co-Immunoprecipitation of LPP activity with Caveolin-1

Caveolin-1 contains a scaffolding binding domain with a hydrophobic amino acid sequence which enables it to interact with a variety of signaling proteins including PLD and PKC. The caveolin-1 binding domain consensus sequences include $\phi x\phi xxx\phi$, $\phi xxxx\phi xx\phi$, or $\phi x\phi xxxx\phi x\phi$ where ϕ = F, Y, W and x is any amino acid (35). Examination of the amino acid sequences of LPPs indicate that they may also possess such a domain in the first intracellular loop: LPP1 and LPP1a contain

YFNVLHSNSFVSNHYIATIYKAVGAFLF, LPP3 contains FYRIYYLKEKSRSTIQNPYVALYKQVGCFLF, and hLPP2 contains YTDRLYSRSDFNNYVAAVYKVLGTFLF. The LPP2 sequence has the closest homology to the caveolin-1 consensus binding sequence. However, using MLE15 CED fractions, LPP activity failed to co-immunoprecipitate with caveolin-1. The caveolin-1 was detected in the pellet fraction from MLE-15 cell caveolin-enriched fractions as determined by western blotting. The apparent failure of caveolin-1 to immunoprecipitate LPP activity does not necessarily indicate a lack of association. Since n-octyl β-glucopyranoside was used in the immunoprecipitation buffer, it is possible that this detergent could have released LPP from the caveolae membrane.

5.4 Discussion

5.4.1 LPP Activity in Lung and Type II Cell CEDs

As it was recently shown in the literature that CEDs were highly enriched in PLD (18, 19, 20, 21) and Edg1 (22), we sought to establish whether pulmonary LPP could be present in these domains. LPP activity (31.2±0.7% of total) was found to be enriched in CEDs isolated from rat lung tissue, which were isolated based on their detergent insolubility in Triton X-100. Lung is an endothelial-rich source where caveolin-1 demonstrates its highest levels of expression (24). Lung is composed of a high proportion of endothelial cells (42% of cell population) as well as muscle cells, fibroblasts, macrophages, type I cells, type II cells, and other cells. LPP activity was present in rafts (8.1±0.8% of total) isolated from freshly isolated rat type

II cells, which are lacking in caveolae. The type II cell represents approximately 10% of the cell population and covers less than 5% of the alveolar epithelial surface. In contrast, type I cells cover greater than 95% of the alveolar surface area and have twice the volume and four times the surface area of endothelial cells (24). LPP activity in lung CEDs could, therefore, arise mostly from type I and endothelial cells which are reported to have large numbers of caveolae. We had previously reported (4) that LPP activity in type II cells was only slightly enriched relative to whole lung homogenate, which is indicative of another cellular localization. Rat lung fibroblasts, moreover, had low LPP activity (4) although caveolae are reported to be abundant in this cell type. However, the isolated fibroblasts could have deviated from their normal phenotype during culture, as is known to occur for isolated type II cells and endothelial cells. Furthermore, these fibroblasts were sparsely distributed and it is well established that the levels of caveolin-1 increase and its localization shifts to areas of cell-cell contact upon confluence and is further affected by serum starvation and growth factor stimulation (36).

5.4.2 LPP Activity in Caveolae and Lipid Rafts

Because homogenates or whole cell lysates were used in the initial studies, the lipid rich domains from the TGN and vesicles most likely contaminated these caveolae fractions. Therefore, using cationic colloidal silica particles, caveolae were isolated from MLE15 cells, a transformed mouse lung type II epithelial cell line. These caveolae (V) were highly enriched in LPP activity as well as caveolin-1. In contrast, the P-V fraction was enriched in 5'-nucleotidase activity and lacking both

in caveolin-1 and LPP activity. Lipid rafts (LR) contained both 5'-nucleotidase and LPP activity but displayed little caveolin-1 immunoreactivity. Hence, LPP activity is present within both caveolae and rafts from MLE15. Isolated rat type II cells contain lipid rafts with LPP activity but no caveolin-1 immunoreactivity based on western blotting. Both caveolae and rafts exist in a liquid ordered (l_o) phase where the tight acyl chain packing and strong lipid-lipid interactions contribute to their detergent insolubility (37).

We propose that in type II cells, an LPP isoform(s) could participate in signaling from lipid rafts. LPP could act sequentially to PLD in the P_{2u} receptor cascade for surfactant phospholipid secretion where it would generate DAG from PC derived PA, thereby sustaining PKC activation and surfactant secretion (5). Recovery from lung injury involves type II cell proliferation and migration to restore the damaged type I cell population. Subsequently, the type II cells undergo a transdifferentiation process in order to re-establish alveolar epithelial integrity. These latter processes may require elevated DAG levels, generated by LPP for PKC activation leading to expression of specific genes involved in this process. Thus, the concerted actions of PLD, LPP and PKC could be necessary for these signaling events to occur in caveolae. These plasmalemmal invaginations would most likely have different functions to rafts and these structures appear when type II cells undergo transdifferentiation. It is unclear whether these plasma membrane rafts are involved in the function of caveolae.

5.4.3 The Identity of LPP in Lung Epithelial Cell CEDs

The cloning of LPPs from rat lung and isolated rat type II cells (Chapter 3) indicates the presence of LPP1, LPP1a, and LPP3. The LPP2 isoform was detected in brain but was absent in lung. The LPP1 and LPP1a isoforms are most probably derived from alternative splicing with regions of divergence at the end of the first transmembrane domain, the beginning of the second transmembrane domain, and various residues in the first extracellular loop. The availability of mouse-reactive C-terminal LPP1/1a and N-terminal LPP3 antibodies allowed the investigation of their localization to CEDs and purified caveolae by western blotting. The LPP1/1a protein was present in MLE15 purified caveolae while the LPP3 isoform was undetectable in this cell line and localized to the detergent soluble fractions in MLE12 cells. The relatively low expression level of the LPP1/1a isoforms in purified caveolae compared to total plasma membranes indicates that LPP1/1a may be present in an activated state within caveolae.

LPP3 protein was found to localize predominantly in CEDs isolated from rat lung tissue and could arise mostly from type I and endothelial cells which are reported to have abundant caveolae. The recent localization of the Edg1 receptor to CEDs (22), the observation that S-1-P promotes endothelial cell migration and angiogenic differentiation (38), and LPP can hydrolyze this phospholipid growth factor (39) implicate LPP in the control of endothelial cell vasculogenesis and angiogenesis. The localization of LPP3 protein predominantly in CEDs from an endothelial-rich source adds further support to this hypothesis.

Sciorra and Morris (40) have reported the localization of endogenous and overexpressed LPP3 to CEDs isolated from Swiss 3T3 and HEK293, respectively.

Therefore, LPP1/1a and LPP3 appear to have a cell-type specific localization depending on the function of the cell. Different isoforms of PLD have been reported in different cell lines. Czarny *et al.* (20, 21) demonstrated that PLD2 is preferentially targeted to CEDs in CHO, HaCaT human keratinocytes, and U937 cells. In contrast, Kim *et al.* (18, 19) have localized PLD1 to CEDs in 3Y1 rat fibroblasts and COS7 cells. Recently, Sciorra and Morris (41) have provided evidence that LPP3 but not LPP1 can generate DAG derived from PLD in HEK293 cells. These authors also demonstrate that these LPP3 overexpressing cells accumulated significantly more DAG when stimulated with phorbol ester (41). Hence, the particular LPP and the PLD isoforms directed to CEDs both can depend on the cell type.

It should be noted that the presence and activation of LPP activity in caveolae-rafts could be explained by the presence of other unidentified forms of LPP. However, examination of the mouse database of expressed sequence tags (dbESTs), using consensus sequences based on the active sites for LPPs did not lead to identification of other candidate LPPs.

5.4.4 Modulation of LPP Activity

LPP activity in CEDs from MLE12 cells treated with PMA revealed a 3.8-fold redistribution of total LPP activity to these domains. Western blotting showed that LPP1/1a protein expression was higher in the total plasma membranes compared to the low levels in MLE15 caveolae although this purified vesicular fraction was more highly enriched in LPP activity. These results suggest that LPP1/1a may become phosphorylated followed by its recruitment into specific microdomains.

Hence, phosphorylated, activated LPP1/1a could be present within caveolae and the lesser active form in the general plasma membrane. Although LPPs have potential PKC phosphorylation sites in the N and C-terminal regions and was shown to be a phosphoprotein (41), further experimental support is needed to determine whether LPPs are, indeed, regulated by phosphorylation thus recruiting them to caveolae-rafts.

Kim *et al.* (18) describe a mechanism for the regulation of the PKC-α dependent PLD activity through molecular interactions between PLD1, PKC-α, and caveolin-1 in caveolae. They demonstrated that both the phosphorylation and activation of PLD1 by PKC occurs in caveolae of 3Y1 cells (19). We propose a similar mechanism for LPP regulation which would involve activation through phosphorylation followed by movement into caveolae-rafts. This would be similar to the mechanism recently reported for the Edg1 receptor (22). The identification of factors that regulate LPP upon cell activation is required to further define the role of LPP in the regulation of surfactant secretion and/or proliferation.

5.4.5 Summary

These results presented in this study show that endogenous LPP activity is enriched in CEDs, isolated based on their detergent insolubility in Triton X-100, from rat lung and mouse lung epithelial cell lines, namely MLE12 and MLE15 cells. The LPP3 protein is predominantly localized in rat lung CED. Furthermore, caveolae from MLE15 cells, purified by the cationic colloidal silica method, indicated

enrichment in LPP activity. Moreover, these cells, when transdifferentiated, become a type-I-like cell and we report an increase in LPP activity as well as corresponding increases in caveolin-1, PKC and PLD protein levels. The increase in LPP activity in transdifferentiated type II cells suggests another function in addition to regulation of surfactant secretion and in controlling cellular proliferation. Furthermore, we demonstrate that in MLE12 cells, the total percent of LPP activity increases within CEDs with PMA treatment and the LPP1/1a protein may be regulated by phosphorylation followed by its recruitment into caveolae-rafts.

5.5 Acknowledgements

We would like to express our gratitude to Dr. D. Stolz (University of Pittsburgh, Pennsylvania) for providing the cationic colloidal silica. We are grateful to Dr. D. Brindley (University of Alberta, Edmonton) for stimulating discussions. We also thank Anne Brickenden for her invaluable technical advice. This work was supported by a group grant from the Medical Research Council of Canada, grants from the Ontario Thoracic Society, and the Child Health Research Institute, London Health Science Center. MN was the recipient of an OGSST award during part of these investigations.

5.6 References

1. **Brindley DN and Waggoner DW.** 1996. Phosphatidate phosphohydrolase and signal transduction. Chem. Phys. Lipids. **80**: 45-57.

2. **Walton PA and Possmayer F.** 1985. Mg^{+2}-dependent phosphatidate phosphohydrolase of rat lung: developmental of an assay employing a defined chemical substrate which reflects the phosphohydrolase activity measured using membrane-bound substrate. Anal. Biochem. **151**: 479-486.

3. **Walton PA and Possmayer F.** 1986. Translocation of Mg^{+2}-dependent phosphatidate phosphohydrolase between cytosol and endoplasmic reticulum in a permanent cell line from human lung. Biochem. Cell Biol. **64**:1135-1140.

4. **Nanjundan M and Possmayer F.** 2000. Characterization of pulmonary NEM-insensitive phosphatidate phosphohydrolase. Exp. Lung.Res. **26**: 361-381.

5. **Rooney SA and Gobran LI.** 1991. Activation of phospholipase D in rat type II pneumocytes by ATP and other surfactant secretagogues. Am. J. Phys. **264**: L133-L140.

6. **Brindley D and Waggoner D.** 1998. Mammalian lipid phosphate phosphohydrolases. J. Biol. Chem. **273**: 24281-24284.

7. **Stukey J and Carman GM.** 1997. Identification of a novel phosphatase sequence motif. Protein Science. **6**: 469-472.

8. **Xu J, Zhang QX, Pilquil C, Berthiaume LG, Waggoner DW, and Brindley DN.** 2000. Related lipid phosphate phosphohydrolase-1 in the regulation of lysophosphatidate signaling. Ann. N.Y. Acad. Sci. **905**:81-90.

9. **Ishikawa T, Kai M, Wada I, and Kanoh H.** 2000. Cell surface activities of the human type 2b phosphatidic acid phosphatase. J. Biochem. (Tokyo). **127**: 645-651.

10. **An S.** 2000. Identification and characterization of G protein-coupled receptors for lysophosphatidic acid and sphingosine-1-phosphate. Ann. N.Y. Acad. Sci. **905**:25-33.

11. **Xu J, Love LM, Singh I, Zhang QX, Dewald J, Wang DA, Fisher DJ, Tigyi G, Berthiaume LG, Waggoner DW, and Brindley DN.** 2000. Lipid phosphate phosphatase-1 and Ca^{+2} control lysophosphatidate signaling through EDG-2 receptors. J. Biol. Chem. **275**: 27520-27530.

12. **Anderson RG.** 1998. The caveolae membrane system. Ann. Rev. Biochem. **67**:199-225.

13. **Schnitzer JE, Liu J, and Oh P.** 1995. Endothelial caveolae have the molecular transport machinery for vesicle budding, docking, and fusion

including VAMP, NSF, SNAP, and annexins, and GTPases. J. Biol. Chem. **270**: 14399-14404.

14. **Oh P, McIntosh DP, and Schnitzer JE.** 1998. Dynamin at the neck of caveolae mediates their budding to form transport vesicles by GTP-driven fission from the plasma membrane of endothelium. J. Cell Biol. **141**: 101-114.

15. **Mineo C, Ying YS, Chapline C, Jaken S, and Anderson RG.** 1998. Targeting of protein kinase C-alpha to caveolae. J. Cell Biol. **141**: 601-610.

16. **Anderson RG, Kamen BA, Rothberg KG, and Lacey SW.** 1992. Potocytosis: sequestration and transport of small molecules by caveolae. Science. **255**: 410-411.

17. **Bist A, Fielding PE, and Fielding CJ.** 1997. Two sterol regulatory element-like sequences mediate up-regulation of caveolin gene transcription in response to low density lipoprotein free cholesterol. Proc. Natl. Acad. Sci. U S A. **94**: 10693-10698.

18. **Kim JH, Han JM, Lee S, Kim Y, Lee TG, Park JB, Lee SD, Suh PG, and Ryu SH.** 1999. Phospholipase D1 in caveolae: regulation by protein kinase C-α and caveolin-1. Biochemistry. **38**: 3763-3769.

19. **Kim Y, Han JM, Han BR, Lee KA, Kim JH, Lee SD, Jang IH, Suh PG, and Ryu SH.** 2000. Phospholipase D1 is phosphorylated and activated by protein kinase C in caveolin-enriched microdomains within the plasma membrane. J. Biol. Chem. **275**: 13621-13627.

20. **Czarny M, Lavie Y, Fiucci G, and Liscovitch M.** 1999. Localization of phospholipase D in detergent-insoluble, caveolin-rich membrane domains. Modulation by caveolin-1 expression and caveolin-182-101. J. Biol. Chem. **274**:2717-2724.

21. **Czarny M, Fiucci G, Lavie Y, Banno Y, Nozawa Y, and Liscovitch M.** 2000. Phospholipase D2: functional interaction with caveolin in low-density membrane microdomains. FEBS Lett. **467**: 326-332.

22. **Igarashi J and Michel T.** 2000. Agonists-modulated targeting of the EDG-1 receptor to plasmalemmal caveolae: eNOS activation by sphingosine-1-phosphate and the role of caveolin-1 in sphingolipid signal transduction. J. Biol. Chem. **275**: 32363-32370.

23. **Campbell L, Hollins AJ, Al-Eid A, Newman GR, von Ruhland C, and Gumbleton M.** 1999. Caveolin-1 expression and caveolae biogenesis during

cell transdifferentiation in lung alveolae epithelial primary cultures. Biochem. Biophys. Res. Commun. **262**: 744-751.

24. **Newman GR, Campbell L, von Ruhland C, Jasani B, and Gumbleton M.** 1999. Caveolin and its cellular and subcellular immunolocalisation in lung alveolar epithelium: implications for alveolar epithelial type I cell function. Cell Tissue Res. **295**: 111-120.

25. **Wikenheiser KA, Vorbroker DK, Rice WR, Clark JC, Bachurski CJ, Oie HK, and Whitsett JA.** 1993. Production of immortalized distal respiratory epithelial cell lines from surfactant protein C/simian virus 40 large tumor antigen transgenic mice. Proc. Natl. Acad. Sci. U S A. **90**: 11029-11033.

26. **Dobbs L.** 1990. Isolation and culture of alveolar type II cells. Am. J. Physiol. **258**:L134-L147.

27. **Lisanti MP, Scherer PE, Vidugiriene J, Tang, Hermanowski-Vosatka A, Tu YU, Cook RF, and Sargiacomo M.** 1994. Characterization of caveolin-rich membrane domains isolated from an endothelial-rich source: implications for human disease. J. Cell Biol. **126**: 111-126.

28. **Stolz DB and Jacobson BS.** 1992. Examination of transcellular membrane protein polarity of bovine aortic endothelial cells in vitro using the cationic colloidal silica microbead membrane-isolation procedure. J. Cell Sci. **103**:39-51.

29. **Schnitzer JE, Oh P, Jacobson BS, and Dvorak AM.** 1995. Caveolae from luminal plasmalemma of rat lung endothelial: microdomains enriched in caveolin, Ca^{+2}-ATPase, and inositol trisphosphate receptor. Proc. Natl. Acad. Sci. U S A. **92**: 1759-1763.

30. **Schnitzer JE, McIntosh DP, Dvorak AM, Liu J, and Oh P.** 1995. Separation of caveolae from associated microdomains of GPI-anchored proteins. Science. **269**: 1435-1439.

31. **Lowry OH, and Rosebrough NJ, Farr AL, and Randall RJ.** 1951. Protein measurement with the folin phenol reagent. J. Biol. Chem. **193**:265-275.

32. **Langlet C, Bernard AM, Drevot P, and He HT.** 2000. Membrane rafts and signaling by the multichain immune recognition receptors. Curr. Opin. Immunol. **12**: 250-255.

33. **Oh P and Schnitzer JE.** 1999. Immunoisolation of caveolae with high affinity antibody binding to the oligomeric caveolin cage. Toward understanding the basis of purification. J. Biol. Chem. **274**: 23144-23154.

34. **Liu J, Oh P, Horner T, Rogers RA, and Schnitzer JE.** 1997. Organized endothelial cell surface signal transduction in caveolae distinct from glycosylphosphatidylinositol-anchored protein microdomains. J. Biol. Chem. **272**: 7211-7222.

35. **Razani B, Schlegel A, and Lisanti MP.** 2000. Caveolin proteins in signaling, oncogenic transformation, and muscular dystrophy. J. Cell Sci. **113**: 2103-2109.

36. **Volonte D, Galbiati, and Lisanti MP.** 1999. Visualization of caveolin-1, a caveolar marker protein, in living cells using green fluorescent protein (GFP) chimerase. The subcellular distribution of caveolin-1 is modulated by cell-cell contact. FEBS Lett. **445**:431-439.

37. **Brown DA and London E.** 2000. Structure and function of sphingolipid- and cholesterol-rich membrane rafts. J. Biol. Chem. **275**: 17221-17224.

38. **English D, Welch Z, Kovala AT, Harvey K, Volpert OV, Brindley DN, and Garcia JG.** 2000. Sphingosine 1-phosphate released from platelets during clotting accounts for the potent endothelial cell chemotactic activity of blood serum and provides a novel link between and angiogenesis. FASEB J. **14**:2255-2265.

39. **Waggoner DW, Gomez-Munoz A, Dewald J, and Brindley DN.** 1996. Phosphatidate phosphohydrolase catalyzes the hydrolysis of ceramide 1-phosphate, lysophosphatidate, and sphingosine 1-phosphate. J Biol Chem. **271**:16506-16509.

40. **Sciorra VA and Morris AJ.** 1999. Sequential actions of phospholipase D and phosphatidic acid phosphohydrolase 2b generate diglyceride in mammalian cells. Mol. Biol. Cell. **10**: 3863-3876.

41. **Wagonner DW, Martin A, Dewald J, Gomez-Munoz A, and Brindley DN.** 1995. Purification and characterization of novel plasma membrane phosphatidate phosphohydrolase from rat liver. J. Biol. Chem. **270**: 19422-19429.

Chapter 6

Overall Discussion

6.1 Summary

Previous studies performed in lung have demonstrated the existence of two different forms of PAPases, namely PAP1 and PAP2 (LPP). The former pulmonary magnesium -dependent enzyme is N-ethylmaleimide (NEM)-sensitive, heat labile, and is involved in phospholipid biosynthesis. This thesis advances our knowledge of the latter isoform, the NEM-insensitive and magnesium-independent lipid phosphate phosphohydrolases (LPPs) in lung and type II cells and establishes the foundation for further studies.

As described in Chapter 2, LPP was inhibited by various sphingoid bases including sphingosine and substrate analogs such as LPA, C-1-P, and, to a lesser extent, S-1-P. LPP activity was slightly enriched in isolated type II cells and low in isolated rat lung fibroblasts. These studies show that lung contains LPP activity in plasma membranes and type II cells where it could play a role in signal transduction, specifically in surfactant phospholipid secretion in the P_{2u} purinergic signaling cascade acting sequentially to PLD. LPP activity was enriched in purified lung plasma membranes where both PA and LPA were good substrates. In contrast, S-1-P was a relatively poor substrate and LPP activity against this substrate was not enriched in lung plasma membranes. The substrate specificity of pulmonary LPP was different to that reported for purified plasma membrane rat liver LPP (1) which suggested the potential presence of a novel LPP in lung.

Chapter 3 identifies the LPP isoforms present in both rat lung and isolated type II cells. The RT-PCR generated LPP1, up to three LPP1 variants, and LPP3 cDNAs. The three LPP1 variants include LPP1a and two novel isoforms, LPP1b and LPP1c. Expression of LPP1, LPP1a, and LPP3 cDNAs in HEK 293 cells established that they encode functional lipid phosphate phosphohydrolases. In contrast, the novel isoforms, LPP1b and LPP1c, contain frameshifts, which would result in premature termination producing putative catalytically inactive polypeptides. Further investigation of the LPP1b isoform revealed that it was present across a variety of tissues and exists in equal abundance to the LPP1/1a isoform in lung tissue. As expected, transient mammalian expression of LPP1b failed to alter phosphatidate phosphohydrolase activity.

Developmental patterns of the cloned LPPs in rat lung, described in Chapter 4, were performed as a preliminary step towards investigating the possible functions of the cloned LPP isoforms. The developmental patterns for LPP as well as for PLD, the LPA and S-1-P subtypes of the Edg receptors, and PKC isoforms indicate potential roles in the control of lung vasculogenesis, epithelial growth, alveolar development, and surfactant phospholipid secretion. A more detailed investigation of LPPs and their role in surfactant secretion awaits improved type II cell systems.

Studies presented in Chapter 5 investigate the localization of LPP in lipid-rich signaling platforms as it was recently reported that PLD isoforms (2, 3, 4, 5) and Edg1 receptor (6) were localized to these lipid-rich signaling domains. LPP activity was found to be enriched in lipid-rich signaling platforms isolated from rat lung tissue, isolated rat type II cells, and type II cell - mouse lung epithelial cell lines

(MLE12 and MLE15). LPP3 protein localized predominantly to rat lung CEDs. Elevated LPP activity and LPP1/1a protein are present in purified caveolae from MLE15 cells prepared using the cationic colloidal silica method. In contrast, total plasma membranes had a higher abundance of LPP1/1a protein with low LPP activity. Phorbol ester treatment caused a 3.8-fold increase in LPP specific activity in MLE12 CEDs. Thus, the activated form of LPP1/1a may be recruited into caveolae-rafts. Moreover, LPP1/1a and LPP3 appear to have cell-type specific localizations. Transdifferentiation of type II cells into a type I-like cell demonstrated enrichment in caveolin-1 levels and LPP activity. These results indicate that LPP is localized in caveolae and/or rafts in lung tissue, isolated type II cells, and type II cell lines consistent with a role for LPP in both caveolae/raft signaling and caveolar dynamics.

6.2 Experimental Limitations

Our laboratory as well as other investigators have attempted to produce antibodies against the LPP isoforms with little success. There exist only antibodies reactive against LPP1/1a and LPP3. These antibodies do not immunoreact well with the rat isoforms. As many of the studies reported in this thesis were performed with rat, appropriate antibodies for advancing these investigations were not available. Furthermore, the C-terminal mouse LPP1 antibody does not distinguish between LPP1 and LPP1a since they cannot be separated by SDS-PAGE as their size differs in only one amino acid. The lack of appropriate isoform-specific antibodies hindered immunohistochemical studies in rat lung sections to address the cellular and

subcellular localization of the endogenous LPP isoforms. The mLPP1 antibody is not suitable for immunofluorescence studies as reported by Brindley and colleagues (7) who have, instead, examined localization of LPPs by overexpressing LPP as GFP fusion proteins. Hence, the localization of endogenous LPPs in the MLE12 and MLE15 cell lines will be addressed once appropriate antibodies become available.

Primary type II cells are very difficult to isolate and rapidly undergo drastic changes in morphology and function when cultured on tissue culture plastic (8). Furthermore, they are not easily transfected due to their low mitotic index (9). Wikenheiser *et al.* (10) have isolated a number of mouse lung epithelial cell lines from transgenic mice expressing the large T antigen driven by the SP-C promoter. The SV40 large T antigen is known to bind to tumor suppressor gene products such as p53 and retinoblastoma (Rb) resulting in uncontrolled cellular proliferation (11). However, these type II-like cell lines do not possess lamellar bodies and do not secrete surfactant (12). Nonetheless, expression of the cloned cDNAs was initially attempted in the SV-40 large T antigen transformed MLE12 and MLE15 cell lines to characterize the various cloned LPPs. However, transfections were without success as cell death resulted with the MLE12 cell line and increases in LPP enzyme activity were not detected in the MLE15 cell line using an inducible tetracycline system.

Dobbs *et al* (13) have described a method for maintaining differentiated type II cells on collagen gels by culture with an apical air surface for up to three weeks in culture. These type II cells are able to secrete surfactant and have numerous lamellar bodies. This culture system will allow some studies of surfactant synthesis,

secretion, and recycling to be performed with more ease. However, the three week culture period will only allow for transient transfections. More recently, deMello *et al* (14) have been successful in generating an immortal differentiated lung type-II epithelial cell line from a transgenic H-2K^b-tsA58 mouse. This transgene consists of the 5'-flanking promoter sequence and the transcriptional initiation site of the mouse major histocompatibility complex coupled to the coding sequence of a temperature-sensitive form of the SV40 T antigen. When cells from these mice are isolated and grown under permissive conditions, 33^{0}C in the presence of γ-interferon (IFN), the SV40 T antigen is expressed causing the cells to proliferate. Upon removal of the IFN and transfer to 39^{0}C, the T antigen expression is turned off, the cells differentiate, possess numerous lamellar bodies, and respond to surfactant secretagogues (14). Such a cell line would be invaluable to investigate the role of LPP in surfactant secretion and in the control of cell growth.

LPP2 knockout mice were recently generated with, however, no obvious phenotype (15). Since it is expected that the generation of knockout LPP1, LPP1a, and LPP3 mice may be potentially lethal or could lead to defects in lung development, conditional knockout mice can be generated using an inducible system using the SP-C promoter to direct expression of the transgene in type II cells at a certain time during development or under various conditions.

6.3 Regulation of Lipid Phosphate Phosphohydrolases

We propose that the LPP1 gene undergoes differential splicing generating LPP1, LPP1a, and LPP1b mRNA products. It was reported by Leung and

colleagues (16) that low mRNA levels of LPP1/1a were present in human colon tumors compared to normal colon tissue. The LPP1b mRNA may be produced at higher levels in various lung conditions such as cancer as a result of differential splicing leading to decreased LPP1/1a mRNA expression. The possibility that LPP1b RNA will be translated into a protein product could be addressed by generating an antibody against the C-terminal ten amino acids of the sequence (DDYWRNSVCLL), which differs to that of the LPP1 and LPP1a isoforms as a result of a frameshift. The localization of LPP1b and the potential modulation of endogenous LPP activity could then be investigated by overexpressing LPP1b in a mammalian cell line.

As shown with the PMA activation studies in caveolin-enriched domains (Chapter 5), there was an increase in the LPP enzyme activity in the detergent insoluble fractions. This could be interpreted as activation of LPP followed by its recruitment from the general plasma membrane to lipid-rich microdomains. The isoform present within MLE15 cells, a type II-like cell line, is LPP1/1a, which appears to be in an activated form within caveolae. Brindley and colleagues (17) have shown that purified LPP is a phosphoprotein and have recently demonstrated that LPP1 is phosphorylated at tyrosine 99 (Brindley DN, unpublished observations) which is located within the proposed caveolin binding domain. However, attempts to immunoprecipitate LPP with caveolin-1 were unsuccessful. The cloned LPPs also have a number of consensus sites for serine/threonine phosphorylation which may be involved in its regulation (18). LPP1/1a may have a role during lung injury by regulating LPA-mediated effects through the Edg receptor (19).

The localization of the LPPs within the nuclear or plasma membrane will be an important determining factor in its ability to dephosphorylate exogenous substrates and intracellular bioactive lipids. The predicted topology of the LPPs within the membrane indicates that the active site faces extracellularly or luminally. However, if these LPPs were to act sequentially to PLD, its active site should face intracellularly since it is thermodynamically and kinetically difficult for the negatively charged PA species to readily flip-flop within the membrane as which occurs for the neutral DAG species (20). Phospholipid translocases and scramblases do not appear to be involved in the flip-flop of PA (21, 22). There may exist other lipid phosphate phosphohydrolases which have their active sites facing intracellularly such as that described for sphingosine-1-phosphate phosphohydrolase (23).

Pulmonary LPP catalyzes the hydrolysis of PA, LPA, and to a lesser extent, S-1-P in rat lung microsomes (Chapter 2). However, S-1-P was a poor substrate in contrast to PA and LPA in purified rat lung plasma membranes suggesting that the LPP isoform in the plasma membrane does not hydrolyze S-1-P. Kanoh and colleagues (24) observed that the activity of overexpressed LPP3 in HeLa cell total membranes was 10-fold lower compared to LPA and PA while overexpressed LPP1 failed to hydrolyze S-1-P. However, Brindley and colleagues (1, 7) reported that both purified rat liver LPP and mouse LPP1 were capable of hydrolyzing these lipid phosphates including S-1-P with similar efficiencies. These differences in substrate specificity may be explained by the presence of other LPPs, which specifically degrade plasma membrane S-1-P. Thus, the presence and localization of S-1-P phosphohydrolase in lung and type II cells must be established. It is also possible

that other membrane components may affect the ability of the LPP enzymes to hydrolyze various lipid phosphates. The LPP3 isoform, determined by western blotting, appears to localize predominantly to CEDs from rat lung, an endothelial-rich source (Chapter 5) where it could have a role in the control of endothelial cell vasculogenesis and angiogenesis (25). Moreover, the recent localization of the Edg1 receptor to caveolin-enriched domains from COS7 cells (6) and the observation that S-1-P can promote endothelial cell migration (BPAEC and HUVEC cells) (26) suggest that LPP3 may regulate the effects of S-1-P through the Edg receptor.

Database analyses indicate that the human LPP1, LPP2, and LPP3 isoforms are localized to chromosome 5, 19, and 1, respectively (NCBI LocusLink). The genomic analysis of the LPP1 and LPP3 genes has not yet been reported. Promoter studies will provide information regarding the transcriptional regulation of the various LPP isoforms. It was reported that in human prostatic LNCaP cells, LPP1 mRNA levels were upregulated upon androgen treatment (27). LPP3 mRNA levels were increased in EGF-treated HeLa cells (24). Furthermore, LPA-phosphohydrolase activity was reported to increase in ovarian cancer cells in response to gonadotropin releasing hormone, GnRH (28). In fetal lung, PAP2 activity increased with glucocorticoid treatment (29, 30). Whether there are hormone responsive elements in the promoter regions of the LPP genes has yet to be established.

6.4 Implications of LPP in Signaling Platforms

We have shown that LPP activity exists in type II cell rafts although the LPP

isoform(s) was not identified. We propose that an LPP isoform(s) could participate in signaling from type II cell rafts where it would act sequentially to PLD, which produces PA from the abundant PC, to produce DAG for sustained PKC activation in the P_{2u} receptor cascade for surfactant phospholipid secretion.

Also during lung injury, type II cells proliferate and migrate to restore the type I cell population through a transdifferentiation process in order to re-establish the alveolar epithelium. These processes may require elevated DAG levels generated by LPP for PKC activation leading to activation of genes involved in this process. We have shown that there are increases in LPP activity as well as in other lipid signaling enzymes during transdifferentiation of isolated type II cells to type I-like cells *in vitro*. The isoform(s) involved in these processes was not identified. The recent localization of the Edg receptor (6) to caveolae and the involvement of LPP in the attenuation of LPA-mediated effects (19) further implicate LPP in the control of cell proliferation.

The dramatic increase in LPP activity and caveolin-1 in type I-like cells are consistent with a potential role for caveolae in controlling cell growth. It has been proposed that caveolin-1 may be a tumor suppressor as its protein levels appear to inversely correlate with the proliferative capacity of the cell (31). Decreased levels of caveolin-1 and caveolae have been reported in a variety of transformed (ras and src) cell lines (31). Interestingly, ras transformed rat 2 fibroblasts have lower LPP activity and higher PA/DAG ratios compared to normal rat 2 fibroblasts (32). PA, a substrate for LPP, is a potent mitogen responsible for the activation of a variety of signal transduction processes including the translocation of Raf-1, which contains

a PA binding site, to membranes, which leads to the activation of the MAP kinase pathway. Recently, caveolin-1 gene expression was found to be downregulated by the activation of this signaling cascade (33). Increased LPP activity would be able to modulate the activation of this kinase pathway through the dephosphorylation of PA to diacylglycerol leading to increases in caveolin-1 expression (Figure 6.1A). Thus, LPP, within caveolae, acting sequentially to PLD could have a role in the control of cell growth. This overall scheme may apply whether caveolin expression is directly involved in down-regulating cell division or caveolin expression represents an aspect of terminal differentiation, which correlates with diminished cell growth.

Caveolae are well known to be enriched in sphingomyelin (34). It was recently reported that these organelles are also enriched in neutral sphingomyelinase (34) and that ceramide is compartmentalized within these domains (35). Caveolae may be the signaling center where stimuli such as TNF-α initiate an apoptotic cascade of events. Tepper *et al.* (36) have recently reported that the loss of phospholipid asymmetry in Jurkat T cells leads successively to sphingomyelin hydrolysis, redistribution of cholesterol, membrane blebbing, and eventually vesicle formation at the cell surface. Hydrolysis of sphingomyelin by sphingomyelinases generates ceramide. LPPs may also be capable of generating ceramide since these enzymes possess broad substrate specificity, which includes its ability to dephosphorylate C-1-P. Although ceramide has been implicated in cell death (37), it is unknown whether the generation of ceramide by LPP is involved in apoptosis. Likewise, it is unknown whether ceramide kinase, another enzyme involved in the regulation of ceramide levels, is present in caveolae. Nonetheless,

Figure 6.1. Potential roles of LPP in caveolae/raft signaling and caveolar dynamics. A, LPP may be involved in the control of cell growth. LPP activity can modulate the activation of the MAP kinase cascade through the dephosphorylation of PA. The balance between the MAP kinase and LPP/PKC pathways may regulate the transcription of caveolin-1. B, LPP may have a role in caveolae dynamics. We propose that LPP may be involved in terminating the PA and C-1-P signals generating DAG to regulate the budding, internalization, and fusion of caveolae.

A Control of Cell Growth

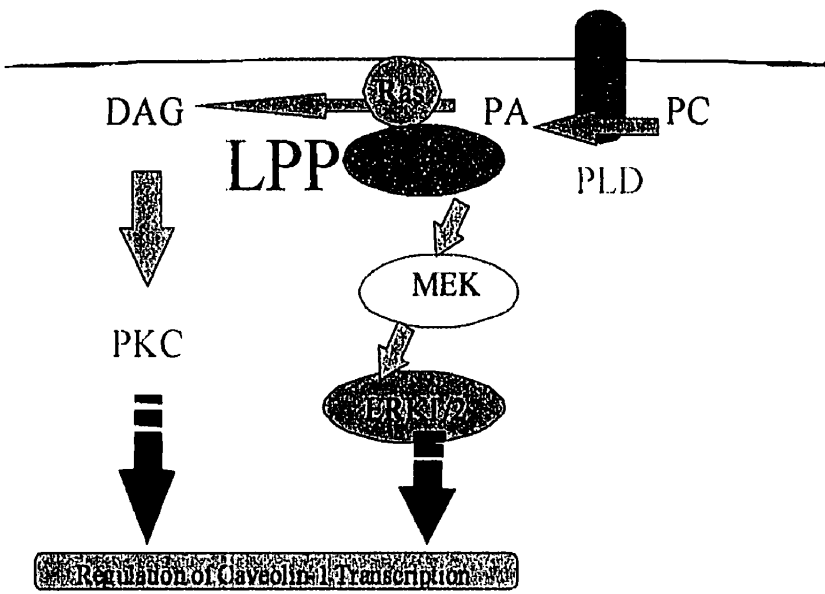

B Caveolar Dynamics

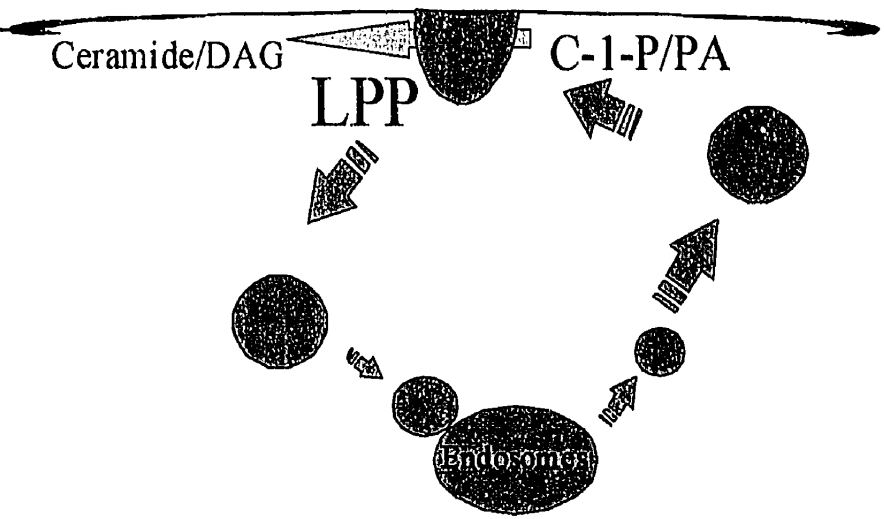

the lipid-membrane environment in caveolae would implicate LPP in the potential regulation of these sphingolipids whose products modulate the activity of PKC and PLD. Hence, LPP could be responsible for the elimination of various signals (PA, LPA, C-1-P, and S-1-P) and the subsequent generation of new signals (DAG, ceramide, and sphingosine) within caveolae. The involvement of LPP in the "cross-talk" between the sphingolipid and glycerolipid pathways could likely occur within these lipid rich microdomains.

LPP may have a potential role in caveolar dynamics. It is known that the phospholipid composition of cellular vesicles plays an important role in their fusion with the plasma membrane. For example, PA generated by PLD was shown to be involved in the process of vesicle budding from Golgi membranes (38, 39). Furthermore, Hinkovska-Galcheva *et al* demonstrated that C-1-P enhanced phospholipid-dependent vesicle fusion to the plasma membrane in polymorphonuclear leukocytes (40). Since LPP has the ability to hydrolyze both C-1-P and PA, it may be involved in regulating the termination of such membrane fusion events and possibly even the budding and fusion of caveolae (Figure 6.1B).

6.5 LPP and Epithelial Cell Growth Control

In rat lung development, increases in the protein expression of cyclin A and D were reported in isolated airway epithelial cells (AECs) during the proliferative phase (19 days of gestation) (41, 42). Moreover, these cyclins were more highly expressed in transformed adult AECs compared to normal cells. The induction of these G_1 phase regulatory cyclins contributes to the continued passage of the cell

through G_1 and into the S phase. Interestingly, it was observed that the cyclin D1 gene was transcriptionally repressed by caveolin-1 (43). Thus, in transformed alveolar epithelial cells and 19 days of gestation epithelial cells, the levels of caveolin-1 are expected to be low with high cyclin D1 expression, increased DNA synthesis, elevated PA to DAG ratios, and low LPP activity. Racine *et al* (44) observed that caveolin-1 expression was reduced in cell lines derived from tumors of epithelial origin compared to normal bronchial epithelial cells. In contrast to transformed cells, normal cells senesce after a finite number of population doublings which could be related to high caveolin-1 protein expression (45), increased LPP activity, higher DAG to PA ratios, low cyclin D1 levels, and diminished DNA synthesis.

The sequence of events that occur during lung injury include the loss of type I cells, proliferation of type II cells, and the transdifferentiation of type II to type I cells. It was reported that caveolin expression in the alveolar epithelium is downregulated after irradiation-induced lung injury (46). The investigators demonstrate a dramatic loss of caveolin immunoreactivity in type I cells compared to endothelial cells which have increased caveolin-1 expression. During normal lung development and lung injury, activation of sphingomyelinase may generate ceramide leading to programmed cell death (Figure 6.2). The concerted actions of PLD, LPP, and PKC may attempt to counter the effects of ceramide in order to maintain the cells in the G_0 phase of the cell cycle and prevent progression to apoptosis. During the proliferative phase of lung development and also during recovery after injury as part of the regeneration of the alveolar epithelium, type II

Figure 6.2. LPP and epithelial cell growth control. The sequence of events that occur during lung injury include the loss of type I cells, proliferation of type II cells, and the transdifferentiation of type II to type I cells. During normal lung development and lung injury, activation of sphingomyelinase may generate ceramide leading to programmed cell death. The concerted actions of PLD, LPP, and PKC may attempt to counter the effects of ceramide. The proliferative phase of lung development and the regeneration of the alveolar epithelium may involve reduced LPP activity, increased PA levels, activation of the MAP kinase signaling cascade, and increased cell division. The transdifferentiation of type II to type I cells during lung development and the resolution phase of lung injury may require elevated caveolin-1 levels, increased LPP activity, and PKC activation.

LPP and Epithelial Cell Growth Control

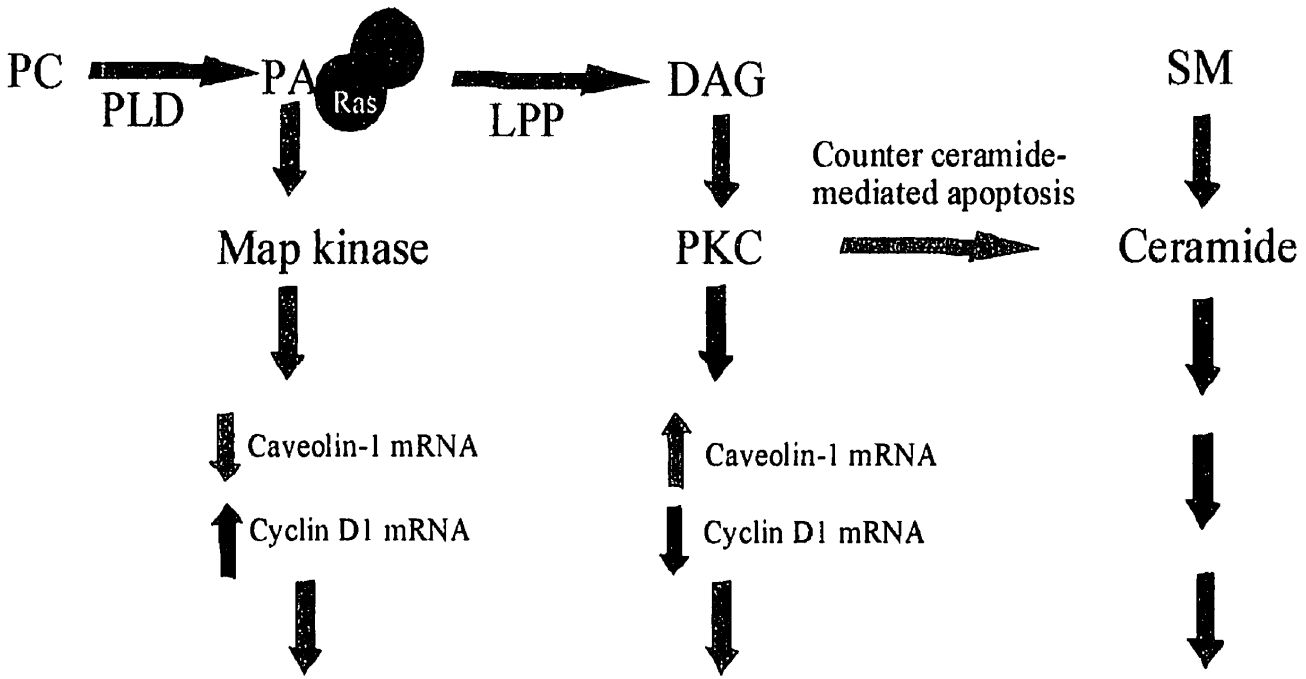

epithelial cells proliferate. This may involve reduced LPP activity, increased PA levels, and activation of the MAP kinase signaling cascade. The transdifferentiation of type II to the type I cells, during the canalicular phase of development and the resolution phase of injury, may require elevated caveolin-1 levels, increased LPP activity, and PKC activation leading to the activation of genes required for this process or for a type I cell function.

6.6 Summary

This thesis further expands our knowledge and understanding of pulmonary lipid phosphate phosphohydrolases. LPP activity is enriched in lung caveolin-enriched domains, plasma membranes, and in type II cell lipid-rich domains where it could be involved in signal transduction. LPP is proposed to act sequentially to PLD in the signaling cascade as well as in regulating the effects of phospholipid growth factors, LPA and S-1-P, which mediate their effects through Edg receptors to elicit various biological responses including cellular proliferation, differentiation, migration, and inhibition of apoptosis. The temporal expression profiles of LPPs, as well as Edg receptors and PLD isoforms, across development implicate these lipid signaling components in the control lung vasculogenesis, surfactant phospholipid secretion, alveolar remodelling. The localization of LPP3 in lung CEDs and the ability to hydrolyze phospholipid growth factors suggests that this isoform could be involved in the control of lung vascularization and angiogenesis. The localization of activated LPP1/1a in caveolae from a type II-like cell line indicates that it may be involved in the control of type II cell growth and in phospholipid surfactant secretion.

The concerted actions of LPP, PLD, and PKC may be implicated in the transdifferentiation of type II cells to a type I cell during lung development as well as during injury.

6.7 References

1. **Waggoner DW, Gomez-Munoz A, Dewald J, and Brindley DN.** 1996. Phosphatidate phosphohydrolase catalylzes the hydrolysis of ceramide-1-phosphate, lysophosphatidate, and sphingosine-1-phosphate. J. Biol. Chem. **271**: 16506-16509.

2. **Kim JH, Han JM, Lee S, Kim Y, Lee TG, Park JB, Lee SD, Suh PG, and Ryu SH.** 1999. Phospholipase D1 in caveolae: regulation by protein kinase C-α and caveolin-1. Biochemistry. **38**: 3763-3769.

3. **Kim Y, Han JM, Han BR, Lee KA, Kim JH, Lee SD, Jang IH, Suh PG, and Ryu SH.** 2000. Phospholipase D1 is phosphorylated and activated by protein kinase C in caveolin-enriched microdomains within the plasma membrane. J. Biol. Chem. **275**: 13621-13627.

4. **Czarny M, Lavie Y, Fiucci G, and Liscovitch M.** 1999. Localization of phospholipase D in detergent-insoluble, caveolin-rich membrane domains. Modulation by caveolin-1 expression and caveolin-182-101. J. Biol. Chem. **274**:2717-2724.

5. **Czarny M, Fiucci G, Lavie Y, Banno Y, Nozawa Y, and Liscovitch M.** 2000. Phospholipase D2: functional interaction with caveolin in low-density membrane microdomains. FEBS Lett. **467**: 326-332.

6. **Igarashi J and Michel T.** 2000. Agonists-modulated targeting of the EDG-1 receptor to plasmalemmal caveolae: eNOS activation by sphingosine-1-phosphate and the role of caveolin-1 in sphingolipid signal transduction. J. Biol. Chem. **275**: 32363-32370.

7. **Jasinska R, Zhang QX, Pilquil C, Singh I, Xu J, Dewald J, Dillon DA, Berthiaume LG, Carman GM, Waggoner DW, and Brindley DN.** 1999. Lipid phosphate phosphohydrolase-1 degrade exogenous glycerolipid and sphingolipid phosphate esters. Biochem J. **340**: 677-686.

8. **Dobbs L.** 1990. Isolation and culture of alveolar type II cells. Am. J. Physiol. **258**: L134-L147.

9. **Fortunati E, Bout A, Zanta MA, Valerio D, and Scarpa M.** 1996. *In vitro* and *in vivo* gene transfer to pulmonary cells mediated by cationic liposomes. Biochim. Biophys. Acta. **1306**: 55-62.

10. **Wikenheiser KA, Clark JC, Linnoila RI, Stahlman MT, and Whitsett JA.** 1992. Simian virus 40 large T antigen directed by transcriptional elements of the human surfactant protein C gene produces pulmonary adenocarcinomas in transgenic mice. Cancer Res. **52**:5342-5352.

11. **Miyata Y and Yahara I.** 2000. p53-independent association between SV40 large T antigen and the major cytosolic heat shock protein, HSP90. Oncogene. **19**:1477-1484.

12. **Wikenheiser KA, Vorbroker DK, Rice WR, Clark JC, Bachurski CJ, Oie HK, and Whitsett JA.** 1993. Production of immortalized distal respiratory epithelial cell lines from surfactant protein C/simian virus 40 large tumor antigen transgenic mice. Proc Natl Acad Sci U S A. **90**:11029-11033.

13. **Dobbs LG, Pian MS, Maglio M, Dumars S, and Allen L.** 1997. Maintenance of the differentiated type II cell phenotype by culture with an apical air surface. Am J Physiol. **273**:L347-L354.

14. **deMello DE, Mahmoud S, Padfield PJ, and Hoffmann JW.** 2000. Generation of an immortal differentiated lung type-II epithelial cell line from the adult H-2K(b)tsA58 transgenic mouse. In Vitro Cell Dev Biol Anim. **36**:374-382.

15. **Zhang N, Sundberg JP, and Gridley T.** 2000. Mice mutant for ppap2c, a homolog of the germ cell migration regulator wunen, are viable and fertile. Genesis. **27**:137-140.

16. **Leung DW, Tompkins CK, and White T.** 1998. Molecular cloning of two alternatively spliced forms of human phosphatidic acid phosphatase cDNAs that are differentially expressed in normal and tumor cells. DNA and Cell Biol. **17**: 377-385.

17. **Waggoner DW, Martin A, Dewald J, Gomez-Munoz A, and Brindley DN.** 1995. Purification and characterization of novel plasma membrane phosphatidate phosphohydrolase from rat liver. J Biol Chem. **270**:19422-19429.

18. **Brindley DN and Waggoner DW.** 1996. Phosphatidate phosphohydrolase and signal transduction. Chem Phys Lipids. **80**:45-57.

19. **Xu J, Love LM, Singh I, Zhang QX, Dewald J, Wang DA, Fisher DJ, Tigyi G, Berthiaume LG, Waggoner DW, and Brindley DN.** 2000. Lipid phosphate phosphatase-1 and Ca^{+2} control lysophosphatidate signaling through EDG-2 receptors. J. Biol. Chem. **275**: 27520-27530.

20. **Pagano RE and Longmuir KJ.** 1985. Phosphorylation, transbilayer movement, and facilitated intracellular transport of diacylglycerol are involved in the uptake of a fluorescent analog of phosphatidic acid by cultured fibroblasts, J. Biol. Chem. **260**:1909-1916.

21. **Dekkers DW, Comfurius P, Schroit AJ, Bevers EM, and Zwaal RF.** 1998. Transbilayer movement of NBD-labeled phospholipids in red blood cell membranes: outward-directed transport by the multidrug resistance protein 1 (MRP1). Biochemistry. **37**:14833-14837.

22. **Zhou Q, Zhao J, Stout JG, Luhm RA, Wiedmer T, and Sims PJ.** 1997. Molecular cloning of human plasma membrane phospholipid scramblase. A protein mediating transbilayer movement of plasma membrane phospholipids. J Biol Chem. **272**:18240-18244.

23. **Mandala SM, Thornton R, Galve-Roperh I, Poulton S, Peterson C, Olivera A, Bergstrom J, Kurtz MB, and Spiegel S.** 2000. Molecular cloning and characterization of a lipid phosphohydrolase that degradessphingosine-1-phosphate and induces cell death. Proc Natl Acad Sci U S A. **97**:7859-7864.

24. **Kai M, Wada I, Imai S, Sakane F, and Kanoh H.** 1997. Cloning and characterization of two human isozymes of Mg^{2+}-independent phosphatidic acid phosphatase. J Biol Chem. **272**:24572-24578.

25. **Schwarz M, Lee M, Zhang F, Zhao J, Jin Y, Smith S, Bhuva J, Stern D, Warburton D, and Starnes V.** 1999. EMAP II: a modulator of neovascularization in the developing lung. Am. J. Physiol. **276**: L365-L375.

26. **English D, Welch Z, Kovala AT, Harvey K, Volpert OV, Brindley DN, and Garcia JG.** 2000. Sphingosine 1-phosphate released from platelets during clotting accounts for the potent endothelial cell chemotactic activity of blood serum and provides a novel link between and angiogenesis. FASEB J. **14**:2255-2265.

27. **Ulrix W, Swinnen JV, Heyns W, and Verhoeven G.** 1998. Identification of the phosphatidic acid phosphatase type 2a isozyme as an androgen-regulated

gene in the human prostatic adenocarcinoma cell line LNCaP. J. Biol. Chem. **273**: 4660-4665.

28. **Imai A, Furui T, Tamaya T, and Mills GB.** 2000. A gonadotropin-releasing hormone-responsive phosphatase hydrolyses lysophosphatidic acid within the plasma membrane of ovarian cancer cells. J Clin Endocrinol Metab. **85**:3370-3375.

29. **Brehier A, Benson BJ, Williams MC, Mason RJ, and Ballard PL.** 1977. Corticosteroid induction of phosphatidic acid phosphatase in fetal rabbit lung. Biochem Biophys Res Commun. **77**:883-890.

30. **Possmayer F, Duwe G, Metcalfe R, Stewart-DeHaan PJ, Wong C, Heras JL, Harding PG.** 1977. Cortisol induction of pulmonary maturation in the rabbit foetus. Its effects on enzymes related to phospholipid biosynthesis and on marker enzymes for subcellular organelles. Biochem J. **166**:485-494.

31. **Anderson RG.** 1998. The caveolae membrane system. Ann. Rev. Biochem. **67**:199-225.

32. **Martin A, Gomez-Munoz A, Waggoner DW, Stone JC, and Brindley DN.** 1993. Decreased activities of phosphatidate phosphohydrolase and phospholipase D in ras and tyrosine kinase (fps) transformed fibroblasts. J. Biol. Chem. **268**: 23924-23932.

33. **Engelman JA, Zhang XL, Razani B, Pestell RG, and Lisanti MP.** 1999. p42/p44 MAP kinase-dependent and -independent signaling pathways regulate caveolin-**1** gene expression. Activation of Ras-MAP kinase a signaling cascades transcriptionally down-regulated caveolin-1 promoter activity. J. Biol. Chem. **274**: 32333-32341.

34. **Liu J and Schnitzer JE.** 1999. Analysis of lipids in caveolae. Methods Mol. Biol. **116**: 61-72.

35. **Liu P and Anderson RG.** 1995. Compartmentalized production of ceramide at the cell surface. J. Biol. Chem. **270**: 27179-27185.

36. **Tepper AD, Ruurs P, Wiedmer T, Sims PJ, Borst J, and van Blitterswijk WJ.** 2000. Sphingomyelin hydrolysis to ceramide during the execution phase of apoptosis results from phospholipid scrambling and alters cell-surface morphology. J. Cell Biol. **150**: 155-164.

37. **Hannun YA.** 1994. The sphingomyelin cycle and the second messenger function of ceramide. J. Biol. Chem. **269**: 3125-3128.

38. **Ktistikis NT, Brown A, Sternweis PC, and Roth MG.** 1995. Phospholipase D is present on Golgi-enriched membranes and its activation by ADP ribosylation factor is sensitive to brefeldin A. Proc. Natl. Acad. Sci. U S A. **92**: 4952-4956.

39. **Ktistikis NT, Brown A, Waters GM, Sternweis PC, and Roth MG.** 1996. Evidence that phospholipase D mediates ADP ribosylation factor-dependent formation of Golgi coated vesicles. J. Cell Biol. **134**: 295-306.

40. **Hinkovska-Galcheva VT, Boxer LA, Mansfield PJ, Harsh D, Blackwood A, and Shayman JA.** 1998. The formation of ceramide-1-phosphate during neutrophil phagocytosis and its role in liposome fusion. J. Biol. Chem. **273**: 33203-33209.

41. **Bui KC, Wu F, Buckley S, Wu L, Williams R, Carbonaro-Hall D, Hall FL, and Warburton D.** 1993. Cyclin A expression in normal and transformed alveolar epithelial cells. Am J Respir Cell Mol Biol. **9**:115-125.

42. **Wu F, Buckley S, Bui KC, and Warbuton D.** 1995. Differential expression of cyclin D2 and cdc2 genes in proliferating and nonproliferating alveolar epithelial cells. Am. J. Respir. Cell Mol. Biol. **12**: 95-103.

43. **Hulit J, Bash T, Fu M, Galbiati F, Albanese C, Sage DR, Schlegel A, Zhurinsky J, Shtutman M, Ben-Ze'ev A, Lisanti MP, and Pestell RG.** 2000. The cyclin D1 gene is transcriptionally repressed by caveolin-1. J Biol Chem. **275**:21203-21209.

44. **Racine C, Belanger M, Hirabayashi H, Boucher M, Chakir J, and Couet J.** 1999. Reduction of caveolin 1 gene expression in lung carcinoma cell lines. Biochem Biophys Res Commun. **255**:580-586.

45. **Park WY, Park JS, Cho KA, Kim DI, Ko YG, Seo JS, and Park SC.** 2000. Up-regulation of caveolin attenuates epidermal growth factor signaling in senescent cells. J Biol Chem. **275**:20847-20852.

46. **Kasper M, Reimann T, Hempel U, Wenzel KW, Bierhaus A, Schuh D, Dimmer V, Haroske G, and Muller M.** 1998. Loss of caveolin expression in type I pneumocytes as an indicator of subcellular alterations during lung fibrogenesis. Cell Biol. **109**:41-48.

Appendices